VNIVERSITAT DE VALÈNCIA Facultat de Ciències Biològiques

PhD Thesis

Núria Banyuls i Ferrando

2017

# Characterisation of the structure-function relationship of the *Bacillus thuringiensis* Vip3A insecticidal proteins.


**Supervisor Dr. Juan Ferré Manzanero**

Catedràtic d'Universitat

Departament de Genètica

ERI de Biotecnologia i Biomedicina

Universitat de València

PhD Thesis

2017

Núria Banyuls i Ferrando

# Characterisation of the structure-function relationship of the *Bacillus thuringiensis* Vip3A insecticidal proteins.

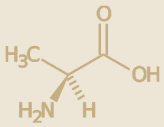


Supervisor: Dr. Juan Ferré Manzanero

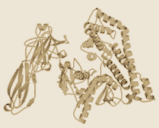

VNIVERSITAT DE VALÈNCIA Facultat de Ciències Biològiques

Tractor and farmer icons are taken from 2015 ISAA infographics *ISAA Brief No. 51*

VNIVERSITAT DE VALÈNCIA | BIOTECMED
Estructura de Recerca Interdisciplinar en Biotecnologia i Biomedicina

Dr. En Juan Ferré Manzanero, Catedràtic del Departament de Genètica de la Facultat de Ciències Biològiques de la Universitat de València,

Informa:

Que Na. Núria Banyuls i Ferrando, Llicenciada en Ciències Biològiques, ha realitza sota la seva direcció el treball d'investigació recollit en esta memòria que porta per títol "Characterisation of the structure-function relationship of the *Bacillus thuringiensis* Vip3A insecticidal proteins (Caracterització de la relació estructura-funció de les proteïnes insecticides Vip3A de *Bacillus thuringiensis*.)", per tal d'optar al Grau de Doctor per la Universitat de València.

I per fer constància, d'acord amb la legislació vigent, signa la present a Burjassot, a 31/05/2017.

Director: Dr. En. Juan Ferré Manzanero

**ERI BIOTECMED**
Estructura de Recerca Interdisciplinar de la Universitat de València
Dpto. Genética, Universitat de València. Dr. Moliner 50, 46100 Burjassot. España.
Tel. +34 96 3544506 e-mail: isicbtm@uv.es web: www.uv.es/biotecmed

*"Whether it be the sweeping eagle in his flight, or the open apple-blossom, the toiling work-horse, the blithe swan, the branching oak, the winding stream at its base, the drifting clouds, over all the coursing sun, form ever follows function, and this is the law. Where function does not change, form does not change. The granite rocks, the ever-brooding hills, remain for ages; the lightning lives, comes into shape, and dies, in a twinkling.*

*It is the pervading law of all things organic and inorganic, of all things physical and metaphysical, of all things human and all things superhuman, of all true manifestations of the head, of the heart, of the soul, that the life is recognizable in its expression, that* ***form ever follows function****. This is the law."*

(Sullivan, 1896)

## AGRAÏMENTS

En primer lloc m'agradaria agrair al Professor Juan Ferré per haver-me donat l'oportunitat de realitzar esta Tesi, en un camp tan diferent de la meva formació acadèmica prèvia. Moltes gràcies Juan per la il·lusió i pel compromís amb la investigació científica; per mantindre l'optimisme tot i les meves constants "males notícies"- com tu deies; per totes les discussions, a voltes acalorades. Moltíssimes gràcies per la disponibilitat a llegir-me i corregir-me els esborranys en temps rècord, especialment en aquesta última etapa que ha sigut *express* i en la que no m'ha faltat el teu recolzament. Moltes gràcies també per sempre trobar la paraula exacta, per atendre als petits detalls que sempre s'escapen i per haver-me donat la flexibilitat i llibertat en enfocar els resultats.

També vull expressar el meu agraïment a les persones que han sigut clau en el camí que duu a la defensa d'esta Tesi Doctoral. En primer lloc, gràcies al Prof. J.A. Jaques per haver-me infectat amb el *bitxo* de la investigació experimental, per tot el recolzament i comprensió i per haver confiat en mi. I també gràcies al Dr. A. Urbaneja, a la Dra. T. Pina, i a tots els companys del Departament d'Entomologia Aplicada de l'IVIA que contribuïren a que el *bitxo* es fera més i més gran. Així mateix, gràcies als Professors R. Albajes i J. Recasens per haver-me espentat i recolzat en el perfil investigador –tot i en contra de la meva voluntat en aquell moment. Finalment, no pot faltar el meu agraïment al Professor J.A. Gil-Delgado; gracias por invitarme a hacer algún *trabajillo* de campo cuando aún era una niña y mi vida daba vueltas de campana. Gracias por enseñarme a ser paciente y a observar con otros ojos; por tu amistad y por la naturalidad y la naturaleza. Gracias por siempre tener un punto de vista diferente, por crecer y también gracias por *no-crecer*, aprendí a poner límites.

Tinc agraïments per a tots els companys/es de GbqBt (CBP) que m'han acompanyat durant estos anys; sovint em vaig sentir aïllada amb els meus mutants i els *screenings* eterns. Sort de l'oportunitat per fer riures i els "*meriendamos"* sempre presents. Maria, Gloria, Cris, Rosi, Patri, Hanane, Agata, Salva, Maissa, Leila, Anabel, Àngel, Natàlia, Alejandro, Camila, Ximo, Sílvia, Melania, Eva, Carles, Sara, Yoli, Balta i Juan; A tots gràcies pel compromís, per les vostres contribucions a les reunions de línia i als *journal-club* i per la il·lusió per la ciència.
Balta, gracias por tus palabras de apoyo que me llegaron en momentos clave. Sara, a pesar de que te fuiste demasiado pronto me espabilaste con solo una tarde; aprecio mucho tus contribuciones y críticas que siempre son constructivas y bien equilibradas. Salva, què podria dir-te a tu que no hagem ja "parlat a crits"! amb tu tots els agraïments són descripcions binomials, gràcies per tots els bons moments- que són els que perduren, pel teu entusiasme i per totes les divertides pilleries.
Maissa i Yoli, amb qui he compartit el treball (a voltes desesperant) amb les Vip i la il·lusió i les discussions tant estimulants de la *Vip Bang theory* o *Escalereta*, juntament

amb Juan i amb Balta. Maissa, muchas gracias por el *contrabando* de proteínas, por siempre estar dispuesta a echarme una mano y por tu risa contagiosa. Yoli moltíssimes gràcies per introduir-me en les nocions essencials (tan importants!) per què poguera desenvolupar-me per mi mateixa; la forma d'organitzar-me el treball i les anotacions, de les bones pràctiques experimentals i les coses específiques del treball amb toxines de Bt. Gràcies pels teus savis consells i trucs, i per sempre trobar solucions.
Rosi, qué alegría haberte disfrutado y qué gratitud tengo de haber trabajado contigo. Tu bondad, tu profesionalidad, tu disponibilidad a ayudar, tu constante capacidad y ganas de aprender y de hacer que las coses parezcan fáciles me siguen despertando admiración.
Patri, para ti todos los agradecimientos se me quedan cortos, si más no me preocupa pues todo lo sabes ya. Gracias por haberme guiado, por el apoyo, por la paciencia, por encontrar tiempo para enseñarme técnicas nuevas, por hablarme de artículos que nunca tenía tiempo de leer, por compartir desinteresadamente tu experiencia y conocimiento, por creer en la ciencia colaborativa, por la curiosidad, por el respeto, por tu filantropía, por tu buen humor, por no esconder la niña que llevas (que todos llevamos) dentro, por ser tan divertida, por tu amistad. Mil gracias por todo, dentro y fuera del lab.
Agata, sin duda contar contigo es una de las recompensas más preciadas que me llevo de esta aventura. Me acuerdo muy bien del primer día que te conocí en las escalares del 6º piso, y no podía imaginar entonces la de cervezas que nos esperaban juntas. Tu amistad ha calado silenciosamente en mí y ya no hay remedio para esta *sitcom*. Dziękuje por todo. ¡Y gracias también por enseñarme a hacer *minipreps*-DIY!
¡Cristii, Es difícil pensar en ti y que no se me ocurran mil chorradas absurdas, divertidas y/o azucaradas que escribir! Muchas gracias por tu apoyo, por las risas y la ilusión constante, los días de piscina, los días de derribos, por tu amistad. Muchas gracias también por asistirme telemáticamente con los programas de alineamiento de secuencias, incluso cuando ya no estabas en el lab.
Leila muchas gracias por tu gentileza, por tu risa constante y por habernos emocionado juntas con el trabajo de aglutinación, que a mi pesar no he podido incluir en este documento. Gracias por tu disponibilidad, la flexibilidad y el compromiso. Muchas gracias a ti y a Maissa por haberme mostrado unos pedacitos de vuestra cultura, tan diferente y tan cercana a la vez.
María y Gloria, muchas gracias por las *charraetas*, por darme otro punto de vista de las Fallas y por siempre estar dispuestas ayudar.
Anabel y Natalia, a las dos gracias por ¡el sentido del humor ácido y picajoso en el justo punto de sal!...Anabel...pels teus acudits...quina pena que no tornares abans!
Vull agrair també a la resta de companys i companyes del 6é pis, per la companyonia i per les festes de Nadal. Gràcies també al personal de Secretaria Javi, Nuria i Paco i al personal de suport a la investigació Vicky, Fede i Jose Carlos.

Gràcies a tots els amics i família pel suport i per haver entès la meva absència dels últims mesos. Gràcies als nou-vinguts Susana, Mauri i Pablo i a les ja conegudes

Camila O. i Camila D. pels constants ànims. Especialment gràcies a la *família Bioloca*, per compartir les experiències d'este procés, per enriquir-me el dia a dia, per la germanor, pel suport mutu i continu fins i tot en la distància d'esta nova diàspora que és la dels Biòlegs. En especial gràcies a Cate, Regi, Oscar i Adri (*que rule l'amor!).*

Gràcies als meus pares, Irene i Luís, en especial per haver-me transmès el respecte i l'amor pel món rural i la natura, i l'interès per la ciència. Gràcies al meu germà Lluís Vicent, per la creativitat, per mostrar-me una forma diferent de vore el món que ens envolta i per fer que valore cada dia més la diversitat i el respecte.

Gràcies a Xavi per tot el suport, la paciència i el recolzament constant. Per decidir cada dia fer este camí junts.
A la Golfeta, que ha sigut companya fidel i pacient en les infinites hores de quietud.

Esta tesi ha sigut finançada amb una beca FPI (Grant Ref. BES-2010-039487) del Ministeri de Ciència i Innovació del Govern d'Espanya.

# INDEX OF CONTENTS

# INDEX OF FIGURES

# INDEX OF TABLES

# SUMMARIES

# RESUM

L'agricultura contemporània exigeix cada cop més un ús sostenible d'agroquímics per tal de reduir l'impacte ambiental i el risc per la salut del consumidor. Alguns bacteris entomopatògens produeixen proteïnes insecticides que s'acumulen en cossos d'inclusió o cristalls paraesporales (com ara les proteïnes Cry i Cyt), així com proteïnes insecticides que són secretades al medi de cultiu. Entre les últimes, hi ha les proteïnes Vip, que es divideixen en quatre famílies d'acord amb la seva identitat d'aminoàcids. Les proteïnes Vip1 i Vip2 actuen com toxines binàries i són tòxiques per a alguns coleòpters i hemípters. Per la família de les Vip4, que és l'última família de proteïnes Vip descoberta, encara no s'hi coneixen espècies susceptibles. Les proteïnes Vip3 no presenten homologia de seqüència amb cap altra família de proteïnes conegudes i són tòxiques per a una àmplia varietat d'espècies de lepidòpters. El mode d'acció de les Vip3 encara no està completament dilucidat, però s'assumeix una mecanisme similar al de les proteïnes Cry en termes generals (activació proteolítica, unió a la membrana epitelial en forma de raspall de l'intestí mitjà, i formació de porus). Les proteïnes Vip3A no comparteixen els mateixos llocs d'unió amb les proteïnes Cry, per la qual cosa són bones candidates per co-expressar-se amb proteïnes Cry en plantes transgèniques (cultius-Bt) amb la finalitat de prevenir o retardar l'aparició de fenòmens de resistència en insectes susceptibles, i per ampliar l'espectre insecticida. Les proteïnes Vip3A són, per tant, una eina important per a la protecció de cultius contra plagues d'erugues en la protecció integrada de cultius (PIC).

Aquesta tesi té com a objectiu principal caracteritzar més profundament la funció i l'estructura de les proteïnes Vip3A. Primerament es va avaluar la toxicitat de 5 proteïnes Vip3A diferents contra 8 espècies d'erugues plaga al capítol 1; les protoxines de Vip3Aa, Vip3Ab, Vip3Ad, Vip3Ae i Vip3Af i les seves corresponents formes activades amb tripsina comercial es van assajar per determinar la seva toxicitat contra *Agrotis ipsilon*, *Helicoverpa armigera*, *Mamestra brassicae*, *Spodoptera exigua*, *Spodoptera frugiperda*, *Spodoptera littoralis*, *Ostrinia nubilalis* i *Lobesia botrana.* No es van trobar diferències de toxicitat importants entre les formes de protoxina i toxina activada. Les proteïnes Vip3Aa, Vip3Ae i Vip3Af mostraren en general una bona activitat insecticida contra totes les espècies d'insectes amb l'excepció d' *O. nubilalis*. De fet, *O. nubilalis* es va mostrar tolerant a l'acció de les Vip3A i només la Vip3Af va causar una mortalitat marginal. La proteïna Vip3Ad no va resultar tòxica per a cap de les espècies assajades, mentre que la Vip3Af va mostrar un ventall d'activitat més ampli.

L'estructura 3D de les proteïnes Vip3A no és coneguda; per esta raó, els següents passos d'esta tesis es centraren en aconseguir un millor coneixement de l'estructura de les proteïnes Vip3A i del seu plegament. Les proteïnes Vip3 s'expressen en forma de precursor el qual necessita un pas previ d'activació mitjançant les proteases del tracte digestiu de l'insecte. Al segon capítol, l'estabilitat d'una Vip3Aa front l'acció de les proteases es va investigar en presència de SDS. La protoxina de la Vip3Aa16 (que

té un pes de 89 kDa) es va tractar amb tripsina comercial i amb extracte de proteases de d'intestí mitjà d' *A. ipsilon* a concentracions elevades. Quan les reaccions no van ser neutralitzades adientment, els resultats de l'anàlisi de l'electroforesi en SDS-PAGE equívocament sugerien que la protoxina es processa per complet, tot i que la mostra digerida encara retenia íntegrament la toxicitat contra *A. ipsilon*. No obstant això, quan la reacció proteolítica es va aturar de manera eficient, es va fer patent que la protoxina només s'escindeix en un lloc de tall primari, independentment de la quantitat de tripsina o d'extracte de l'intestí mitjà de l'insecte utilitzat. Els dos pèptids de 66 kDa i de 19 kDa generats com a conseqüència de l'activació co-elueixen després de la cromatografia de filtració en gel, indicant que ambdós romanen units després de l'escissió. Es va confirmar, per tant, que el fragment de 66 kDa és extremadament resistent a l'acció de les proteases i que la degradació observada a l'electroforesi quan la reacció enzimàtica de les proteases no es correctament neutralitzada és producte de la interacció de l'SDS amb la Vip3Aa. Estos resultats es varen reproduir en el capítol 3er amb la proteïna Vip3Af1 i la espècie plaga *S. frugiperda*. La degradació aparent de la toxina es va observar quan la Vip3Af es va tractar amb la major concentració de peptidases. La Vip3Af aparentment degradada també fou tòxica contra les larves nounades de *S. frugiperda*. Encara més, quan la Vip3Af que havia estat sotmesa al tractament amb tripsina durant 72h es va tractar amb quantitats addicionals de tripsina, la degradació aparent del pèptid de 62 kDa no es vaobservar més. En conclusió, es proposa que l'activació proteolítica de les proteïnes Vip3A es produeix de manera esglaonada, per mitjà de la qual la protoxina es divideix en dos pèptids principals, seguit d'un canvi subtil de plegament del fragment de 62-66 kDa amb probablement implicat en l'acció insecticida.

En el 4t capítol, la tècnica de l'escaneig d'alanina es va realitzar en 558 d'un total de 788 aminoàcids que formen la proteïna Vip3Af1. L'escaneig d'alanina és una tècnica molt utilitzada per identificar i localitzar posicions crucials o epítops en la seqüència d'una proteïna i permet aprofundir en la relació estructura-funció de les proteïnes. De les 558 substitucions analitzades, 19 comprometeren l'expressió de la proteïna i 11 disminuïren considerablement la toxicitat contra *S. frugiperda*. Les substitucions que van reduir l'activitat insecticida s'agrupen principalment en dues regions de la seqüència (entre els aminoàcids 167-272 i entre els aminoàcids 689-741). La majoria de les substitucions que afectaren l'activitat front *S. frugiperda* ho feren de manera similar contra *A. segetum*. La caracterització de la sensibilitat front a proteases de les 11 proteïnes mutants seleccionades per disminuir la toxicitat va revelar 6 patrons de proteòlisi diferents, identificats mitjançant electroforesi en SDS-PAGE. L'estudi de la fluorescència intrínseca de tots els mutants seleccionats només va revelar canvis lleus en el pic d'emissió, indicant que probablement les mutacions provoquen només canvis menors en l'estructura terciària. L'estructura tridimensional de la Vip3Af1 es va predir *in silico* per primera vegada.

Finalment, en el capítol 5è, 12 mutants diferents es van generar mitjançant mutagènesi dirigida en diferents posicions al llarg de la seqüència de la proteïna Vip3Af1. La mutagènesi dirigida és una aproximació comú per a la millora la funcionalitat de les proteïnes, així com per aprofundir en els coneixement de les

proteïnes a nivell molecular, especialment quan l'estructura de la proteïna és desconeguda. Deu dels 12 mutants generats es varen expressar amb èxit i tots ells foren funcionalment actius, la qual cosa subratlla l'alta resilència de la seqüència de la Vip3Af1. No va ser possible millorar significativament la potència insecticida contra *S. frugiperda* en cap de les mutacions. Les mutacions en la posició 689 (G689S, G689E i N682K-G689S), així com les mutacions E483H i W552H van donar patrons proteolítics diferents al perfil natiu de la Vip3Af (tipus salvatge). Els espectres d'emissió de fluorescència intrínseca no suggereixen un canvi en el plegament significatiu. En este capítol es discuteixen les possibles implicacions que les mutacions tenen sobre les interaccions intramoleculars i s'infereix en la conformació de la proteïna.

Els resultats obtinguts en esta tesi aporten una millor comprensió de l'estructura i funció de les proteïnes Vip3A. Esta informació és útil per a la presa de decisions quan s'empra *B. thuringiensis* o les seves proteïnes insecticides com un recurs fitosanitari en els programes de control integrat de plagues i en estratègies de maneig de la resistència .

## SUMMARY

Modern agriculture demands for more sustainable agrochemicals to reduce the environmental and health impact. Some entomopathogenic bacteria produce insecticidal proteins which accumulate in inclusion bodies or parasporal crystals (such as the Cry and Cyt proteins), as well as insecticidal proteins which are secreted to the culture media. Among the latter, there are the Vip proteins, which are divided into four families according to their amino acid identity. The Vip1 and Vip2 proteins act as binary toxins and are toxic to some Coleoptera and Hemiptera. For the most recently reported Vip4 family, no target insects have been found as yet. Vip3 have no sequence similarity to any other proteins families known and are toxic to a wide variety of Lepidoptera. Its mode of action is yet not completely elucidated but a general mode of action similar to that of the Cry proteins (proteolytic activation, binding to the brush border membrane of the midgut epithelium, and pore formation) is assumed. Vip3A proteins do not share binding sites with Cry proteins, which makes them good candidates to be combined with Cry proteins in transgenic plants (Bt-crops) to prevent or delay insect resistance, and to broaden the insecticidal spectrum. Vip3A are an important tool for crop protection against caterpillar pests in integrated pest management (IPM) strategies.

This thesis aimed to deeper characterise the function and structure of the Vip3A proteins. In chapter 1, the toxicity of 5 different Vip3A proteins against 8 different caterpillar pests was first assessed: Vip3Aa, Vip3Ab, Vip3Ad, Vip3Ae and Vip3Af and their corresponding trypsin-activated toxins were tested for their toxicity against *Agrotis ipsilon*, *Helicoverpa armigera*, *Mamestra brassicae*, *Spodoptera exigua*, *Spodoptera frugiperda*, *Spodoptera littoralis*, *Ostrinia nubilalis* and *Lobesia botrana.* No major differences were found when comparing protoxins *vs*. trypsin-activated toxins. Vip3Aa, Vip3Ae and Vip3Af displayed overall good insecticidal activity against all insect species with the exception of *O. nubilalis*, which was found to be tolerant to all Vip3A tested and only marginal mortality was caused by the Vip3Af. Vip3Ad protein was not toxic to any of the tested species whereas Vip3Af showed the broadest range of activity.

The·3D-structure of the Vip3A proteins are not known, therefore, consecutives steps were performed to achieve a better insight on the Vip3Aprotein folding and structure. Vip3 proteins are expressed as a precursor that is to be activated by the insect gut proteases. In the 2nd chapter, stability of the Vip3Aa against proteases was investigated in the presence of SDS. Vip3Aa16 protoxin (of 89 kDa) was treated at high concentrations of trypsin and *Agrotis ipsilon* midgut juice. When the reactions were not properly neutralized, the results of SDS-PAGE analysis (as well as those with *Agrotis ipsilon* midgut juice) equivocally indicated that the protoxin could be completely processed, although it retained full toxicity against *A. ipsilon*. However, when the proteolytic reaction was efficiently stopped, there was revealed that the protoxin was only cleaved at a primary cleavage site, regardless the amount of trypsin

used. The 66 kDa and the 19 kDa peptides generated by the proteases co-eluted after gel filtration chromatography, indicating that they remain together after cleavage. The 66 kDa fragment was found to be extremely resistant to proteases and that the misleading degradation observed in the SDS-PAGE was a consequence of the inefficient neutralisation of the enzymatic reaction and the interaction of the SDS molecules with the Vip3A protein. These results were reproduced in the 3d chapter with the different Vip3Af protein and the different pest species *S. frugiperda*. The misleading degradation previously reported for the closely related Vip3Aa16 was also observed in the Vip3Af at the highest concentration of peptidases used. The apparently degraded protein was active against *S. frugiperda* neonates. When the trypsin-activated toxin was further treated with trypsin, the misleading over-processing of the 62 kDa core was no longer observed in the SDS-PAGE. The proteolytic activation of the Vip3A is proposed to be stepwise fashion, which first step involves the formation of a toxin core of 62-66 kDa fragment that undergoes a subtle folding change likely involved in the insecticidal mechanism.

In the 4$^{th}$ chapter, the alanine scanning technique was performed on 558 out of the total of 788 amino acids of the Vip3Af1 protein. Alanine scanning is a successful technique for mapping crucial positions or epitopes in a protein and allows a greater insight into protein structure-function relationships. From the 558 residue substitutions, 19 impaired protein expression and 11 compromised the insecticidal activity against *S. frugiperda*. Substitutions that reduced insecticidal activity mainly clustered in two regions of the protein sequence (amino acids 167-272 and amino acids 689-741). Most of the substitutions that impaired the activity to *S. frugiperda* behave likewise to *Agrotis segetum*, with few exceptions. The characterisation of the sensitivity to proteases of these 11 mutant proteins displaying decreased insecticidal activity revealed 6 different band patterns as evaluated by SDS-PAGE. The study of the intrinsic fluorescence of all selected mutants revealed only slight shifts in the emission peak, likely indicating only minor changes in the tertiary structure. An *in silico* modelled 3D structure of Vip3Af1 is proposed for the first time.

Finally, in the 5$^{th}$ chapter, 12 different mutants were generated by site-directed mutagenesis all along the Vip3Af1 protein sequence. Site-directed mutagenesis is a common approach to function improvement as well as to deepen in the protein knowledge, especially when the protein structure is unknown. Ten of these mutants were successfully expressed and were functionally active, highlighting the high resilience of the Vip3Af1 sequence. None of the Vip3Af mutations caused an improvement of the insecticidal potency against *S. frugiperda*. Mutations in position 689 (G689S, G689E and N682K-G689S), as well as mutations E483H and W552H gave proteolytic patterns different to the native profile of the wild type. The intrinsic emission fluorescence spectra did not show a significant folding change. Implications on the intramolecular interactions and on the conformation of the protein are further discussed.

The results obtained in this Thesis give to a better understanding of the protein structure and function of Vip3A proteins, which will be helpful for the decision making

when and how using *B. thuringiensis* or its insecticidal proteins as a phytosanitary resource in pest management programs and resistance management strategies.

# INTRODUCTION

Part of this section is included in:

Chakroun M, Banyuls N, Bel Y, Escriche B, Ferré J. Bacterial Vegetative Insecticidal Proteins (Vip) from Entomopathogenic Bacteria (2016). Microbiol Mol Biol Rev.;80: 329–350. doi:10.1128/MMBR.00060-15

## GENERAL ASPECTS OF *Bacillus thuringiensis*

*Bacillus thuingiensis* (Berliner) is an endospore-forming Gram-positive bacterium that is widely used as microbial control agent of insect pests. It was firstly found in 1902 by the japanesse biologist Shigetane Ishiwatari in dead insects of the silkworm *Bombyx mori* (Lepidoptera: Bombycidae) being responsible of an unknown disease affecting the silk industry. The bacterium was named by then as *Bacillus sotto* in reference to the aspect of the infected larvae, but it was not until 10 years later that Ernst Berliner properly characterized the bacterium from infected insects of the Mediterranean flour moth *Ephestia kuehniella* (Lepidoptera: Pyralidae) collected from the province of Thuringe, in Germany, and in reference to the origin of the isolate he named it *Bacillus thuringiensis.* In the late 20's, the applicability of the microorganism was used for the first time and during the last 50 years for the biological control of *Ostrinia nubilalis* (Lepidoptera: Crambidae) (Melo et al., 2016; Sanchis, 2011).

*Bacillus thuringiensis* (Bt) is a saprophytic, cosmopolitan and ubiquitous microorganism belonging to the *Bacillus cereus* group. Bt-spores are found in a variety of environmental compartments such as soil, dead and living insects, stored grains, phylloplane and in stagnant waters surfaces associated to the presence of mosquitoes cadavers. Whereas the persistence and growing of Bt in soils and leaves surfaces is controversial, it does not need insects for multiplication and the reported cases of epizootia are rare. Thus, Bt is best considered as an opportunist pathogen (de Maagd et al., 2001; Dubois et al., 2012; Martin, 1994).

## *Bacillus thuringiensis* APPLICATIONS

Although the Invertebrate Pathology is a recent science of the mid-twentieth Century, the first quotes on insect pathology date back to 2500 BC in China or in 350 BC in Greece, with reference to natural preparations for counteract silkworm and honeybee diseases. Since then, an enormous number of bacteria, virus, fungus, nematodes and insects have been considered useful for the protection of goods. The use of microbiological control agents (MCA) begun in the 19$^{th}$ Century with the investigation of *Beauveria bassiana*, although it was not a widespread practice until the discovery of *Bacillus thuringiensis*. Since then, several bacterial species have been identified including *Bacillus thuringiensis* (Bt) sub-species, *Lysinibacillus sphaericus, Paenibacillus* spp. and *Serratia entomophila* (Lacey et al., 2015, 2001; Sanchis, 2011).

*Bacillus thuringiensis* produce several proteins which are active against a variety of invertebrate organisms. The δ-endotoxins (Cry and Cyt proteins) are produced as parasporal crystalline inclusions (Fig. I-1) when the bacterial growth reach the stationary phase, whereas Vip proteins are soluble and secreted to the surroundings during the exponential growth phase. Other virulent factors that account for the toxicity are α-exotoxins, β-exotoxins, hemolysins, enterotoxins, chitinases and

phospholipases which contribute to the necrotrophic biology. Additionally, the spores have shown a synergistic effect of the insecticidal activity (de Maagd et al., 2001).

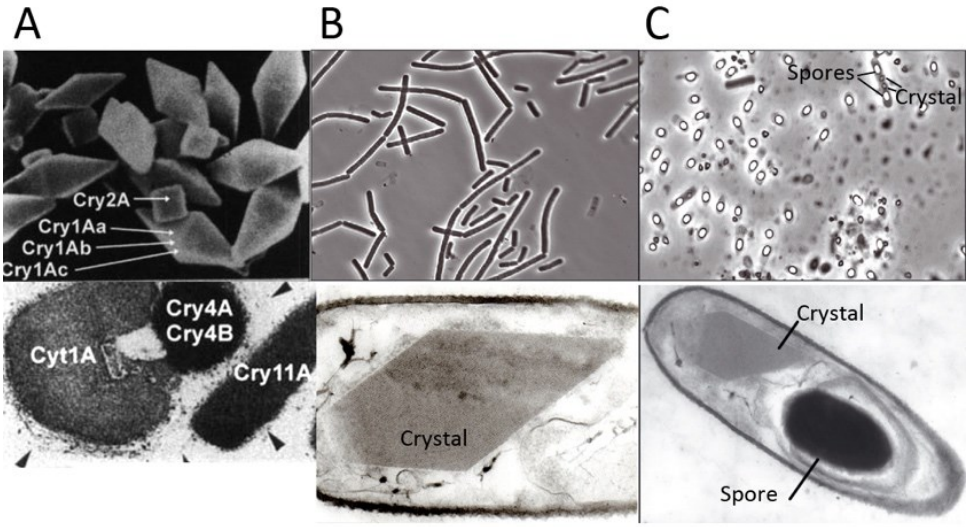


*Fig. I- 1. Sporulated culture and parsporal bodies of* Bacillus thuringiensis.
*A. Parasporal body protein inclusions containing Cry proteins (in* Federici, 1998). *B and C (upper images) phase photomicrographs of vegetative cells (left) and spores (right), 1000X and (lower images) transmission electron micrographs of longitudinal sections of* Bacillus thuringiensis (*in Sanchis, 2011)* .

The different proteins of Bt are active against different orders of insects such as Coleoptera, Lepidoptera, Hemiptera, Diptera (mosquitoes and black flies), Hymenoptera, Mallophaga and Blattodea, but also against some nematodes, acari (mites and ticks), snails or the protozoan causing human trichomaniasis. Some Cry toxins have also been reported to have bactericidal and lectin-like activity (Lacey et al., 2015; Melo et al., 2016; Palma et al., 2014). However, Bt is not restricted solely to its use as entomopathogen. It has also been reported to promote plant growth (PGPR) and it has gained attention in the medical area due to the strong activity against human-cancer cell lines of some parasporins. Other interesting industrial applications include bioremediation of heavy metals, biosynthesis of silver nanoparticles or the production of polyhydroxyalkanoate biopolymer (Jouzani et al., 2017; Melo et al., 2016; Palma et al., 2014)

The use of entomopathogens can be done by the 3 strategies of classical, conservative and augmentative biological control, although the most common way for pest control is the augmentative-inundative application of MCA. The success of the use of Bt as MCA is largely due to the practical similarity to conventional pesticides: Bt-based products are relatively cheap and easy to formulate, have long shelf life and can be applied using conventional application equipment. Furthermore, the wide range of pests covered and the high selectivity, as well as the safety and low environmental impact makes Bt a desirable tool for crop protection. In addition, the

use of Bt is compatible with other strategies for crop management such as agricultural practices, biological control using natural enemies and chemical treatments. Bt-formulations are by far the MCA most used at a global scale (Fig. I-2) and account for almost 98% of the bacterial MCA (Lacey et al., 2015).

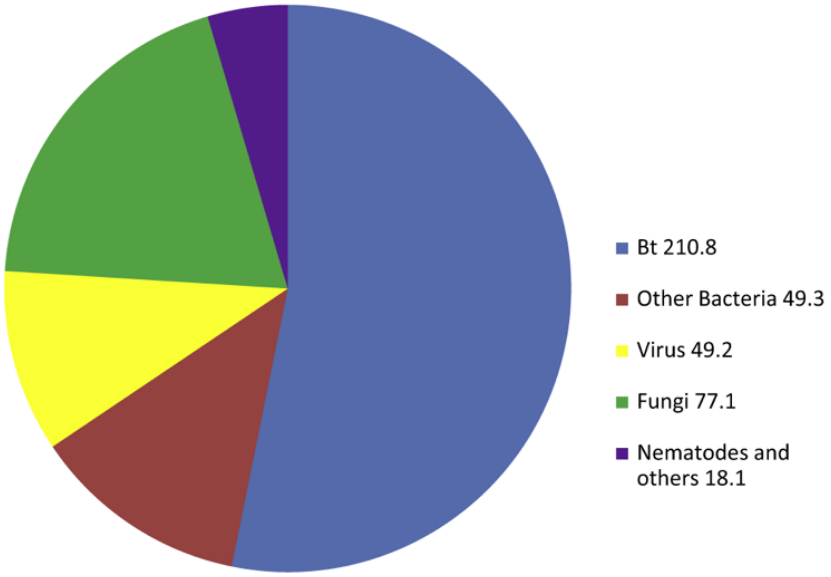


***Fig. I- 2. Estimated world biopesticide sales by type in 2010 (millions of $US).***
*CPL Business Consultants (2010). The 2010 Worldwide Biopesticides Market Summary, vol. 1. CAB International Centre, Wallingford in Lacey et al., (2015).*

The first Bt biopesticides used commercially were Sporéine, Thuricide and Bactospéine throughout the 1930s and 1960s. After the WorldWar II there was an increase in the production and usage of broad spectrum synthetic pesticides as the agriculture systems became more intensified (Alexandratos and Bruinsma, 2012; Sanchis, 2011). As a consequence of the overused of chemical pesticides, some undesirable effects such as environment contamination, health problems for consumers and operators and the loss of effectiveness due to insect resistance prompted the urgency to develop a more sustainable agriculture. Since the 90's, there is a more rationale use of synthetic pesticides in developed countries but still up to 3.8 million tonnes of pesticides are spread annually whereas MCA account only for 1-2% of the pesticides global market (De et al., 2014; EPA, 2017; Lacey et al., 2015; Tilman et al., 2001). From the total amount of pesticides used worldwide, the large part accounts for herbicides followed by insecticides and fungicides, though this distribution varies within different regions in the planet (Fig. I-3) (Carvalho, 2006; De et al., 2014; EPA, 2017; EUROSTATS).

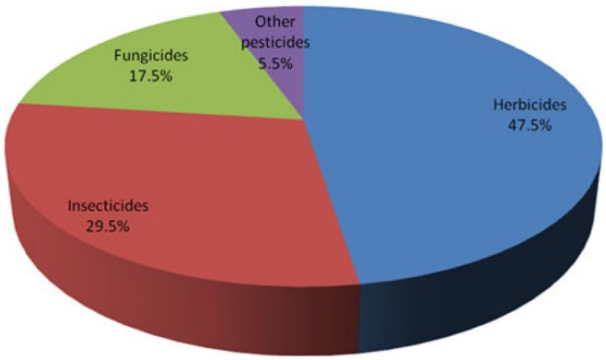


*Fig. I- 3. Worldwide consumption of pesticide in De et al., (2014).*

Efforts on discovering new MCA or their applications are made from the last 20 years in order to face a more sustainable and safe agriculture. Bt products were typically formulated as water dispersible granules or wettable powders whereas nowadays, low impact formulas based on micro- and nano-formulations are being implemented to microbial sprays. Additionally, toxin microencapsulation in inert cells of *Pseudomonas fluorescens* have also been used (De et al., 2014; Hernández-Rodríguez et al., 2013; Jouzani et al., 2017; Mahadeva Swamy and Asokan, 2013; Panetta, 1993). Bt insecticidal proteins are also being expressed in genetically modified crops (Bt-crops). Among the biotechnology-based improved crops, Bt-crops are the most largely cultivated, together with glyphosate tolerant crops (ISAA; James, 2015; Moar et al., 2017). Other type of genetically modified crops (GMO) conferring valuable properties such as drought resistance stress or diverse viral disease resistance are already available. Furthermore, attempts to apply the utmost cutting edge technologies of gene silencing and genome editing such the breakthrough CRISPR/CAS technology to biotech-crops are lately being reported (Kupferschmidt, 2013; Lacey et al., 2015; Li et al., 2012; Shan et al., 2013; Wang et al., 2014).

The use of entomopathogens fits well into integrated pest management (IPM) systems. The practical value of MCA do not rely only on the efficacy and the production cost, but on additional advantages as the low impact to the environment, the unnecessary re-entry and pre-harvest intervals after applications, the safety to human consumers and the harmless effect to non-target organisms, which allow the preservation of natural enemies and a greater biodiversity in the agrosystem.

## INSECTICIDAL PROTEINS

Entomopathogenic bacteria have enormous potential for insect control and they can provide us with an arsenal of insecticidal compounds (de Maagd et al., 2003). By far, the most widely used and best known insecticidal proteins are the Cry proteins from *Bacillus thuringiensis.* These proteins accumulate in the parasporal crystal at the time of sporulation and are released into the culture medium only after the cell wall disintegrates. Formulations based on *B. thuringiensis* crystals and spores have been successfully used to control a wide range of lepidopteran pests, as well as some coleopteran, blackfly, and mosquito species (Sanahuja et al., 2011; Sanchis, 2011). The insecticidal potency of some Cry proteins is such that their respective *cry* genes have been transferred to plants, conferring total or very high protection against the most damaging pests (Estruch et al., 1997; James, 2014; Shelton, 2012).

Despite the wide success of Cry proteins in insect control, some important pests were found to be highly tolerant to Cry proteins, such as *Agrotis ipsilon* (Lepidoptera: Noctuidae) and *Diabrotica* spp. (Coleoptera: Chrysomelidae), which cause significant damage to corn seedlings. Screening programs that aimed to evaluate insecticidal active components in culture supernatants from *Bacillus* isolates identified a culture supernatant from *Bacillus cereus* AB78, which resulted in 100% mortality of *Diabrotica virgifera virgifera* and *Diabrotica longicornis barberi* larvae (Warren, 1997). The active component in this supernatant was found to be proteinaceous. Anion exchange chromatography followed by SDS-PAGE showed that the insecticidal activity was due to two different proteins of 80 and 45 kDa, which were named Vip1Aa and Vip2Aa, respectively (from Vegetative Insecticidal Protein). Sequences with homology to the respective *vip1Aa* and *vip2Aa* genes were found in about 12% of the 463 *B. thuringiensis* strains tested (Warren, 1997). In the same study, the vegetative culture supernatant from *B. thuringiensis* strain AB88 contained an 88.5 kDa protein that was highly toxic to *A. ipsilon* and other lepidopteran larvae, which was named Vip3Aa. More recently, Vip4Aa was reported by direct sequence submission to the NCBI GenBank (accession number AEB52299). *In silico* analysis predicted a molecular mass of approximately 108 kDa for Vip4Aa (Palma et al., 2014). Alternative names for Vip proteins were also given before the standardization by the Bt Toxin Nomenclature Committee (Crickmore et al., 2014) (Fig. I-4), such as Insecticidal Secreted Proteins (Isp), with the classes Isp1, Isp2, and Isp3 (NCBI GenBank accession numbers AJ871923, AJ871924, AJ872070), which are homologous to Vip1, Vip2, and Vip3, respectively. It should be mentioned that another secreted insecticidal protein from *B. thuringiensis*, named Sip, has been reported. This protein shares no homology to the Vip proteins and should not be mistaken with one of them (Donovan et al., 2006).

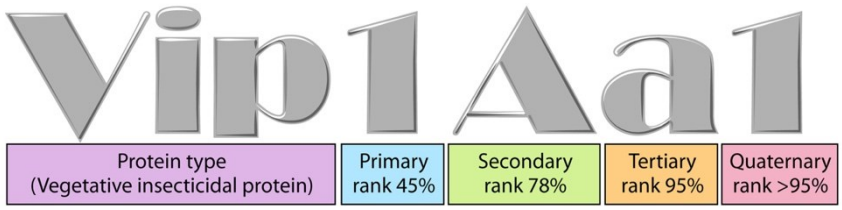


***Fig. I- 4. Nomenclature system for Vip proteins.***
*The system consists of four ranks based on the amino acid sequence identity* (Crickmore et al., 2014). *The primary, secondary, and tertiary ranks distinguish proteins with less than approximately 45, 78, and 95% sequence identity, respectively. The quaternary rank distinguishes proteins sharing >95% sequence identity, which can be considered products of "allelic" forms of the same gene, but can also have the same sequence which originated from different isolates.*

To date, 15 Vip1, 20 Vip2, 105 Vip3, and one Vip4 proteins have been reported (Crickmore et al., 2014, accessed on May 2017). Fig. I-5 shows the dendrogram with the hierarchy of the Vip proteins based on their degree of amino acid identity. Vip1 and Vip2 act as binary toxins for some Coleoptera and Hemiptera (Feitelson et al., 2003; Sattar and Maiti, 2011; Schnepf et al., 2003; Warren, 1997; Yu et al., 2011a), and Vip3 are active against a wide range of species of Lepidoptera (Estruch et al., 1996; Ruiz de Escudero et al., 2014). No target insects have been found as yet for Vip4. In contrast to the Cry protein family, Vip1, Vip2, and Vip3, and Vip4 share almost no sequence homology among each other, with Vip1 and Vip4 being the most similar (34% amino acid identity).

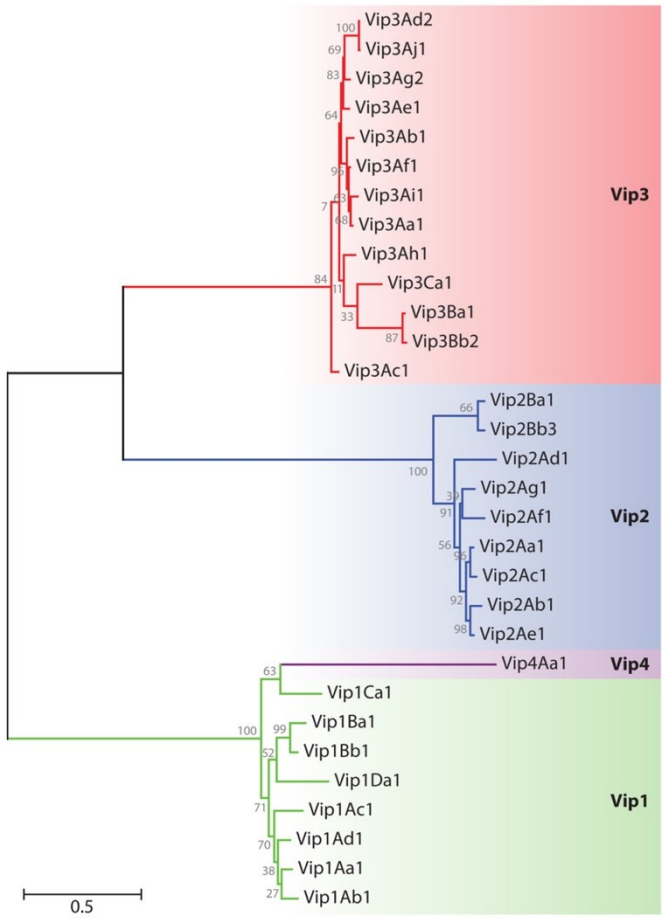


***Fig. I- 5. Dendogram showing the relationships among Vip proteins based on their degree of amino acid identity.***
*Amino acid sequences were aligned using the Clustal X interface* (Thompson et al., 1997)**.** *The evolutionary distance was calculated by the maximum likelihood analysis and the tree was constructed using the MEGA5 program* (Tamura et al., 2011). *Accession numbers of the protein sequences used in this analysis: Vip1Aa1 ([Seq. ID no.] 5 in* Warren et al., 1998)*, Vip1Ab1 (Seq. ID no. 21 in* Warren et al., 1998)*, Vip1Ac1 (accession number HM439098), Vip1Ad1 (accession number JQ855505), Vip1Ba1 (accession number AAR40886), Vip1Bb1 (accession number AAR40282), Vip1Ca1 (accession number AAO86514), and Vip1Da1 (accession number CAI40767), Vip2Aa1 (RCSB Protein Data Bank accession number 1QS1A), Vip2Ab1 (Seq. ID no. 20 in* Warren et al., 1998)*, Vip2Ac1 (accession number AAO86513), Vip2Ad1 (accession number CAI40768), Vip2Ae1 (accession number EF442245), Vip2Af1 (accession number ACH42759), Vip2Ag1 (accession number JQ855506), Vip2Ba1 (accession number AAR40887), Vip2Bb3 (accession number KJ868170), Vip3Aa1 (accession number AAC37036), Vip3Ab1 (accession number AAR40284), Vip3Ac1 (named PS49C; Seq. ID no. 7 in Narva and Merlo patent application US20040128716), Vip3Ad2 (accession number CAI43276), Vip3Ae1 (accession number CAI43277), Vip3Af1 (accession number CAI43275), Vip3Ag2 (accession number FJ556803), Vip3Ah1 (accession number DQ832323) Vip3Ai1 (accession number KC156693), Vip3Aj1 (accession number KF826717), Vip3Ba1 (accession number AAV70653), Vip3Bb2 (accession number ABO30520), Vip3Ca1 (accession number ADZ46178), Vip4Aa1 (accession number HM044666).*

## The binary Vip1/Vip2 toxin

In addition to *B. cereus* and *B. thuringiensis*, *vip1* and *vip2* genes have also been found in other bacterial species, such as *Lysinibacillus sphaericus* (formerly known as *Bacillus sphaericus*) and *Brevibacillus laterosporus* (Ruiu, 2013; Schnepf et al., 2003). Studies on the distribution of *vip1* and *vip2* genes have shown that they are found in around 10% of *B. thuringiensis* strains (Hernández-Rodríguez et al., 2009; Sattar et al., 2008; P.R. Shingote et al., 2013; Warren, 1997; Yu et al., 2011b). These two genes have been found in the same operon, and with two different open reading frames separated by an intergenic spacer of 4 to 16 bp within a 4 to 5 kb genomic sequence (Bi et al., 2015; Shi et al., 2007; Warren, 1997), and in a megaplasmid (around 328 kb length) in *B. thuringiensis* strain IS5056 (Murawska et al., 2013). At the time of writing this thesis the "*Bacillus thuringiensis* Toxin Nomenclature" data base lists the following *vip1* and *vip2* genes: 3 *vip1Aa*, 1 *vip1Ab*, 1 *vip1Ac*, 1 *vip1Ad*, 2 *vip1Ba,* 3 *vip1Bb*, 1 *vip1Bc*, 2 *vip1Ca*, and 1 *vip1Da*, and 3 *vip2Aa*, 1 *vip2Ab*, 2 *vip2Ac*, 1 *vip2Ad*, 3 *vip2Ae*, 2 *vip2Af*, 2 *vip2Ag*, 2 *vip2Ba,* and 4 *vip2Bb* (Crickmore et al., 2014).
Vip1 and Vip2 proteins are expressed concomitantly, and translation from the same transcript appears to be essential to ensure high levels of both proteins. They are produced during the vegetative growth phase of *B. thurigiensis* and their levels remain high until after the sporulation stage. The gene transcripts are detected at the start of the logarithmic phase, reaching their maximum expression in the stationary phase, and remaining at high levels in the sporulation stage (Bi et al., 2015; Estruch et al., 1996; Shi et al., 2007, 2004).

### Protein Structure and Function

Classical bacterial A-B toxins, such as the cholera toxin, interact with cells as a complex composed of one or several polypeptides associated in solution (in the case of the cholera toxin, the A component is surrounded by 5 B-polypeptides). Alternatively, Gram positive bacilli from the genera *Clostridium* and *Bacillus* produce proteins (A+B toxins) with a synergistic binary mode of action in which the two proteins do not form an aggregate before binding to the cell surface (Barth et al., 2004). The Vip1/Vip2 toxin is an example of an A+B toxin related to mammalian toxins from *Clostridium* spp. (*C. botulinum*, *C. difficile*, *C. perfringens*, and *C. spiroforme*) and *B. anthracis*. Sequence homology with the mammalian toxins, the lack of toxicity of the individual proteins, translational frameshift mutation experiments of the *vip1* gene, along with toxicity bioassays against susceptible insects confirmed the binary mode of action of these proteins (Warren, 1997).
Sequence analysis of the Vip1Aa and Vip2Aa proteins revealed the presence of an N-terminal signal peptide of about 30 and 50 amino acids, respectively (Shi et al., 2007, 2004; Warren et al., 1998). The signal peptide was shown to be cleaved during secretion, rendering mature proteins of approximately 82 kDa (for Vip1Aa) and 45 kDa (for Vip2Aa) (Bi et al., 2015; Warren, 1997). Sequence alignment revealed that the N-terminus of Vip1 is highly conserved (75-91% identity) (Fig. I-6). In contrast, the

C-terminus of Vip1 is much less conserved (23-35% identity) (Shi et al., 2007, 2004; Warren, 1997).

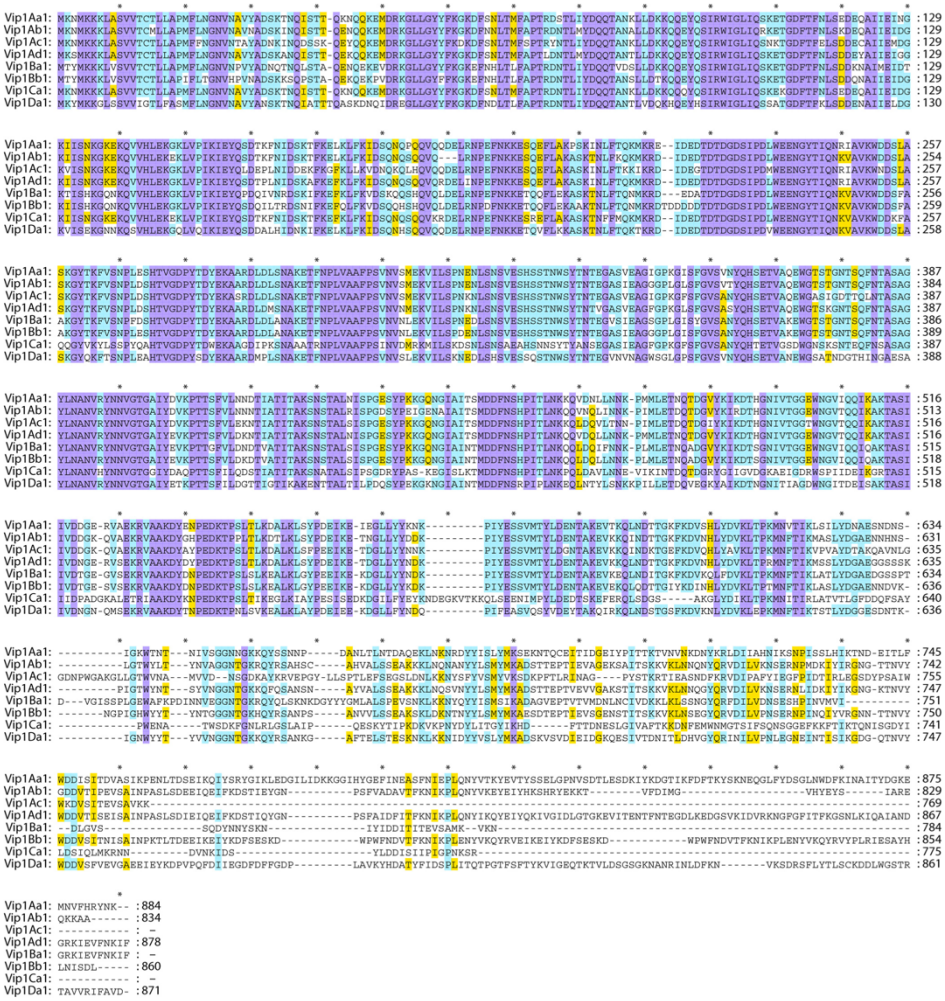

***Fig. I- 6. Multiple-sequence alignment of the Vip1 proteins.***

*Sequence identity is indicated by shading, where violet is 100% sequence identity, pale blue is 80–100%, yellow is 60–80%, and white is < 60%. Intervals of 10 amino acids are marked with "*". "SP": Signal Peptide. Proteins used in this analysis are as follows: Vip1Aa1 (Seq. ID no. 5 in* Warren et al., 1998*), Vip1Ab1 (Seq. ID no. 21 in* Warren et al., 1998*), Vip1Ac1 (accession number HM439098), Vip1Ad1 (accession number JQ855505), Vip1Ba1 (accession number AAR40886), Vip1Bb1 (accession number AAR40282), Vip1Ca1 (accession number AAO86514), and Vip1Da1 (accession number CAI40767).*

Vip1 has moderate sequence identity with the binding component C2-II of the C2 *C. botulinum* toxin (29%), and the Ib of the iota toxin from *C. perfringens* (31%). It also shares 33 to 38% identity with the *C. spiroforme* toxin and the *B. anthracis* protective antigen, and with the toxin B of *C. difficile* at amino acids 142-569 (Leuber et al., 2006; Shi et al., 2007, 2004). Vip2 shares more than 30% sequence identity with the

clostridial Rho-ADP-ribosylating exotoxin C3 (Han et al., 1999). These similarities suggested that the Vip1 protein is the "B" component, and that the Vip2 protein is the "A" component of the binary toxin (Barth et al., 2004). Thus, Vip1 would act as the binding and translocation component (channel forming protein) (Blaustein et al., 1989; Knapp et al., 2002; Schmid et al., 1994), and Vip2 would enter the cell and exert its toxic effect.

Vip2 is an NAD-dependent actin-ADP-ribosylating toxin (Jucovic et al., 2008) which has two distinctive domains: the N-terminal domain (comprised of the amino acids from 60-265) and the C-terminal domain (comprised of the amino acids from 266-461), which is the NAD-binding domain (Fig. I-7) (Han et al., 1999).

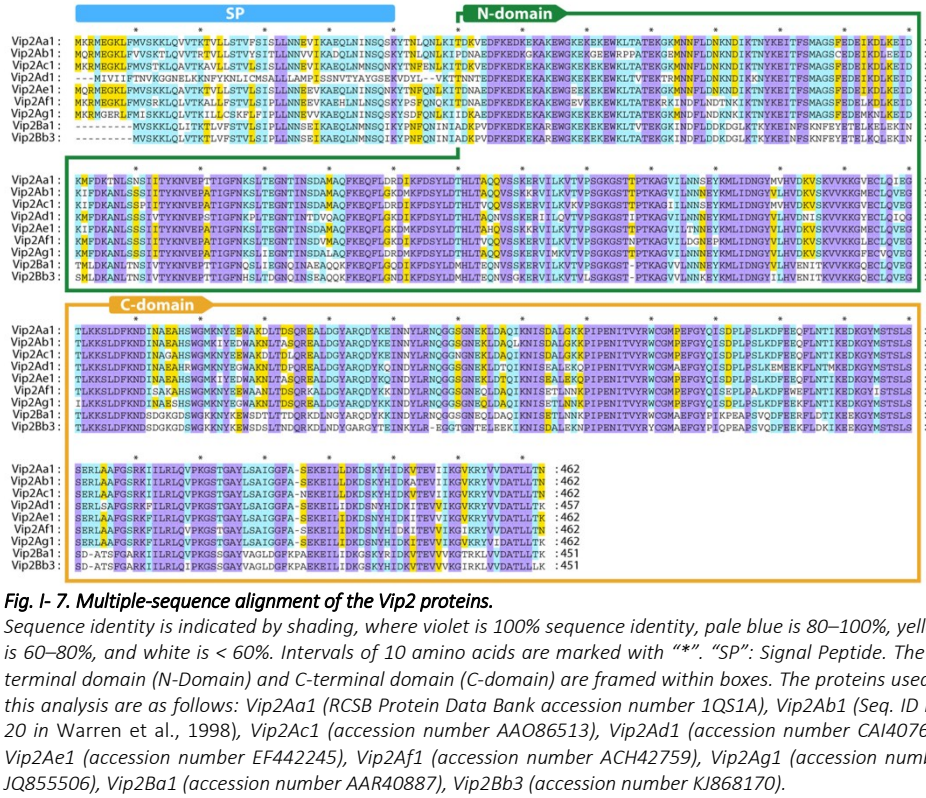


*Fig. I- 7. Multiple-sequence alignment of the Vip2 proteins.*

*Sequence identity is indicated by shading, where violet is 100% sequence identity, pale blue is 80–100%, yellow is 60–80%, and white is < 60%. Intervals of 10 amino acids are marked with "*". "SP": Signal Peptide. The N-terminal domain (N-Domain) and C-terminal domain (C-domain) are framed within boxes. The proteins used in this analysis are as follows: Vip2Aa1 (RCSB Protein Data Bank accession number 1QS1A), Vip2Ab1 (Seq. ID no. 20 in* Warren et al., 1998*), Vip2Ac1 (accession number AAO86513), Vip2Ad1 (accession number CAI40768), Vip2Ae1 (accession number EF442245), Vip2Af1 (accession number ACH42759), Vip2Ag1 (accession number JQ855506), Vip2Ba1 (accession number AAR40887), Vip2Bb3 (accession number KJ868170).*

Despite their limited sequence homology to each other, the crystallography structure analysis of the Vip2 N- and C-terminal domains showed homology in their structure (Fig. I-8). Each domain core is formed mainly by the perpendicular packing of a five-stranded mixed β-sheet with a three-stranded antiparallel β-sheet. The three-stranded sheet is flanked by four consecutive α-helices, and the five-stranded sheet by an additional α-helix (Han et al., 1999). The overall fold of each domain resembles the catalytic domains of classical A-B toxins. In fact, crystal structure superposition of Vip2 and the clostridial toxin C3, along with sequence alignment, suggests that the class of Vip2 toxins has arisen by a single gene duplication of an ancestral ADP-ribosyl

transyl transferase. This duplication event would have been followed by further divergence by which the N-terminal domain would have lost the catalytic function and evolved into a binding component, to finally give rise to a new protein family with the ability to bind to other carrier proteins (e.g., Vip1), and thereby act as binary toxins (Barth et al., 1998; Han et al., 2001, 1999).

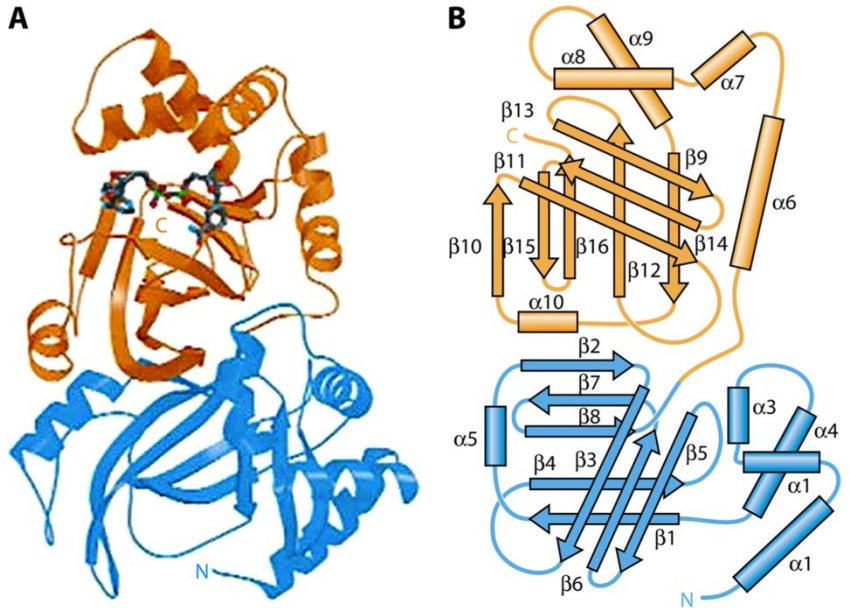


***Fig. I- 8.: Tridimensional structure of Vip2 showing the two domains in different colors (N-domain in blue and C-domain in orange).***
*(a) Schematic ribbon representation showing the NAD molecule (in blue) bound to the C-terminal domain. (b) Schematic drawing with secondary structure nomenclature (reprinted from* Han et al., (1999) *by permission from Macmillan Publishers Ltd.).*

## Insecticidal Activity

The toxicity of Vip1, Vip2, and their combination has been tested against a number of insect species belonging to the orders Coleoptera, Lepidoptera, Diptera, and Hemiptera, as well as in nematodes (Table I-1). So far, toxicity has been found against 10 coleopteran species (Bi et al., 2015; Boets et al., 2011; Feitelson et al., 2003; Schnepf et al., 2003; Prashant R Shingote et al., 2013; Warren, 1997) and to the hemipteran *Aphis gossypii* (Sattar and Maiti, 2011; Yu et al., 2011a).
Testing of individual Vip1 or Vip2 proteins against a number of insect species from different orders has confirmed the fact that they must act together to be toxic, since alone neither displayed any toxic activity against the species tested (Table I- 1). Another interesting feature of these toxins comes from experiments combining different pairs of proteins. The binary toxin Vip1Aa/Vip2Aa (carried and expressed from the same operon) is active against *D. virgifera virgifera*, but Vip1Ab/Vip2Ab (carried and expressed from the same operon) has no activity against this insect. Interestingly, the Vip1Aa/Vip2Ab combination is active, whereas its counterpart

Vip1Ab/Vip2Aa is not, suggesting that the lack of toxicity of the Vip1Ab/Vip2Ab pair to *D. virgifera virgifera* is due to the Vip1Ab component (Warren, 1997).

***Table I- 1. Activity spectrum of individual Vip1 and Vip2 protoxins and their combinations as binary toxins (1/2).***

| Protein | Insect order | Insect species | Activity[a] ($LC_{50}$) |
|---|---|---|---|
| Vip1Aa | Coleoptera | *D. virgifera virgifera* | NA |
| Vip1Ac | Coleoptera | *C. suppressalis*, *Holotrichia oblita* | NA |
| | | *Tenebrio molitor* | NA |
| | Lepidoptera | *H. armigera*, *S. litura* | NA |
| | | *S. exigua* | NA |
| | Diptera | *C. quinquefasciatus* | NA |
| | Hemiptera | *A. gossypii* | NA |
| Vip1Ad | Coleoptera | *Anomala corpulenta*, *H. oblita*, *Holotrichia parallela* | NA |
| Vip1Ae | Hemiptera | *A. gossypii* | NA |
| Vip1Da | Coleoptera | *D. virgifera virgifera* | NA |
| Vip2Aa | Coleoptera | *D. virgifera virgifera* | NA |
| Vip2Ac | Coleoptera | *T. molitor* | NA |
| | Lepidoptera | *H. armigera*, *S. exigua*, *S. litura* | NA |
| Vip2Ad | Coleoptera | *D. virgifera virgifera* | NA |
| Vip2Ae | Coleoptera | *H. oblita*, *T. molitor* | NA |
| | Lepidoptera | *C. suppressalis*, *H. armigera*, *S. exigua* | NA |
| | Diptera | *C. quinquefasciatus* | NA |
| | Hemiptera | *A. gossypii* | NA |
| Vip2Ag | Coleoptera | *A. corpulenta*, *H. oblita*, *H. parallela* | NA |
| Vip1Aa + Vip2Aa | Coleoptera | *Diabrotica longicornis barberi* | +++ (NI) |
| | | *Diabrotica undecimpunctata howardi* | + (NI) |
| | | *D. virgifera virgifera* | +++ (40/20[b] ng/g diet) |
| | | *Leptinotarsa decemlineata*, *T. molitor* | NA |
| | Lepidoptera | *A. ipsilon*, *H. virescens*, *H. zea*, *M. sexta*, *O. nubilalis*, *S. exigua*, *S. frugiperda* | NA |
| | Diptera | *Culex pipiens* | NA |
| Vip1Aa + Vip2Ab | Coleoptera | *D. virgifera virgifera* | +++ (NI) |
| Vip1Ab + Vip2Aa | Coleoptera | *D. virgifera virgifera* | NA |
| Vip1Ab + Vip2Ab | Coleoptera | *D. virgifera virgifera* | NA |
| Vip1Ac + Vip2Ac | Coleoptera | *T. molitor* | NA |
| | Lepidoptera | *H. armigera*, *S. exigua*, *S. litura* | NA |
| Vip1Ac + Vip2Ae | Coleoptera | *H. oblita*, *T. molitor* | NA |
| | Lepidoptera | *C. suppressalis*, *H. armigera*, *S. exigua* | NA |
| | Diptera | *C. quinquefasciatus* | NA |
| | Hemiptera | *A. gossypii* | +++ (87.5 ng/ml) |
| Vip1Ad + Vip2Ag | Coleoptera | *A. corpulenta* | +++ (220 ng/g soil) |
| | | *H. oblita* | +++ (120 ng/g soil) |
| | | *H. parallela* | +++ (80 ng/g soil) |
| Vip1Ae + Vip2Ae | Hemiptera | *A. gossypii* | ++ (96/481[b] ng/ml) |
| Vip1Ca + Vip2Aa | Coleoptera | *T. molitor* | NA |
| | Lepidoptera | *H. armigera*, *S. exigua*, *S. litura* | NA |
| | Diptera | *C. quinquefasciatus* | NA |
| Vip1Da + Vip2Ad | Coleoptera | *Anthonomus grandis* | + (207 μg/ml) |
| | | *D. longicornis barberi* | +++ (213 ng/ml) |

*For information on the source of the toxicity data, please refer to Chakroun* et al.*, 2016a,2016b.*

*Table I- 1. Activity spectrum of individual Vip1 and Vip2 protoxins and their combinations as binary toxins (continued, 2/2).*

| Protein | Insect order | Insect species | Activity[a] ($LC_{50}$) |
|---|---|---|---|
| | | *D. undecimpunctata howardi* | ++ (4.91 μg/ml) |
| | | *D. virgifera virgifera* | +++ (437 ng/ml) |
| | | *L. decemlineata* | +++ (37 ng/ml) |
| | Lepidoptera | *H. virescens*, *H. zea*, *M. sexta*, *O. nubilalis*, *Sesamia nonagrioides*, *S. littoralis*, *S. frugiperda* | NA |
| Vip1Ac-like/Vip2Ac-like | Coleoptera | *Sitophilus zeamais* | ++ (NI) |
| Vip1/Vip2 | Nematoda | *Caenorhabditis elegans*, *Pristionchus pacificus* | NA |
| Vip1Ba1-Vip2Ba1 | Coleoptera | *D. virgifera virgifera* | +++ (NI) |
| Vip1Aa2-Vip2Aa2 | Coleoptera | *D. virgifera virgifera* | +++ (NI) |
| | Lepidoptera | *H. virescens*, *H. zea* | NA |
| Vip1Bb1-Vip2Bb1 | Coleoptera | *D. virgifera virgifera* | +++ (NI) |
| | Lepidoptera | *H. virescens*, *H. zea* | NA |

[a] The number of "+" symbols reflects the activity level. NA, not active; NI, no information on the $LC_{50}$.
[b] Proportion of Vip1/Vip2 that gives 50% mortality.

*For information on the source of the toxicity data, please refer to Chakroun* et al.*, 2016a,2016b.*

## Mode of Action

The molecular mechanism of the insecticidal activity of the Vip1/Vip2 toxin is not totally understood (Fig. I-9). The multistep process begins with the ingestion of the toxin by the larva, probably followed by the proteolytic activation in the midgut by trypsin-like proteases. The activated monomer of Vip1Ac has been shown to form oligomers containing seven Vip1 molecules (Leuber et al., 2006). These oligomers would recognize specific receptors in the midgut brush border membrane, where the toxin would then insert into the membrane. Evidence that the Vip1 component is involved in receptor recognition was in part provided by the fact that Vip1Aa cannot be replaced by Vip1Ab without losing toxicity to *D. virgifera virgifera* (Warren, 1997). The first Vip1-binding protein receptor described for a Vip1 protein by ligand blot experiments was identified in *A. gossypii* by ligand blot and was approximately 50 kDa in size; concomitantly, no binding of Vip1 was observed to brush border membrane vesicles (BBMV) from non-susceptible insect species (Sattar and Maiti, 2011).

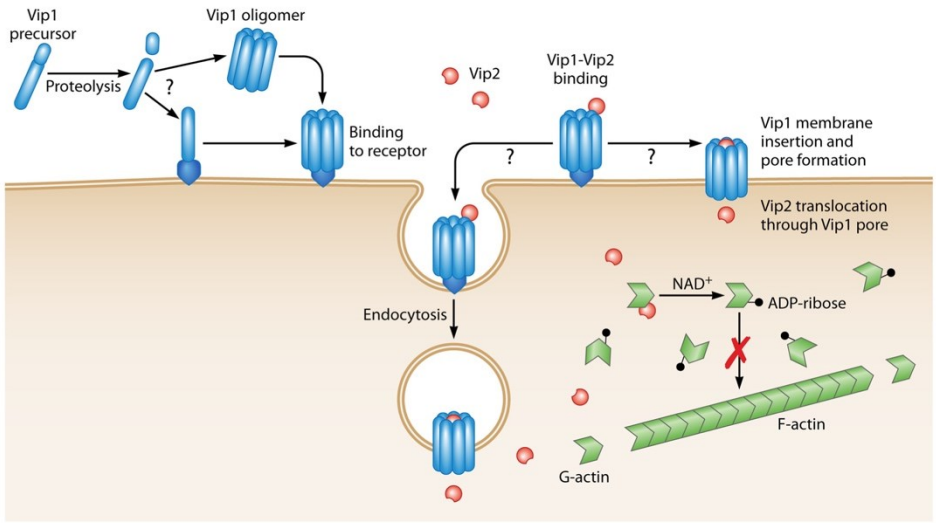


*Fig. I- 9. Proposed mode of action of the binary Vip1/Vip2 toxin. The Vip1 protoxin is proteolytically processed by midgut proteases. The activated toxin binds to specific receptors either as a monomeric form or after oligomerization. Vip2 then binds to the oligomeric Vip1 protein and enters the cell either by endocytosis of the whole complex or directly through the pore formed by Vip1. Once inside the cytosol, Vip2 would catalyze the transfer of the ADP-ribose group from NAD to the actin monomers, preventing their polymerization.*

*In vitro* experiments showed that Vip1 formed membrane pores in artificial lipid bilayers (Leuber et al., 2006). The pores had two different conductance states, suggesting the simultaneous formation of two different channels. Vip1Ac channels are asymmetric and moderately anion selective. The putative channel-forming domain of Vip1 contains two negatively charged (E340 and E345) and two positively charged (K351 and H363) amino acids, which are hypothesized to contribute to the selectivity of the channel (Leuber et al., 2006).

The mechanism by which Vip2 enters the cell is still unknown, but based on its homology with the C2-I component of the C2 clostridial binary toxin, it seems likely that Vip2 enters the cell via receptor-mediated endocytosis (Barth et al., 2004). Leuber et al. (2009) have proposed that a second possibility, in which the strong outward proton gradient across the midgut brush border membrane of insect cells (maintained by the highly alkaline midgut fluids of the larvae) could favor that Vip2Ac be "directly" delivered into the cytoplasm of the midgut cells via the channel formed by Vip1Ac. Experimental evidence favoring either one of these mechanisms is lacking. Once inside the cytosol, the catalytic Vip2 domain would catalyze the transfer of the ADP-ribose group from NAD to actin, preventing its polymerization and thus inhibiting microfilament network formation (Han et al., 1999; Jucovic et al., 2008).

### Expression in Plants

Despite the economic importance of Vip1 and Vip2 as effective toxins against the major corn pest *D. virgifera virgifera*, the expression of the binary toxin *in planta* has not been possible due to the cytotoxic activity of the Vip2 protein. In fact, Vip2 expression in yeast resulted in serious developmental pathology and phenotypic alterations (Jucovic et al., 2008). To overcome this problem, Jucovic et al. (2008) designed a new zymogene strategy which consisted of the expression of a zymogenic form of Vip2 called "ProVip2". The Vip2 proenzyme was obtained by extension of the C-terminal portion of the protein in such a way that it masked the enzymatic activity. The additional C-terminal peptide was effectively eliminated by the proteolytic action of *D. virgifera virgifera* midgut enzymes, and insects on a diet containing ProVip2 transgenic corn and Vip1 were all killed. Transformed plants had a phenotype unrecognizable from controls.

## The Vip3 lepidopteran-active protein

Similarly to the Vip1 and Vip2 proteins, Vip3 proteins are produced during the vegetative growth phase of *B. thuringiensis* and can be detected in culture supernatants from 15 h post-inoculation to beyond sporulation, which reflects their high stability (Estruch et al., 1996; Mesrati et al., 2005). A study of the *vip3Aa16* gene reported that the transcription start point was located at 101 bp upstream of the start codon, and that the -35 and -10 promoter regions were very similar to the *B. subtilis* promoters that are under the control of the $\sigma^E$ holoenzyme. These results strongly suggested that the *vip3Aa16* gene is transcribed by a $\sigma^{35}$ holoenzyme, the *B. thuringiensis* homolog of $\sigma^E$ (Mesrati et al., 2005).

Genes coding for Vip3 proteins are commonly found among *B. thuringiensis* strains, and hence some studies have found them even in 50 and up to 87% of the strains tested, and in more than 90% of strains carrying *cry1* and *cry2* genes (Beard et al., 2008; Espinasse et al., 2003; Hernández-Rodríguez et al., 2009; Liu et al., 2007; Mesrati et al., 2005; Rice, 1999; Yu et al., 2011b). *vip3* genes are approximately 2.4 kb in length and they are normally carried on large plasmids (Mesrati et al., 2005; Wu et al., 2004), although in some cases they have been proposed to be located in the bacterial chromosome (Franco-Rivera et al., 2004). Many screening strategies of *B. thuringiensis* isolates have been performed with the aim of isolating new *vip3* genes (Abulreesh et al., 2012; Asokan et al., 2012; Baranek et al., 2015; Bhalla et al., 2005; Franco-Rivera et al., 2004; Hernández-Rodríguez et al., 2009; Liu et al., 2007; Loguercio et al., 2002; Murawska et al., 2013; Rang et al., 2005; Sattar et al., 2008). At the time of writing this document, there are 63 *vip3Aa*, 2 *vip3Ab*, 1 *vip3Ac*, 6 *vip3Ad*, 1 *vip3Ae*, 4 *vip3Af*, 15 *vip3Ag*, 1 *vip3Ah*, 1 *vip3Ai*, 2 *vip3Aj*, 2 *vip3Ba*, 3 *vip3Bb*, and 4 *vip3Ca* genes reported (Crickmore et al., 2014, accessed on May 2017). It is not surprising that most of the studies on the Vip3 proteins have been carried out with the most abundant Vip3Aa proteins, and hence very little information is available on Vip3B and Vip3C proteins and on other less common proteins of the Vip3A family

(Vip3Ab, Vip3Ac, etc.). Unfortunately, early papers omitted the tertiary rank in the Vip3 name, referring just to Vip3A. Although these studies were most likely carried out on Vip3Aa, in this document it was followed the nomenclature provided by the authors whenever we found not possible to identify the protein by either the accession number or by any other means.

## Protein Structure and Function

The number of amino acids in any particular Vip3 protein is around 787, and the protein has an average molecular mass of approximately 89 kDa. The N-terminus of Vip3 is highly conserved, while the C-terminal region is highly variable (Rang et al., 2005; Ruiz de Escudero et al., 2014; Wu et al., 2007) (Fig. I-10) and it has been proposed to be involved in target specificity (Wu et al., 2007).

Vip3A proteins contain three cysteine residues. Point mutations in each of these three residues resulted in loss of activity. However, this loss of activity was related with trypsin sensitivity rather than to the disruption of potential disulfide bonds (Dong et al., 2012b).

The N-terminus of Vip3 proteins contains a signal peptide which is responsible for the translocation of the protein to the periplasmic space across the cell membrane. It consists of a few positively charged amino acids, followed by a hydrophobic region, which are not removed after secretion from the bacterial cell (Chen et al., 2003; Doss et al., 2002; Estruch et al., 1996). Without a clear putative cleavage site, the extent of the signal peptide varies depending on the protein sequence itself and on the program used for prediction, and ranges from 11 to 28 amino acids (Chen et al., 2003; Doss et al., 2002; Estruch et al., 1996). Since the secretion of proteins commonly implies the excision of the signal peptide, the secretion mechanism for the Vip3 proteins is still unclear.

The highly conserved amino acid sequence of the N-terminal region of Vip3A proteins is an indication that this region likely plays an important role in either the protein folding or by directly affecting binding to the membrane receptors. However, contradictory results have been obtained in experiments testing the insecticidal activity of mutant Vip3A proteins with deletions at the N-terminal end. Deletion of the first 198 amino acids (which corresponds to the 22 kDa proteolytic fragment described by Estruch and Yu (Estruch and Yu, 2001) abolished the toxicity to *Helicoverpa armigera* (Lepidoptera: Noctuidae) and *Spodoptera exigua* (Lepidoptera: Noctuidae) (Li et al., 2007).

Deletion of the first 27 N-terminal amino acids from Vip3Aa rendered the protein inactive due to total loss of solubility (Chen et al., 2003). The deletion of the first 39 N-terminal amino acids from Vip3Aa differentially affected the toxicity of this protein toward the two susceptible insect species: *Spodoptera litura* (Lepidoptera: Noctuidae) and *Chilo partellus* (Lepidoptera: Crambidae) (Selvapandiyan et al., 2001).


*Fig. I- 10. Multiple-sequence alignment of the Vip3 proteins.*

*Sequence identity is indicated by shading, where violet is 100% sequence identity, pale blue is 80–100%, yellow is 60–80%, and white is < 60%. Intervals of 10 amino acids are marked with "*". "SP": Signal Peptide. "T": 65-kDa fragment after proteolysis: "PPS1" and "PPS2", first and second processing sites, respectively (as described in Rang et al., 2005). The proteins used in this analysis are as follows: Vip3Aa1 (accession number AAC37036), Vip3Ab1 (accession number AAR40284), Vip3Ac1 (named PS49C; Seq. ID no. 7 in Narva and Merlo patent application US20040128716), Vip3Ad2 (accession number CAI43276), Vip3Ae1 (accession number CAI43277), Vip3Af1 (accession number CAI43275), Vip3Ag2 (accession number FJ556803), Vip3Ah1 (accession number DQ832323) Vip3Ai1 (accession number KC156693), Vip3Aj1 (accession number KF826717), Vip3Ba1 (accession number AAV70653), Vip3Bb2 (accession number ABO30520), Vip3Ca1 (accession number ADZ46178), Vip4Aa1 (accession number HM044666).*

Contrary to the above results, Gayen et al. (2012) found that deletion of the first 200 N-terminal amino acids enhanced the insecticidal potency of the core active toxin about 2 to 3-fold against *H. armigera*, *A. ipsilon*, *Spodoptera littoralis* (Lepidoptera: Noctuidae), and *Scirpophaga incertulas* (Lepidoptera: Pyralidae). Similarly, in another study (Bhalla et al., 2005), deletion of 33 amino acids from the Vip3Aa N-terminus caused no loss of toxicity against *S. litura, Plutella xylostella* (Lepidoptera: Plutellidae), and *Earias vitella* (Lepidoptera: Noctuidae).

The function of some C-terminal modifications has also been studied without leading to a general conclusion. Usually, the effect of the same change varies among different insect species, preventing a consensus about the contribution of certain regions or amino acid positions to the toxicity of Vip3A proteins (Bhalla et al., 2005; Chen et al., 2003; Gayen et al., 2012; Li et al., 2007; Selvapandiyan et al., 2001). There is general agreement in that the last amino acids of the C-terminus are critical for the activity and stability of Vip3 proteins, since their deletion, substitution by non-conservative residues, or addition of amino acids to the end of the protein, completely abolishes the protein activity (Gayen et al., 2012; Selvapandiyan et al., 2001) and the susceptibility to proteases (Estruch and Yu, 2001; Li et al., 2007). A triple mutation at the C-terminus of Vip3Aa1 resulted in an unstable protein that was completely hydrolyzed by the midgut juice of *A. ipsilon* larvae but retained toxicity against Sf9 cells (Estruch and Yu, 2001).

An analysis of the Vip3 protein sequences conducted by the authors of this review, and performed with the NCBI-CDD database (Marchler-Bauer et al., 2011), revealed the presence of a carbohydrate binding motif (CBM_4_9 superfamily, pfam02018) in all of the Vip3 proteins with the exception of Vip3Ba (Fig. I- 11). The CBM spans from position 536 to a position near amino acid 652, with a consistent e-value between 10 $e^{-4}$ and 10 $e^{-17}$, depending on the Vip3 protein considered. The analysis of Vip3 sequences also revealed positive hits with different multi-domains in the N-terminal region, with lower e-values of around 10 $e^{-4}$, and with differences depending on the Vip3 protein being considered. We did not detect any hydrophobic region susceptible to forming a transmembrane domain other than the short succession of hydrophobic amino acids in the signal peptide (Doss et al., 2002; Estruch et al., 1996).

Comparison of the Vip3Aa1 sequence with that of the Vip3B and Vip3C type proteins reveals differences distributed throughout the length of the protein (Fig. I-10). Nevertheless, maximum divergence was found at the C-terminus, as occurs among Vip3A family proteins. The N-termini of the putative signal sequences of Vip3B and Vip3C are almost identical to that of all Vip3A proteins. The proteolytic processing sites are less conserved among the three Vip3 proteins, but major differences are found in the middle of the protein sequence; the insertion of 5 amino acids downstream of the first processing site for Vip3Ca1, and 17 amino acids downstream of the second processing site for Vip3Ba1 are responsible for the change in the expected size of the toxin “active form” from 66 kDa to 69 kDa. The Vip3B inserted sequence consists of three repetitions of the pattern DCCEE, which is characterized by its high content of negatively charged amino acids (D and E) and cysteine residues. From a total of 11 cysteine residues found in Vip3B proteins, eight (78%) are located

in this inserted sequence (Palma et al., 2012; Rang et al., 2005). Whether the insertion of this repetitive pattern contributes to the limited insecticidal activity of the Vip3B proteins is not known.

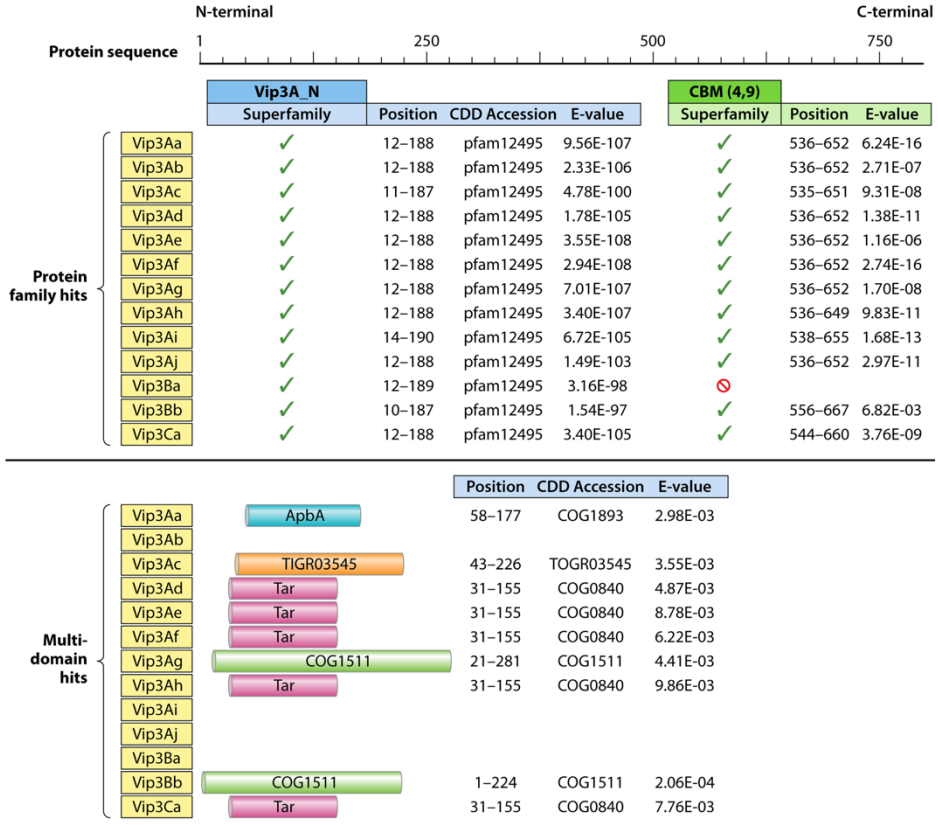


***Fig. I- 11. Conserved Domain (CDD) Analysis of representative Vip3 proteins.***
*The same sequences as in Fig.I- 10 were used. CBM: carbohydrate binding motif; ApbA: ketopantoate reductase motif; Tar: methyl-accepting chemotaxis protein motif; COG1511: motif of a predicted protein membrane of unknown function; TIGR03545 represents a relatively rare but broadly distributed uncharacterized protein family of proteins, distributed in 1-2% of bacterial genomes.*

The chrystallographic 3D structure of Vip3 proteins has not yet been elucidated. It has been recently described that Vip3A proteins form heterotetramers as pro-toxins and toxins (Kunthic et al., 2016; Palma et al., 2017). Secondary structure prediction suggests that the N-terminus is mainly composed of α-helix structures, whereas the essential components of the C-terminus are β- structures and coils, which would be consistent with its proposed role in insect specificity (Rang et al., 2005; Wu et al., 2007). The fact that Vip3 proteins do not show homology to any protein outside their group prevents *in silico* modeling based on structure homology. Only a partial tertiary structure of the Vip3 protein corresponding to the last 200 amino acids has been modelled by homology to domain II of the Cry proteins (Wu et al., 2007).

## Insecticidal Activity

Most of the information on the insecticidal activity of Vip3 proteins has been obtained with the most abundant variants of the Vip3Aa subfamily, and very little data exists on the toxicity of Vip3B, Vip3C, and other Vip3A proteins outside of the Vip3Aa subfamily.

**Insecticidal spectrum of Vip3 proteins.** Vip3A proteins are toxic to a large number of lepidopteran species. It is worth mentioning that Vip3A proteins are very active against insect species from the genus *Agrotis*, which are known to be tolerant to Cry proteins, and also to species from the genus *Spodoptera,* which display low susceptibility to Cry proteins (Van Frankenhuyzen and Nystrom, 2009). In this regard, it has been shown that deletion of the *vip3A* gene from the *B. thuringiensis* HD1 strain significantly decreased its toxicity towards *A. ipsilon* and *S. exigua* (Donovan et al., 2001). On the other hand, other species susceptible to Cry proteins, such as *Ostrinia nubilalis* (Lepidoptera: Crambidae), *Culex quinquefasciatus* (Diptera: Culicidae), and *Chironomus tepperi* (Diptera: Chironomidae), are marginally or not susceptible to any Vip3A protein tested (Doss et al., 2002; Estruch et al., 1996; Yu et al., 1997, 2012). With Vip3 proteins, depending on the Vip3 protein and the insect species considered, it is not uncommon to find that, while the mortality is reached at a high concentration of Vip3 protein, a strong growth inhibition (or even complete growth arrest) is observed at lower concentrations (Abdelkefi-Mesrati et al., 2011b; Ben Hamadou-Charfi et al., 2013; Jamoussi et al., 2009; Palma et al., 2012; Ruiz de Escudero et al., 2014). Therefore, the "functional mortality" (dead insects plus those remaining at L1) better represents the effectivity of the Vip3 protein in those cases (Ali and Luttrell, 2011; Chakroun et al., 2012; Ruiz de Escudero et al., 2014).

Table I- 2 summarizes the results which have been reported on the insecticidal activity of proteins of the Vip3Aa subfamily. Only the values of the protoxin form are given since there are no reports indicating relevant differences in the insecticidal activity between the protoxin and the activated form (Ruiz de Escudero et al., 2014), with the exceptions of Vip3Aa16 against *S. exigua* and Vip3Af1 against *Spodoptera frugiperda* (Lepidoptera: Noctuidae) (Chakroun et al., 2012; Hernández-Martínez et al., 2013). Despite the very small differences among Vip3Aa sequences, some proteins may exhibit significant differences in toxicity to the same insect species (Palma et al., 2013a; Ruiz de Escudero et al., 2014; Selvapandiyan et al., 2001). For example, among all Vip3Aa proteins tested, only Vip3Aa1 and Vip3Aa14 have been described as low or non-active against *H. armigera* (Table I-2). Nonetheless, considering that most of the data in Table I-2 were obtained in different laboratories, insecticidal differences are likely to come from factors other than slight differences in protein sequence, such as the protocol used for protein preparation, purity of the sample, method of quantification, bioassay conditions, or variability among insect populations. Independent laboratories have observed a decrease in the toxicity of some Vip3A proteins after purification with metal-chelate chromatography (Baranek et al., 2015; Hernández-Martínez et al., 2013). The effect of the method of purification on the toxicity depends on both the type of protein and the insect species

*Table I- 2. Spectrum of Activity and toxicity of the Vip3Aa subfamily proteins (1/2).*

| Protein | Insect species | Larval instar[c] | Assay type | $LC_{50}$ (ng/cm$^2$)[a] | Scoring time (days) |
|---|---|---|---|---|---|
| Vip3Aa | *A. ipsilon* | 2nd–3rd | Diet incorporation | <200.0 | 2 |
| | *O. nubilalis* | 2nd–3rd | Diet incorporation | NA | 2 |
| | *S. frugiperda* | 2nd–3rd | Diet incorporation | <200.0 | 2 |
| | *H. armigera* | Neonate | Surface contamination | 155 | 7 |
| | *Helicoverpa punctigera* | Neonate | Surface contamination | 22 | 7 |
| | *H. virescens* | Neonate | Diet incorporation | NI | 7 |
| | *H. zea* | Neonate | Diet incorporation | NI | 7 |
| | *A. ipsilon* | 1st | Surface contamination | 17.1 | 5 |
| | *Danaus plexippus* | 1st | Surface contamination | NA | 5 |
| | *H. zea* | 1st | Surface contamination | 112.5 | 5 |
| | *M. sexta* | 1st | Surface contamination | 176.3 | 5 |
| | *O. nubilalis* | 1st | Surface contamination | NA | 5 |
| | *S. frugiperda* | 1st | Surface contamination | 55.9 | 5 |
| | *H. armigera* | Neonate | Diet incorporation | 89 | 5 |
| | *A. ipsilon* | Neonate | Diet incorporation | 63 | 5 |
| | *S. littoralis* | Neonate | Diet incorporation | 36 | 5 |
| | *S. incertulas* | Neonate | Diet incorporation | 60 | 5 |
| Vip3Aa1 | *A. ipsilon* | Neonate | Diet incorporation | <28 | 6 |
| | *H. virescens* | Neonate | Diet incorporation | <420 | 6 |
| | *H. zea* | Neonate | Diet incorporation | ≥420 | 6 |
| | *O. nubilalis* | Neonate | Diet incorporation | >420 | 6 |
| | *S. exigua* | Neonate | Diet incorporation | <28 | 6 |
| | *S. frugiperda* | Neonate | Diet incorporation | <70 | 6 |
| | *B. mori* | Neonate | Surface contamination | 1,986 | 7 |
| | *H. zea* | Neonate | Surface contamination | 27.7 | 7 |
| | *S. frugiperda* | Neonate | Surface contamination | 6.9 | 7 |
| | *S. frugiperda* | Neonate | Surface contamination | 49.3 | 7 |
| | *A. ipsilon* | Neonate | Surface contamination | 14 | 7 |
| | *S. frugiperda* | Neonate | Surface contamination | 620 | 7 |
| | *H. armigera* | Neonate | Surface contamination | 1,660 | 7 |
| | *Lobesia botrana* | Neonate | Diet incorporation | 1.3 µg/ml | 7 |
| | *Mamestra brassicae* | Neonate | Surface contamination | 14.4 | 7 |
| | *S. littoralis* | Neonate | Surface contamination | 4.0 | 7 |
| Vip3Aa7 | *H. armigera* | Neonate | Leaf dip | 35.6 ng/ml | 3 |
| | *P. xylostella* | 3rd | Diet incorporation | 28.9 ng/ml | 3 |
| | *S. exigua* | Neonate | Diet incorporation | 46.1 ng/ml | 7 |
| | *P xylostella* | 3rd | Leaf dip | 4.9 | 3 |
| Vip3Aa9 | *A. ipsilon* | 1st | Leaf dip | 2,165 | 1 |
| | *C. partellus* | 1st | Leaf dip | 8 | 1 |
| | *Phthorimaea operculella* | 1st | Leaf dip | 370 | 1 |
| | *P xylostella* | 1st | Leaf dip | 36 | 1 |
| | *S. litura* | 1st | Leaf dip | 5 | 1 |
| Vip3Aa10 | *A. ipsilon* | Neonate/1st | Surface contamination | 80.7 | 6 |
| | *B. mori* | Neonate/1st | Surface contamination | NA | 6 |
| | *C. quinquefasciatus* | Neonate/1st | In water | NA | 6 |
| | *H. armigera* | Neonate/1st | Surface contamination | 325.2 | 6 |
| | *P. xylostella* | Neonate/1st | Leaf dip | 220.7 | 6 |
| | *S. litura* | Neonate/1st | Surface contamination | 45.4 | 6 |
| Vip3Aa11 | *H. armigera* | 1st | Diet incorporation | 25.7 ng/mg | 7 |
| | *Ostrinia furnacalis* | 1st | Diet incorporation | 720 µg/ml | 7 |
| | *P. xylostella* | 1st | Leaf dip | 4.2 mg/ml | 4 |
| | *S. exigua* | 1st | Diet incorporation | 1.3 ng/mg | 7 |
| Vip3Aa13 | *H. armigera* | Neonate | Diet incorporation | 160 ng/ml | 2 |
| | *S. exigua* | Neonate | Diet incorporation | 740 ng/ml | 2 |
| | *S. litura* | Neonate | Diet incorporation | 270 ng/ml | 2 |

*Table I-2. Spectrum of Activity and toxicity of the Vip3Aa subfamily proteins (continued, 2/2).*

| Protein | Insect species | Larval instar[c] | Assay type | $LC_{50}$ ($ng/cm^2$)[a] | Scoring time (days) |
|---|---|---|---|---|---|
| Vip3Aa14 | *Earias vitella* | Neonate | Leaf dip | 794 | 3 |
| | *H. armigera* | Neonate | Leaf dip | NA | 3 |
| | *Pieris brassicae* | Neonate | Leaf dip | NA | 3 |
| | *P. xylostella* | Neonate | Leaf dip | 120 | 3 |
| | *S. litura* | Neonate | Leaf dip | 12 | 3 |
| | *H. armigera* | Neonate | Diet incorporation | NA | 3 |
| | *P. xylostella* | Neonate | Leaf dip | NA | 3 |
| | *S. litura* | Neonate | Leaf dip | 0.1 | 3 |
| Vip3Aa16 | *P. oleae* | 3rd | Leaf dip | NI | 5 |
| | *S. littoralis* | 1st | Surface contamination | 305 | 6 |
| | *E. kuehniella* | 1st | Diet incorporation | 36 | 6 |
| | *S. exigua* | Neonate | Surface contamination | 2,600 | 7 |
| | | | | 290 | 10 |
| | *S. frugiperda* | Neonate | Surface contamination | 340 | 7 |
| | | | | 24 | 10 |
| | *A. segetum* | 1st | Surface contamination | 86 | 6 |
| | *Tuta absoluta* | 3rd | Leaf dip | 335 | 3 |
| | *Ectomyelois ceratoniae* | Neonate | Diet incorporation | 40[b] | 5 |
| Vip3Aa19 | *H. armigera* | 1st | Diet incorporation | 24.1 ng/mg | 7 |
| | *O. furnacalis* | 1st | Diet incorporation | >100 µg/ml | 7 |
| | *P. xylostella* | 1st | Leaf dip | 59.8 µg/ml | 4 |
| | *S. exigua* | 1st | Diet incorporation | 1.4 ng/mg | 7 |
| | *H. virescens* | 1st | Diet incorporation | 1.35 µg/ml | 7 |
| | *P. xylostella* | 1st | Leaf dip | 2236 µg/ml | 5 |
| | *H. zea* | Neonate | Surface contamination | 500 | 7 |
| Vip3Aa29 | *C. quinquefasciatus* | — | In water | NA | 2 |
| | *C. suppressalis* | — | Diet incorporation | 24.0 µg/ml | 5 |
| | *C. tepperi* | — | In water | NA | 2 |
| | *H. armigera* | — | Diet incorporation | 22.6 µg/ml[d] | 5 |
| | *S. exigua* | — | Diet incorporation | 36.6 µg/ml | 5 |
| Vip3Aa43 | *S. albula* | Neonate | Surface contamination | 3.9 | 7 |
| | *S. cosmioides* | Neonate | Surface contamination | 2.8 | 7 |
| | *S. eridania* | Neonate | Surface contamination | 3.4 | 7 |
| | *S. frugiperda* | Neonate | Surface contamination | 24.7 | 7 |
| Vip3Aa45 | *Chrysodeixis chalcites* | Neonate | Surface contamination | 1,044.6 | 7 |
| | *L. botrana* | Neonate | Diet incorporation | 1.96 µg/ml | 7 |
| | *M. brassicae* | Neonate | Surface contamination | 39.7 | 7 |
| | *S. exigua* | Neonate | Surface contamination | 119.7 | 7 |
| | *S. littoralis* | Neonate | Surface contamination | 18.7 | 7 |
| Vip3Aa50 | *Anticarsia gemmatalis* | Neonate | Surface contamination | 20.3 | 7 |
| | *S. frugiperda* | Neonate | Surface contamination | 79.6 | 7 |
| Vip3Aa58 | *S. exigua* | Neonate | Surface contamination | 16 | 10 |
| | *Cydia pomonella* | Neonate | Surface contamination | 238 | 10 |
| | *Dendrolimus pini* | 2nd | Leaf dip | 2,355 | 10 |
| Vip3Aa59 | *S. exigua* | Neonate | Surface contamination | 19 | 10 |
| | *C. pomonella* | Neonate | Surface contamination | 275 | 10 |
| | *D. pini* | 2nd | Leaf dip | 1,626 | 10 |

*[a] Unless otherwise stated, $LC_{50}$s are given in nanograms per square centimeter and refer to the protoxin form of the proteins. NA, not active; NI, no information on the $LC_{50}$ is available, although the protein was active.*

*[b] Although the $LC_{50}$ is given in nanograms per square centimeter, the bioassay was performed by using diet incorporation.*

*[c] —, not specified.*

*[d] The 50% inhibitory concentration is shown instead of the $LC_{50}$.*

*For information on the source of the toxicity data, please refer to Chakroun* et al.*, 2016a,2016b.*

tested. The length of the bioassay can also drastically affect the final outcome with some proteins, as has been shown for Vip3Aa16 with *S. exigua* and *S. frugiperda*, for which the $LC_{50}$ values decreased by a factor of 10 when mortality was scored at 10 d instead of 7 d (Chakroun et al., 2012). Ali and Lutrell (2011) found that the insecticidal response of *Helicoverpa zea* and *Heliothis virescens* (Lepidoptera: Noctuidae) to Vip3Aa varied greatly among different batches of the same protein as well as with the buffer used.

Table I- 3 summarizes the bioassay data on Vip3A proteins other than those of the Vip3Aa subfamily, and Table I-4 that of Vip3 proteins other than those of the Vip3A family.

*Table I- 3 Spectrum of Activity and toxicity of the Vip3A proteins other than those of the Vip3Aa subfamily.*

| Protein | Insect species | Larval instar | Assay type | $LC_{50}$ (ng/cm$^2$)[a] |
|---|---|---|---|---|
| Vip3Ab1 | *A. ipsilon* | Neonate | Surface contamination | 62 |
| | *S. exigua* | Neonate | Surface contamination | 597 |
| | *S. frugiperda* | Neonate | Surface contamination | 2,020 |
| | *S. littoralis* | Neonate | Surface contamination | 163 |
| Vip3Ac1 | *Anopheles gambiae* | —[b] | — | NA |
| | *B. mori* | Neonate | Surface contamination | 44.8 |
| | *D. virgifera virgifera* | — | — | NA |
| | *H. zea* | Neonate | Surface contamination | 133.7 |
| | *O. nubilalis* | Neonate | Surface contamination | NA |
| | *S. frugiperda* | Neonate | Surface contamination | 11.6 |
| Vip3Ad2 | *A. ipsilon* | Neonate | Surface contamination | >4,000 |
| | *S. frugiperda* | Neonate | Surface contamination | >4,000 |
| Vip3Ae1 | *A. ipsilon* | Neonate | Surface contamination | 4 |
| | *S. frugiperda* | Neonate | Surface contamination | 28 |
| | *S. exigua* | Neonate | Surface contamination | 11.1 |
| | *S. frugiperda* | Neonate | Surface contamination | 20 |
| | *H. armigera* | Neonate | Surface contamination | 4,460 |
| | *L. botrana* | Neonate | Diet incorporation | 0.2 μg/ml |
| | *M. brassicae* | Neonate | Surface contamination | 258 |
| | *S. littoralis* | Neonate | Surface contamination | 8 |
| Vip3Af1 | *S. frugiperda* | Neonate | Surface contamination | 49.3 |
| | *A. ipsilon* | Neonate | Surface contamination | 18 |
| | *S. frugiperda* | Neonate | Surface contamination | 60 |
| | *H. armigera* | Neonate | Surface contamination | 840 |
| | *L. botrana* | Neonate | Diet incorporation | 0.8 μg/ml |
| | *M. brassicae* | Neonate | Surface contamination | 6 |
| | *S. littoralis* | Neonate | Surface contamination | 43.2 |
| Vip3Ag4 | *C. chalcites* | Neonate | Surface contamination | 45.5 |
| | *L. botrana* | Neonate | Diet incorporation | 1.1 |
| | *M. brassicae* | Neonate | Surface contamination | >2,500 |
| | *S. exigua* | Neonate | Surface contamination | 265.2 |
| | *S. littoralis* | Neonate | Surface contamination | 34.9 |

[a] $LC_{50}$s refer to mortality at 7 days for the protoxin form of the proteins and are given in nanograms per square centimeter unless otherwise stated; NA, not active.
[b] —, information not available.

*For information on the source of the toxicity data, please refer to Chakroun* et al.*, 2016a,2016b.*

*Table I- 4. Spectrum of activity and toxicity of Vip3B and Vip3C protein families.*

| Protein | Insect species | Larval instar[b] | Assay type | $LC_{50}$ (ng/cm$^2$)[a] | Scoring time (days) |
|---|---|---|---|---|---|
| Vip3Ba1 | *O. nubilalis* | Neonate | Surface contamination | NA | 7 |
| | *P. xylostella* | 2nd | Leaf dip | NA | 7 |
| Vip3Bb2 | *A. gossypii* | Nymph | Diet incorporation | NA | 7 |
| | *C. tepperi* | 4th | Liquid solution | NA | 4 |
| | *H. armigera* | Neonate | Surface contamination | NI | 7 |
| | *H. punctigera* | Neonate | Surface contamination | NI | 7 |
| | *Tribolium castaneum* | — | Diet incorporation | NA | 10 |
| Vip3Ca3 | *A. ipsilon* | Neonate | Surface contamination | >4,000 | 10 |
| | *C. chalcites* | Neonate | Surface contamination | <400 | 10 |
| | *H. armigera* | Neonate | Surface contamination | <4,000 | 10 |
| | *L. botrana* | Neonate | Diet incorporation | >100 µg/ml | 10 |
| | *M. brassicae* | Neonate | Surface contamination | <4,000 | 10 |
| | *O. nubilalis* | Neonate | Surface contamination | >4,000 | 10 |
| | *S. exigua* | Neonate | Surface contamination | >4,000 | 10 |
| | *S. frugiperda* | Neonate | Surface contamination | >4,000 | 10 |
| | *S. littoralis* | Neonate | Surface contamination | <4,000 | 10 |
| | *T. ni* | Neonate | Surface contamination | <4,000 | 10 |

*For information on the source of the toxicity data, please refer to Chakroun* et al.*, 2016a,2016b.*

**Interactions with other insecticidal proteins.** Synergism has been observed between the Vip3Aa and Cyt2Aa proteins against *Chilo suppressalis* (Lepidoptera: Crambidae) and *S. exigua* after their co-expression in *E. coli*; contrarily, this protein combination was slightly antagonistic on *C. quinquefasciatus* (Yu et al., 2012). Bergamasco et al*.,* (2013) reported synergism between Vip3A and Cry1Ia in three *Spodoptera* species (*S. frugiperda*, *S. albula*, and *S. cosmioides* (Lepidoptera: Noctuidae)) but slight antagonism in *Spodoptera eridania* (Lepidoptera: Noctuidae). Antagonism between Vip3A and Cry1A or Cry1Ca proteins was described in *H. virescens* (Lemes et al., 2014): antagonism was found in combinations of Cry1Ca with Vip3Aa, Vip3Ae, or Vip3Af, and of Vip3Af with either Cry1Aa or Cry1Ac. In the same study, Vip3Aa and Cry1Ca showed antagonism in *S. frugiperda*, whereas the same combination was synergistic in *Diatraea saccharalis* (Lepidoptera: Crambidae). The mechanisms underlying synergism and antagonism are unknown. For the antagonism between the Vip3A and Cry1C proteins, Lemes et al*.,* (2014) hypothesized a physical interaction of the two proteins impairing the access of the binding epitopes to the membrane receptor. Hetero-oligomer formation with increased ability of membrane insertion or pore formation has been proposed to explain synergism between Cry1Ac and Cry1Aa (Lee et al., 1996). However this possibility between Vip3 and Cry1 proteins seems very unlikely because of their lack of homology.

**Genetically engineered *vip3A* genes.** Genetic engineering allows the construction of chimeric genes that code for parts of different proteins to obtain new proteins with novel or improved properties. Knowledge of the domains of a protein is of great advantage in the design of chimeric proteins. Despite the lack of information on the tertiary structure of Vip3A proteins, two chimeras have been created by sequence swapping between the *vip3Aa* and *vip3Ac* genes with the aim to increase host specificity (Fang et al., 2007). These chimeras between Vip3Aa and Vip3Ac were created by combining around 600 amino acids from the N-terminus of

one protein and around 180 amino acids of the C-terminus of the other (Table I-5). The two chimeric proteins exhibited new toxicity properties: Vip3AcAa (with the N-terminus of Vip3Ac) was more toxic than the two original proteins towards all the insects tested, and it even caused growth inhibition towards the Vip3A-tolerant *O. nubilalis*. In contrast, Vip3AaAc was less toxic than its counterpart and the original proteins, and it even lost completely the activity against *Bombyx mori* (Lepidoptera: Bombycidae) (Fang et al., 2007) (Table I- 5). Li et al*.,* (2007) achieved an 18-fold increase in toxicity against *S. exigua* by changing the last two amino acids of the chimeric Vip3AcAa protein (from IK to LR).

Similar attempts have been conducted by combining the *vip* and *cry* genes. Fusion of the *vip3Aa* gene with *cry1A* rendered a fusion protein that retained the toxicity of Cry1Ac, but partially lost that of Vip3Aa, possibly due to incorrect Vip3A folding (Saraswathy et al., 2008). In another study, the *vip3Aa* gene was fused with the 5' region of c*ry9Ca*, and the resultant chimeric protein was more toxic than the individual proteins and the mixture of them, probably because Vip3Aa increased the solubility of the Cry9Ca protein (Dong et al., 2012a). In an attempt to improve the Vip3Aa yield, a mutant *vip3Aa* gene (with the signal peptide deleted) was fused with the promoter and the 3' terminal half of *cry1C*, with the result of a 9-fold increase in the expression of the recombinant protein which was concentrated in inclusion bodies. Unfortunately, this protein showed lower insecticidal activity than the original Vip3Aa protein against the insects tested*,* probably due to low solubilization or improper folding of the protein (Song et al., 2008) (Table I- 5).

*Table I- 5. Genetic engineered Vip3A proteins and effects on insect toxicity.*

| Protein | Modification type(s) | Description[b] | Effect(s) of modification[a] |
|---|---|---|---|
| Vip3AcAa | Domain swapping | Chimera of Vip3Ac N terminus (600 aa) and Vip3Aa C terminus (189 aa) | Gain of toxicity against *O. nubilalis*; IA against *S. frugiperda*, *H. zea*, and *B. mori* |
| Vip3AaAc | Domain swapping | Chimera of Vip3Aa1 N terminus (610 aa) and Vip3Ac C terminus (179 aa) | DA against *S. frugiperda* and *H. zea*; LA against *B. mori* |
| Vip3Aa14 | Protein fusion | Chimera of Vip3Aa14 and Cry1Ac | As effective as Cry1Ac against *H. armigera* and *P. xylostella* but DA compared to Vip3Aa against *S. litura* |
| Vip3Aa7 | Gene promoter change and protein fusion | Chimera of Cry1C promoter with truncated Vip3Aa7 (39 aa deleted at N terminus) and Cry1C C-terminal region | Higher yield of Vip3Aa7, Vip relocation in Bt inclusion bodies but DA against *P. xylostella*, *H. armigera*, and *S. exigua* |
| Vip3Aa7 | Protein fusion | Chimera of Vip3Aa7 and Cry9Ca N terminus | IA against *P. xylostella* |

[a] DA, decrease of activity; IA, increase of activity; LA, loss of activity.
[b] aa, amino acids.
*For information on the source of the toxicity data, please refer to Chakroun* et al*., 2016a,2016b.*

Another type of approach has been the introduction and expression of *vip3A* genes in *B. thuringiensis* strains expressing different *cry* genes, to create new strains to be used in insecticidal formulations with broader spectrum of action. Commercial formulations of *B. thuringiensis* strains contain low amounts of Vip proteins, since these are secreted to the growth medium which is mostly discarded during the

processing of the formulation (Lisansky et al., 1993). This problem can be alleviated by directing the expression of the *vip3A* gene to the sporulation stage using sporulation-dependent promoters and specific transcription sequences from different *cry* genes (Arora et al., 2003; Sellami et al., 2011; Thamthiankul Chankhamhaengdecha et al., 2008; Zhu et al., 2006). The engineered strains in all these cases showed improved production of Vip3A proteins and higher toxicity towards the insects tested. Cloning and expression of the *vip3Aa* gene in *Pseudomonas fluorescens* has also been accomplished with the aim of producing spray insecticides based on the Vip3A protein, either combined or not with Cry proteins (Hernández-Rodríguez et al., 2013). The heterologously expressed Vip3Aa protein, which was not secreted to the media and remained "encapsulated" within the bacterial cell, retained full toxicity.

## Mode of Action

Study of the mode of action of the Vip3 proteins started soon after their discovery in 1996 by Estruch et al. (1996), who proposed that Vip3 proteins would exert their toxicity via a process different from that of the Cry proteins, based on the lack of structural homology of these two types of proteins. Despite being so different, both types of toxins exert their toxic action through apparently the same sequence of events: activation by midgut proteases, crossing the peritrophic membrane, binding to specific proteins in the apical membrane of the epithelial midgut cells, and pore formation (Lee et al., 2003) (Fig. I- 12). Recently, Jiang et al. (2016) have reported evidence on an apoptotic pathway in addition to the pore formation event. So far, all published studies on the mode of action of Vip3 proteins have been carried out with those of the Vip3A family, and mostly on those of the Vip3Aa subfamily. A recent study on the Vip3Ca protein indicate that this protein has a similar mode of action to the Vip3A proteins (Gomis-Cebolla et al., 2017).

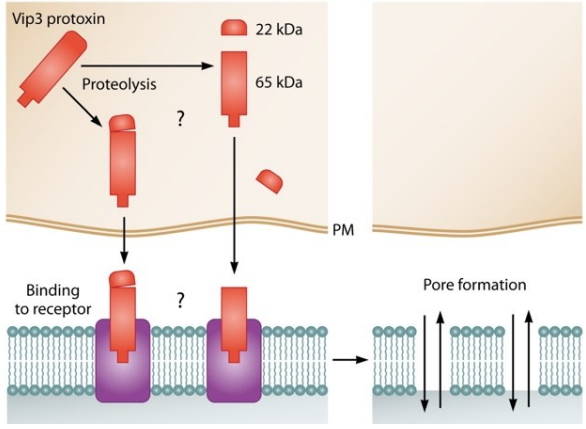


***Fig. I- 12. Proposed mode of action of the Vip3 proteins.***
*The full length protoxin is proteolytically processed by midgut proteases. The 65 kDa fragment binds to specific receptors (either with the 22 kDa fragment still bound or not). Pores are then formed that lead to the death of the cell.*

**Behavioral and histopathological effects.** The behavioral symptoms observed in susceptible insects after ingestion of the Vip3Aa protein resemble the ones observed after Cry intoxication: feeding cessation, loss of gut peristalsis, and overall paralysis of the insect (Yu et al., 1997). After ingestion of the Vip3Aa protein, the analysis of gut cross-sections of susceptible insects shows extensive damage in the midgut, with disrupted, swollen and/or lysed epithelial cells, and leakage of cellular material to the lumen (Abdelkefi-Mesrati et al., 2011a, 2011b; Ben Hamadou-Charfi et al., 2013; Boukedi et al., 2015; Chakroun and Ferré, 2014; Sellami et al., 2015; Yu et al., 1997). No damage was observed either in the foregut or in the hindgut, and neither in the midgut of non-susceptible insects (Yu et al., 1997).

**Proteolytic processing.** *In vitro* proteolysis of full length Vip3Aa proteins using insect midgut juice showed that they are processed to several major proteolytic products, generally of around 62-66, 45, 33, and 22 kDa (Abdelkefi-Mesrati et al., 2011a, 2011b; Ben Hamadou-Charfi et al., 2013; Chakroun and Ferré, 2014; Yu et al., 1997). The 22 kDa fragment corresponds to the N-terminus of the protein (from amino acids 1 to 198 in Vip3Aa1), the 66 kDa fragment to the remainder of the protein (from amino acid 199 to the end in Vip3Aa1), and the 45 and 33 kDa fragments are thought to be derived from the 66 kDa portion (Estruch and Yu, 2001).

The minimal toxic fragment of the Vip3Aa protein has also been studied. Although an early study claimed that the minimal fragment that retained insecticidal activity after proteolysis was the 33 kDa fragment (Estruch and Yu, 2001), all subsequent studies are in favor of the 62-66 kDa fragment as being the Vip3Aa toxic core (Abdelkefi-Mesrati et al., 2011a, 2011b; Ben Hamadou-Charfi et al., 2013; Caccia et al., 2014; Chakroun et al., 2012; Chakroun and Ferré, 2014; Gayen et al., 2012; Hernández-Martínez et al., 2013; Lee et al., 2006, 2003; Li et al., 2007; Liu et al., 2011). Interestingly, the 20 kDa fragment produced upon proteolytic processing of the Vip3Aa16 protoxin co-purifies with the 62 kDa fragment, suggesting that, after activation of the full length protein, the two fragments remain together (Chakroun and Ferré, 2014).

Compared to Cry proteins, the 62-66 kDa toxic core of Vip3A proteins is more susceptible to the action of proteases. Incubation of either Vip3Aa or Vip3Ae with commercial serine-proteases or insect midgut juice showed the unstable nature of the 62 kDa fragment, which started to break down even before all the protoxin is processed (Abdelkefi-Mesrati et al., 2011a; Ben Hamadou-Charfi et al., 2013; Caccia et al., 2014; Chakroun and Ferré, 2014; Yu et al., 1997). Partial purification of peptidases from the *S. frugiperda* midgut juice showed that cationic trypsin-like and anionic chymotrypsin-like peptidases are involved in the formation of the Vip3A 62 kDa fragment, whereas cationic chymotrypsin-like peptidases participated in its further processing (Caccia et al., 2014).

In general, the proteolytic activation does not seem to be a critical step in determining Vip3A insect toxicity and specificity. It has been shown that the midgut juice of a non-susceptible insect (*O. nubilalis*) could process Vip3A *in vitro* to a 65 kDa fragment which was fully toxic when fed to susceptible insects (Yu et al., 1997). However, in some cases the rate of processing of the full length protein has been

proposed to account for differences in the toxicity of a given Vip3A protein to different insect species (Abdelkefi-Mesrati et al., 2011a; Caccia et al., 2014; Chakroun et al., 2012). Indeed, some studies have shown that differences in mortality disappeared when the trypsin activated protein was used instead of the full length protein (Chakroun et al., 2012; Hernández-Martínez et al., 2013).

**Binding to the larval midgut epithelium.** *In vivo* immunolocalization studies have shown that Vip3A binds to the apical microvilli of midgut epithelial cells (Chakroun and Ferré, 2014; Yu et al., 1997) (Fig. I-13). Specific binding to the brush border membrane vesicles (BBMV) prepared from susceptible insects was first shown using biotin-labeled Vip3Aa and Vip3Af (Abdelkefi-Mesrati et al., 2011b; Ben Hamadou-Charfi et al., 2013; Bergamasco et al., 2013; Lee et al., 2006, 2003; Liu et al., 2011; Sena et al., 2009). Interestingly, Vip3Aa also binds specifically to the BBMV of the non-susceptible *O. nubilalis* (Lee et al., 2003), which indicates that specific binding is necessary but not sufficient to produce toxicity.

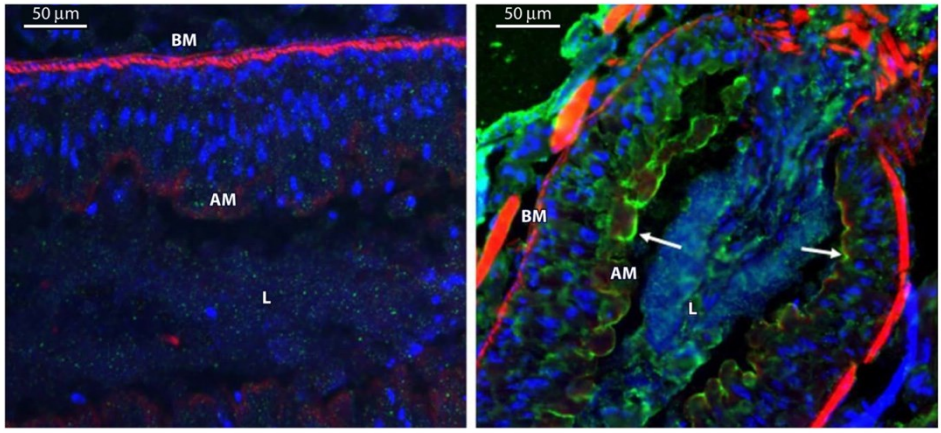


***Fig. I- 13. Immunolocalization of Vip3Aa in midgut tissue sections after ingestion by*** S. frugiperda ***larvae.***
*Left panel: Control larvae. Right panel: Larvae that ingested Vip3Aa. Nuclei were stained blue, and the apical and the basal membranes were stained red. Binding of Vip3Aa to the apical membrane is shown in green. BM: basal membrane, AM: apical membrane, L: gut lumen. (reprinted from* Chakroun and Ferré, 2014).

Quantitative binding parameters were obtained using the $^{125}$I-labeled Vip3Aa and *S. frugiperda* BBMV. This binding was found to be saturable, mostly irreversible, and differentially affected by the presence of divalent cations (Chakroun and Ferré, 2014). Vip3A proteins were also found to have lower affinities but higher numbers of binding sites compared with the Cry1A and Cry2A proteins. Interestingly, homologous competition showed that both the 62 kDa and the 20 kDa fragments of the trypsin-activated $^{125}$I-Vip3Aa bound to BBMV, and both were displaced by the addition of non-labeled Vip3Aa. By contrast, using biotin-labeled Vip3Aa, Liu et al. (2011) found that only the 62 kDa fragment was able to bind to the BBMV of *H. armigera*, and also that the 20 kDa fragment was found exclusively in the supernatant of the binding reaction.

Competition binding assays showed the absence of shared binding sites between Vip3A and Cry proteins. This has been shown for Vip3Aa with Cry1Ac, Cry1Ab, Cry1Fa, Cry2Ae, and Cry2Ab in all insect species tested, and for Vip3Af with Cry1Ab and Cry1F in *S. frugiperda* (Ben Hamadou-Charfi et al., 2013; Chakroun and Ferré, 2014; Gouffon et al., 2011; Lee et al., 2006; Liu et al., 2011; Sena et al., 2009). However, Bergamasco et al. (2013) reported partial competition of Cry1Ia for the Vip3Aa binding sites in *S. eridania* BBMV, but not in *S. frugiperda*, *S. albula*, and *S. cosmioides* BBMV. Competition among proteins of the Vip3A family has only been tested in *S. frugiperda* (Chakroun and Ferré, 2014). Vip3Ae, Vip3Af, and even the non-active Vip3Ad, competed for the Vip3Aa binding sites with no significant differences in their binding parameters. A general model of the binding sites of Vip3A proteins in relation to Cry proteins is shown in Fig. I- 14.

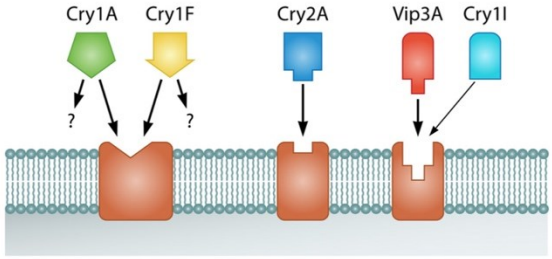


***Fig. I- 14. General binding site model for the Cry and Vip proteins in the midgut epithelial membrane of lepidopteran larvae.***
*Cry1Fa and Cry1A proteins, in addition to the shared binding site, may have other sites depending on the insect species considered. Recognition of Vip3Aa sites by Cry1Ia has been found only in* S. eridania *(out of four* Spodoptera *species tested).*

Interaction of Vip3Aa with the BBMV of the susceptible insects involves specific binding molecules different from the ones recognized by Cry1A proteins. Ligand blot analyses revealed that Vip3Aa recognized 80 and 110 kDa proteins in *Manduca sexta* (Lepidoptera: Sphingidae), while Cry1Ab bound to proteins of 120 and 210 kDa (Lee et al., 2003). The same study showed that Vip3Aa was unable to bind to the purified aminopeptidase N (APN) and the cadherin ectodomain toxin-binding region (TBR) from *M. sexta*, both membrane proteins known to bind Cry proteins (Lee et al., 2003). In *Prays oleae* (Lepidoptera: Yponomeutidae) and *Agrotis segetum* (Lepidoptera: Noctuidae) Vip3Aa bound to a 65 kDa protein, while Cry1Ac bound to a 210 kDa band in *P. oleae* and to a 120 kDa band in *A. segetum* (Abdelkefi-Mesrati et al., 2009; Ben Hamadou-Charfi et al., 2013). In *S. littoralis*, Vip3Aa bound proteins of 55 and 100 kDa (Abdelkefi-Mesrati et al., 2011b), and in *Ephestia kuehniella* (Lepidoptera: Pyralidae), *S. frugiperda*, *S. albula*, *S. cosmioides*, and *S. eridania*, to a protein of 65 kDa (Abdelkefi-Mesrati et al., 2011a; Bergamasco et al., 2013), to which Cry1Ia also bound in the four *Spodoptera* species (Bergamasco et al., 2013).
Very few studies have addressed the identity of the Vip3A binding molecules in the insect midgut. Two Vip3Aa binding molecules have been identified so far using the yeast two hybrid system. The first one was a 48 kDa protein from *A. ipsilon* with

homology to a family of extracellular glycoproteins called tenascins, which could be associated with apoptotic processes (Estruch and Yu, 2001). The second binding molecule was the S2 ribosomal protein from *S. litura*, identified as a Vip3A receptor in Sf21 cells (Singh et al., 2010). Silencing of the S2 gene reduced the toxicity of Vip3A to both Sf21 cells and fifth-instar *S. litura* larvae. Both S2 and Vip3Aa co-localized in the surface and cytoplasm of Sf21 cells, suggesting that the interaction takes place in the cell surface and, once pores are produced, the Vip3-S2 complex internalizes (Singh et al., 2010). How this S2-Vip3A protein interaction could trigger the lysis of the cells was not explained and remains unknown. In *H. armigera*, the molecules that bind to Vip3Aa were found to be slightly associated with lipid rafts (Sena et al., 2009). In an attempt to understand how midgut cells respond to the intoxication by Vip3 proteins, gene expression profiles of *S. exigua* larvae treated with a sublethal dose of Vip3Aa were obtained using a genome-wide microarray that included more than 29,000 unigenes (Bel et al., 2013). No alteration was found in the expression levels of the two Vip3A binding proteins described above (S2 and the tenascin X-tox-like protein), nor in genes related to the mode of action of the Cry proteins. It was concluded that the lack of significant changes in the transcription levels of the genes analyzed was most likely due to the fact that either they were not involved in the Vip3 mode of action, or because the mechanisms of defense against Vip3A toxins do not rely on the regulation of the members involved in the mode of action.

Pore formation. Despite the absence of any predicted pore-forming domains in the Vip3 proteins, the pore formation activity of the Vip3Aa protein activated with trypsin or midgut juice has been demonstrated by voltage clamping assays with dissected midguts of *M. sexta* (Lepidoptera: Sphingidae) and also in planar lipid bilayers (Lee et al., 2003). In contrast, the full length Vip3Aa protein was unable to form pores. The ion channels were able to destroy the transmembrane potential, and they were voltage independent and cation selective (Lee et al., 2003).The pore forming ability of the activated Vip3Aa was also demonstrated by fluorescence quenching using *H. armigera* BBMV (Liu et al., 2011). The formation of Vip3Aa ion channels was restricted to susceptible insects, and they have been found to have biophysical properties that differ from those of Cry1Ab in *M. sexta* (Lee et al., 2003).

## Resistance and Cross-Resistance

Very few cases have been reported on resistance to Vip3 proteins. Laboratory selection of a *H. virescens* colony led to 2,040-fold resistance to Vip3Aa compared to the unselected population (Pickett, 2009). Resistance was found to be polygenic with possible paternal influence, and ranged from almost completely recessive to incompletely dominant; fitness costs were temperature dependent, with reduced mating success, fecundity, and fertility (Gulzar et al., 2012). After 12 generations of selection with Vip3A, a freshly established laboratory colony of *S. litura* reached a resistance level of 285-fold compared to a susceptible colony (Barkhade and Thakare, 2010). The resistant insects were found to lack two casein-degrading bands in non-

denaturing electrophoretic gels and to have reduced proteolytic activity (2-fold) toward several protease substrates.

The presence of Vip3Aa resistance alleles in field populations was studied in *H. armigera* and *H. punctigera* (Lepidoptera: Noctuidae) was studied in Australia by using the F2 screening method (Mahon et al., 2012). The results showed that resistance alleles in both insect species existed as natural polymorphisms at a relatively high frequency (0.027 and 0.008 respectively), above mutation rates normally encountered (Mahon et al., 2012). Interestingly, within each species, the resistance of two different F2 families was due to alleles at the same locus, and resistance was found to be essentially recessive, most probably conferred by a single gene, and did not confer cross-resistance to Cry1Ac or Cry2Ab (Mahon et al., 2012). The frequency of resistant alleles in *H. armigera* did not increase over the following four seasons (until 2014/2015), and resistant insects were found to activate the Vip3Aa protoxin more slowly than susceptible insects, although no significant differences in binding to membrane receptors were found (Chakroun et al., 2016c). Further studies on the resistant *H. punctigera* strain confirmed that there was no linkage between the Vip3A and the Cry2Ab resistance loci (Walsh et al., 2014). A study on the presence of Vip3Aa resistance alleles in field populations of *S. frugiperda* from different states of Brazil, using the F2 method, estimated an overall frequency of 0.0009, which is relatively low (Bernardi et al., 2015).

The increased use of Vip3 toxins in pyramided *Bacillus thuringiensis* treated crops (Bt-crops) to improve both pest control and resistance management, sparked interest in the evaluation of cross-resistance between Cry and Vip3A proteins (Kurtz, 2010). So far, no significant cross-resistance between these two classes of proteins has been described. Vip3Aa was found to be equally toxic to a susceptible and to three Cry resistant *H. virescens* strains (YHD2, resistant to Cry1Ac, Cry1F, and slightly cross-resistant to Cry2A, and CXC and KCBhyb, both resistant to Cry1Ac, Cry1Aa, Cry1Ab, Cry1F, and Cry2Aa2) (Jackson et al., 2007). Two studies on Cry1Acresistant strains of *H. zea* showed no significant cross-resistance to Vip3A or Cry2Ab (Anilkumar et al., 2008; Welch et al., 2015). A study on two *H. armigera* populations from Cry1Ac-cotton planting regions in China showed a lack of significant correlation between the responses to Vip3Aa and those to Cry1Ac, suggesting little or no cross-resistance between these two toxins (An et al., 2010). Cross-resistance to Vip3A has also been studied in two *S. frugiperda* Cry1F-resistant populations, one collected from Bt maize fields in Puerto Rico and the other collected from the southeast United States. Both populations were very susceptible to Vip3Aa, indicating the absence of cross-resistance between the Vip3Aa and Cry1F proteins (Huang et al., 2014; Vélez et al., 2013). A study using a different Vip3A protein, Vip3Ac, showed that it was equally toxic to susceptible and Cry1Ac-resistant *Trichoplusia ni* (Lepidoptera: Noctuidae) strains (Fang et al., 2007). However, in this case, the resistant strain was slightly less susceptible to Vip3Aa (resistance ratio of 2.1) and to two Vip3A chimeric proteins (resistance ratios of 1.8 and 3.2) (Fang et al., 2007).

## Expression in Plants

The *vip3Aa* gene has been successfully introduced in cotton and in corn, and later combined with other *cry* genes to confer higher protection and delay insect resistance (https://www.epa.gov/ingredients-used-pesticide-products/current-and-previously-registered-section-3-plant-incorporated). VipCot™ and Agrisure Viptera™ were registered in the USA in 2008 and 2009, respectively (Syngenta Seeds, Inc.). The former is the result of event COT102 in cotton, which produces the Vip3Aa19 protein (http://www.isaaa.org/gmapprovaldatabase/gene/default.asp?GeneID=24&Gene=vip3A(a); http://en.biosafetyscanner.org/schedaevento.php?evento=208), whereas the latter contains the event MIR162 in corn, which produces the Vip3Aa20 protein (http://iaspub.epa.gov/apex/pesticides/f?p=CHEMICALSEARCH:30#p). Both events have been pyramided with *cry1Ab* (VipCot™ Vip3Aa + mCry1Ab, and Agrisure Viptera™ Vip3Aa + Cry1Ab), and later with *cry1Fa* (VipCot™ Vip3Aa + Cry1Ac + Cry1Fa, and Agrisure Viptera™ Vip3Aa + Cry1Ab + Cry1Fa) to confer a wider and more robust protection against Lepidoptera(Adamczyk and Mahaffey, 2008; Burkness et al., 2010; Kurtz et al., 2007). Furthermore, the corn event MIR162 has been stacked with other *cry* genes expressing proteins active against Coleoptera (Cry3A and eCry3.1Ab) to confer protection against these two insect orders (Carrière et al., 2015). A three-year study on the field performance of VipCot™ expressing just the Vip3Aa protein indicated that the plants were highly efficacious against *H. armigera* early in the season, but that the efficacy declined as the season progressed, though not so drastically as Cry1Ac in Bollgard™ or Ingard™ cotton (Llewellyn et al., 2007). In 2015, the first modified Vip3A, with improved toxicity, was introduced in tobacco conferring almost total protection towards *H. armigera*, *A. ipsilon*, and *S. littoralis* (Gayen et al., 2015).

Cotton has also been transformed with a synthetic *vip3A* gene fused to a chloroplast transit peptide coding sequence (Wu et al., 2011). The Vip3A protein accumulated in the chloroplasts and its concentration in the plant was higher than in plants transformed with just the synthetic gene. Transformed plants provoked 100% mortality to larvae of *S. frugiperda*, *S. exigua*, and *H. zea.*

# OBJECTIVES

# OBJECTIUS

L'objectiu general d'esta Tesi Doctoral és aportar nova informació en relació a l'estructura molecular i la conformació de les proteïnes Vip3A i la seva relació amb l'acció insecticida sobre plagues de lepidòpters d'interès agrícola. Amb un millor coneixement de l'estructura de les proteïnes Vip3A es pretén contribuir a una major comprensió de les bases moleculars del mode d'acció i de l'avaluació de risc, així com dels fenòmens de resistència que puguen sorgir com a conseqüència del seu ús habitual en la protecció integrada de cultius.

Per a este efecte, es varen plantejar els següents objectius específics:

1. Caracteritzar l'espectre insecticida de diferents proteïnes Vip3A.
   1.1. Provar l'eficàcia en condicions preliminars de les proteïnes Vip3Aa, Vip3Ab, Vip3Ae, Vip3Af i Vip3Ad front a 8 espècies de lepidòpters de tres famílies diferents. Establir paràmetres quantitatius de l'eficàcia del control ($LC_{50}$) de les combinacions proteïna/insecte més significatives. Analitzar possibles diferències en l'eficàcia de les pro-toxines i les toxines activades del les Vip3A en estudi.
   1.2. Establir la combinació toxina-insecte model amb què desenvolupar l'estudi de la relació estructura-funció de les Vip3A.

2. Analitzar l'estabilitat front l'acció de les proteases digestives en presència de detergent (SDS). Inferir en aspectes estructurals de la Vip3Aa i de la Vip3Af.
   2.1. Analitzar les cinètiques d'activació de les proteïnes front diferents concentracions de serín-proteases.
   2.2. Provar la influència de l'SDS en el procés digestiu i en la caracterització dels fragments d'activació en SDS-PAGE mitjançant l'ús d'inhibidors específics i la separació de fragments per cromatografia de filtració en gel.
   2.3. Identificar els principals fragments resultants de l'activació de la pro-toxina mitjançant seqüenciació de la N-terminal i la petjada peptídica.

3. Establir els aminoàcids i regions crítiques per a l'activitat insecticida i l'estabilitat d'una proteïna Vip3A mitjançant l'escaneig d'alanina.
   3.1. Bio-assajar la col·lecció de mutants d'alanina front a una espècie susceptible de plaga i seleccionar les mutacions que causen una disminució significativa en la funció insecticida. Confirmar els resultats sobre una segona espècie.
   3.2. Caracteritzar la contribució de les posicions crítiques seleccionades a l'estabilitat de la proteïna front tripsina i front l'extracte de proteases digestives de les espècies susceptibles bio-assajades. Identificar els fragments principals produïts després del tractament proteolític mitjançant seqüenciació de la N-terminal i/o petjada peptídica.

3.3. Analitzar les diferències en el plegament de les proteïnes mutades amb reduïda activitat insecticida mitjançant l'obtenció de l'espectre d'emissió de fluorescència intrínseca.
3.4. Proposar una model tridimensional d'una proteïna Vip3A.

4. Realitzar mutacions dirigides per tal d'incrementar el potencial insecticida de la Vip3Af i inferir en aspectes estructurals.

# OBJECTIVES

The main goal of this thesis is to shed some light on the molecular structure and spatial architecture of Vip3A proteins and their relationship with their insecticidal action on lepidopteran pests of agricultural interest. A better understanding of the Vip3A structure will contribute to ease the safety risk assessment and to a greater understanding of the molecular mode of action, as well as to the resistance events that may arise as a result of their common use for crop protection.

To that end, the following specific objectives were stablished:

1. Characterize the insecticidal spectra of different Vip3A proteins.
   1.1. To perform preliminary assays for the assessment of the effectiveness of 5 Vip3A proteins (Vip3Ab, Vip3Ae, Vip3Af Vip3Ad) against 8 caterpillar species of three different taxonomic families. To establishing quantitative parameters of the effectiveness ($LC_{50}$) for the protein / insect combinations with most promising results. Address the possible differences of the pro-toxins and the activated toxins.
   1.2. To select the insect-toxin combination for further development of the structure-function relationship study.

2. Analyze the stability against digestive proteases in the presence of SDS and inference of structural aspects of the Vip3Aa and Vip3Af proteins.
   2.1. To analyze the activation kinetics of the Vip3A proteins treated with different concentrations of proteases.
   2.2. To test the influence of the SDS on the digestion using specific inhibitors and the characterization of the resulting proteolytic fragments by gel filtration chromatography.
   2.3. To identify the main proteolytic fragments by N-terminal sequencing and peptide mass fingerprinting.

3. Identify critical amino acid positions for the insecticidal performance and to set "*hot spots*" in the Vip3A primary sequence by alanine-scanning.
   3.1. To test the alanine-mutant collection against a susceptible pest and select mutations that cause a significant decrease in the insecticide activity. Confirmation of the results on a second species.
   3.2. Describe the contribution of selected positions to the protein stability against trypsin and midgut juice from the susceptible species tested. Identify the main proteolytic fragments by N-terminal sequencing and / or peptide mass fingerprinting.

3.3. To analyze the differences in protein folding of the mutated proteins with a reduced insecticidal activity by obtaining the intrinsic fluorescence emission spectra.
3.4. To propose a three-dimensional model of a Vip3A protein.

4. Perform site-directed mutagenesis of a Vip3A protein in order to attempt an increase of the insecticide potency and infer structural aspects.

# CHAPTER I

## 1. A screening of five *Bacillus thuringiensis* Vip3A proteins for their activity against lepidopteran pests.

Results from this chapter are included in:

Ruiz de Escudero I, Banyuls N, Bel Y, Maeztu M, Escriche B, Muñoz D, Caballero P, Ferré J,. (2014). A screening of five *Bacillus thuringiensis* Vip3A proteins for their activity against lepidopteran pests. J Invertebr Pathol.; 117: 51–55.

## 1.1. Introduction

Vip3 insecticidal proteins are produced by *Bacillus thuringiensis* during the vegetative growth phase and most of them have activity against lepidopteran species. The Vip3 proteins are currently classified in three subfamilies based on their amino acid identity: Vip3A, Vip3B and Vip3C (Crickmore et al., 2014). Most studies on the insecticidal activity of Vip3 proteins have been carried out with Vip3Aa, which is the first protein discovered of this family (Estruch et al., 1996). This protein has been shown to have a broad activity spectrum against lepidopteran pests (for a review see (Milne et al., 2008). Vip3A proteins have been shown to target receptors in the insect midgut different to those used by Cry proteins (Gouffon et al., 2011; Lee et al., 2006; Liu et al., 2011; Sena et al., 2009), which makes them a good alternative or complement to Cry proteins for resistant management. Plants expressing the *vip3Aa* gene along with *cry* genes have been developed and transgenic corn and cotton expressing *vip3Aa* have been commercialized for the control of lepidopteran pests (Raybould and Quemada, 2010).
Since the discovery of Vip3Aa, *B. thuringiensis* collections have been screened for new *vip3* genes, with the result of a considerable increase in the number of new members in the *vip3* family (Asokan et al., 2012; Beard et al., 2008; Hernández-Rodríguez et al., 2009; Mesrati et al., 2005; Palma et al., 2012; Rang et al., 2005). Despite this, there are still very few data on the activity of Vip3 proteins other than Vip3Aa variants. In this paper we have tested the insecticidal activity of five Vip3 proteins against eight lepidopteran pests and the results have revealed important differences in their insecticidal spectrum despite the high amino acid identity among some of them.

## 1.2. Materials and methods

### 1.2.1. Insect colonies.

Insects were grown in the insectaries of the Public University of Navarra and of the University of Valencia under controlled conditions of temperature, humidity and photoperiod (25±2 ºC, 70±5 % RH, and L16:D8 h). Insects were reared on different semi-synthetic diet. *Agrotis ipsilon, Helicoverpa armigera*, *Mamestra brassicae*, *Spodoptera exigua, Spodoptera frugiperda* and *Spodoptera littoralis* (Lepidoptera: Noctuidae) were maintained in a growth wheat germ-based semi-synthetic diet (Greene et al., 1976). For *Ostrinia nubilalis* (Lepidoptera: Crambidae) and *Lobesia botrana* (Lepidoptera: Tortricidae), a flour corn diet was used (Ruiz de Escudero et al., 2007).

### 1.2.2. Source of vip3 genes and protein preparation.

*Escherichia coli* clones carrying plasmids carrying the genes *vip3Aa1* (pGA85, NCBI accession No. AAC37036), *vip3Ab* [pGA65; identical to *vip3Ab1* (NCBI accession No. AAR40284) except in that the 2nd codon is GAC (encoding D) rather than AAT (encoding N)], *vip3Ad2* (pGA59, NCBI accession No. CAI43276), *vip3Ae1* (pGA60, NCBI accession No. CAI43277) and *vip3Af1* (pGA58, NCBI accession No. CAI43275), were kindly provided by Bayer CropScience NV (Ghent, Belgium) and were expressed in *E. coli* WK6. A multiple amino acid sequence alignment was performed using ClustalX v2.1 (Larkin et al., 2007) and the percent identity among proteins was calculated using the Multiple Sequence Aligment Editor software GeneDoc 2.7.0 (Nicholas et al., 1997) (Table 1.1).

*Table 1. 1. Percent identity between Vip3A proteins at the amino acid level.*

| | *Vip3Aa1* | *Vip3Ab* | *Vip3Ad2* | *Vip3Ae1* | *Vip3Af1* |
|---|---|---|---|---|---|
| *Vip3Aa1* | - | | | | |
| *Vip3Ab* | *83* | - | | | |
| *Vip3Ad2* | *85* | *80* | - | | |
| *Vip3Ae1* | *81* | *90* | *82* | - | |
| *Vip3Af1* | *88* | *86* | *80* | *83* | - |

Protein expression was done by picking out one single colony of recombinant *E. coli* and inoculating in preculture of LB medium (20 ml) with ampicillin (100 µg/ml). After overnight incubation at 37 °C in an orbital shaker at 180 rpm, 5 ml of preculture were transferred to a 500 ml of the same culture medium and incubated at 37 °C in an orbital shaker at 180 rpm. When the $OD_{600}$ reached a value between 1.6 and 1.8, 1 mM isopropyl-D-thiogalactopyranoside (IPTG) was added for induction of *vip3* gene expression. The culture was grown overnight at 37 °C in a shaking incubator at 180 rpm. Cells were centrifuged at 8,800 *g* for 30 min. The pellet was resuspended (3 ml per gram of pellet) in lysis buffer (20 mM phosphate buffer pH 7.4, 0.5 M NaCl, 3 mg/ml lysozyme, 10 µg/ml DNAse and 100 µM phenylmethylsulfonyl fluoride) and incubated with shaking for 30 min at 37 °C. Cells were lysed by sonication of 15 ml aliquots in a Bandelin Sonoplus sonicator HD 2070 (on ice, twice for 60 s, with a 10 s pause in between, at 70% maximal power). The Vip3A proteins in the supernatant were recovered following centrifugation at 27,000 *g* and then filtered through a 0.45 µm filter followed by a second filtration through a 0.2 µm filter. To obtain the trypsin-activated Vip3A proteins, the protoxin samples were incubated with 1% bovine pancreas trypsin (Sigma-Aldrich) (wt of Vip protein/wt trypsin) at 37 °C for 1 h. Because we had observed instability of the VipA proteins when stored at −20 °C directly in the *E. coli* lysate extract, both protoxins and activated toxins were subjected to ammonium sulfate precipitation (70%). After centrifugation at 10,000*g* for 15 min, the pellet was stored at −20 °C until required.

Vip3A production, solubilization and activation were checked by 12% sodium dodecyl sulfate polyacrilamide gel electrophoresis (SDS-PAGE). All the protoxin forms had an apparent molecular mass of around 89 kDa and the trypsin-activated proteins of

around 66 kDa (Fig. 1.1). Concentration of the protoxins and activated toxins was estimated densitometrically from the intensity of the corresponding bands in the gel with a 1D Manager ver. 2.0 program (TDI Tecnología de Diagnóstico e Investigación).

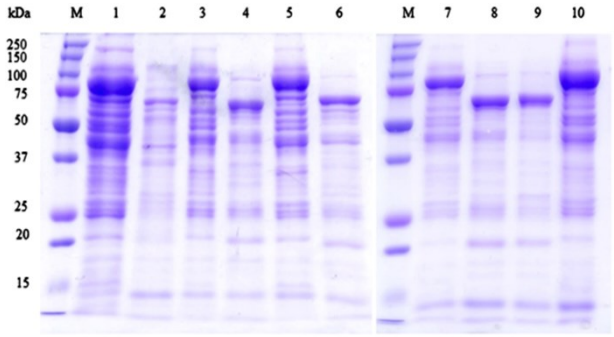


***Fig. 1. 1. Electrophoresis of*** E. coli ***extracts expressing either Vip3A protoxins or activated toxins.***
*M: Molecular Weight Marker (Bio-RadPrecision Plus Protein Unstained Standards), 1: Vip3Aa protoxin, 2: Vip3Aa toxin, 3: Vip3Ab protoxin, 4: Vip3Ab toxin, 5: Vip3Ad protoxin, 6: Vip3Ad toxin, Vip3Ae protoxin, 8: Vip3Ae toxin, 9: Vip3Af toxin, and 10:Vip3Af protoxin.*

### 1.2.3. Bioassays.

Before being used in bioassays, the precipitated Vip3A protoxins were solubilized in 20 mM phosphate buffer, 0.5 M NaCl, pH 7.4. Surface contamination assays were carried out by applying 50 µl of the sample dilutions on artificial diet (in 2 $cm^2$ multiwell plates). Qualitative bioassays were carried out in duplicate at a single protein concentration (2.5 µg/$cm^2$) and with 16 neonate larvae per replicate. For *L. botrana* bioassays, protoxins and toxins were incorporated in the diet at a final concentration of 50 µg/ml of diet as described in Ruiz de Escudero et al. (2007). Controls with just buffer were run in parallel. Only those bioassays with mortality in the controls lower than 10% were considered. Trays were incubated at 25±2 ºC, 70±5 % RH, and L16:D8 h and mortality was scored at 7 and 10 days. "Functional mortality" was defined as dead larvae plus larvae arrested at L1. This parameter was included because Vip3A proteins with low activity against some insect species could still be chosen for their potential interest by arresting larval development, which under field conditions can be as effective to control the pest as killing the larvae. Quantitative bioassays were replicated at least three times using between five and seven concentrations of Vip3A protein samples and 16 neonate larvae for each concentration. Estimation of $LC_{50}$ in dose-response bioassays was performed using the Polo-PC software (LeOra-software, Berkeley, CA). $LC_{50}$ values were considered significantly different when fiducial limits of Relative Potency did not include the unit or they did not overlap.

## 1.3. Results and Discussion

As a first approach to determine which of the five Vip3A proteins were active against the eight test insect species, a qualitative screening assay was first carried out. Vip3A proteins were tested at a high concentration to select those species that were most susceptible. Table 1.2 shows the results obtained with the protoxin form of the proteins and Table 1.3 with the activated toxins. Comparing the results in both tables, no major differences were found in the toxicities of the protoxins *vs*. the activated toxins. Therefore, the lack of toxicity of the proteins against some of the insect species is most likely not due to a problem in the conversion of the protoxin to the toxin form. The result obtained with Vip3Aa and *S. exigua* is in contrast with that of a previous publication in which the activated toxin was significantly more active than the protoxin (Chakroun et al., 2012). This discrepancy may be explained by the different type of Vip3Aa protein used (Vip3Aa16 instead of Vip3Aa1) and/or the different preparation of the protoxin.

*Table 1. 2. Effect of Vip3A protoxins at 2.5 µg/cm² [percent mortality (M) or functional mortality (FM)] on neonate larvae from different insect species[a].*

| Insect species | Vip3Aa | | | Vip3Ab | | | Vip3Ad | | | Vip3Ae | | | Vip3Af | | |
|---|---|---|---|---|---|---|---|---|---|---|---|---|---|---|---|
| | 7 d | | 10 d | 7 d | | 10 d | 7 d | | 10 d | 7 d | | 10 d | 7 d | | 10 d |
| | M | FM | M | M | FM | M | M | FM | M | M | FM | M | M | FM | M |
| *A. ipsilon* | 98[b] | 98[b] | 100[b] | 91 | 100 | 93 | 10[b] | 10[b] | -[c] | 99[b] | 99[b] | 100[b] | 99[b] | 99[b] | 100[b] |
| *H. armigera* | 49 | 100 | 64 | 29 | 59 | 36 | 6 | 16 | 16 | 43 | 97 | 72 | 75 | 100 | 91 |
| *M. brassicae* | 100 | 100 | 100 | 4 | 4 | 8 | 4 | 4 | 8 | 88 | 88 | 88 | 100 | 100 | 100 |
| *S. exigua* | 80 | 100 | 99 | 71 | 100 | 83 | 0 | 0 | 0 | 100 | 100 | 100 | 23 | 77 | 65 |
| *S. frugiperda* | 100[b] | 100[b] | 100[b] | 88 | 100 | 100 | 0[b] | 0[b] | 0[b] | 99[b] | 100[b] | 100[b] | 99[b] | 100[b] | 100 |
| *S. littoralis* | 100 | 100 | 100 | 100 | 100 | 100 | 4 | 4 | 4 | 100 | 100 | 100 | 100 | 100 | 100 |
| *O. nubilalis*[d] | 21 | 26 | 22 | 7 | 7 | 8 | 0 | 0 | 3 | 20 | 22 | 22 | 26 | 41 | 29 |
| *L. botrana* | 90 | 90 | 95 | 10 | 10 | 10 | 10 | 10 | 10 | 100 | 100 | 100 | 100 | 100 | 100 |

[a] *Values represent the mean of two replicates.*
[b] *Data extrapolated from Hernández-Martínez* et al.*, (2013).*
[c] *Not tested.*
[d] *Values are the mean of four replicates.*

*Table 1. 3. Effect of Vip3A activated toxins at 2.5 µg/cm² [percent mortality (M) or functional mortality (FM)] on neonate larvae from different insect species[a].*

| Insect species | Vip3Aa | | | Vip3Ab | | | Vip3Ad | | | Vip3Ae | | | Vip3Af | | |
|---|---|---|---|---|---|---|---|---|---|---|---|---|---|---|---|
| | 7 d | | 10 d | 7 d | | 10 d | 7 d | | 10 d | 7 d | | 10 d | 7 d | | 10 d |
| | M | FM | M | M | FM | M | M | FM | M | M | FM | M | M | FM | M |
| *A. ipsilon* | 96[b] | 96[b] | -[c] | 92 | 100 | 95 | 10[b] | 10[b] | -[c] | 99[b] | 99[b] | - | 93[b] | 93[b] | - |
| *H. armigera* | 72 | 100 | 91 | 16 | 66 | 22 | 16 | 16 | 16 | 66 | 97 | 94 | 81 | 100 | 93 |
| *M. brassicae* | 100 | 100 | 100 | 0 | 0 | 0 | 8 | 13 | 17 | 83 | 83 | 83 | 100 | 100 | 100 |
| *S. exigua* | 89 | 100 | 100 | 71 | 92 | 71 | 0 | 0 | 0 | 100 | 100 | 100 | 44 | 100 | 58 |
| *S. frugiperda* | 100[b] | 100[b] | 100[b] | 100 | 100 | 100 | 0[b] | 0[b] | 0[b] | 96[b] | 100[b] | 100[b] | 99[b] | 100[b] | 100[b] |
| *S. littoralis* | 100 | 100 | 100 | 100 | 100 | 100 | 4 | 4 | 4 | 100 | 100 | 100 | 100 | 100 | 100 |
| *O. nubilalis*[d] | 21 | 21 | 21 | 2 | 2 | 2 | 9 | 9 | 9 | 19 | 19 | 19 | 41 | 50 | 45 |
| *L. botrana* | 100 | 100 | 100 | 45 | 45 | 45 | 5 | 5 | 10 | 100 | 100 | 100 | 100 | 100 | 100 |

[a] *Values represent the mean of two replicates.*
[b] *Data extrapolated from Hernández-Martínez* et al.*, (2013).*
[c] *Not tested.*
[d] *Values are the mean of four replicates.*

To evaluate the results of this first screening assay, we considered of "potential interest" those proteins for which the protoxin affected at least 80% of the insects in any of the parameters measured (mortality or functional mortality). According to this criterion, the proteins active against most of the insect species were Vip3Aa, Vip3Ae and Vip3Af, followed by Vip3Ab. Vip3Ad was not toxic to any of the species tested.
Considering the results in Tables 1.2 and 1.3 by insect species, *A. ipsilon*, *S. frugiperda* and *S. littoralis* were susceptible to Vip3Aa, Vip3Ab, Vip3Ae and Vip3Af; *S. exigua* was susceptible to Vip3Aa and Vip3Ae, and moderately susceptible to Vip3Ab; *M. brassicae* and *L. botrana* were susceptible to Vip3Aa, Vip3Ae and Vip3Af; *H. armigera* was moderately susceptible to Vip3Aa, Vip3Ae and Vip3Af, and *O. nubilalis* was tolerant to all Vip3A proteins tested, although it showed some susceptibility to Vip3Af.
To confirm the qualitative results and to obtain quantitative parameters of the most active proteins (Vip3Aa, Vip3Ab, Vip3Ae and Vip3Af), concentration-mortality assays were performed with those combinations of protein/insect for which the Vip3A protein was considered of "potential interest" according to the criterion indicated above. The results are shown in Table 1.4. Vip3Ab was found highly toxic to *A. ipsilon* ($LC_{50}$ = 62 ng/cm$^2$) (a species non-susceptible to Cry toxins), and moderately toxic to the three *Spodoptera* species tested ($LC_{50}$ values from 163 to 2020 ng/cm$^2$). Compared with Vip3Aa, Vip3Ae and Vip3Af, Vip3Ab was less active to *S. littoralis* (Table 1.4).

*Table 1. 4. Quantitative parameters from concentration-mortality responses (at 7 days) of most active Vip3A protoxins on their respective insect species.*

| Treatment | Regression line | | $LC_{50}$ | 95% F. L.[a] | | Goodness of fit | Relative potency | 95% F. L.[a] | |
|---|---|---|---|---|---|---|---|---|---|
| | Slope±SE | a[b]±SE | (ng/cm$^2$) | Lower | Upper | $\chi^2$ | | Lower | Upper |
| ***A. ipsilon*** | | | | | | | | | |
| Vip3Ab | 0.9±0.1 | 4.6±0.2 | 62 | 37 | 100 | 9.5 | - | - | - |
| ***H. armigera*** | | | | | | | | | |
| Vip3Aa | 1.4±0.2 | 1.4±0.7 | 1660 | 1040 | 2470 | 7.4 | 3.2 | 1.4 | 7.7 |
| Vip3Ae | 1.7±0.2 | -1.2±0.9 | 4460 | 2770 | 7200 | 18.9 | 1 | - | - |
| Vip3Af | 1.0±0.1 | 3.8±0.3 | 840 | 394 | 2030 | 27.7 | 6.5 | 3.0 | 14.5 |
| ***M. brassicae*** | | | | | | | | | |
| Vip3Aa | 1.5±0.1 | 3.3±0.1 | 14.4 | 10.5 | 17.7 | 0.9 | 18.9 | 13.1 | 27.3 |
| Vip3Ae | 1.5±0.1 | 1.4±0.2 | 258 | 200 | 334 | 2.4 | 1 | - | - |
| Vip3Af | 1.5±0.1 | 3.9±0.1 | 6.0 | 4.4 | 7.7 | 0.9 | 44.2 | 30.2 | 65.0 |
| ***S. exigua*** | | | | | | | | | |
| Vip3Ab | 1.5±0.2 | 0.8±0.5 | 597 | 426 | 810 | 1.2 | - | - | - |
| ***S. frugiperda*** | | | | | | | | | |
| Vip3Ab | 0.9±0.1 | 2.0±.03 | 2020 | 1290 | 3840 | 2.5 | - | - | - |
| ***S. littoralis*** | | | | | | | | | |
| Vip3Aa | 3.3±04 | 3.0±0.3 | 4.0 | 3.0 | 4.5 | 0.6 | 46.0 | 32.9 | 64.2 |
| Vip3Ab | 2.3±0.2 | -0.03±0.56 | 163 | 130 | 201 | 0.8 | 1 | - | - |
| Vip3Ae | 2.0±0.2 | 3.0±0.3 | 8.0 | 6.1 | 9.5 | 1.4 | 21.2 | 15.2 | 29.5 |
| Vip3Af | 1.8±0.2 | 2.0±0.4 | 43.2 | 33.0 | 55.0 | 0.7 | 3.7 | 2.7 | 5.1 |
| ***L. botrana*** | | | | | | | | | |
| Vip3Aa | 1.1±0.1 | 4.9±0.1 | 1.3[c] | 0.9 | 1.8 | 1.8 | 1 | - | - |
| Vip3Ae | 2.1±0.3 | 6.4±0.2 | 0.2[c] | 0.1 | 0.3 | 6.1 | 6.3 | 2.9 | 14.1 |
| Vip3Af | 2.8±0.4 | 5.2±0.1 | 0.8[c] | 0.7 | 1.0 | 0.9 | 1.6 | 0.8 | 3.4 |

[a] *Fiducial limits.*
[b] *Intercept*
[c] L. botrana *$LC_{50}$ values are given in µg of protein per ml of diet.*

The relative potencies of Vip3Aa, Vip3Ae and Vip3Af depended of the insect species considered, revealing the difference of activity among different proteins despite the similarity of the sequences (Table 1.1 and Fig. 1.2). For example, Vip3Ae was the most active protein against *A. ipsilon*, *S. frugiperda* and *L. botrana* whereas it was the least toxic of the three proteins against *M. brassicae* (Table 1.4) (Hernández-Martínez et al., 2013). The quantitative results confirmed the low susceptibility of *H. armigera* to the Vip3A proteins observed in the toxicity screening (the $LC_{50}$ values were above 840 ng/cm$^2$). *M. brassicae* and *L. botrana* were found to be very susceptible to Vip3Aa, Vip3Ae, and Vip3Af, with $LC_{50}$ values similar or lower than these obtained by Palma et al., (2013). It is also worth noting the higher susceptibility of *S. littoralis* to Vip3Aa and Vip3Ab compared to the other two *Spodoptera* species, as well as its fast dose-

mortality response to the Vip3A proteins tested as evidenced by the values of the slopes (Table 1.4) (Chakroun et al., 2012; Hernández-Martínez et al., 2013).

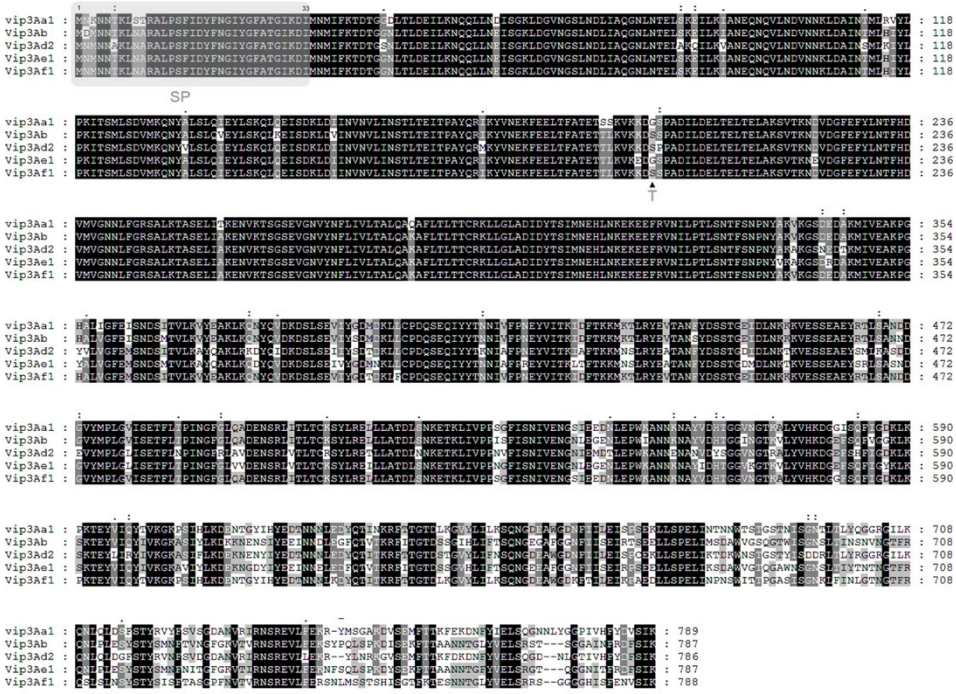


*Fig. 1. 2 Multiple sequence alignment of the 5 Vip3A proteins used for the insecticidal screening*
*Sequence identity is indicated by shading: black for 100%, dark grey for 80-100%, light grey for 60-80%, and white for less than 60% identity. Symbols above the sequences indicate divergent amino acids in Vip3Ad2 as compared to the other four Vip3A proteins: single dots indicate conservative changes, double dots indicate non-conservative changes, and a "-" sign indicates a deletion. Grey shadow indicates the "Signal Peptide" (SP) (Rang* et al*., 2005) and the triangle (◢) indicates the beginning of the 65 kDa toxin (T) fragment characterized in Vip3Aa1 by* Estruch and Yu (2001).

The present study is the first one that compares the toxicity of a relatively large number of Vip3A proteins with a considerable number of insect species. The results presented here, along with those already available in the literature for the Vip3 protein family, will help to design new combinations of insecticidal protein genes (e.g., with *cry* genes) in transgenic crops or in recombinant bacteria (Hernández-Rodríguez et al., 2013).

## 1.4. Conclusions

Five *B. thuringiensis* Vip3A proteins (Vip3Aa, Vip3Ab, Vip3Ad, Vip3Ae and Vip3Af) and their corresponding trypsin-activated toxins were tested for their toxicity against eight lepidopteran pests: *A. ipsilon*, *H armigera*, *M brassicae*, *S exigua*, *S frugiperda*, *S littoralis*, *O. nubilalis* and *L. botrana.* Toxicity was first tested at a high dose at 7 and

10 days. No major differences were found when comparing protoxins *vs*. trypsin-activated toxins. The proteins that were active against most of the insect species were Vip3Aa, Vip3Ae and Vip3Af. Vip3Ad was not toxic to any of the species tested. Considering the results by insect species, *A. ipsilon* and *S. frugiperda* were susceptible to Vip3Aa, Vip3Ab, Vip3Ae and Vip3Af; *M. brassicae* and *L. botrana* were susceptible to Vip3Aa, Vip3Ae and Vip3Af; *H. armigera* was moderately susceptible to Vip3Aa, Vip3Ae and Vip3Af, and *O. nubilalis* was tolerant to all Vip3 proteins tested, although it showed some susceptibility to Vip3Af. After assessing the toxicity range of the 5 different Vip3A proteins to different target pests, it was decided to continue the work of this thesis by further exploring the Vip3Aa and Vip3Af proteins as were the most active proteins.

# CHAPTER II

## 2. Insights into the structure of the Vip3Aa insecticidal protein by protease digestion analysis

Results from this chapter are included in:

Bel Y, Banyuls N, Chakroun M, Escriche B, Ferré J. Insights into the Structure of the Vip3Aa Insecticidal Protein by Protease Digestion Analysis. Toxins (Basel). 2017;9: 131. doi:10.3390/toxins9040131

## 2.1. Introduction

*Bacillus thuringiensis* (Bt) is a ubiquitous Gram-positive sporulating bacterium that produces several entomopathogenic proteins. The proteins that have received more attention, and are thus the best known, are the δ-endotoxins (Cry and Cyt toxins), produced as parasporal crystalline inclusions during the stationary phase of growth. Other proteins associated with insecticidal activity, including the Vip proteins, are secreted into the medium during the vegetative growth phase(Palma et al., 2014). Some Cry and Vip proteins (such as Vip3A proteins) show high insecticidal activity against a wide range of insect species (for a review, see van Frankenhuyzen 2009 for Cry proteins, and Chakroun et al. 2016 for Vip proteins), and the genes encoding them have been transferred to crop plants to protect them against insect pests.

Vip3 proteins do not share sequence homology with other Bt insecticidal toxins and their 3D structure is yet unknown. The proposed mode of action of Vip3A proteins shares some similarities with that of the Cry proteins in that both undergo activation (proteolytic processing) in the insect midgut, bind to receptors on the surface of the midgut cells and, finally, make pores that lead to cell lysis, septicemia, and eventually, death of the insect (Adang et al., 2014; Caccia et al., 2016; Chakroun et al., 2016a; Lee et al., 2003; Liu et al., 2011). The molecular processes behind this cascade of events are still unclear for Vip3A proteins and differ from those of the Cry proteins. The binding sites of the Vip3A proteins in the midgut are different from those described for the Cry proteins (Abdelkefi-Mesrati et al., 2011b, 2009; Ben Hamadou-Charfi et al., 2013; Lee et al., 2006; Sena et al., 2009), and the cell pores formed are structurally and functionally different (Lee et al., 2003). The high insecticidal activity of the Vip3A proteins, along with the differences in the mode of action with Cry proteins, has prompted their use in crop protection and pest management. Some Bt-cotton and Bt-corn varieties combine the expression of Vip3Aa with one or more Cry proteins (ISAA).

Vip3A proteins (MW about 89 kDa) have an N-terminal signal sequence that, unlike most secreted proteins, is not processed when the protein is delivered to the media (Estruch et al., 1996). Once in the midgut of the insect, as a first step in the mode of action, the Vip3A proteins are activated. The activation is necessary since the full length Vip3Aa is unable to form pores *in vitro* (Lee et al., 2003), and differences in the rate of activation have been related with differences in susceptibility amongst lepidopteran species (Abdelkefi-Mesrati et al., 2011a; Chakroun et al., 2012; Gomis-Cebolla et al., 2017). Furthermore, reduced protease activity has been found in a Vip3Aa-resistant strain of *Helicoverpa armigera* (Lepidoptera: Noctuidae) (Chakroun et al., 2016c), and it has been proposed as the mechanism of resistance in a Vip3Aa resistant strain of *Spodoptera litura* (Lepidoptera: Noctuidae) (Barkhade and Thakare, 2010).

The activation of the Vip3Aa protein by the insect midgut juice (MJ) was described soon after its discovery. Incubation of Vip3Aa with insect MJ led to four major

proteolysis products of about 62, 45, 33, and 22 kDa (Yu et al., 1997). Similar patterns of proteolysis (with a band of about 65 kDa and several other bands of lower molecular weight) have been observed by other authors with MJ from many insect species protein (Abdelkefi-Mesrati et al., 2011a, 2011b; Ben Hamadou-Charfi et al., 2013; Caccia et al., 2014; Lee et al., 2003; Marucci et al., 2015; Sellami et al., 2015). Similarly, the *in vitro* activation of Vip3A proteins with trypsin produces a major fragment of about 62-65 kDa, along with other fragments, mainly one of about 20 kDa that would correspond to the N-terminal region (Estruch and Yu, 2001). Although the 33 kDa fragment was proposed to be the minimum toxic fragment after proteolysis(Estruch and Yu, 2001), further studies have led to the 62-65 kDa protein being considered the protease resistant core and the active form of the protein (Abdelkefi-Mesrati et al., 2011a, 2011b; Baranek et al., 2015; Ben Hamadou-Charfi et al., 2013; Caccia et al., 2014; Chakroun et al., 2012; Hernández-Martínez et al., 2013; Lee et al., 2003; Liu et al., 2011; Ruiz de Escudero et al., 2014). However, some studies on the stability of Vip3A proteins to proteases seemed to show that the 62-65 kDa core was not stable, as revealed by SDS-PAGE, since the 62-65 kDa fragment was processed to smaller fragments when the concentration of proteases was increased (Caccia et al., 2014; Li et al., 2007; Song et al., 2016a).

In the present work, the activation process for Vip3 proteins was closely examined in order to better understand the Vip3Aa protein stability and to shed light on its structure. In our hands, the SDS-PAGE analysis of the Vip3Aa protein processed at high concentrations of trypsin (or MJ), indicated an apparently fast and complete degradation of the protein. However, when the proteolytic reaction was efficiently stopped, it was revealed that the protoxin had been only cleaved at a primary cleavage site, regardless the amount of proteases used, generating two bands of 66 kDa and 19 kDa. These findings are important for the interpretation of many published results in which Vip3A processing is shown. Finally, the trypsin treatment of the protoxin in the presence of SDS revealed the presence of secondary cleavage sites that have allowed us to propose a relationship between the predicted secondary structure of the protein and its stability.

## 2.2. Materials and Methods

### 2.2.1. Vip3Aa expression and purification

The Vip3Aa protein was obtained from the vip3Aa16 gene fused to a six histidine-tail and cloned in *Escherichia coli* (Abdelkefi-Mesrati et al., 2009). Expression of the vip3Aa16 gene was achieved as described elsewhere (Abdelkefi-Mesrati et al., 2011a), except for that the pre-culture was allowed to reach an OD of 1.2 before being transferred to the main culture medium, and that isopropyl-β-D-thiogalactopyranoside (IPTG) was added to the latter when it reached an OD of 0.4. After 5 h at 37 °C, the cells were harvested by centrifugation and then lysed

(Abdelkefi-Mesrati et al., 2011a). After centrifugation at 17,000 *g*, the supernatant containing the Vip3Aa protein was collected and used for subsequent purification.
Affinity chromatography purification of Vip3Aa was carried out using His TrapTM FF crude columns (GE Healthcare Bio-Sciences AB, Uppsala, Sweden). The column was equilibrated with Phosphate-Buffered Saline solution (PBS, Roche, Germany) pH 7.4, with 10 mM of imidazole. The supernatant was then loaded onto the column and washed with PBS with 45 mM imidazole. The Vip3Aa protein was eluted with elution buffer (PBS containing 150 mM imidazole) and 1 ml fractions were collected in tubes containing 50 µl of 0.1 M EDTA. Fractions with a high protein concentration (as determined photometrically at 280 nm) were combined and dialyzed overnight against 20 mM Tris-HCl, 0.15 M NaCl, 5 mM EDTA, pH 8.6, or against 50 mM carbonate buffer, 5 mM EDTA, pH 10.5. The final concentration of Vip3Aa was determined either by densitometry after SDS-PAGE or by the Bradford's method (Bradford, 1976), using bovine serum albumin (BSA) as a standard.

### 2.2.2. Vip3A proteolytic processing

The Vip3Aa protein was subjected to different proteolysis treatments. Aliquots were taken out at desired times, mixed with SDS-PAGE loading buffer (10 µl sample with 5 µl loading buffer), heated at 99°C for 10 min, snap frozen in liquid nitrogen, and stored at -20°C until use. When trypsin inhibitors were used, the aliquots were mixed with trypsin inhibitors and either immediately or after a short incubation time (10 min at RT), the loading buffer was added to the samples to be processed for SDS-PAGE as usually. The loading buffer composition was 0.2 M Tris-HCl pH 6.8, 1 M sucrose, 5 mM EDTA, 0.1% bromophenol blue, 2.5% SDS, and 5% β-mercaptoethanol.

### 2.2.3. Trypsin treatments

The affinity-purified Vip3Aa protein was subjected to proteolytic activation with commercial trypsin (trypsin from bovine pancreas, SIGMA T8003) in either Tris-HCl buffer (20 mM Tris-HCl, 0.15 M NaCl, 5 mM EDTA, pH 8.6) or carbonate buffer (50 mM carbonate buffer, 5 mM EDTA, pH 10.5). Vip3Aa was incubated with trypsin at either 1:100, 24:100, or 120:100 ratios (trypsin:Vip3A, w:w) at both 4°C and 30°C.
The irreversible inhibitors used to stop the trypsin action, were: PMSF (phenylmethanesulfonyl fluoride, from SIGMA), TLCK (Nα-tosyl-L-lysine chloromethyl ketone hydrochloride, from SIGMA), AEBSF protease inhibitor (4-(2-aminoethyl)benzenesulfonyl fluoride hydrochloride, from ThermoFisher), and E64 (trans-epoxysuccinyl-L-leucylamido(4-guanidino)butane, from SIGMA). The denaturing agent used, urea, was added directly to the sample tubes to reach the concentration of 8 M.

### 2.2.4. Midgut juice (MJ) treatment

MJ was obtained from *Agrotis ipsilon* 5th instar larvae. For that purpose, 15 larvae were dissected and their peritrophic membranes, containing the food bolus, were pulled out and transferred into an ice-cold container, homogenized, and centrifuged for 10 min at 16,100 *g* at 4°C. The supernatant was collected and centrifuged again for 10 additional min. The final supernatant was quickly distributed into small aliquots, snap frozen in liquid nitrogen, and stored at -80°C. The protein content was quantified by the Bradford (Bradford, 1976) method using BSA as a standard.
Vip3Aa was incubated with MJ at a ratio of 40:100 (MJ:Vip3A, w:w). The sample was incubated at 30°C for 30 min.

### 2.2.5. MALDI TOF/TOF analyses

The analyses were performed in a 5800 MALDI TOF/TOF (ABSciex) at the proteomics facility of the SCSIE (Servei Central de Suport a la Investigació Experimental), at the University of Valencia, Valencia, Spain. Protein fingerprinting was performed on tryptic fragments separated by SDS-PAGE.
To perform the molecular weight analyses, the Vip3Aa protein was first treated with trypsin (24:100 trypsin:Vip3A, w:w) and the mixture was incubated at 30°C for 3 days. The analyses of the Vip3Aa molecular weight were performed after diluting the sample 1:2 in trifluoroethanol with SA as a matrix. The analyses were performed in a positive linear mode in a mass range of 10000-100000 m/z. The spectra were analyzed by the mMass software (Strohalm et al., 2008), Version 5.5.0 .

### 2.2.6. Gel filtration chromatography

Gel filtration chromatography was performed with an ÄKTA explorer 100 chromatography system (GE Healthcare) in a Superdex-75 10/300 GL column (GE Healthcare Life sciences, USA) equilibrated and eluted with 20 mM Tris-HCl, 300 mM NaCl, pH 8.9, to a flow rate of 1 ml/min.

### 2.2.7. Toxicity tests

The biological activity of the Vip3A samples was assessed with *A. ipsilon* first instar larvae. The *A. ipsilon* colony was established with insects obtained from Andermatt Biocontrol AG (Stahlermatten, Switzerland) which had been reared in the laboratory for more than 14 generations. The insects were reared on an artificial diet and maintained in a rearing chamber at 25 ± 3°C, with 70 ± 5 RH and a 16/8h light/dark photoperiod.
Surface contamination assays were carried out with a single larva in each 2 $cm^2$ well in multiwell plates. The toxicity of full length Vip3Aa or the processed Vip3Aa was tested using protein concentrations of 40 and 65 $ng/cm^2$ (which corresponds to the $LC_{90}$ value extrapolated from published data (Hernández-Martínez et al., 2013)). For each replicate, 16 to 32 neonate larvae were used. Mortality was scored after 7 days.

The larvae remaining in the first instar stage after 7 days were also recorded and added to the number of dead larvae to obtain the "functional mortality".

### 2.2.8. Protein structure prediction software

The secondary structure prediction was generated by the Geneious software, version 10.1.1. (Kearse et al., 2012).

## 2.3. Results

### 2.3.1. Stability of Vip3Aa protoxin to trypsin processing

Trypsin treatment of the Vip3Aa protein in Tris-HCl buffer (pH 8.6), at 1:100 trypsin:Vip3A (w:w) for 30 min (corresponding to the conditions used in most studies) rendered a major band of around 66 kDa (usually identified as the Vip activated toxin) as well as other smaller bands of about 42, 32, 29, and 19 kDa (Fig. 2. 1a). Whereas the concentration of the smaller bands decreased with the incubation time, the 66 kDa band seemed to become more intense as the incubation proceeded. To confirm this observation, the experiment was repeated using different ratios of trypsin:Vip3A (24:100 and 120:100, w:w). In these conditions, the accumulation with time of the 66 kDa band became even more evident, and at the same time the smaller bands eventually disappeared (Fig. 2. 1b and c). This phenomenon was also observed when trypsin digestion was performed at a lower temperature (4°C), as well as when the Tris buffer was substituted by carbonate buffer (pH 10.5) (data not shown).

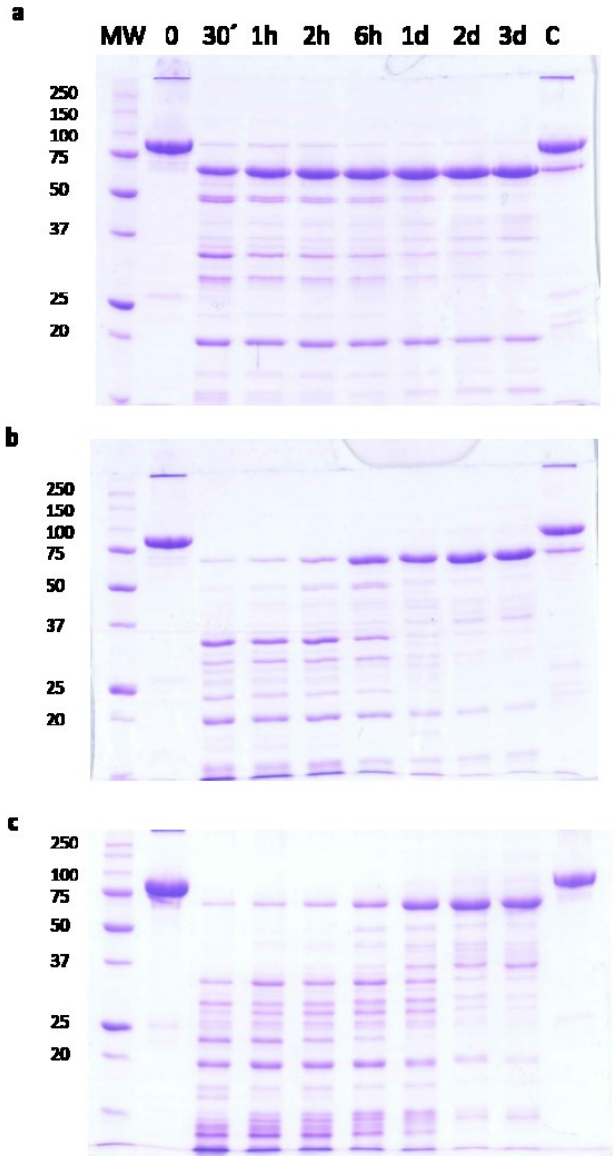


*Fig. 2. 1. Time course of trypsin processing of Vip3Aa as revealed by SDS-PAGE.*
*Reactions were performed at 30°C at different concentrations of trypsin in Tris-HCl buffer. The ratios of trypsin:Vip3A (w:w) were: (a): 1:100, (b): 24:100, and (c): 120:100. Aliquots were withdrawn at different times, as shown at the top of each lane. Molecular weight markers (MW) are indicated in kDa. C = protoxin after 3 days of incubation at 30°C.*

Gel filtration chromatography of the 30 min processed Vip3Aa protein (with 24:100 trypsin:Vip3Aa) showed a main peak at 8.3 min, corresponding to the void volume of the column (the exclusion limit for globular proteins of this column was 100 kDa), and a peak at 13.0 min (of around 23 kDa by SDS-PAGE), which corresponded to trypsin

(Fig. 2. 2, fraction 12). SDS-PAGE analysis of the fractions containing the first peak showed two main bands, one of 66 kDa and the other of 19 kDa (Fig. 2. 2, lanes 8 and 9 in inset), suggesting that the band pattern obtained at short incubation times in Fig. 2. 1 is the result of the trypsin acting on Vip3Aa while in the loading buffer. Furthermore, the presence of both polypeptides in these fractions indicated that, once cleaved, the 19 kDa peptide remains bound to the 66 kDa polypeptide. The elution of the cleaved Vip3Aa protein in a peak corresponding to a molecular size larger than 100 kDa indicates that either the cleaved Vip3Aa protein occurs in solution either as an oligomeric protein, or that it adopts a non-globular shape.

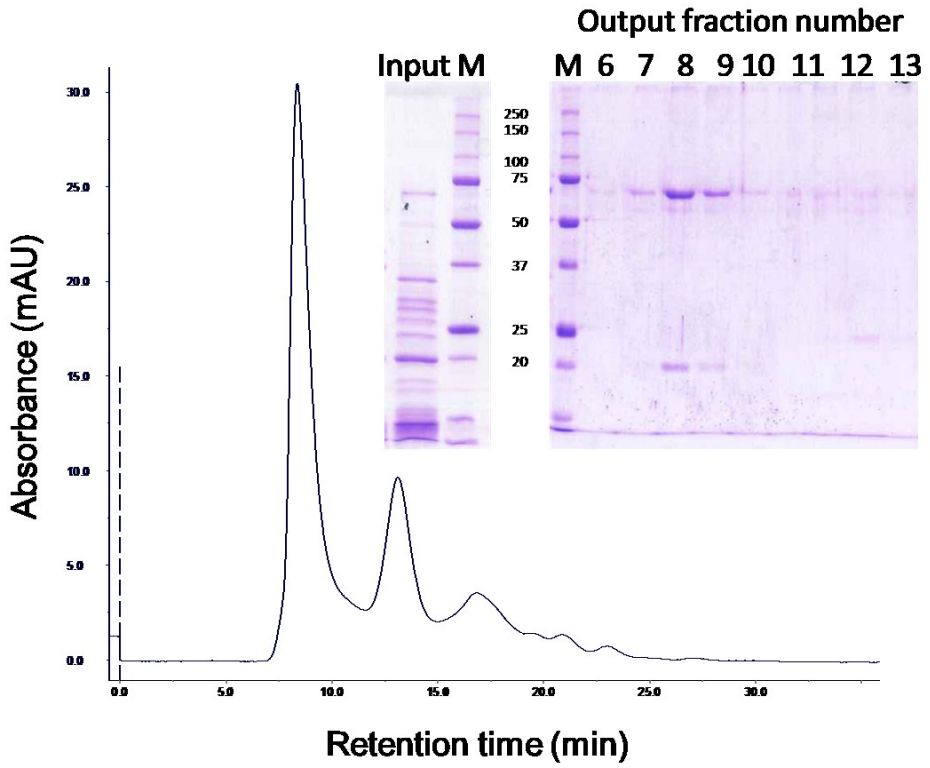


*Fig. 2. 2. Gel filtration chromatography of Vip3Aa treated with trypsin.*
*Vip3Aa was incubated with trypsin (24:100 trypsin:Vip3A, w:w) for 30 min ("Input" in figure inset). The sample was loaded into a Superdex-75 10/300 GL column and elution fractions (1 ml each) were analysed by SDS-PAGE ("Output" in figure inset). Molecular weight markers (M) are indicated in kDa.*

### 2.3.2. Checking the efficiency of protease inhibitors or high concentration urea on stopping the trypsin action

Several irreversible trypsin protease inhibitors (PMSF, TLCK, AEBSF, E64), as well as a denaturant agent (8 M urea), were used to stop the action of trypsin upon Vip3Aa prior to SDS-PAGE. The protease inhibitors or the urea were added after 30 min of Vip3Aa incubation with trypsin (24:100 trypsin:Vip3Aa, w:w). The loading buffer was

added either immediately or 10 min after addition of the inhibitors or the urea, and then the samples were heated for SDS-PAGE. The inhibitors were used at the highest concentration recommended in the literature. The results showed that none of the tested trypsin inhibitors stopped the action of trypsin when the loading buffer was added just after the addition of the inhibitors (Fig. 2. 3a). In these conditions only E64 was able to partially stop the reaction. However, if the addition of loading buffer was delayed 10 min, the AEBSF inhibitor was able to completely stop the trypsin action, rendering a pattern in SDS-PAGE of three bands: the 66 and 19 kDa peptides derived from the Vip3Aa protoxin, and a 23 kDa band corresponding to trypsin (lane 6 in Fig. 2. 3b). Unexpectedly, after preincubation, E64 performed worse than in the previous conditions. These experiments were replicated using a lower rate of trypsin:Vip3Aa (10:100, w:w) and a concentration of inhibitors 10 times higher, and the results did not change (data not shown). Therefore, except for AEBSF, the rest of inhibitors tested were not able to inhibit completely the activity of trypsin, even used at very high concentration. On the other hand, 8 M urea was very efficient stopping the action of trypsin, rendering a profile similar to that obtained with AEBSF (Fig. 2. 3a). Some minor bands could be observed after a 10 min preincubation in the presence of urea (Fig. 2. 3b), probably because a small fraction of Vip3Aa became digested by trypsin while becoming denatured.

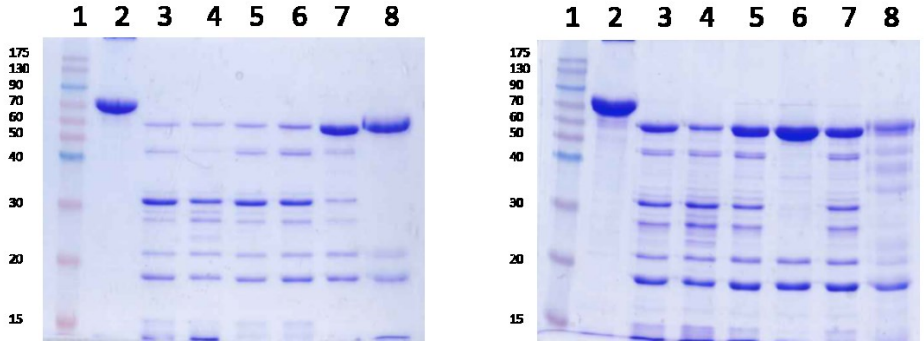


*Fig. 2. 3. Trypsin digestion of Vip3Aa using inhibitors to stop the reaction.*
*The reactions were stopped with the addition of irreversible trypsin protease inhibitors or urea. Loading buffer was added either immediately (a) or 10 min after addition of the inhibitors or the urea (b) and the samples heated and subjected to SDS-PAGE. Lanes 1: molecular weight markers; lanes 2: untreated protoxin; lanes 3: control with no inhibitors; lanes 4: 1 mM PMSF; lanes 5: 0.1 mM TLCK; lanes 6: 1 mM AEBSF; lanes 7: 10 mM E64; lanes 8: 8 M urea. Molecular weight markers are indicated in kDa.*

Taken together, the above experiments show that when the trypsin activity is completely inhibited (by either AEBSF or 8 M urea) before SDS-PAGE, only two tryptic fragments are generated, of 66 kDa and 19 kDa, even at extremely high concentrations of trypsin (24:100 trypsin:Vip3A, w:w). Thus, Vip3Aa has just one primary cleavage site under native conditions, as opposed to the several secondary cleavage sites revealed under denaturing conditions.

### 2.3.3. Analysis of the biological activity of the trypsin-treated Vip3A protein

To determine whether the samples treated with high concentration of trypsin (24:100 trypsin:Vip3A, w:w) for different times (and with very different SDS-PAGE profiles) differed in their insecticidal activity, bioassays were performed with *A ipsilon* (Lepidoptera: Noctuidae) neonate larvae. The results showed that the Vip3Aa samples treated for either 30 min or 3-4 days retained the insecticidal activity similarly to the unprocessed protein (Table 2. 1). Since the 19 kDa fragment disappears with time, the results suggest that this fragment is not essential for toxicity.

*Table 2. 1. Toxicity of Vip3Aa before and after different trypsin treatments.*
*Bioassays were performed with A. ipsilon neonates and the mortality scored after 7 days. Functional mortality is defined as the number of dead larvae plus 1st instar arrested larvae. Values represent the mean and standard error of n replicates. Mortality in the controls (just buffer or buffer with trypsin added) was always ≤10%.*

| Vip3Aa treatment | 40 ng/cm$^2$ Vip3Aa | | | 65 ng/cm$^2$ Vip3Aa | | |
|---|---|---|---|---|---|---|
| | n | % Mortality | % Functional M. | n | % Mortality | % Functional M. |
| Untreated | 2 | 71 ± 30 | 97 ± 4 | 3 | 81 ± 19 | 100 |
| 30 min trypsin-treated | 2 | 67 ± 33 | 94 ± 8 | 2 | 94 ± 6 | 100 |
| 3 - 4 days trypsin-treated | 2 | 66 ± 35 | 100 | 3 | 84 ± 16 | 100 |

### 2.3.4. Vip3Aa processing by trypsin in the presence of SDS and β-mercaptoethanol

Since the SDS-PAGE loading buffer contains SDS and β-mercaptoehanol, experiments were performed in which the Vip3Aa protoxin was incubated with trypsin (for 30 min at a 24:100 trypsin:Vip3A, w:w), in the presence of SDS and/or β-mercaptoehanol (at the same concentrations that they would be once the loading buffer is added to the sample). The reactions were stopped with 1 mM AEBSF, let stand for 10 min at RT, and processed for SDS-PAGE as usual. The results showed that the presence of SDS reproduced the same band pattern observed when the trypsin reaction is not stopped with protease inhibitors before SDS-PAGE (Fig. 2. 4), evidencing that bands other than 19 and 66 kDa appear by the action of trypsin in the presence of SDS on secondary cleavage sites.

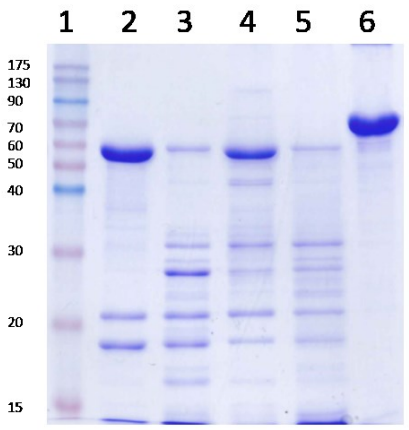


***Fig. 2. 4. Trypsin processing of Vip3Aa in the presence of SDS and β-mercaptoethanol.***
*Vip3Aa was treated with trypsin (24:100 trypsin:Vip3A, w:w) with or without SDS or β-mercaptoethanol, incubated for 30 min at 30°C and subjected to SDS-PAGE. Lane 1: molecular weight markers; lane 2: control without SDS or β-mercaptoethanol; lane 3: with SDS; lane 4: with β-mercaptoethanol; lane 5: with SDS and β-mercaptoethanol; lane 6: Vip3Aa without trypsin (protoxin). All reactions were stopped with 1 mM AEBSF followed by 10 min incubation at RT. Molecular weight markers (kDa) are indicated in the left. The band of around 23 kDa corresponds to trypsin.*

### 2.3.5. Identification of peptides generated by the trypsin treatment

Molecular weight analysis by MALDI TOF/TOF of the trypsin-treated Vip3Aa protein incubated for 3 days (at 24:100 trypsin:Vip3A, w:w) revealed peaks of mass/charge of 66539, 33246, and 22169, which corresponded to a 66 kDa polypeptide (66.539 kDa exact molecular weight) with one, two, and three charges, respectively (see Supplementary Fig. S-2.1 in the Annex section).
The tryptic peptide mass fingerprint was obtained for the main bands obtained after trypsin treatment followed by SDS-PAGE. The results allowed us to putatively identify the SDS-PAGE bands based on the Vip3Aa16 sequence (GenBank Acc. No. AAW65132.1). Unfortunately, this type of analysis does not always allow one to pinpoint the exact N- and C-terminus of the peptides, since some tryptic fragments which are generated are either too small or too large to allow detection. The fingerprinting results unambiguously indicated that the band of 66 kDa consisted of a polypeptide starting at amino acid residue D-199 and ending at the C-terminus of the protein (amino acid K-789). The fingerprint of the band of approx. 19 kDa matched with sequences from the N-terminal region of the protein, starting at the N-terminus and ending at either K-195, K-197, or K-198 (most likely the latter). The bands of approx. 42, 32, and 29 kDa all gave matches with the C-terminal part of the protein. The start residue of the band of 29 kDa was confirmed by Edman's degradation, and was identified as S-509; the last residue of this band coincided with the protein C-terminus. The bands of 42 and 32 kDa yielded tryptic fragments matching the region covered by the band of 29 kDa, indicating that they are larger versions of the 29 kDa fragment.

### 2.3.6. Stability of Vip3Aa protoxin to *A. ipsilon* midgut juice

When the Vip3Aa protein, apparently degraded after treatment with a very high concentration of MJ (40:100, MJ:Vip3A, w:w) (Fig. 2. 5, lane of Input in inset), was subjected to gel filtration chromatography, the Vip3Aa protein eluted as a single main peak at 8.35 min, along with several other peaks associated with the MJ (Fig. 2. 5). SDS-PAGE of the fractions that contained the 8.35 min peak showed two main bands, one of 66 kDa and the other of 19 kDa (Fig. 2. 5, lane A1 in inset). This result confirmed the existence of a core of 66 kDa extremely stable to MJ proteases and showed that the apparent degradation of Vip3Aa at high concentrations of MJ, as observed by SDS-PAGE, was an artefact.

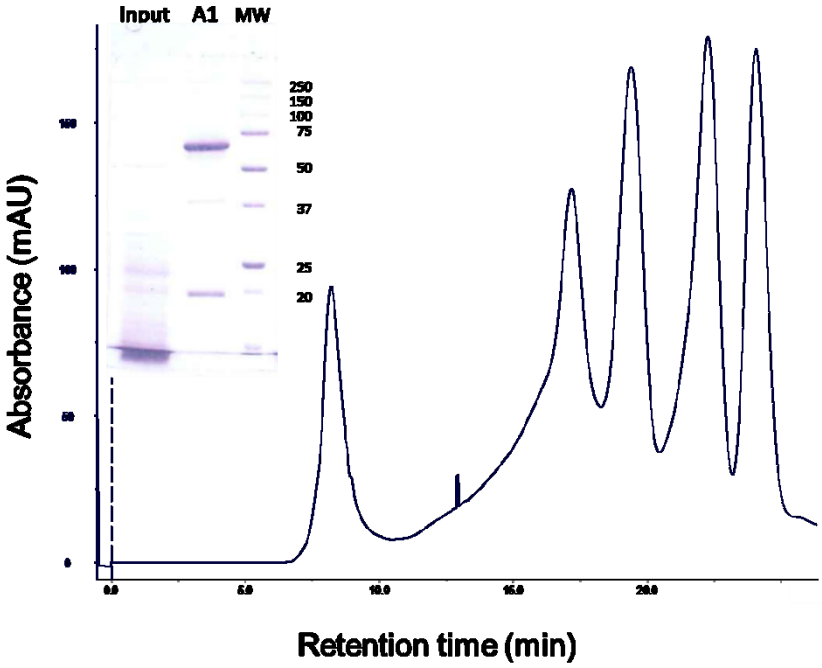


*Fig. 2. 5. Gel filtration chromatography of Vip3Aa treated with* A. ipsilon *midgut juice (MJ).*
*Vip3Aa was incubated with 40:100 MJ:protein (w:w) for 1 h ("Input" in figure inset). The sample was loaded into the column and the elution fractions (1 ml each) were analysed by SDS-PAGE. The protein profile of the output (fraction A1) is shown in the figure inset. Molecular weight markers (MW) are indicated on the right in kDa.*

## 2.4. Discussion

Since the discovery of Vip3 proteins, the mode of action on susceptible insects has been assimilated to that of the much better known Cry proteins. Though with important differences, especially at the membrane target sites, the main steps have been mirrored in those of the Cry proteins, including the activation of the protein by proteases in the midgut. Therefore, the full length Vip3Aa protein, or protoxin, is activated in the insect midgut producing a protease resistant core, the one identified as the 62-66 kDa fragment. This fragment has been proposed to be the one crossing

the peritrophic membrane and binding to specific sites in the epithelial membrane. However, this model has been challenged by results which have pointed out to that the 62-66 kDa fragment is not as resistant as supposed to proteases. Although the 62-66 kDa fragment appears as the main proteolysis band in SDS-PAGE when the concentration of trypsin or midgut juice is low, it is no longer the main band in SDS-PAGE gels when higher concentrations of proteases are used (Caccia et al., 2014; Li et al., 2007; Song et al., 2016a). Many other studies have shown the apparent instability of the 62-66 kDa fragment (Abdelkefi-Mesrati et al., 2011a, 2011b; Lee et al., 2003; Liu et al., 2011; Marucci et al., 2015) and similar results have been obtained with the closely related Vip3Ca protein (Chakroun and Ferré, 2014).

Our results show that, when exposed to trypsin or MJ proteases (even at very high concentrations), the Vip3Aa protoxin is cleaved at a primary cleavage site, between amino acids 198 and 199, rendering two fragments of 19 kDa and 66 kDa which are stable to further processing. The stability to further processing of the 66 kDa core is extremely high: it withstands concentrations as high as 120:100 trypsin:Vip3Aa and 40:100 *A. ipsilon* MJ:Vip3Aa, no matter the incubation times, a situation close to that encountered *in vivo*, when the protoxin is ingested by the larva.

The apparent degradation of the 66 kDa fragment at high concentrations of trypsin or MJ is due to the action of the proteases upon addition of SDS with the loading buffer. This is inferred from the results when the sample is subjected to gel filtration chromatography and trypsin is separated from the activated Vip3Aa prior to SDS-PAGE analysis (Fig. 2. 2) or when the reaction is properly stopped (Fig. 2. 3). As clearly shown in Figure 2. 4, trypsin can act on the target protein even in the presence of this concentration of denaturant, presumably because Vip3Aa unfolds before trypsin is inactivated, making available less accessible cleavage sites. The unexpected increase of the 66 kDa band with time at high concentrations of trypsin (Fig. 2. 1) is explained because, since trypsin autodigests, the shorter the incubation time of the Vip3Aa protein with trypsin, the higher the trypsin concentration still present in the sample, and thus, the more efficient processing of the 66 kDa peptide by trypsin under denaturing conditions.

Gel filtration chromatography shows that the proteolytically processed Vip3Aa protein elutes as a high molecular mass protein. The SDS-PAGE analysis of the elution peak shows two bands of 66 kDa and 19 kDa, which indicates that these two molecules remain associated under native conditions, as it was previously reported (Chakroun and Ferré, 2014). The elution of the processed protein from the gel filtration column as a high molecular mass protein (the exclusion limit of the column is 100 kDa) is in agreement with a recent study that shows that the trypsin-activated Vip3Aa protein aggregates in solution to form an oligomer or because the protein may adopt a non-globular shape (Kunthic et al., 2016). Other examples are known of proteins that, after activation, the two main fragments remain together and co-elute chromatographically. The MJ-activated Cry8Da protein (64 kDa) can be further digested giving two bands of 54 kDa and 8 kDa by SDS-PAGE, but which elute together by gel filtration chromatography (Yamaguchi et al., 2010). Also, Cry4A is cleaved into two fragments of 20 kDa and 45 kDa by protease activation that cannot be separated

by gel filtration chromatography (Yamagiwa et al., 1999). Two fragments of 55 kDa and 8-11 kDa, which cannot be separated by size exclusion chromatography, are also obtained during the activation of the coleopteran active Cry3Aa protein (Carroll et al., 1997).

The role of the 19 kDa in the toxicity of the activated Vip3Aa is controversial. While Li et al. (Li et al., 2007) found that deletion of the N-terminal first 189 amino acids abolished the insecticidal activity of a chimeric Vip3AcAa protein, Gayen et al. (2012) found that a Vip3Aa deletion mutant lacking the first 200 amino acids of the protein not only did not abolish the activity, but it slightly enhanced it against the three insect species tested, and that the expression of this deleted protein in tobacco plants provided even higher plant protection against several feeding insects than the expression of the wild type protein (Gayen et al., 2015). It is possible that the discrepancy between these two studies is due to the method used for the expression and purification of the deletion mutants, if not to the different Vip3A proteins used. Other studies with smaller deletions also gave contradictory results (Bhalla et al., 2005; Chen et al., 2003; Selvapandiyan et al., 2001). According to our results, the presence of the 19 kDa fragment in the toxicity seems not to be essential, since similar insecticidal activities were found for the samples incubated at 24:100 trypsin: Vip3Aa for 30 min or 3 days (Table 2. 1), with the latter almost lacking the 19 kDa fragment (Fig. 2. 1).

An unexpected result from this study is the difficulty in completely terminating the reaction of Vip3Aa with trypsin. Even the highest concentration of inhibitors recommended by the suppliers was unable to stop the reaction, except for AEBSF, and this only after incubation for 10 min. This lack of efficacy, along with the susceptibility of Vip3Aa to SDS unfolding, is responsible for the degradation patterns of Vip3 proteins obtained when analyzed by SDS-PAGE. In the light of our results, all previous data on Vip3 proteins proteolysis, either by commercial proteases or by MJ, should be revised, since most reported band patterns would reflect the susceptibility of the Vip3 protein under denaturing conditions. This would affect more severely to those experiments performed at high concentrations of either trypsin or insect midgut juice. It is very likely that the lack of termination of the trypsin reaction would be the reason why the 33 kDa fragment was originally proposed to be the minimum toxic fragment after proteolysis (Estruch and Yu, 2001).

No 3D structure of any Vip3 protein has yet been resolved. To shed light on the Vip3Aa structure, we have exploited the susceptibility of this protein to trypsin digestion under denaturing conditions (i.e., in the presence of SDS) to uncover secondary trypsin sites. The main bands obtained upon trypsin treatment of Vip3Aa in the presence of SDS were analyzed by MALDI TOF/TOF and the tryptic fragments were identified based on the Vip3Aa16 sequence (GenBank Acc. No. AAW65132.1). The analysis provided the exact molecular weight of the main fragment (66.539 kDa) and identified the 19 kDa fragment as the N-terminal fragment generated by the primary cleavage site. Secondary cleavage sites yielded the bands of approx. 42, 32, and 29 kDa, whose tryptic fragments gave matches with the C-terminal part of the protein, suggesting that this region is the most stable region of the 66 kDa core.

Interestingly, the predicted secondary structure of the Vip3Aa protein shows a cluster of beta sheets in the C-terminal region of the protein (where the putative carbohydrate-binding motif is also located), whereas the rest of the protein is mainly composed of alpha helices (Fig. 2. 6). This bias in the secondary structure suggests that the beta sheets might form a structure that stabilizes this region.

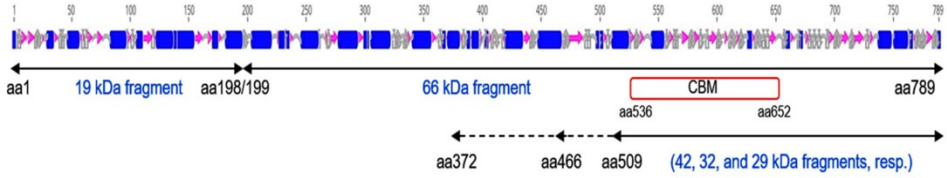


***Fig. 2. 6. Schematic representation of the Vip3Aa secondary structure and identification of the peptides generated by trypsin digestion of Vip3Aa.***

*Alfa helices are represented as blue cylinders, beta sheets are represented as purple arrows and turns are represented in gray. CBM = Predicted Carbohydrate Binding Motif. Black arrows under the secondary structure represent the polypeptides identified by Mass fingerprinting. Insect rearing and bioassays.*

## 2.5. Conclusions

The results presented here show that Vip3A proteins, and by extension other Vip3 proteins, are readily cleaved at a primary site by proteases rendering the 19-22 kDa and 62-66 kDa fragments. Despite the fact that the two fragments remain attached, the long-time exposure to proteases seems to eventually digest the small fragment. In contrast, the largest fragment is extremely stable to trypsin or MJ proteases. However, its susceptibility to SDS unfolding, along with the low efficacy of trypsin inhibitors to stop the proteolytic reaction, makes the SDS-PAGE analysis reveal secondary cleavage sites which give artefactual band patterns and, in some cases (at high concentration of MJ or trypsin), even the apparent complete degradation of the protein. The information provided here is useful for further biochemical and structural studies with the Vip3Aa and other Vip3 proteins, and may help explain some reproducibility problems faced when working with these type of proteins.

# CHAPTER III

## 3. Inference of structural traits of the Vip3Af1 from proteolytic digestion under the influence of SDS.

## 3.1. Introduction

Microbial control agents (MCA) have become a widespread resource for agricultural pest management since the 20th century. MCA-based products are environmental-safe with no risk to human consumers, allowing a more sustainable production of food. Nowadays there is a great variety of green products based on microbial agents, whereas *Bacillus thuringiensis* (Bt) based strategies are by far the most used (Lacey et al., 2015).

*Bacillus thuringiensis* Berliner is a Gram-positive sporulating bacterium which produces several entomopathogenic toxins and enzymes of agronomic interest. Among them, δ-endotoxins (Cry and Cyt proteins) are produced during the sporulation growth phase in parasporal inclusions and are highly toxic to a variety of insect pests. Different to them, vegetative insecticidal proteins (Vip) are soluble proteins that are secreted during the vegetative growth phase of Bt. Vip3 proteins are a family of Vip proteins active specific against lepidopteran pests. Cry and Vip proteins differ in their practical mode of action and therefore their combination in the same pest management strategy is becoming a common practice. Nowadays Cry1 and Vip3A proteins are often found co-expressed in some biopesticides and in commercial transgenic plants (Bt-crops) (Carrière et al., 2015; Chakroun et al., 2016a; EFSA, 2012; Kurtz et al., 2007; Moar et al., 2017; Sanchis, 2011), constituting an important tool for both conventional and organic farming.

The details in the mode of action of Vip3A proteins are not exempt of controversy. It is acknowledged that after ingestion different gut peptidases process the protein rendering the active toxin, which then crosses the peritrophic membrane and binds to specific receptors in the brush border midgut epithelium (Chakroun et al., 2016a; Chakroun and Ferré, 2014; Lee et al., 2003; Palma et al., 2014; Sena et al., 2009). Soon after the ingestion, the insect larvae stop feeding and moving (Yu et al., 1997). The starvation contributes to the disruption of the peritrophic matrix exposing the ectoperitrophic space to the lumen content(Caccia et al., 2016). Following the specific binding event, the Vip3 toxins might be inserted into the membrane and form pores (Lee et al., 2003; Liu et al., 2011), bound to the S2 ribosomal protein and translocated into the cell cytoplasm (Singh et al., 2010), or trigger a signaling cascade that activates an apoptotic process (Estruch and Yu, 2001; Jiang et al., 2016); In all cases, this succession of events leads to the histopathologic alteration in the gut epithelium and the eventual death of the insect (Abdelkefi-Mesrati et al., 2011b; Chakroun and Ferré, 2014; Gomis-Cebolla et al., 2017; Song et al., 2016b; Yu et al., 1997).

Proteolytic processing is a key starting point on the insecticidal performance. The activation step and the protease sensitivity has been often related to different insecticidal response (Abdelkefi-Mesrati et al., 2011b; Caccia et al., 2014; Chakroun et al., 2016c, 2012; Estruch and Yu, 2001; Hernández-Martínez et al., 2013; Li et al., 2007). Right from the beginning, Estruch and Yu (Estruch and Yu, 2001) proposed that

the 89 kDa Vip3A protein acted as a precursor which is promptly cleaved by insect proteases, splitting the protein in two fragments of 20 kDa (corresponding to the 200 first residues of the N-terminal) and of 65 kDa (corresponding to the activated toxin). The identity of these fragments was further confirmed in later works by protein sequencing (as shown in chapter II and chapter IV). Estruch and Yu also described two additional secondary cleavage sites in the 65 kDa fragment which render two overlapping minor bands of 45 kDa and 33 kDa. The described proteolytic profile was also found by other authors (Ben Hamadou-Charfi et al., 2013; Yu et al., 1997), whereas the accumulation of the 65 kDa band was not predominant in the Vip3Aa12 (Song et al., 2016a). In the case of Vip3C proteins, the main core active toxin corresponds to 70 kDa size (Gomis-Cebolla et al., 2017).

Vip3 sequences do not share close nor far homologues with known structures and their conformation structure has been rarely reported. Therefore, structural inferences are mostly reduced to sequence analysis, *in silico* predictions and protein engineering (Dong et al., 2012b; Gayen et al., 2012; Li et al., 2007; Rang et al., 2005; Selvapandiyan et al., 2001; Wu et al., 2007). It has been recently reported that Vip3A proteins can be found either as a globular protein or with an elongated shape, and are able to aggregate forming homo-tetramers (Kunthic et al., 2016; Palma et al., 2017, 2014).

In a previous work, Bel and coworkers (Bel et al., 2017) shown how an apparent degradation of the Vip3Aa16 after activation was a consequence of the interaction of the serine-proteases with the Vip3 proteins denatured by the action of the SDS. This effect can be a useful tool to infer in the different folding states among Vip3 proteins that might account for their specificity against target pests. In this work we present similar results with a different subclass of Vip3A and hypothesize on structural features. The results presented herein and in Bel et al. open the possibility that the loss of the toxicity reported elsewhere could be rather related to different mechanisms other than higher sensibility to proteases, such as an impairment of the binding, a disruption of the putative active site, or a suboptimal folding of the whole protein.

## 3.2. Material and Methods

### 3.2.1. Vip3Af Expression and Purification

The Vip3Af protein was kindly provided Bayer CropScience NV (Ghent, Belgium). The *vip3Af1* gene (GenBank accession No. AJ872070.1) was fused to a His-tag sequence at the N-terminus and cloned in the pMaab10 plasmid (Beard et al., 2008) in BL21 *Escherichia coli* strain. Vip3Af was expressed as reported elsewhere (Ruiz de Escudero et al., 2014).

The protein was purified by metal-chelate affinity chromatography of the crude extract lysate similarly as previously described by Hernández-Martínez et al. (Hernández-Martínez et al., 2013) (2012) using HisTrap FF columns (GE Healthcare).

Eluted fractions were collected in 2 mL tubes containing EDTA at a final concentration of 5 mM. The first 8 fractions were pooled and dialyzed o/n at 4 ºC against 20 mM Tris-HCl, 300 mM NaCl, pH 9. The dialyzed protein was maintained in the refrigerator until use.

### 3.2.2. Midgut Juice and Trypsin Preparation

Midgut juice (MJ) was obtained from midguts from 5$^{th}$ instar larvae of *Spodoptera frugiperda* (Lepidoptera: Noctuidae). The larvae were dissected in cold ice and the bolus content were extracted by carefully excising the midgut epithelium and the peritrophic membrane. Bolus from eight to ten larvae were mixed and centrifuged at 16,000 *g* and 4 °C for 10 min. The supernatant fraction was the immediately snap frozen in liquid nitrogen and stored in deep freezing conditions at -80 °C. Total protein concentration in the midgut juice was quantified with Bradford reagent using BSA as standard (Bradford, 1976).
A stock solution of 10 mg/ml of commercial trypsin from bovine pancreas (Ref. T8003, Sigma-Aldrich) was prepared with pure water, distributed in small aliquots and stored until use at -20 °C up to one month.

### 3.2.3. Proteolytic Kinetics Assays

The kinetics of the Vip3Af were studied as previously described for the close-related Vip3Aa (Bel et al., 2017). 50 to 100 µg of affinity-purified protoxins were incubated with different concentrations of either trypsin or midgut juice of *S. frugiperda* in 100-280 µl final volume of 20 mM Tris, 300 mM NaCl, pH 9 at 30 °C. At the desired time of 0.1, 0.5, 1, 2, 6, 24, 48 and 72 h, a volume equivalent to 3 µg of Vip3Af was taken and mixed with SDS-PAGE loading buffer (0.2 M Tris-HCl pH 6.8, 1 M sucrose, 5 mM EDTA, 0.1% bromophenol blue, 2.5% SDS, and 5% β-mercaptoethanol) (2:1, sample:loading buffer), followed by a heating step of 5 min at 99 °C after which samples were immediately frozen in liquid nitrogen and stored at -20 ºC until use. Proteolytic processing fragments were separated in in 12% SDS-PAGE.
For a quantitative comparison of the processing rate, the amount of Vip3Af protoxin (89 kDa) and activated toxin (62 kDa) at the different incubation times was quantified densitometrically using the TotalLab 1D v 13.01 software. The densitometry values from the 65 kDa, 33 kDa and 20 kDa bands were relativized to the input value in the gel, and the background was corrected. Graphical representation was performed using the software GraphPad Prism v 5.00.

### 3.2.4. Size Exclusion Chromatography

A sample of 180 µg of the Vip3Af protoxin was treated with midgut juice from *S. frugiperda* at a ratio of 5:100 (MJ:Vip, w:w) in a final volume of 380 µl at 30 °C for 72 h. The reaction product was subjected to gel filtration chromatography with an ÄKTA explorer 100 chromatography system (GE Healthcare) in a Superdex-75 10/300

GL column (GE Healthcare Life sciences, Uppsala, Sweden) equilibrated and eluted with 20 mM Tris-HCl, 150 mM NaCl, pH 9, to a flow rate of 1 mL/min.

### 3.2.5. Protease Stability of the Vip3Af Activated Toxin

Once the samples of the kinetics experiments were incubated for 72 h, the remaining activated samples were cold down and set aside at 4 °C for 48 h. In order to indirectly detect any conformational change in the activated Vip3Af, each samples were divided into two equivalent volumes and further treated with either 24:100 trypsin (trypsin:Vip, w:w) or 1.5:100 (MJ:Vip, w:w) midgut fluid form *S. frugiperda* and incubated at 30 °C for 0.1, 0.5, 1, 2 and 24 h. A volume equivalent to 3 µg of Vip3Af was taken from the reaction mixture as described above.

### 3.2.6. Biological Activity of the Digested Vip3Af

The toxicity of the Vip3Af activated with midgut juice of *S. frugiperda* at a ratio of 5:100 (MJ:Vip, w:w) at 30 °C for 30 min was tested against *S. frugiperda*. Insect population of *S. frugiperda* was reared on a semi-synthetic diet (Greene et al., 1976) and maintained under controlled conditions (25 ± 2° C, 70 ± 5% RH and 16:8h L:D). Surface contamination bioassays were conducted by applying 50 µl of the Vip3Af in 2 $cm^2$ diameter well in a multiwell plates filled with the semi-synthetic diet and let dry. A protein concentration of 150 ng/$cm^2$ was chosen based on the reported $LC_{50}$ of the Vip3Af1 affinity purified (Hernández-Martínez et al., 2013). A single neonate was placed in each well, 16 neonates per treatment. Bioassays were replicated twice and mortality was scored at 7 days. Trays were maintained in the insect rearing chamber.

## 3.3. Results

### 3.3.1. Kinetics of the Activation of Vip3Af Protoxin with Trypsin and Insect Gut Proteases

The treatment of Vip3Af with 24:100 trypsin (trypsin:Vip, w:w) in Tris-HCl buffer (pH 9) gave the two characteristic bands of 65 kDa and 20 kDa in all time points analysed, plus additional minor bands of ca. 45 kDa, 33 kDa, and 30 kDa at 30 min of the reaction start (Fig. 3. 1a). As the time course of the reaction progressed, the intermediate bands progressively vanished in parallel to the degradation of the trypsin yet visible in the SDS-PAGE, whereas the intensity of 65 kDa band slightly increased. It is also newsworthy the odd emergence of a dim band of 90 kDa from 6 h onwards. When Vip3Af was treated with an even higher concentration of trypsin (120:100 trypsin:Vip, w:w), this effect was more remarkable (Fig. 3. 1b). At the initial time point of 0.1 h, the higher digestion of the 65 kDa band, and the later increment in the band intensity was more notorious, whereas the band of 45 kDa is not

conspicuously formed. The band of 20 kDa mostly remained stable and only a slight decrease was observed at the very end of the experiment (Fig. 3. 1c).

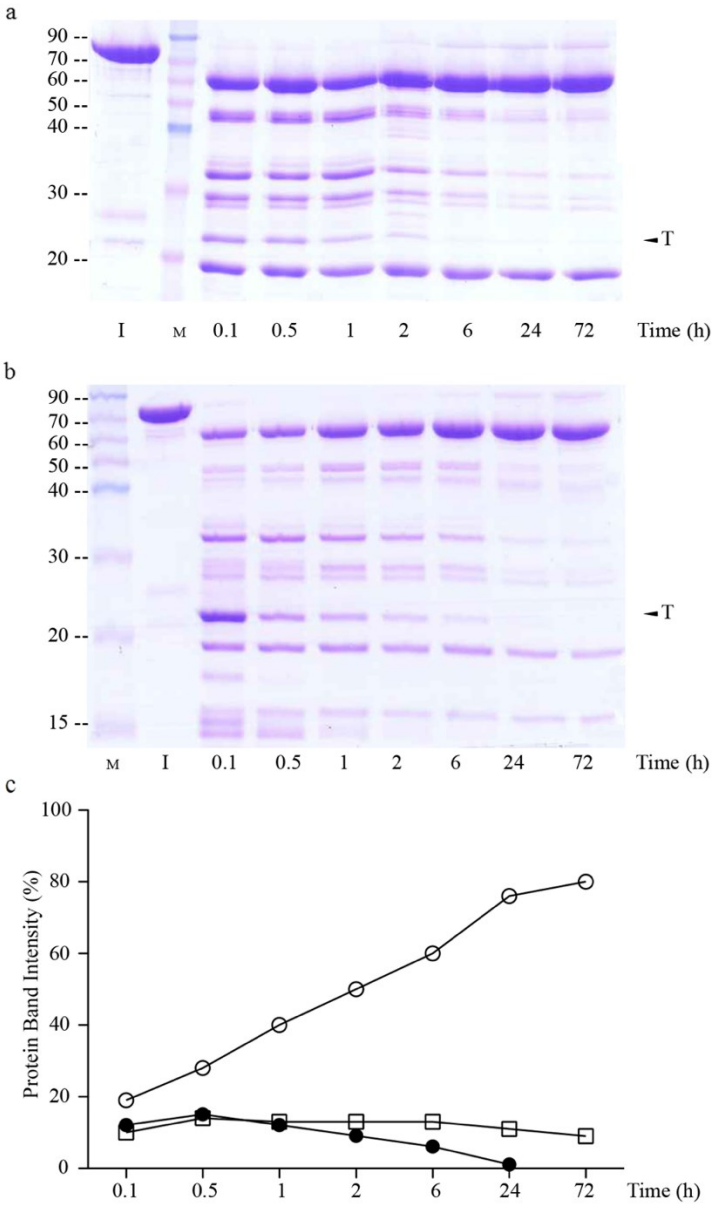


***Fig. 3. 1. Kinetics of Vip3Af1 proteolytic activation with trypsin.***

*Reactions were conducted at 30 °C in Tris-HCl buffer (20 mM Tris, 300 mM NaCl, pH9) and (a) 24:100 trypsin (trypsin:Vip, w:w) or (b) 120:100 trypsin (trypsin:Vip, w:w). A sample volume corresponding to 3 µg of Vip protein was taken at different time intervals and subjected to SDS-PAGE. Bands of 62 kDa (○), 20 kDa (●) and 33 kDa (□) were quantified by desitometry (c). "I": input protoxin. "M": molecular weight marker (kDa). "T": band corresponding to the trypsin.*

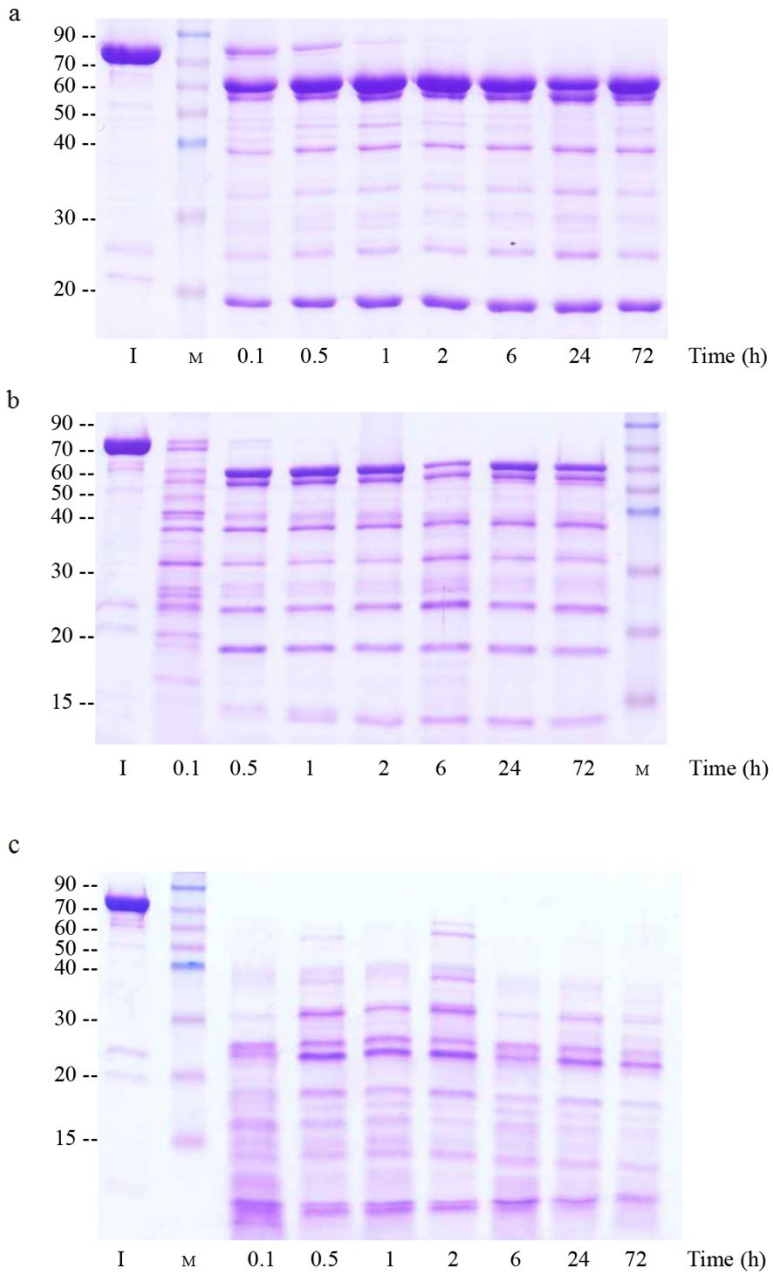


***Fig. 3. 2. Kinetics of Vip3Af1 proteolytic activation with* S. frugiperda *midgut juice (MJ).***
*Reactions were conducted at 30 °C in Tris-HCl buffer (20 mM Tris, 300 mM NaCl, pH9) and (a) 0.5:100, (b) 1.5:100 or (c) 5:100 midgut juice (MJ total protein:Vip, w:w). A sample volume corresponding to 3 µg of Vip protein was taken at different time intervals and subjected to SDS-PAGE. "I": input protoxin. "M": molecular weight marker (kDa).*

A different effect was observed when Vip3Af was treated with different ratios of midgut juice. An uncomplete processing of the 89 kDa protoxin was achieved during the first 30 min at a ratio of 0.5:100 (MJ:Vip, w:w) (Fig. 3. 2a). The main bands of 65 kDa and 20 kDa accumulated over time as the protoxin band (89 kDa) disappeared, accounting for complete digestion of the protoxin form. The increment of the 65 kDa band was not observed over time at higher concentrations of midgut juice (Fig. 3. 2a and Fig. 3. 2b) when the protoxin form was completely digested. Interestingly, a lower band of around 60 kDa was formed since the beginning of the reaction at the concentrations of 0.5:100 (MJ:Vip, w:w) and more significantly at 1.5:100 (MJ:Vip, w:w) (Fig. 3. 2a and Fig. 3. 2b). Other minor bands of about 38 kDa, 33 kDa and 25 kDa appeared to be more intense as the midgut juice concentration was increased (Fig. 3. 2b). Complete digestion of the 65 kDa band was observed in the SDS-PAGE when Vip3Af was treated with midgut juice at the ratio of 5:100 (MJ:Vip, w:w) (Fig. 3. 2c).

### 3.3.2. Size exclusion Chromatography of the Vip3Af Treated with High Concentrations of Midgut Juice

The Vip3Af treated with high concentrations of midgut juice (5:100, MJ:Vip, w:w) for 72 h appeared to be completely digested (Fig. 3. 2c and inset in Fig. 3. 3). Gel filtration of this preparation revealed a single peak coincidental with the void volume of the column used, which corresponds to a globular proteins size larger than 100 kDa. The analysis of this peak by SDS-PAGE showed only a band of about 65 kDa. The 20 kDa band is not observed probably due to the low sample concentration after elution.

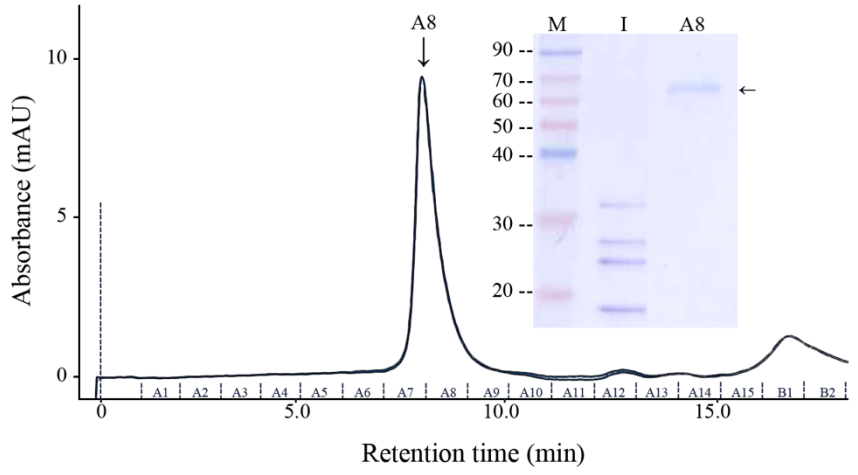


***Fig. 3. 3. Gel filtration chromatography of Vip3Af1 treated with*** S. frugiperda ***midgut juice (MJ).***
*The incubation took place at 30 ºC, 5:100 midgut juice (MJ total protein:Vip w:w) for 72 hours. The treated sample was injected into a Superdex 75 10/300 GL column in a flow rate of 1mL/min. The inset shows the input*

*sample ("I") and the elution fraction A8 as revealed by SDS-PAGE. "M": molecular weight marker (kDa). Absorbance measured at 280 nm.*

### 3.3.3. Stability of the Vip3Af differently activated to further protease treatment.

Trypsin-activated toxin and MJ-activated toxin gave different SDS-PAGE profiles after further protease treatment. When the trypsin-activated form was further treated with midgut juice (Fig. 3. 4a- "midgut juice"), the result was similar to that from the protoxin digestion (Fig. 3. 2b). Likewise, the MJ-activated form (Fig. 3. 4b- "midgut juice") revealed an apparent degradation of the protein, similar to that observed when the protoxin was treated with the highest concentration of midgut juice (Fig. 3. 2c). This effect is likely explained by an accumulation effect of the peptidases from the midgut fluids, probably due to a higher stability of these proteases compared to trypsin.

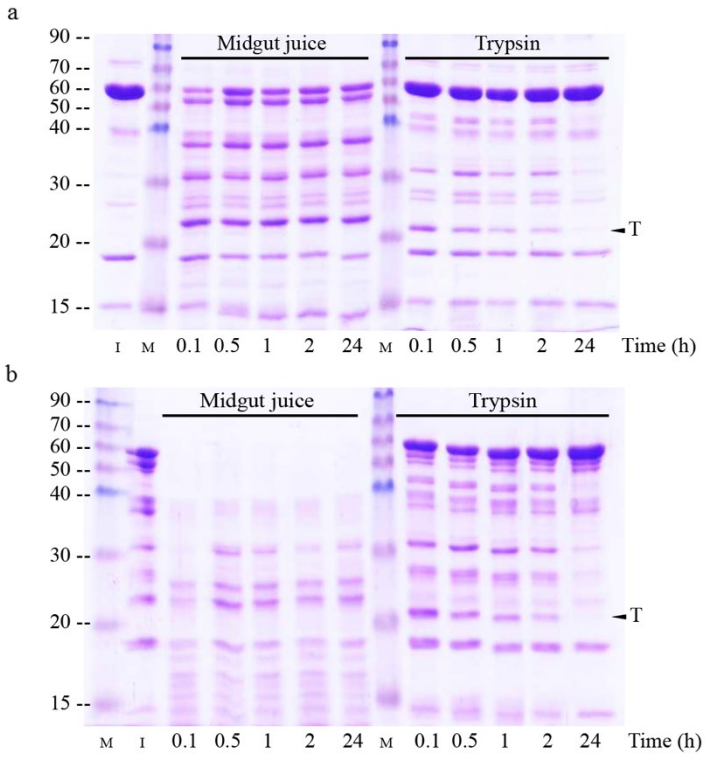


***Fig. 3. 4. Protease stability of the 62 kDa fragment core of the Vip3Af1.***
*The activated toxin (Input) was obtained after 72 h treatment of the Vip3Af1 protoxin with (panel a) trypsin (corresponding to the last lane in Fig. 1a) or with (panel b)* S. frugiperda *midgut juice (corresponding to last lane in Fig. 2a). Both activated forms were treated again with either with 24:100 trypsin (trypsin:Vip, w:w) ("Trypsin") or with 1.5:100* S. frugiperda *midgut juice (MJ total protein:Vip, wt:wt) ("Midgut juice") at 30 ºC for 24 h. Reactions were conducted at 30 ºC in Tris-HCl buffer (20 mM Tris, 300 mM NaCl, pH9). Samples (3 µg) were taken at different time points and loaded into a SDS-PAGE. "I": Input samples. "M": molecular weight marker (kDa). "T": band corresponding to the trypsin.*

Different to the results observed after protoxin digestion with trypsin (Fig. 3. 1a), when the trypsin-activated form was further treated with trypsin (Fig. 3. 4a- "trypsin"), the band intensity of the 65 kDa fragment did not increased over time. This highlights a remarkable stability of the 65 kDa "core" and the 20 kDa fragment to trypsin digestion. Conversely, when the MJ-activated form was further treated with trypsin (Fig. 3. 4b- "trypsin") the proteolytic profile resembled that from the protoxin treatment (Fig. 3. 1a).

### 3.3.4. Toxicity test.

The single dose bioassays at 150 ng/cm$^2$ (Table 3. 1) gave a mortality and functional mortality higher than 69% in both Vip3Af protoxin and the Vip3Af treated with 5:100 midgut juice (MJ:Vip, w:w) for 72 h at 30 ºC, indicating that the profile observed in the SDS-PAGE of an apparently degraded protein (Fig. 3. 2c) completely retains the insecticidal function.

***Table 3. 1. Susceptibility of*** S. frugiperda ***to Vip3Af1 before and after 72 h treatment with 5:100*** S. frugiperda ***midgut juice (MJ:Vip, w:w).***

*Treated and untreated Vip3Af1 were applied at 150 ng/cm$^2$ in surface contamination bioassays with neonates and the mortality was scored after 7 days. Functional mortality: dead larvae + stunting larvae (L1 instar). Values represent the mean and standard error of 2 replicates. Mortality in the controls (20 mM Tris, 150mM NaCl, pH 9) was ≤15%.*

| Vip3Af treatment | % Mortality (mean ± SE) | % Functional Mortality (mean) |
|---|---|---|
| Vip3Af Protoxin | 69 ± 9 | 100 |
| Vip3Af treated with MJ | 88 ± 18 | 100 |

## 3.4. Discussion

Secondary cleavage sites in the Vip3Aa protein after treatment with high concentration of trypsin or insect midgut juice have been recently described by Bel and co-workers (Bel et al., 2017). The apparent degradation of Vip3Aa toxins observed in the SDS-PAGE was proved to be an *in vitro* effect caused by the denaturing interaction of the SDS present in the SDS-PAGE loading buffer. While Vip3Aa proteins are progressively unfolded by the SDS, the trypsin and other peptidases present in the insect midgut juice resist the denaturation and retain enzymatic activity even at the high temperature gradually achieved during the sample heating step, acting upon inaccessible cutting sites under Vip3Aa-native conditions.

A similar effect to high concentration of proteases was observed in the Vip3Af1 protein, suggesting that this might be a common phenomenon in the Vip3A proteins. Some minor differences with regards to the Vip3Aa are however noticed. Though the 65 kDa fragment apparently accumulated over time as the trypsin self-digests, in

contrast to what occurs in the Vip3Aa16 a complete digestion of the 65 kDa fragment at the first time-points of the kinetics was not observed, not even at the highest ratio of trypsin (120:100 trypsin:Vip, w:w) (Fig. 3. 1). Moreover, the N-terminus fragment of 20 kDa almost completely disappeared in the Vip3Aa16, whereas in the Vip3Af1 this band is yet enough intense after 72 h incubation (Fig. 3. 1c). The interaction of the SDS with protein during denaturation has been commonly assumed to give long unfolded peptides. Nowadays it is known that secondary structures such as α-helices or β-sheets might be formed as a consequence of the protein interaction with the SDS micelles (Parker and Song, 1992). Furthermore, the way in which SDS differently interacts with proteins can be used to define domains and infer in the proteins structure, (e.g. by "gel shifting" of mutated proteins) (Shi et al., 2012). Therefore, the differences found between Vip3Af1 and the Vip3Aa16 might reflect a different interaction of both proteins to SDS molecules, which might account to some differences in their native structure.

The results obtained herein showed that a misleading degradation also occurs in the Vip3Af after being treated with *S. frugiperda* midgut juice (Fig. 3. 2). The progressively emergence of the 65 kDa fragment in the SDS-PAGE over time was not observed at high concentrations of midgut juice (Fig. 3. 2, Fig. 3. 4). This difference with the trypsin treatment (Fig. 3. 1) is likely explained by the higher stability of the different proteases content of the midgut juice, which must be still present in the reaction mix after 72 h. This apparently degraded sample retained full toxicity against *S. frugiperda* (Table 3. 1). When the deceiving over-digested protein was subjected to gel filtration chromatography, a single band of about 65 kDa corresponding to the "core" active toxin was observed (Fig. 3. 3). This phenomenon accounts for the differential size separation of Vip3Af and the proteases, which have lower molecular weight of around 25 kDa and 27 kDa for chymotrypsin and trypsin, respectively. The fraction of the Vip3Af eluted from the chromatography, free of proteases, is therefore no longer digested when the loading buffer containing SDS is added. The Vip3Af eluted with the void volume, indicating a protein size larger than 100 kDa. Assuming a globular conformation of the Vip3A proteins, the activated form would be eluted at a peak corresponding to 90 kDa max. (the sum of the 65 kDa band and the 20 kDa band which co-elute together (Bel et al., 2017; Chakroun and Ferré, 2014; Kunthic et al., 2016)). However, the seemingly higher size of the native Vip3Af indicates a native conformation either as a predominantly elongated chain or a globular fold with a quaternary structure, in agreement to what has been recently shown for other Vip3A proteins (Bel et al., 2017; Kunthic et al., 2016; Palma et al., 2017).

Researchers commonly activate Vip3A proteins by adding 1:100 to 5:100 trypsin:Vip (w:w) for 1-2 h. After one hour, the protoxin is completely processed at the primary cleavage sites into the 65 kDa and the 20 kDa bands. When the protoxin is treated with higher amounts of trypsin (Fig. 3. 1a), after 1 h incubation there are yet many "non-native" secondary bands. Further addition of the same amount of trypsin (24:100 trypsin:Vip, w:w) after 72 h, gave only dim secondary bands (Fig. 3. 4a – "Trypsin"), suggesting some differences in the activated-toxin conformation. We

propose that once the protoxin is first treated with trypsin, the excision of the 200 amino acids from the N-terminus probably triggers a compaction of the "core" into a globular form, in agreement to Kunthic et al*.,* (2016). Furthermore, Lee et al*.,* (2003) showed that the activation step was crucial for the formation of pores in brush border vesicles membranes (BBMV) of susceptible insects, perhaps facilitated by the compacting into a globular shape. It is worth to consider that, *in vivo*, further activation steps might occur in the brush border membranes of the insect midguts by exopeptidases, such as aminopeptidase and carboxypeptidases, which could account for further folding changes (Caccia et al., 2014; Song et al., 2016a; Srinivasan et al., 2006).

Although the X-ray structure of Vip3 proteins is not yet disclosed, an *in silico* model of the 3D-structure of the Vip3Af1 (see chapter IV) shows the C-terminal part of the protein predominantly formed by β-sheets, in compliance to the C-terminus model proposed by Wu et al. (Wu et al., 2007). Additionally, there is Carbohydrate Binding Motif (CBM 4,9; from $Ser^{536}$ to $Gln^{652}$ in the Vip3Af1) predicted within this region, which typically is mainly composed by β-sheets (Chakroun et al., 2016a). The secondary structures are differently affected by SDS; while α-helices are quickly unfolded, β-sheets are more robust and resistant to SDS restructuration (Nielsen et al., 2007). Accordingly, Bel and colleagues (Bel et al., 2017) proved that the smaller band of 29 kDa matched the C-terminal end of the Vip3Aa sequence and was not further processed by trypsin in the presence of SDS, not even at the highest enzyme concentration. Here we show that a 33 kDa band is also steady maintained at high concentrations of trypsin, which is likely to account for the C-terminal end of the Vip3Af protein.

Further addition of midgut juice to the activated toxin gave similar results to that from the protoxin digestion with midgut juice, regardless of the peptidase used in the first treatment (trypsin or mj) (Fig. 3. 4). In *S frugiperda* larvae, the protease composition account mostly by chymotrypsin-like peptidases (87%), trypsin (7%) and elastase (1%) (Caccia et al., 2014; Srinivasan et al., 2006). Provided that in the midgut juice there is a cocktail of serine proteases with different isoforms, these results might be explained by the contribution of the different protease-types in each reaction, regardless on the protein folding.

To check whether the misleading degradation effect previously described was rather anecdotic or on the contrary could be generalized to other Vip3A, regardless the Vip3 subclass or the insect gut specific proteases, we reproduced the main experiments published by Bel et al., (2017) with a different Vip3A and a different insect species. The results obtained here supports that this is a common effect observable in Vip3A proteins and confirm the high stability of the Vip3A "active core". Some dissimilarities in the way Vip3A proteins interact with SDS micelles at more detailed scale might reflect conformation differences that can underpin the variety of pests susceptible to different Vip3 proteins.

# CHAPTER IV

## 4. Critical amino acids for the insecticidal activity of Vip3Af from *Bacillus thuringiensis*. Inference on structural aspects.

## 4.1. Introduction

Vegetative insecticidal proteins (Vip) are entomotoxic proteins of increasing importance in the framework of sustainable pest management and crop protection strategies. Different to the well-known δ-endotoxins, Vip proteins are produced during the vegetative growth phase of *Bacillus thuringiensis* (Berliner) (Bt) and secreted to the growth medium as soluble proteins. Of particular interest are Vip3A proteins, which were first described in the late 90's and were found to be active against lepidopteran species with potencies different to those of the widely used Cry proteins, such as the Cry-tolerant *Agrotis ipsilon* (Lepidoptera: Noctuidae) or of many other species from the *Spodoptera* genus (Estruch and Yu, 2001; Gayen et al., 2012; Warren, 1997). Despite their discovery more than 20 years ago, the details on the mode of action of Vip3A proteins as insecticidal toxins are not fully understood. Nevertheless, there is wide consensus on a general mechanism similar to that of Cry proteins, consisting of a proteolytic activation in the insect lumen gut, binding to specific receptors on the midgut epithelium, and formation of ion channels which lead to the insect death (Lee et al., 2003; Liu et al., 2011). A different, though not mutually exclusive mechanism, including an apoptotic pathway was initially suggested (Estruch and Yu, 2001; Lee et al., 2003). It has been recently proposed that Vip3A proteins act via mitochondrial swelling and caspase activation on Sf9 cells (Jiang et al., 2016). Although it has been shown that specific binding of Vip3A proteins can occur in non-susceptible species (Chakroun et al., 2016c; Chakroun and Ferré, 2014; Lee et al., 2003), both mechanisms described above have in common that Vip3 and Cry proteins bind to different specific receptors and, therefore, their combination in the same pest management strategy is a promising tool to hinder the evolution of resistance to Bt toxins in addition to increasing the insecticidal potency and diversifying the range of target pests. Nowadays, the co-expression of Vip3 proteins with other entomotoxic proteins, such as Cry toxins, are available to growers both in some Bt-based biopesticides and in pyramided Bt crops (Carrière et al., 2015; Chakroun et al., 2016a; EFSA, 2012; Gayen et al., 2015; Kurtz et al., 2007; Moar et al., 2017; Sanchis, 2011), whereas promising applications based on nanoparticles and microencapsulation in bacterial cells are under exploration to render on-demand and more flexible green products based on Bt toxins (Hernández-Rodríguez et al., 2013; Mahadeva Swamy and Asokan, 2013; Panetta, 1993).

To date, 105 alleles of Vip3A proteins are known (Crickmore et al., 2014), most of which have been tested and are active to a wide range of lepidopteran species with high selectivity at the species level. Whereas the spatial conformation in three domains of some of the Cry proteins is well established, Vip3 proteins do not share homology with any other known protein and the elucidation of their protein structure is a milestone yet to be achieved (de Maagd et al., 2003; Palma et al., 2014; Palma and Berry, 2016; Wu et al., 2007). However, recent studies have shown that Vip3A

are globular proteins with a quaternary structure (Kunthic et al., 2016; Palma et al., 2017, 2014).
Alanine scanning is a successful technique for mapping crucial positions or epitopes in a protein and allows a greater insight into protein structure-function relationships. It consists of a systematic change, one by one, of the native amino acid residues to alanine residues. Alanine is the amino acid with the second smallest side chain, after glycine. It is composed of a chemically inert methyl group. The substitution of a residue to an alanine 'removes' the specific properties of a particular side chain while maintaining the β-carbon, ensuring the most frequent dihedral angle that connect the side chain with the amino acid backbone. Thus, the alanine mutagenesis simplifies the analysis of systematic residue substitutions in a protein sequence without changing the preferred secondary structure by introducing new chemical or steric properties that might blur the interpretation of the results (Cunningham and Wells, 1989; Morrison and Weiss, 2001).
In the present work, an extensive examination of the Vip3Af1 primary structure was performed for the first time by means of the alanine scanning technique. A total of 558 out of the 788 residues of the Vip3Af1 sequence were changed to alanine and studied in detail. This is a first step in a better understanding of the Vip3A protein structure and the relationship to its biochemical hallmarks insecticidal activity.

## 4.2. Materials and Methods

### 4.2.1. Alanine Mutants Library

The *vip3Af1* gene (GenBank accession No. AJ872070.1) encoding the 788 amino acid protein Vip3Af1 (NCBI accession No. CAI43275, from now on: Vip3Af1(WT)), was modified to encode a His-tag sequence at the N-terminus. The alanine mutants library consisted of a total of 558 clones in *Escherichia coli* strain DH5α. Each clone differed from the others by a single amino acid codon which had been changed to an alanine codon from the Vip3Af1(WT) sequence cloned in the pMaab10 plasmid (Beard et al., 2008). The changes were performed using the QuickChange Lightning Site-directed Mutagenesis Kit (Agilent Technologies, Inc.). The sequence positions that were not changed to Ala were (Table 4. 1): i) the $Met^1$ corresponding to the start codon; ii) N-terminus region (from amino acids 15 to 165), assuming that this region is not involved in the specificity of the toxin; iii) the 30 Ala residue positions in the Vip3Af1(WT), and iv) 48 positions for which mutagenesis failed and no mutant protein could be obtained. The collection was kindly provided by Bayer CropScience NV (Ghent, Belgium).

*Table 4. 1. List of missing positions of the Vip3Af1(WT) protein which could not be tested.*
*Amino acid positions correspond to the Vip3Af1 protein sequence (accession No. CAI43275).*

| Description | Residues position | Num. of redidues |
|---|---|---|
| List of clones within the library with no expression of the modified-Vip3Af1 protein | $Asn^{5}$, $Ile^{176}$, $Asn^{180}$, $Phe^{183}$, $Phe^{286}$, $Arn^{293}$, $Asp^{302}$, $Tyr^{409}$, $Phe^{416}$, $Tyr^{420}$, $Glu^{458}$, $Leu^{511}$, $Leu^{520}$, $Asn^{541}$, $Thr^{564}$, $Gly^{569}$, $Gly^{639}$, $Ile^{780}$, $Ser^{786}$ | 19 |
| List of missing clones from the library: | | |
| First amino acid (start codon) | $Met^{1}$ | 1 |
| Gap at the N-terminus region | From $Ser^{15}$ to $Thr^{165}$ | 151 |
| Alanine in the wt sequence ($Ala^{x}$) | x= 10, 12, 172, 189, 203, 216, 248, 252, 257, 280, 283, 285, 299, 336, 345, 351, 356, 375, 440, 462, 469, 496, 517, 554, 559, 572, 657, 670, 690, 725 | 30 |
| Failed mutagenesis | $Lys^{7}$, $Val^{179}$, $Lys^{294}$, $Leu^{296}$, $His^{310}$, $Leu^{311}$, $Asn^{312}$, $Lys^{313}$, $Glu^{316}$, $Tyr^{335}$, $Gly^{340}$, $Glu^{374}$, $Asp^{386}$, $Leu^{399}$, $Pro^{417}$, $Glu^{437}$, $Val^{480}$, $Thr^{518}$, $Asp^{519}$, $Phe^{581}$, $Tyr^{595}$, $Ile^{607}$, $Leu^{609}$, $Lys^{627}$, $Asp^{628}$, $Thr^{640}$, $Leu^{649}$, $Asn^{700}$, $Thr^{706}$, $Arg^{708}$, $Gln^{709}$, $Ser^{715}$, $Tyr^{716}$, $Ser^{720}$, $Ile^{721}$, $Phe^{729}$, $Arg^{734}$, $Val^{739}$, $Ser^{748}$, $Ser^{749}$, $Ser^{751}$, $Phe^{757}$, $Asn^{762}$, $Asn^{763}$, $Val^{768}$, $Ser^{711}$, $Phe^{782}$, $Glu^{783}$ | 48 |
| Total (missing positions) | | 230 |

### 4.2.2. Protein Expression

For the initial screening, Vip3Af Ala-mutant clones and the Vip3Af1(WT) clone were expressed by picking up one single colony and inoculating it into a 3 ml of LB medium with ampicillin (100 µl/ml). After overnight incubation at 37ºC with mild shaking, 2 ml of this preculture was transferred to 20 ml of the same growth medium and incubated at 37ºC with mild shaking until the culture reached an $OD_{600}$ of approximately 4.7. Aliquots of 100 and 1000 µl were taken and centrifuged for 20 min at 16,900 *g* at 4ºC. The supernatant was discarded and the pellets were stored at -20ºC until used, without any further treatment, for the initial toxicity assays.
For the rest of the work, since the *E. coli* strain DH5α is not inducible, selected clones were subjected to plasmid purification and the plasmid was transformed into the IPTG inducible strain *E. coli* WK6. All clones were grown and expressed as previously described (Ruiz de Escudero et al., 2014). After centrifugation, the crude extract supernatant was filtered through a 0.2 µm membrane before purification.

### 4.2.3. Western Blot

After separation by SDS-PAGE, proteins were electroblotted in duplicate onto nitrocellulose membranes. Membranes were blocked with 3% of bovine serum albumin (BSA) in PBST buffer (Phosphate Buffered Saline with 0.1 % Tween 20), and after washing three times with PBST, membranes were incubated either with a

polyclonal antibody raised against anti-Vip3Aa, which cross-reacted against Vip3Af proteins (1:2000 dilution), or with a monoclonal anti-His antibody (1:5000 dilution). Membranes incubated with the anti-Vip3 antibody were probed with an anti-rabbit IgG-conjugated horseradish peroxidase (1:5000 dilution) and bands were visualized with a chemiluminescence detection kit (RPN2209; GE Healthcare) using an ImageQuant LAS400 image analyser (GE Healthcare). Membranes incubated with the anti-His antibody were probed with an anti-mice IgG conjugated to alkaline phosphatase (1:2000 dilution) and the results were visualized with the NBT/BCIP color detection reagent.

### 4.2.4. Protein Purification

Purification of the crude extracts was carried out with a metal-chelate affinity chromatography in a similar way as previously described by Hernández-Martínez et al. (Hernández-Martínez et al., 2013) using HisTrap FF columns (GE Healthcare). Fractions of 1 ml were eluted from the column and collected in tubes containing 50 µl of 0.1 M EDTA. The fractions containing Vip3Af were pooled and dialyzed against 20 mM Tris, 150 mM NaCl, 5 mM EDTA, pH 8.6, before storage at -20ºC.
For purification by isoelectric point precipitation, the pH of the clarified crude extracts was lowered to 4.7 with 0.1 M acetic acid while stirring on ice. The precipitated protein was pelleted by centrifugation and stored at -20ºC.

### 4.2.5. Insect Rearing and Bioassays

Insect colonies of *Spodoptera frugiperda* and *Agrotis segetum* (Lepidoptera: Noctuidae) were reared on a semi-synthetic diet (Greene et al., 1976) in a rearing chamber under controlled conditions of temperature, humidity and photoperiod (25 ± 2 ºC, 70 ± 5% RH and 16:8 h L:D).
Surface contamination bioassays were conducted by applying 50 µl of the Vip3Af protein sample on a 2 $cm^2$ diameter well in multi-well plates filled with the semi-synthetic diet and let dry. A single neonate was used in each well. Bioassay plates were maintained in the insect rearing chamber. All bioassays were scored at 7 days for mortality and functional mortality (dead larvae plus stunt larvae at L1). Three types of bioassays were conducted:

i) For the screening of the alanine mutants library, pellets from 100 µl of bacterial cultures were resuspended in 1 ml of PBS. Every clone was bioassayed at a single concentration (corresponding approximatively to 150-190 ng/$cm^2$ of Vip3Af protein) using 16 individualised neonates of *S. frugiperda*. A negative control (*E. coli* DH5α without the pMAAB plasmid containing the *vip3Af* gene) and a positive control (*E. coli* expressing the Vip3Af1(WT) protein) were always done in parallel. Mutants that displayed no insecticidal activity were selected for having a mutation considered critical for the protein function. Selected mutants were screened twice. In order to dismiss a false positive result, the expression of Vip3Af protein on these samples was checked by SDS PAGE.

ii) For the semi-quantitative bioassays, Vip3Af proteins were expressed and partially purified by isoelectric point precipitation, since it was previously reported that affinity purification with Ni-columns can affect the insecticidal activity of Vip3A proteins (Hernández-Martínez et al., 2013). The precipitated Vip3Af proteins were solubilised in 20 mM Tris, 300 mM NaCl, pH 9, and tested at a concentration of 1 µg/cm$^2$, which is 130-fold higher than the $LC_{50}$ for *S. frugiperda* and 28-fold higher than the $LC_{50}$ for *A. segetum* (Table 4. 2). A total of 16 neonates of *S. frugiperda* were assayed for each mutant. The Vip3Af1(WT) protein purified by isoelectric point precipitation served as a positive control. The mutant proteins for which loss of insecticidal activity was confirmed on *S. frugiperda*, were also bioassayed against *A. segetum* in the same way. Bioassays were repeated two to three times.

***Table 4. 2. Quantitative parameters from concentration-mortality responses (at 7 days) of Vip3Af1(WT) partially purified by isoelectric point precipitation on*** S. frugiperda ***and*** A. segetum***.***

| Lepidopteran species | Regression line | | $LC_{50}$ | 95% F. L.[†] | | Goodness of fit χ2 |
|---|---|---|---|---|---|---|
| | Slope±SE | a [*] ±SE | (ng/cm$^2$) | Lower | Upper | |
| *S. frugiperda* | 1.0±0.1 | 4.2±0.1 | 7.6 | 4.9 | 11.0 | 4.3 |
| *A. segetum* | 0.9±0.1 | 3.5±0.3 | 35.2 | 19.1 | 58.9 | 4.8 |

[†] *Fiducial limits.*

[*] *a: intercept*

iii) Quantitative toxicity assays were performed against *S. frugiperda* and *A. segetum* with Vip3Af1(WT) partially purified by isoelectric point precipitation. As in the semi-quantitative bioassays, the precipitated Vip3Af1(WT) protein was solubilised in 20 mM Tris, 300 mM NaCl, pH 9, and then serially diluted to 7 different concentrations. The solubilisation buffer was used as a control. Regression curves were estimated from at least three replicates using the Polo-PC probit analysis program (LeOra-software, 1987). $LC_{50}$ values were considered significantly different when fiducial limits did not overlap.

### 4.2.6. Midgut Juice Preparation

*Spodoptera frugiperda* and *A. segetum* 5$^{th}$ instar larvae were dissected on ice and the bolus content, along with peritrophic membrane enclosing it, was collected. Once the peritrophic membrane was removed as reported in chapter III, the bolus contents from eight to ten larvae were mixed and centrifuged at 4 ºC for 10 min at 16,000 *g*. The supernatant was collected and distributed in small aliquots, immediately frozen in liquid nitrogen and stored at -80 °C. Total protein concentration in the midgut juice was quantified with Bradford reagent using BSA as standard (Bradford, 1976).

### 4.2.7. Proteolytic Pattern Assays

Affinity purified Vip3Af proteins (5 µg) were incubated with 5:100 trypsin (trypsin:Vip, w:w) or with midgut juice from either *S. frugiperda* or *A. segetum* at 0.4% in a final volume of 40 µl. After 1 h incubation at 37 ºC, PMSF was added at a final concentration of 250 µM, followed by SDS-PAGE loading buffer (0.2 M Tris-HCl pH

6.8, 1 M sucrose, 5 mM EDTA, 0.1% bromophenol blue, 2.5% SDS, and 5% β-mercaptoethanol) (2:1, sample:loading buffer) and then the samples were heated at 99 ºC for 5 min. Samples were either run immediately in 12% SDS-PAGE or frozen in liquid nitrogen and stored at −20 ºC for further analysis. The Vip3Af1(WT) was included as an internal control in all reactions. Reactions without the addition of trypsin or midgut juice were always conducted in parallel as a control for the potential thermolability of the mutant proteins. The whole assay was replicated twice. The size of the SDS-PAGE main bands in each protein sample was determined using the TotalLab 1D v 13.01 software.

To test whether the proteolysis patterns could be affected by the presence of SDS in the loading buffer (Bel et al., 2017), mutants W552A (pattern "b") and E483A (pattern "f") were subjected to incubation with 24:100 trypsin (trypsin:Vip, w:w) for 1 min to up to 3 days at 30ºC. The samples were processed and analysed by SDS-PAGE as indicated above. Additionally, the reaction mixtures after 30 min incubation with 5:100 trypsin (trypsin:Vip, w:w) at 37ºC were subjected to gel filtration chromatography in a Superdex-200 10/300 GL column using an ÄKTA explorer 100 chromatography system (GE Healthcare Life Sciences, Uppsala, Sweden) equilibrated and eluted with 20 mM Tris-HCl, 150 mM NaCl, pH 9, to a flow rate of 0.75 ml/min.

### 4.2.8. Peptide Identification

Trypsin-generated fragments from the affinity-purified Vip3Af1(WT) were electrophoretically separated in 12% SDS-PAGE. For Edman degradation analysis, proteins in the gel were transferred onto a PVDF membrane. Protein bands were then cut out and sent for Edman degradation. N-terminal amino acid sequencing was performed by using a Procise 494 (Applied Biosystems) at CIB-CSIC (Madrid, Spain).

For the peptide mass fingerprinting, protein bands were directly cut out from the gel and digested with trypsin. The peptide mass and sequence was determined by liquid chromatography and tandem mass spectrometry (LC-MS/MS) in a nanoESI qQTOF (5600 TripleTOF, ABSCIEX) at the proteomics facility of the SCSIE (Servei Central de Suport a la Investigació Experimental), at the University of Valencia (Valencia, Spain). The mass transitions were scaned first from 350–1250 m/z and then followed by a second scan from 100–1500 m/z. The peptides sequence identified were compared to the Vip3Af1(WT) protein sequence to match the region corresponding to each SDS-PAGE proteolytic band. Expected molecular weights were calculated using the online SIB Compute pI/Mw tool (Gasteiger et al., 2005).

### 4.2.9. Intrinsic Fluorescence Emission Spectra

The intrinsic fluorescence of the Vip3Af proteins, before and after trypsin treatment, was checked in a Varian Cary Eclipse fluorimeter (Agilent Technologies, Australia) with an excitation at 280 nm (excitation slit of 5 nm) and recording the emission spectra from 300 to 450 nm (emission slit of 20 nm). Fluorescence of the affinity purified proteins (5-10 µg) in 20 mM Tris, 300 mM NaCl, pH 9, was measured in a quartz cuvette in a final volume of 1.3 ml. After recording the spectra, the samples

were subjected to trypsin treatment (24:100 trypsin:Vip, w:w), at 37 ºC for 1 h). Graphic curves represent the average of three scans. The curves were smoothed with the moving average algorithm.

### 4.2.10. *In silico* prediction of the 3D structure of Vip3Af1(WT)

The *ab initio* modelling of the full sequence of the Vip3Af1(WT) protein was done using the fully automated server Robetta available online using guinzo domain prediction (http://robetta.bakerlab.org). The prediction of disulfide bonds were done using Disulfind online server (http://disulfind.dsi.unifi.it) (Ceroni et al., 2006) and the DiANNA 1.1 web server online tool (http://clavius.bc.edu/~clotelab/DiANNA/) (Ferrè and Clote, 2006).

## 4.3. Results

### 4.3.1. Screening of the Alanine Mutants Collection.

As a first step to determine the positions critical for the insecticidal activity of the Vip3Af1(WT), a quick screening was carried out on *S. frugiperda* neonates with *E. coli* cells expressing each of the 588 clones (Table 4. 1). A total of 54 clones were found to show a substantial decrease of the insecticidal activity. In the experimental conditions in which the wild type Vip3Af1 protein (Vip3Af (WT)) produced a mortality higher than 80% and a functional mortality of 100%, these 54 clones produced a mortality lower than 25% and a functional mortality lower than 45%. The expected mutations in these clones were confirmed by PCR amplification and sequencing (Table S-4.1, Annex section). After verifying Vip3Af expression in those clones with low activity by SDS-PAGE (Fig. 4. 1), 19 were found not to express the protein (Table 4. 1). Since sequencing of the *vip3Af* gene and vector indicated no sequence error, we infer that these positions might be critical for the stability of the wild type protein or its expression.

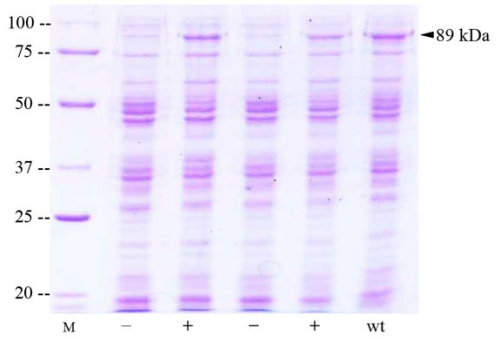


***Fig. 4. 1. Detection of the expression of Vip3Af proteins (89 kDa) in the collection of Ala-mutants used in the screening.***
*Direct broth (10 µl of the culture adjusted to an $OD_{600}$ of 4.7) was loaded and subjected to SDS-PAGE. "M": molecular weight marker (kDa); minus sign (-): absence of Vip3Af expression; plus sign (+): Vip3Af expression, and "wt": Vip3Af1(WT) as a positive control.*

To confirm the above data, the 35 clones expressing Vip3Af which decreased the insecticidal activity were subjected to a more accurate semi-quantitative bioassay testing their Vip3Af proteins partially purified by isoelectric point precipitation. The expression of the Vip3Af proteins was -verified by Western blot (Fig. 4. 2).

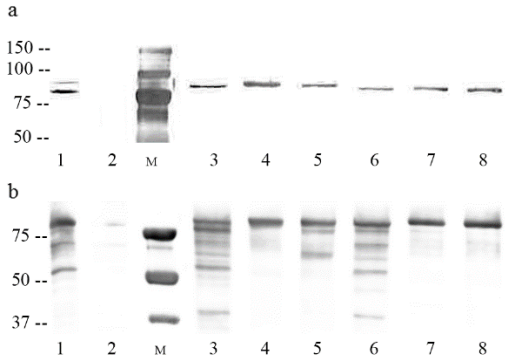


***Fig. 4. 2. Detection of Vip3Af in the crude extract after isoelectric point precipitation.***
*Membranes were probed with monocolonal antibodies against histidine for His-tag detection (a) and with polyclonal antibodies against Vip3A proteins (b). Lane 1: Vip3Af1(WT) as a positive control; lane 2: E. coli wk6Ø as a negative control; lanes 3 to 8: mutants Y272A, W552A, Y719A, M238A, G689A, and E483A, respectively. Western blot was performed to all samples but these mutants were chosen for graphic representation of the results as representative of each of the proteolytic band patterns. "M": molecular weight marker (kDa).*

In a first step, all clones were tested against *S. frugiperda*. Then, the clones exhibiting a significant decrease in toxicity against this insect species were subsequently tested against *A. segetum* (Table 4. 3). For *S. frugiperda*, the top 11 positions driving the strongest activity inhibition (defined as mortality lower than 42% and functional mortality lower than 70%; these values were chosen as to allow to include at least one mutant protein from each SDS-PAGE band pattern, as shown in the next section) were T167A, E168A, F229A, M238A, Y272A, E483A, W552A, G689A, I699A, Y719A,

and G727A. The graphical representation of the distribution of these 11 critical positions, along with other positions for which the decrease of insecticidal activity was less drastic (mortality less than 50%), is shown in Fig. 4. 3. Except for two of these positions (residues 483 and 552), the remaining positions fell into two clusters, one between residues 167 to 272, and the other between residues 689 and 741.

***Table 4. 3. Insecticidal activity of the Vip3Af1(WT) and the mutant proteins on* S. frugiperda *and* A. segetum *at a concentration of 1 µg/cm² (average of two replicates) with indication of the proteolytic band pattern.***

*Bioassays were scored after 7 days. M%: mortality. fM%: functional mortality. ND: not determined due to the lack of His-tag in the protein.*

| Vip3Af protein | Proteolysis band pattern | *S. frugiperda* | | *A. segetum* | |
|---|---|---|---|---|---|
| | | % M | % fM | % M | % fM |
| Vip3Af1(WT) | a | 72 | 100 | 60 | 100 |
| T167A | a | 3 | 6 | 31 | 94 |
| E168A | a | 16 | 22 | 6 | 6 |
| T170A | a | 56 | 94 | | |
| P171A | d | 34 | 72 | | |
| E184A | a | 59 | 100 | | |
| L194A | ND | 81 | 100 | | |
| L209A | d | 47 | 94 | | |
| L212A | a | 81 | 100 | | |
| L215A | d | 72 | 97 | | |
| F229A | d | 22 | 56 | | |
| Y230A | d | 59 | 100 | | |
| M238A | d | 28 | 59 | 13 | 35 |
| N242A | a | 44 | 91 | 59 | 100 |
| F244A | d | 49 | 90 | 72 | 94 |
| R246A | d | 41 | 97 | 47 | 100 |
| K250A | a | 91 | 100 | | |
| E254A | a | 62 | 100 | | |
| L255A | ND | 41 | 81 | | |
| V261A | a | 59 | 97 | | |
| N270A | a | 78 | 100 | | |
| Y272A | a | 10 | 19 | 0 | 0 |
| V277A | ND | 67 | 100 | | |
| L287A | a | 66 | 100 | | |
| I301A | a | 58 | 73 | | |
| M307A | a | 63 | 100 | | |
| E483A | f | 21 | 61 | 63 | 100 |
| F485A | a | 59 | 100 | | |
| W552A | b | 13 | 13 | 13 | 16 |
| G689A | e | 41 | 69 | 16 | 26 |
| I699A | c | 29 | 33 | 0 | 0 |
| L711A | c | 44 | 100 | 44 | 72 |
| Y719A | c | 22 | 25 | 3 | 6 |
| G727A | c | 27 | 27 | 0 | 0 |
| F741A | c | 28 | 94 | 38 | 56 |
| H779A | ND | 56 | 59 | | |

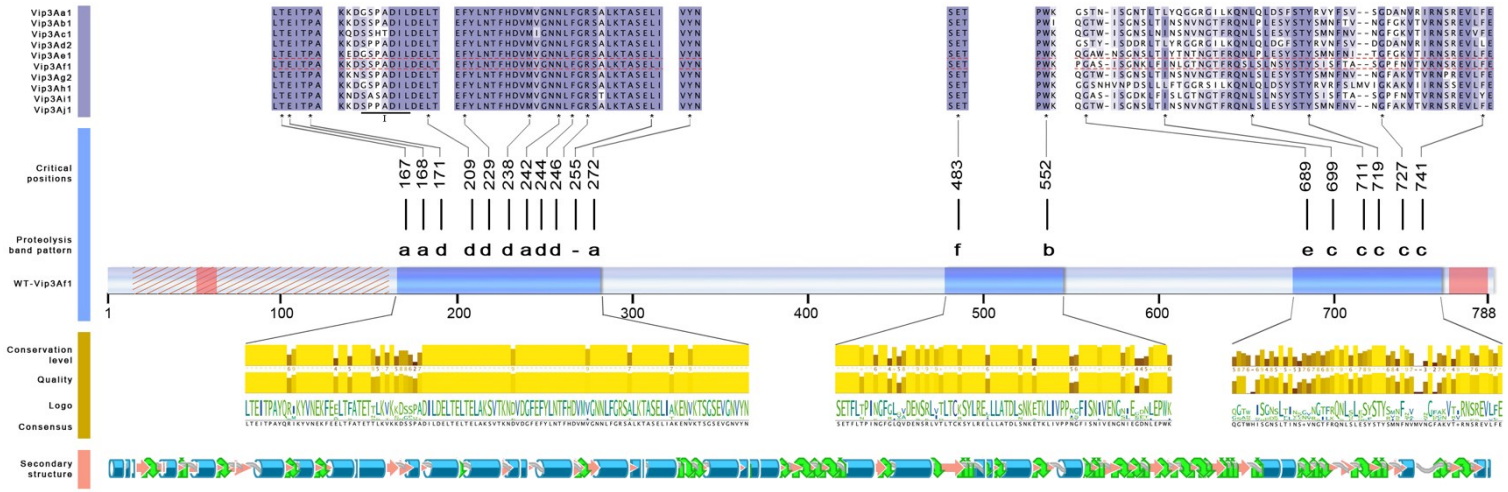


***Fig. 4. 3. Vip3Af1(WT) critical amino acid positions for the insecticidal activity.***

*Vip3Af1(WT) sequence is represented by the grey bar (blue panel). The dashed region was not subjected to alanine scanning; blue segments in the protein bar are the regions where these critical positions are clustered. Red segments indicates the hypothetical contacting region. Above the protein bar, letters "**a**" to "f" illustrate the different proteolysis profiles displayed by the proteins with the substitutions to Ala in these positions (see Fig. 4). Conservation of these sites was evaluated by Clustal Omega msa* (Sievers et al., 2011) *of different Vip3A proteins from* ***Bacillus thuringiensis****: Vip3Aa1 (GenBank accession number AAC37036), Vip3Ab1 (accession number AAR40284), Vip3Ac1 (named PS49C with Seq. ID 7 in U.S. patent application 20.040.128.716 (Narva and Merlo)), Vip3Ad2 (accession number CAI43276), Vip3Ae1 (accession number CAI43277), Vip3Af1 (accession number CAI43275), Vip3Ag2 (accession number ACL97352), Vip3Ah1 (accession number ABH10614), Vip3Ai1 (accession number KC156693) and Vip3Aj1 (accession number KF826717). The msa (purple panel) is coloured according to BLOSUM62 colour scheme. Amino acid conservation, quality (BLOSUM62 score based on observed substitutions), logo visualisation (Buried index: dark green (buried), light green (exposed)) and consensus sequence as visualised by Jalview* (Waterhouse et al., 2009) *is shown in the yellow panel. The lower panel (orange panel) represents the predicted secondary structure using Geneious v. 6.0* (Kearse et al., 2012)*: blue cylinders are α-helixes, pink arrows are β-sheets, green arrows are turns, and grey waves represents coils. "I" marks the beginning of the 66 kDa insecticidal fragment described for the Vip3Aa according to Rang et al.* (Rang et al., 2005).

### 4.3.2. Proteolytic cleavage of the wild type and mutant Vip3Af proteins

To indirectly assess whether the change to Ala could affect the structure of the protoxin, the 35 mutant proteins selected in the screening for decreased insecticidal activity were subjected to proteolytic treatment and classified according to their proteolysis band pattern. Six different band patterns were revealed by SDS-PAGE (Fig. 4. 4). The patterns were comparable no matter whether they were obtained with bovine trypsin or with midgut juice from either *S. frugiperda* or *A. segetum.*

Different sizes of the most conspicuous bands characterise these patterns, especially the bands corresponding to the 62 kDa and 20 kDa fragments, the two more intense bands in the Vip3Af1(WT), which characterize the pattern "a" and which are generated by the action of proteases on the primary cleavage site (Bel et al., 2017). The 62 kDa band was not among the main bands in patterns "b", "c", "e" and "f", and the 20 kDa band was not present in patterns "d" and "f", which showed a major band of 27 kDa. Patterns "b", "e" and "f" were only represented once among the 35 pre-selected mutants. It is also worth to note that patterns "a" and "d" (both maintaining the 62 kDa band) were found in those mutants clustering in the first half of the protein, whereas patterns "c" and "e" (both being very similar except for the faint presence of the 62 kDa band in "e") were found in mutants clustering near the C-terminus. Patterns "b" and "f" were found in the two mutants not included in these two clusters.

It has been recently shown that proteases, in the presence of SDS, can act on secondary cleavage sites of Vip3Aa in the interval between the moment that the loading buffer is added and the moment that the proteins are heat denatured (Bel et al., 2017). To test whether our proteolysis patterns could be affected by the presence of SDS in the loading buffer, mutants W552A (pattern "b") and E483A (pattern "f") were subjected to incubation with trypsin for up to 3 days. The results showed that, regarding the major bands, the pattern that appeared after 1 min incubation was the same as the one obtained after 3-days incubation (when no trypsin remains in the reaction mixture) (Fig. 4. 5 a and b). Similarly, the major bands pattern obtained for these two mutants did not changed after subjecting the reaction mixture to gel filtration chromatography, indicating that removal of trypsin before SDS-PAGE does not have an effect on the major bands that characterize the proteolysis pattern (Fig. 4. 5 c and d). Minor bands are probably a consequence of the SDS effect on the protein. Therefore, under the experimental conditions used, these band patterns reflect the digestion of these mutated protoxin to proteases *in vitro*.

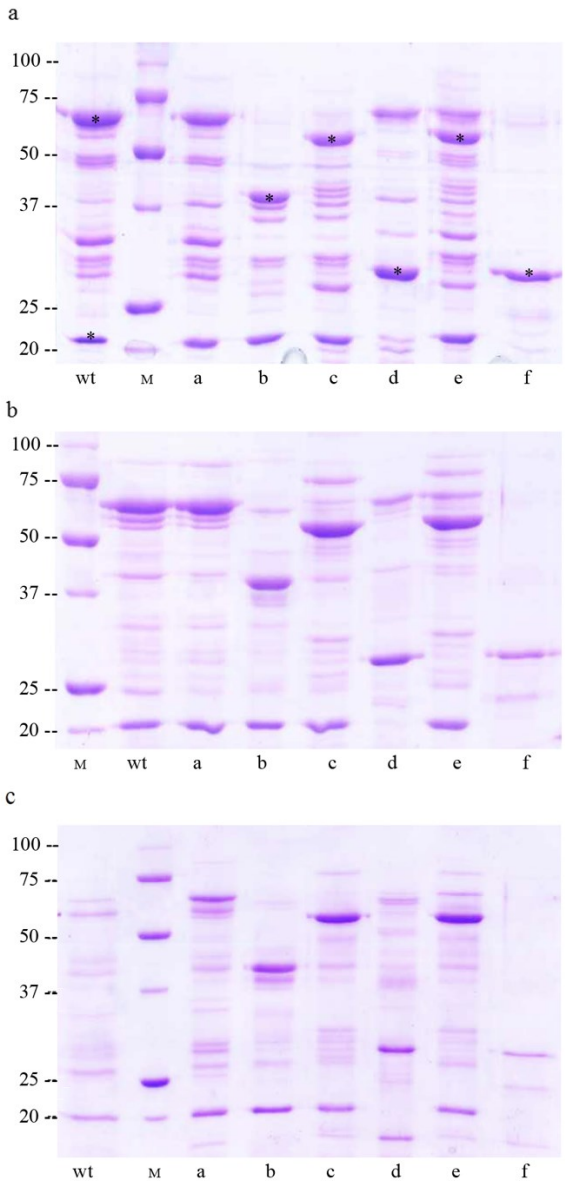


***Fig. 4. 4. Representative proteolytic band patterns of the selected mutant proteins of Vip3Af1(WT) after SDS-PAGE.*** *Protein samples (5 μg) were incubated with 5:100 trypsin (trypsin:Vip, w:w) (a), 0.4% midgut juice from S. frugiperda (b) or 0.4% midgut juice from A. segetum (c) (wt/wt, midgut juice total protein/Vip). Incubations were performed at 37 ºC for 1 h. Lanes "wt": Vip3Af1(WT), "M": molecular weight marker (kDa), "a to "f": mutants Y272A, W552A, Y719A, M238A, G689A and E483A, respectively. The different proteolysis profiles are defined according to their main protein bands after SDS-PAGE as follows: Pattern "a" (corresponding to the "wt): 62 kDa and 20 kDa; pattern "b": 40 kDa and 20 kDa; pattern "c": 53 kDa and 20 kDa; pattern "d": 62 kDa and 27 kDa; pattern "e": 62 kDa, 57 kDa and 20 kDa, and pattern "f": 27 kDa. "*" indicates the bands analysed for peptide identification either by EDMAN degradation or by peptide mass fingerprinting.*

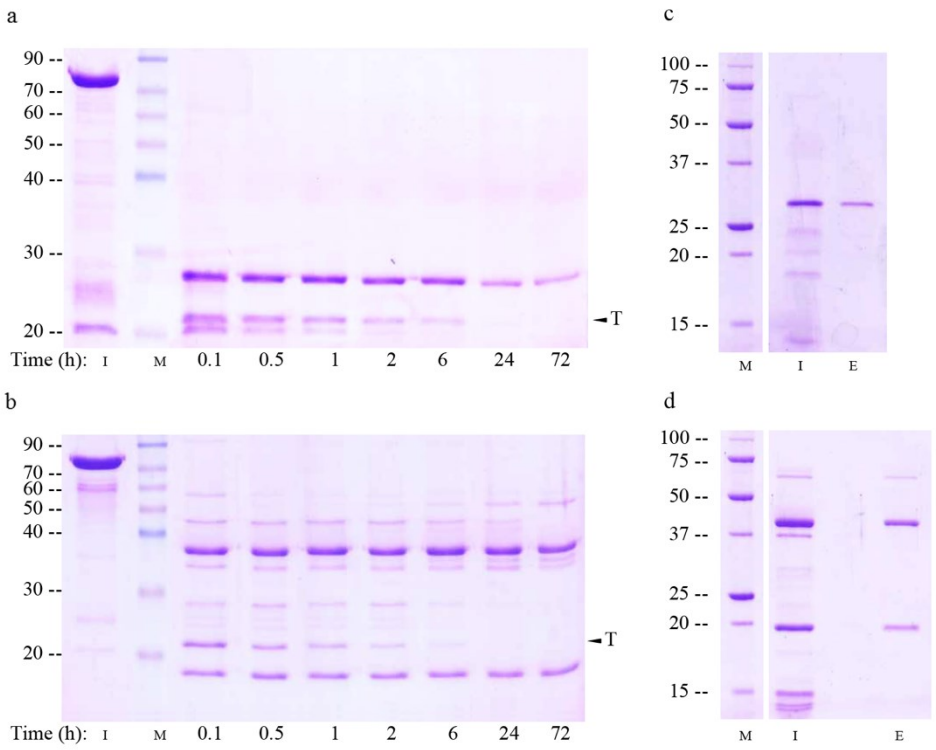


***Fig. 4. 5. Analysis of the effect of the SDS on the proteolytic pattern of Vip3Af-mutant proteins E483A (pattern "f", panels a and c) and W552A ("pattern b", panels b and d) after trypsin treatment.***

*Protein samples were treated with 24:100 trypsin (trypsin:Vip, w:w) at 30 ºC for the kinetics analysis (panels a and b); Each line of the SDS-PAGE corresponds to 3 µg of protein sample. For the size exclusion chromatography (panels c and d), protein samples were treated with 5:100 trypsin (trypsin:Vip, w:w) during 30 min at 37 ºC and injected into a Superdex-200 10/300 GL column. Panels c and d show the input sample and the elution protein fractions as revealed by SDS-PAGE. M": molecular weight marker (kDa), "I": sample input (Protoxin in panels a and b, Toxin in panels c and d), "E": eluted fraction. "T": Trypsin.*

### 4.3.3. N-terminal sequence analysis of tryptic fragments and peptide identification

Some proteolytic fragments were subjected to N-terminal sequencing to determine their position in the protein (see Fig. 4. 4). The 20-kDa fragment, obtained after trypsin treatment of the Vip3Af1(WT), yielded the sequence ALPSF, the first amino acid corresponding to $Ala^{12}$. The N-terminal sequence of the 62-kDa was DXXPA, which only matched with the query sequence on DSSPA (D = $Asp^{199}$) (see "I" in Fig. 4. 4). The protein is thus cleaved after $Lys^{198}$, within a highly conserved region rich in lysine residues, cleaving the protein in two main fragments of 20 kDa and 62 kDa. The N-terminal sequence of the 27 kDa fragment obtained after trypsin treatment of the E483A mutant (pattern f) was IVPPS, which perfectly matches with the sequence starting with $Ile^{528}$ and, considering the molecular weight of the fragment, it spans from $Ile^{528}$ till almost the C-terminus of the protein. This result was in agreement with the region identified using the peptide mass fingerprinting. The

peptide identification of the other bands highlighted with an asterisk in Fig. 4. 4, shows that the 40 kDa band from the mutant W552A (pattern b) is derived from the central region of the protein, matching small peptides from $Ser^{247}$ to $Lys^{602}$, a region that corresponds to a theoretical size of 39.8 kDa. Similarly, the 53 kDa band present in "pattern c" matched different small peptides spanning the region from $Tyr^{178}$ to $Lys^{661}$, which would correspond to a theoretical size of 54.4 kDa. The remaining bands, of 27 kDa present in "pattern d" and of 57 kDa present in the pattern from mutant G689A (the only representative of "pattern e"), matched peptides all over the protein sequence, making it impossible to identify the source of these bands.
Interestingly, all fragments analysed by peptide mass fingerprinting always revealed the presence of 2 small peptides in the N-terminus (53-NQQLLNEISGK-65) and in the C-terminus (743-SNLMSSTSHISGTFKTESNNTGLYVELSR-773).

### 4.3.4. Emission Spectra from Vip3Af1(WT) and Vip3Af-selected mutants

An indirect measure of the spatial conformation and folding of the Vip3Af1(WT) and the selected mutant proteins was obtained by analysing the intrinsic fluorescence emission spectra of the protoxin and the toxin forms (Fig. 4. 6). All Vip3Af protoxins and the processed forms showed emission maxima below 348 nm (the maximum expected for free Trp in water (Teale and Weber, 1957)), indicating that most Trp are buried into the hydrophobic core of the protein. The existing tryptophan in the Vip3Af are located in the C-terminal end at positions W552, W658 and W684. In the transition from protoxin to toxin, there is only one case (M238A) for which the quantum yield decreases, along with a slight shift to the red, suggesting a change in the surrounding of the Trp residues to higher polarity, perhaps by being exposed to the aqueous buffer. For the other mutant proteins, the transition from protoxin to toxin renders either practically no increase in the quantum yield –as was the case for Vip3Af1(WT) - or a significant increase, which suggest either changes to less polar environments or the minor contribution of the single tryptophan from the trypsin molecule.

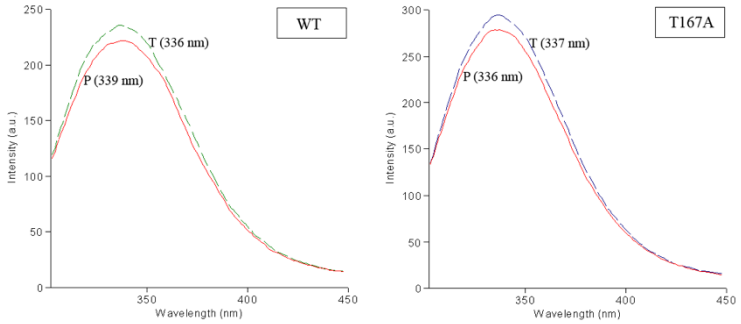


***Fig. 4. 6. Emission spectra of the intrinsic fluorescence of Vip3Af1(WT) and mutant Vip3Af proteins with reduction of their insecticidal activity (1/3).***
*Proteins (3 -8 µg/mL) were excited at 280 nm and the emission was scanned from 300 to 450 nm. "P": protoxin; "T": protoxins treated with 24:100 trypsin (trypsin:Vip, w:w) at 37 ºC for 1 h. The maximum emission peak is indicated within brackets.*

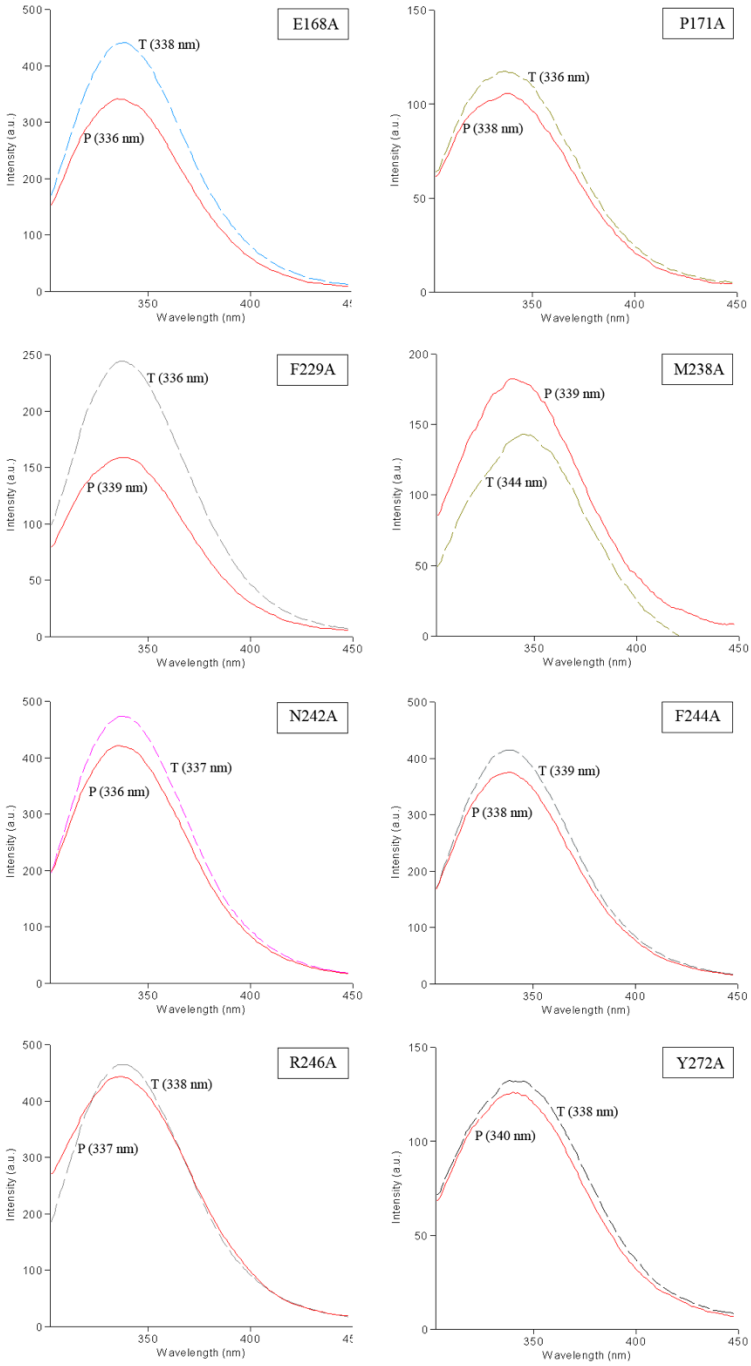


***Fig. 4. 6. Emission spectra of the intrinsic fluorescence of Vip3Af1(WT) and mutant Vip3Af proteins with reduction of their insecticidal activity (2/3).***

*Proteins (3 -8 µg/mL) were excited at 280 nm and the emission was scanned from 300 to 450 nm. "P": protoxin; "T": protoxins treated with 24:100 trypsin (trypsin:Vip, w:w) at 37 ºC for 1 h. The maximum emission peak is indicated within brackets.*

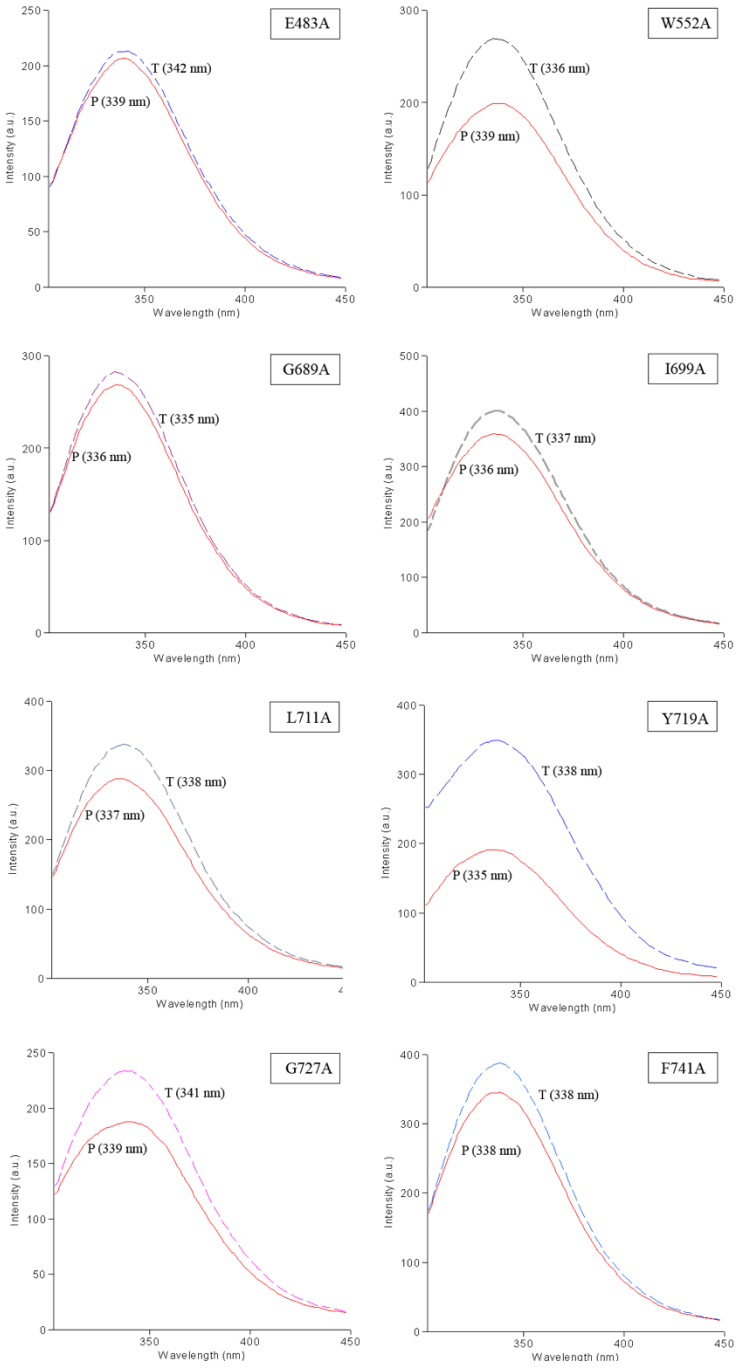


***Fig. 4.6. Emission spectra of the intrinsic fluorescence of Vip3Af1(WT) and mutant Vip3Af proteins with reduction of their insecticidal activity (3/3).***

*Proteins (3 -8 µg/mL) were excited at 280 nm and the emission was scanned from 300 to 450 nm. "P": protoxin; "T": protoxins treated with 24:100 trypsin (trypsin:Vip, w:w) at 37 ºC for 1 h. The maximum emission peak is indicated within brackets.*

### 4.3.5. Structure prediction of the Vip3Af1(WT)

The *in silico* modelling of the Vip3Af1(WT) resulted in a structure parsed into 5 different domains, three of which are modelled by homology whereas the other two are modelled *ab initio*. Domain 1 spans up to amino acid 188 (domain confidence level 0.18, *ab initio*), Domain 2 spans from position 189 to 272 (domain confidence level 0.20), Domain 3 extends from amino acid 273 to 542 (domain confidence level 1.01, *ab initio*), Domain 4 is predicted from residue 543 to residue 715 (domain confidence level 0.42) and Domain 5 spans from amino acid 716 till the end of the protein (domain confidence level 0.83).
The three-dimensional structure of this model (Fig. 4. 7) identifies two main regions: The N-terminus depicted mainly by α-helix structures, and the C-terminus with greater prevalence of ß-sheet structures. The central region of the protein is greatly formed by disordered structures.

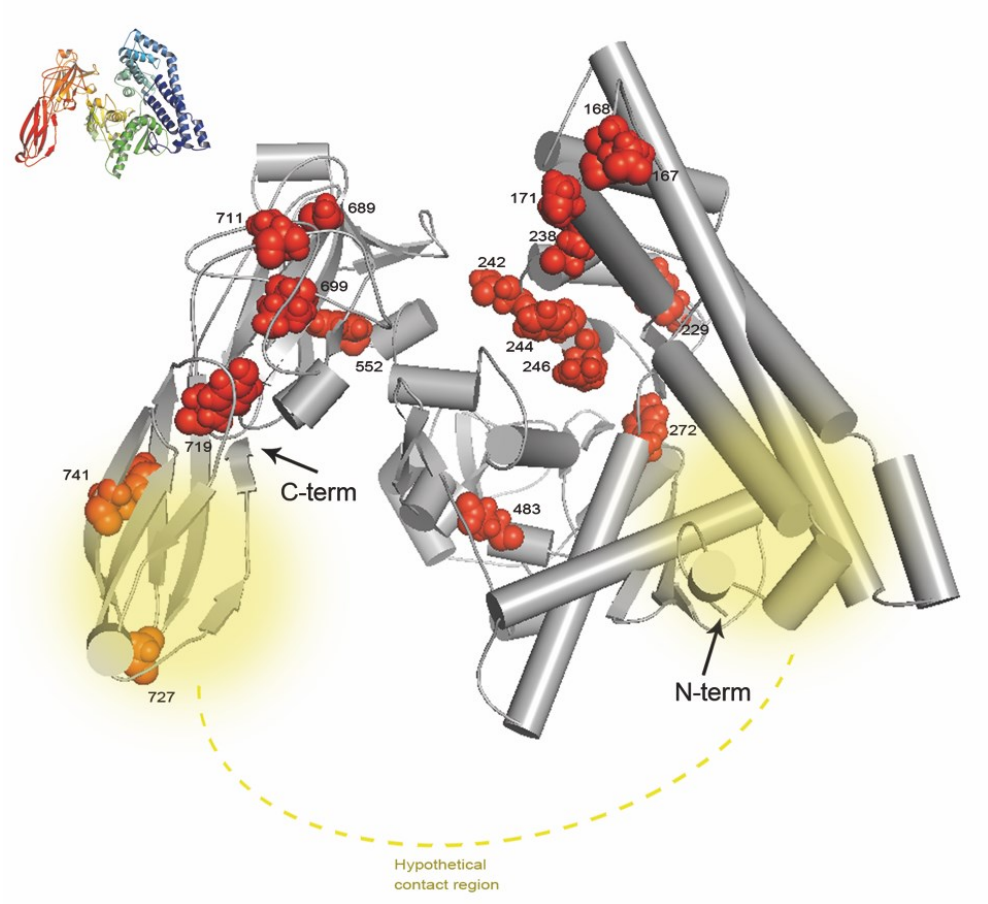


***Fig. 4. 7. Representation of the critical positions in a 3D conformation of the Vip3Af1(WT).***
*The structure was predicetd* ab initio *using Robetta (confidence level of the domains conforming the model vary from 0.18 to 0.83) visualised with PyMOL v 1.8* (Schrödinger, 2015). *The structure in the upper left corner is coloured from blue (N-term) to red (C-term) and serves as a guide to visualize the 5 predicted domains. Yellow shadows indicate the hypothetical contacting region.*

The prediction of whether residues, represented in the alignment shown in Figure 4. 3, were exposed or buried was conducted using the Conseq server (Berezin et al., 2004). No disulphide bonds are expected in any of the 3 cysteine residues along the Vip3Af1(WT) sequence according to the two online servers employed; nevertheless, DiANNA server predicted C401 as a half-cystine with a score of 0.53.

## 4.4. Discussion

A total of 558 out of 788 residues of the Vip3Af1(WT) were analysed for their specific contribution to the insecticidal selectivity and potency, and to protein stability, by means of alanine scanning. Most of the substitutions constituted neutral mutations, stressing the high level of resilience and adaptability of Vip3A proteins to preserve protein function and homeostasis, even when most of these changes involved the substitution of highly conserved residues among the Vip3A subfamily. Only 10% of the residues analysed play a crucial role in either protein stability, protein folding, proteolytic processing or insecticidal activity of the Vip3Af1(WT). In all, we have detected 54 substitutions affecting the function/stability of the protein, 19 out of which accounted for non-synonymous substitutions compromising protein expression, or alternatively rendering such unstable proteins that were degraded immediately after their expression since it was not possible to detect the protein expression in SDS-PAGE (Fig. 4. 1). The remaining 35 substitutions decreased the insecticidal potency against *S. frugiperda* in different degrees (Table 4. 3). Further characterization of these 35 variants by protease analysis was performed in order to indirectly assess the impact of the substituted residues on the tertiary structure of the protein. The clustering of the most critical positions affecting insecticidal activity against *S. frugiperda* revealed 2 main '*hot spots'* along the Vip3Af1(WT) sequence, one located near the N-terminus ($Leu^{167}$ – $Tyr^{272}$) and the other near the C-terminus ($Gly^{689}$ – $Phe^{741}$) (Fig. 4. 3). These clusters correspond to the end of domain 1 and the whole domain 2, and the end of domain 4 and beginning of domain 5, predicted in the *ab initio* tertiary structure, respectively (Fig 4. 6). Likewise, the different proteolytic patterns cluster in preferred regions of the sequence: with the exception of G689A (which gives patter "e"), the 62 kDa band was only present in the variants clustered in the N-terminal region, represented by proteolytic patterns "a" and "d", whereas pattern "c" was only represented in the C-terminus cluster along with patter "e". Most of the changes compromising the insecticidal activity consisted of a variety of hydrophobic amino acids. Alanine is the smallest of the hydrophobic residues, thus, a hydrophobic bulk decrease might imply local steric modifications negatively affecting the protein function.

It is very likely that mutants displaying profile "a" do not alter the tertiary structure of the protein, since this is the band pattern obtained for the wild type protein. Thus, the loss of insecticidal activity in these variants is likely to be due to the change in their respective native residues, which might be critical for the insecticidal function, either by constituting a key structural residue whose change leads to a locally

misfolded protein or by constituting a key functional residue whose change interferes with critical interactions with other molecules. Pattern "a" was characterised by the main bands of 62 kDa and 20 kDa, similarly to the 65 kDa and 22 kDa bands initially described for the Vip3Aa1 by Estruch and Yu (Estruch and Yu, 2001). Peptide identification confirmed that the protein sequence is split in two at $Lys^{198}$, giving two main fragments which match the C-terminal end and the N-terminus, respectively. There is evidence that after proteolytic digestion, these two main fragments co-elute after gel permeation chromatography (Fig. 4. 5), suggesting that they remain bounded after cleavage (Chakroun and Ferré, 2014). It is likely that these regions are spatially close enough in the protoxin native conformation such that intramolecular interactions such as hydrogen bonds or salt bridges, present far from the primary cleavage site, remain intact following proteolytic activation. We propose that the contact regions between this pair could be from residues 53-65 and from residues 743-773, since these peptides always appeared in the mass fingerprinting of the different proteolytic fragments. These two regions are placed close to the two "*hot spots*" in the Vip3Af1(WT) sequence described for the insecticidal activity (Fig. 4. 3 and Fig. 4. 7).

The other band patterns different from "a" (i.e. patterns "b" to "f") reveal changes in the structure that make secondary cleavage sites (those sites different from the main cleavage site after $Lys^{198}$) more easily available to proteases. The fact that the proteolytic patterns obtained are similar after trypsin treatment and after midgut juice treatment from both *S. frugiperda* and *A. segetum* (Fig. 4. 4) suggests that the decrease of toxicity of these mutants is related to the instability to proteases *in vivo*. Since the fluorescence emission spectra indicate that none of the selected mutants lead to a detectable unfolding of the protein, the possible conformational changes made by the residue exchanges must be local, affecting just their immediate vicinity. The absence of a major folding change of the Vip3 proteins after activation is in agreement with the recently published study on the 3D topology of the Vip3Ag4 (Palma et al., 2017). An exception to his general effect is mutant E483A, in which a drastic change in the protein fold after activation takes place as revealed by the unique proteolytic band of only 27 kDa (Fig. 4. 5). This single fragment contains the three Trp of the Vip3Af, suggesting that the partial folding of the β-structure in the C-terminus remains unchanged.

The largest fragment from the trypsin treatment, the 62 - 66 kDa polypeptide, is considered to be the core active toxin (Abdelkefi-Mesrati et al., 2011a, 2011b; Bel et al., 2017; Ben Hamadou-Charfi et al., 2013; Caccia et al., 2014; Chakroun et al., 2012; Chakroun and Ferré, 2014; Estruch and Yu, 2001; Gayen et al., 2015, 2012; Hernández-Martínez et al., 2013; Lee et al., 2006, 2003; Li et al., 2007; Liu et al., 2011). We have found that some of the mutants with proteolytic patterns lacking the 62 kDa band still retain some insecticidal activity, which could suggest that fragments smaller than 62 kDa are toxic (Table 4. 3). However, since the toxicity of these mutants was tested with the protoxin form and not with the processed protein, we cannot attribute the toxicity of the mutants to the fragments smaller than 62 kDa. It is very likely that the toxicity observed *in vivo* with the protoxin is due to an

intermediate 62 kDa core before the processing to a smaller fragment is completed, suggesting that the activation process is a multi-step event with intermediate sized fragments.

Regarding the smallest fragment of 19 – 22 kDa at the N-terminus, there is agreement in that it contains a signal peptide involving the first 34 residues, which is not removed after protein secretion (Chen et al., 2003; Doss et al., 2002; Estruch et al., 1996; Rang et al., 2005). However, Doss et al. (Doss et al., 2002) suggested a putative cleavage site between residue $Thr^{10}$ and $Arg^{11}$ in Vip3Aa based on the S score prediction. It is likely that the signal peptide in the Vip3Af1 is cleaved after $Arg^{11}$, since trypsin cleaves after amino acids Lys or Arg. Few attempts have been made to elucidate the role of the N-terminus of the Vip3A proteins other than identifying the presence of a predicted signal peptide (Bhalla et al., 2005; Chen et al., 2003; Li et al., 2007; Liu et al., 2017; Selvapandiyan et al., 2001) and, among these, the results are controversial: deletion of the first 200 residues in Vip3Aa led to opposite results, from complete suppression of insecticidal activity and total sensitivity to trypsin digestion, to an increase of up to 2.8-fold in the toxicity against different caterpillar species, both when tested as the purified toxin and when expressed in a tobacco transgenic line (Gayen et al., 2015, 2012; Li et al., 2007).

The lack or decrease of toxicity in Vip3Aa mutants with C-terminal modifications was often related to an increase in the sensitivity towards proteases in the gut environment of susceptible insects. A triple mutation in the C-terminal sequence of Vip3Aa1, and also the Vip3Aa3 protein, which lacks the 44 last residues of a typical Vip3Aa sequence, render a highly unstable protein against gut fluids preventing the insecticidal function in susceptible pest species but not against the insect cell line Sf9 (Estruch and Yu, 2001). Either the deletion or the addition of a few residues to the very C-terminal end of a Vip3A chimeric protein was found to lead to complete trypsin hydrolization of the 62 kDa fragment and to abolish the insecticidal activity (Li et al., 2007a). A more drastic deletion of up to 220 residues in the C-terminus of Vip3Aa9 rendered a completely inactive protein whereas the deletion of the last 154 amino acids marginally decreased the toxicity against *Chilo partellus* (Lepidoptera: Crambidae) while this mutant was not toxic against *Spodoptera litura* (Lepidoptera: Noctuidae) (Selvapandiyan et al., 2001). Experiments conducted by C-terminal sequence swapping on Vip3A proteins displayed opposite results depending on the sequence combination of the resulting chimera, including an increase in the insecticidal potency and even a broaden of the target range in comparison to the native proteins (Fang et al., 2007). The importance of the C-terminal region in the protease resistance and toxicity is in agreement with our results clustering critical positions for the protease sensitivity and the toxicity against *S. frugiperda* in a carboxy-terminal region within the last 100 amino acids of the protein (Fig. 4. 3). We propose that the protein stabilisation role of the C-terminus might be achieved by intra-chain interactions (e.g. hydrogen bonding, salt bridges) between the β-sheets of the C-terminus and the α-helices of the N-terminus. The disruption of these interactions by mutation to a residue with different physicochemical properties might lead to the exposure of a secondary cleavage site downstream of the main first

processing (192-XXKVKX-199 (Rang et al., 2005)), perhaps in sequence 259-KENVK-263 for the mutant in pattern "e" and 212-KEK-216 for pattern "c" (Fig. 4. 3 and Fig. 4. 7).

The high divergence of the C-terminal sequences amongst Vip3A proteins has been proposed to be rather related to evolutionary diversification than to the lack of functional constraints (Wu et al., 2007), and thus, we would expect a higher acceptance of alanine substitution in this region without hindering the protein function. Though the C-terminal region of Vip3 proteins is quite diverse, there are still several residues in the C-terminus highly conserved amongst different Vip3A sequences which are likely to pose functional or structural constraints, and therefore not likely to be subjected to positive selection pressure. This is in fact the case for all residues identified to be critical for the insecticidal performance when substituted by an alanine throughout the protein sequence (Table 4. 3, Fig. 4. 3). The alanine replacements in these conserved sites constitute neither a homologous nor a conservative change and, therefore, the chemical properties of the native residues may take part in crucial interactions driving insecticidal response.

The effect of alanine substitutions on the insecticidal activity of Vip3Af is similar for the two caterpillar pest species tested, with some exceptions. Substitutions T167A and E483A apparently are not as critical for *A. segetum* as for *S. frugiperda* (Table 4. 3). In contrast, most of the selected mutations in the C-terminus of the Vip3Af (G689A, I699A, Y719A, and G727A) were more critical for the insecticidal activity against *A. segetum* than for *S. frugiperda*. Wu et al. (Wu et al., 2007) proposed that $Gly^{689}$ in the Vip3Af1(WT) (position 711 in the reference paper) was a site subjected to positive selection pressure and it is likely that this position plays its role in sequence diversification whereas the specific change to an alanine results in a negative mutation. The different behaviour of the above-mentioned mutations between *A. segetum* and *S. frugiperda* supports the hypothesis of the C-terminal sequence being responsible for target diversification and specificity. It is worth noting that both pest species have quite similar susceptibility profile to Vip3A proteins and that larger differences could be observed if other species were tested (for overall different Vip3 susceptibility refer to Chakroun et al. (Chakroun et al., 2016a, 2016b)).

The only mutation rendering the proteolytic pattern "b", W552A, suppressed the insecticidal activity. This position is located within the predicted carbohydrate binding motif (CBM 4,9), which is a common feature in all Vip3 proteins known so far with the exception of Vip3B proteins (Chakroun et al., 2016a). Interestingly, aromatic residues such as tryptophan, tyrosine and, less commonly, phenylalanine, are considered as key residues for CBM ligand recognition and binding (Boraston et al., 2004).

The secondary and the tertiary structure of the Vip3Af1(WT) predicted in the present work suggest that the N-terminal region is mainly composed of α-helices and the C-terminus is predominantly constituted by β-sheets, in agreement with what was described previously for Vip3 proteins (Wu et al., 2007). This disposition might be a common feature among Vip3 proteins as judged from the high homology in their consensus sequences (Fig. I- 10, Introduction section) and is also the secondary

structure disposition among the well-known Cry proteins (Palma et al., 2014). Although a reliable conclusion on the tertiary structure cannot be drawn without further empirical information, the architecture of the Vip3Af1(WT) is predicted to have 5 domains with a high rate of disordered regions, coils and loops in the last 4 domains (Fig. 4. 6). Furthermore, the structure predicted by the Robetta server locates the above discussed $Gly^{689}$ (the position that gives pattern "e" when mutated to Ala) in a loop between two β-sheets just as in the model predicted for the C-terminal region by Wu et al., ( 2007).

In agreement with the *in silico* prediction, none of the cysteine substitutions in C292A, C401A or C507A affected the toxicity against *S. frugiperda*, suggesting the absence of disulphide bonds stabilizing the chain structure. Contrary to our results, the insecticidal activity of the Vip3Aa7 was seriously compromised when each native cysteine was substituted to a serine (Dong et al., 2012b); the loss of the activity of C507S was rather related to trypsin sensitivity, though the authors do not discard the involvement of a disulphide bond between the pair $C^{401}$-$C^{507}$. Interestingly, $C^{401}$ is the only cysteine residue predicted to be oxidized. The role of cysteines is commonly related to protein stabilization by covalent bonding between residue pairs, although the substitution of a half-cystine can be locally compensated by either the new residue or with other amino acid residues in their vicinity, with different type of interactions other than disulphide bonds (e.g. hydrogen bonding, hydrophobic interactions, aromatic and aliphatic π interactions) yet resulting in a functional protein (Christensen et al., 1997; Jagtap et al., 2007; Thangudu et al., 2008). These three cysteine residues are indeed highly conserved among all Vip3A sequences described so far. The main difference between Vip3A and Vip3B proteins is a short sequence insertion rich in cysteines, along with the deletion of the $Cys^{507}$ (Palma et al., 2012; Rang et al., 2005). The presence of the Cys residues could be involved in rapid evolution and diversification of Vip3 insecticidal proteins as it has been extensively described for small multimeric toxins in snake venoms (Calvete et al., 2005, 2003; Juárez et al., 2008; Yeates, 2007).

Despite discovery of the first Vip3 proteins more than 20 years ago, only few surveys addressing structural features implied in their mode of action are available and there is not a clear insight into their adaptive evolutionary role. The large number of Vip3 proteins and the variability of toxicity against certain closely related pest species suggests a tight relationship between structure and function. The critical positions described herein may contribute to improving the insecticidal potency and the stability of Vip3A proteins by more rational and directed molecular modifications.

# CHAPTER V

## 5. Exploring intramolecular organisation of the Vip3Af from *Bacillus thuringiensis* by site-directed mutagenesis.

## 5.1. Introduction

Worldwide agriculture is continuously facing new challenges to adapt to global change and the human density. According to FAO reports, the rate of human population increase is predicted to reach 9 billions of people by 2050 (Alexandratos and Bruinsma, 2012). After the Green Revolution, the agriculture has been deeply transformed by means of intensification and technification in order to obtain higher yields and cope with the food market rules. With the consequent increase of the world arable surface accounting up to 1.6 billion ha (Alexandratos and Bruinsma, 2012), the amount of chemicals released to the environments has increased accordingly, summing up more than 166 million tonnes of fertilizers (Alexandratos and Bruinsma, 2012) and up to 3.8 million tonnes of pesticides annually (De et al., 2014; EPA, 2017; Tilman et al., 2001). From the total amount of pesticides used worldwide, the large part accounts for herbicides followed by insecticides and fungicides, though this distribution varies within different regions in the planet (Carvalho, 2006; De et al., 2014; EPA, 2017; EUROSTATS). The overuse of conventional pesticides during the last decades has led to serious environmental and food security concerns and as a consequence, the approval of many active substances has been drawn back. Pesticides such as DDT or HCH are still widely used in developing countries, whereas in Europe, of the existing 1355 actives substances, only 486 actives remain authorised, 76 out of which are candidates for substitution due to unacceptable hazard (Carvalho, 2006; De et al., 2014; 'EU Pesticides database'). In this context, the development of green plant protection products as well as biotechnology-based improved crops (biotech crops) that permit to reduce the employment of chemical pesticides in combination with local agricultural practices is of upmost priority. *Bacillus thuringiensis* based crops (Bt-crops) are the most largely cultivated biotech crops, together with glyphosate tolerant crops (ISAA). Other type of genetically modified crops (GMO) crops conferring valuable properties such as drought resistance stress, or diverse viral disease resistance are already available. Furthermore, attempts to apply the utmost cutting edge technologies of gene silencing and genome editing such the breakthrough CRISPR/CAS technology to biotech-crops are lately being reported (Kupferschmidt, 2013; Lacey et al., 2015; Li et al., 2012; Shan et al., 2013; Wang et al., 2014). In fact, during 2016, the first non-GMO gene-editing crop, a sulfonylurea herbicides tolerant canola, was marketed in the USA (James, 2015).

Microbial control agents are used as sustainable, health safe and renewable biopesticides, often combined with other chemical pesticides to protect a crop in integrated pest management (IPM) programs. From all known insecticidal microbial control agents, *B. thuringiensis* (Bt) is by far the most used, either as Bt-based bioformulants or as Bt-crops (EPA, 2017; Jouzani et al., 2017; Lacey et al., 2015; Moar et al., 2017). Vip3 proteins from *B. thuringiensis* are insecticidal proteins secreted to the environment during the bacterial vegetative growth phase. The mode of action

of Vip3 and Cry proteins is similar, differing mainly in the binding to specific receptors. This difference has led to the development of stacked crops co-expressing Cry1 and Vip3A proteins as to prevent resistance development of susceptible insects. Likewise, other Cry-expressing crops are being pyramided with insect specific RNAi to counteract insect resistance to Cry-expressing crops (Bernardi et al., 2015, 2014; Carrière et al., 2015; Chakroun et al., 2016a, 2016c; Gayen et al., 2015; Graser et al., 2017; ISAA; Kurtz et al., 2007; Ni et al., 2017; Sanchis, 2011). Furthermore, the genetic engineering of Vip3A proteins in other insecticidal microbial agents such as *Beauveria bassiana* is a promising tool to potentiate the pest management strategies in combination with more conventional approaches (Liu et al., 2013; Qin et al., 2010). Additionally, there is room yet to improve the more classic approach of Bt-based formulations either by toxin microencapsulation in inert cells or by means nanotechnology (De et al., 2014; Hernández-Rodríguez et al., 2013; Jouzani et al., 2017; Mahadeva Swamy and Asokan, 2013; Panetta, 1993).

Vip3 proteins are highly active and selective against caterpillar pests, though they do not cover a wide range of target pests. Broaden the target pest or the insecticidal potency of the already known proteins by molecular techniques is a shorter and cheaper approach to increase the available resources for the agricultural pest management. Unlike Cry toxins, only few studies exist aiming the structure and folding of Vip3 proteins or their performance improvement. In the previous chapter, the totality of the core active toxin of the Vip3Af was analysed by the alanine scanning technique. As a result, some positions in the primary sequence were identified as being crucial for the insecticidal activity, selectivity or protein stability. To achieve a deeper insight of the scope of the selected key residues, some of these positions were further investigated herein by site directed mutagenesis.

## 5.2. Materials and Methods

### 5.2.1. Protein source and site directed mutagenesis

The *vip3Af(wt)* gene is a His-tagged modification of the *vip3Af1* (GenBank accession No. AJ872070.1) as described in chapter IV of this thesis. The clone was kindly provided by Bayer CropScience NV (Ghent, Belgium).

A total of 12 single and double mutants of the *vip3Af(wt)* were generated by site directed mutagenesis by the technique of the whole plasmid amplification. Primer design was based on the proposal by Zheng and co-workers (Zheng et al., 2004) and are detailed in Table 5. 1. Primer requirements according to Zheng and (Zheng et al., 2004) are summarised in Table S-5.1 (Annex section). Besides the introduction of the desired codon substitution in both primers, a silent mutation was introduced at least in one of the primer pairs to insert a restriction site for quick screening purposes. The rationale in choosing each particular substitution was based on i) multiple sequence alignments of the Vip3A proteins and the information on the insecticidal activity of certain positions available in the literature (Chakroun et al., 2016a), ii) the critical

positions for the structure-function relationship of the Vip3Af1 identified in the previous chapter, iii) the *in silico* prediction of reactive-structural and exposed-buried residues prediction (Berezin et al., 2004), iv) the degree of favourable amino acid substitution based on exchange matrices and intrinsic amino acid properties (Betts and Russell, 2003; Bordo and Argos, 1991; NCBI; Russell et al., n.d.) and iv) the positive selected residues described in Wu et al., (Wu et al., 2007).

***Table 5. 1. Primers used for the site directed mutagenesis by the whole plasmid amplification.***
*Primer sequence are grouped in triplets for ease the identification of the appropriate mutated codon (highlighted in bold). The nucleotide change with regards to the wild-type is denoted in lower –case. Underlined sequence indicates the introduction or removal of a restriction site for screening purposes*

| Mutation | Primer | Sequence (5'-3') | Position† | Restriction site modification (screening enzyme) |
|---|---|---|---|---|
| M34L | Fwd | GAC ATT cTG AAT ATG ATT TTc AAA ACG GAT ACA GGT GG | 94 | Deletion (DraI) |
| | Rev | CGT TTT gAA AAT CAT ATT CAg AAT GTC TTT GAT ACC AG | 83 | |
| T167S-E168D-P171G | Fwd | C TCT ACA CTT tCT GAc ATT ACA ggT GCA TAT CAA CGG ATT AAA TAT GTG | 489 | None (EcoRI) |
| | Rev | CCG TTG ATA TGC Acc TGT AAT gTC AGa AAG TGT AGA GTT AAT AAG AAC | 478 | |
| K284Q | Fwd | CTA CAA GCA cAA GCa TTT CTT ACT TTA ACA ACA TGC | 841 | Deletion (HindIII) |
| | Rev | GT AAG AAA tGC TTg TGC TTG TAG AGC TGT TAA TAC | 822 | |
| E483D | Fwd | GTC ATC AGT GAt ACA TTT TTG ACT CCG ATA AAT G | 1438 | None (EcoRI) |
| | Rev | CAA AAA TGT aTC ACT GAT GAC ACC TAA TGG | 1429 | |
| E483Q | Fwd | GTC ATC AGT cAA ACA TTT TTG ACT CCG ATA AAT G | 1438 | None (EcoRI) |
| | Rev | CAA AAA TGT TTg ACT GAT GAC ACC TAA TGG | 1429 | |
| E483H | Fwd | GTC ATC AGT cAc ACA TTT TTG ACT CCG ATA AAT G | 1438 | None (EcoRI) |
| | Rev | CAA AAA TGT gTg ACT GAT GAC ACC TAA TGG | 1429 | |
| W552H | Fwd | GAC AAT TTA GAG CCG cAC AAA GCA AAT AAT AAG AAC GCG | 1639 | Addition (AciI) |
| | Rev | GC TTT GTg CGG CTC TAA ATT GTC CTC TTC TAT GG | 1628 | |
| W552F | Fwd | GAC AAT TTA GAG CCG Ttc AAA GCA AAT AAT AAG AAC GCG | 1639 | None (EcoRI) |
| | Rev | GC TTT gaA CGG CTC TAA ATT GTC CTC TTC TAT GG | 1628 | |
| W552Y | Fwd | GAC AAT TTA GAG CCG Tac AAA GCA AAT AAT AAG AAC GCG | 1639 | Addition (RsaI) |
| | Rev | GC TTT gtA CGG CTC TAA ATT GTC CTC TTC TAT GG | 1628 | |
| G689S | Fwd | CG ACT CCA tcG GCa AGC ATT TCA GGA AAT AAA C | 2057 | Deletion (NheI) |
| | Rev | GA AAT GCT tGC Cga TGG AGT CGT AAT CCA AG | 2048 | |
| G689E | Fwd | CG ACT CCA GaG GCa AGC ATT TCA GGA AAT AAA C | 2057 | Deletion (NheI) |
| | Rev | GA AAT GCT tGC CtC TGG AGT CGT AAT CCA AG | 2048 | |
| N682K-G689S | Fwd | CCG AAc TCT TGG ATT ACG ACT CCA tcG GCT AGC ATT TCA GG | 2038 | Deletion (EcoRI) |
| | Rev | GCT AGC Cga TGG AGT CGT AAT CCA AGA cTT CGG ATT AAT TAA TTC | 2032 | |

*†Position at 5' (forward, "Fwd") and at 3' (reverse, "Rev") primers for each polymerase chain reaction primer pair. Reference gene accession number AJ872070.1.*

The plasmid amplification reaction was performed out with a high fidelity DNA polymerase with strong 3'-5' exonuclease activity and high processivity (KAPAHiFi™ PCR Kit, ref. KK2101, Kapa Biosystems, USA) using the 6 kb pMAAB 10 plasmid (Beard et al., 2008) containing the *vip3Af(wt)* gene as template. The PCR reaction was carried out with 25-50 ng template, 0.6 µM primer pair, 200 µM dNTPs, 0.5 U of polymerase, 5 µL of KAPAHiFi buffer in a final volume of 25 µL. The reaction was initiated with a pre-heating step of 3 min at 95 ºC and 16 cycles of denaturation, annealing and extension phases of 98 ºC for 20 sec, 60 ºC for 30 sec and 72 ºC for 4 min, respectively. The reaction was finalised with 15 min of final extension at 72 ºC.
The parental plasmids remaining in the final reaction were digested with FastDigest DpnI (Thermo Scientific, USA) at 37 ºC for 10 min. The enzymatic digestion of the

DpnI was stopped at 80 ºC for 5 min and the reaction then cooled down on ice. The plasmids carrying the mutant version of *vip3Af* were transformed into *Escherichia coli* DH10ß strain heat-shock cells. Plasmid purification was performed on 2-3 transformed colonies and screened with the specific restriction enzyme to ensure that amplification reactions had not led to wrong plasmid constructions due to strand displacement during the elongation step. The restriction product was checked by agarose gel electrophoresis. Plasmids displaying the expected fragments size were further transformed into *E. coli* BL21 strain for the expression of the mutant Vip3Af protein.

The mutations were further confirmed by DNA sequencing. The gene region containing the mutation of the selected clones was amplified in the same way as done for the site directed mutagenesis, using 5-10 ng template and 30 cycles PCR. The different primer pairs used (Table 5. 2) gave amplification fragments of up to 757 bp. The PCR product was checked by agarose gel electrophoresis and purified using NucleoSpin Gel and PCR clean-up kit (MN, Germany) and sequenced by the Sanger method.

All primers were non-phosphorylated and synthesised by Sigma-Aldrich.

***Table 5. 2. Primers used for testing out the correct change in the mutated proteins and the results of the sequencing***

*Underlined primers were used for the sequencing of the amplification products.*

| Primer | Sequence | Position† in the reference gene | Product size‡ (bp) | Vip3Af mutated protein | Codon (aa) (wt / mutation) |
|---|---|---|---|---|---|
| *Vip3-sc.fw*[1] | 5′ TGCCACTGGTATCAARGA 3′ | 78 - 1078 | 1000 | M34L | ATG (M)/ CTG (L) |
| *wt1.rev* | 5′ ACCCAACCAATGCATGTCCT 3′ | | | | |
| *wt1.fw* | 5′ CGATGCGATAAATACGATGCTTCATA 3′ | 321 - 1078 | 757 | T167S+E168D+P171G | ACT (T) + GAA (E) + CCT (P) / TCT (S) + GAC (D) + GGT (G) |
| *wt1.rev* | 5′ ACCCAACCAATGCATGTCCT 3′ | | | K284Q | AAA (K)/ CAA (Q) |
| *wt2.fw* | 5′ CGGAGGTTATTTATGGTGATACGG 3′ | 1166 - 1793 | 627 | E483D | GAA (E)/ GAT (D) |
| *wt2.rev* | 5′ TGGATTACATACTCAGTTTTCGGT 3′ | | | E483Q | GAA (E)/ CAA (Q) |
| | | | | E483H | GAA (E)/ CAC (H) |
| | | | | W552H | TGG (W)/ CAC (H) |
| | | | | W552F | TGG (W)/ TTC (F) |
| | | | | W552Y | TGG (W)/ TAC (Y) |
| *wt3.fw* | 5′ AAGGACGGAGGATTTTCACAA 3′ | 1729 - 2281 | 552 | N682K+G689S | AAT (N) + GGG (G) / AAG (K) + TCG (S) |
| *wt3.rev* | 5′ TCTACATATAATCCGGTATTATTGG 3′ | | | G689S | GGG (G)/ TCG (S) |
| | | | | G689E | GGG (G)/ GAG (E) |

*†Position at 5′ end of the forward and reverse primers for each polymerase chain reaction primer pair. Reference gene accession number AJ872070.1.*

*‡Using the reference gene as the template.*

*[1]in Hernández-Rodríguez* et al.*(2009)*

### 5.2.2. Protein Expression and Purification

The Vip3Af1(WT) and the mutated variants harboured in *E. coli* BL21 strain were expressed as described by Ruiz de Escudero et al., (2014). Briefly, a single *E. coli* colony was grown in LB-ampicillin culture at 37 ºC with soft shaking. The Vip3Af expression was induced with 1 mM IPTG when the culture reached an $OD_{600}$ between 1.2 and 1.8. After overnight expression, bacterial cells were pelleted and further treated with 1% lysozyme in PBS (phosphate buffered saline, pH 7.4) followed by two sonication steps. The crude lysate was clarified by centrifugation and the resulting supernatant was filtered through a 0.2 µm diameter pore membrane before purification.

Vip3Af proteins were purified from the clarified lysate extracts using pre-packed nickel columns (HisTrap FF columns, GE Healthcare). Purified proteins were eluted from the column in PBS with 150 mM imidazol and collected in tubes containing EDTA (5 mM final concentration). The eluted fractions were dialyzed overnight against 20 mM Tris, 150 mM NaCl, pH 9, and stored at -20 ºC. Protein purity was checked by SDS-PAGE and the protein concentration was calculated densitometrically using the TotalLab 1D v 13.01 software.

### 5.2.3. Proteolytic Pattern Assays

Volumes equivalents to 3 µg of purified Vip3Af proteins were incubated with 5:100 trypsin (trypsin:Vip, w:w) in a final volume of 55 µl at 37 ºC. After 1 h incubation, a final concentration of 250 µM PMSF was added to each reaction, immediately followed by the addition of SDS-PAGE loading buffer (0.2 M Tris-HCl pH 6.8, 1 M sucrose, 5 mM EDTA, 0.1% bromophenol blue, 2.5% SDS, and 5% β-mercaptoethanol) (2:1, sample:loading buffer) and 5 min heating at 99 ºC. Proteolytic fragments were separated in a 12% SDS-PAGE. The Vip3Af1(WT) was used as a control. Untreated samples were assayed in parallel to monitor the thermolability of the mutant proteins in the absence of trypsin. The assay was replicated twice.

### 5.2.4. Intrinsic Fluorescence Emission Spectra

The intrinsic fluorescence emission spectra were obtained by exciting 3-8 µg of purified-protein samples at 280 nm (excitation slit of 5 nm) and recording the emission spectra from 300 to 450 nm (emission slit of 20 nm) in a Varian Cary Eclipse fluorimeter (Agilent Technologies, Australia). Protein samples were placed in a quartz cuvette filled with 1.3 ml of 20 mM Tris, 300 mM NaCl, pH 9 buffer. Graphic curves represent the average of 3 scans. The curves were smoothed with the "moving average" algorithm.

### 5.2.5. Insect Rearing and Insecticidal Activity

The bioassays were performed with a laboratory population of *Spodoptera frugiperda* (Lepidoptera: Noctuidae). The population was maintained on

semi-synthetic diet (Greene et al., 1976) in a rearing chamber at 25 ± 2 ºC, 70 ± 5% RH and 16:8h L:D.

The insecticide potency of the Vip3Af1(WT) and the modified Vip3Af proteins was estimated from the $LC_{50}$ values obtained in quantitative surface contamination assays. A volume of 50 µl of purified protein was applied to the surface of 2 $cm^2$ diameter wells filled with semi-synthetic diet. A range of 7 serially diluted concentrations of Vip3Af samples was tested in each bioassay. Proteins were diluted with 20 mM Tris, 150 mM NaCl, pH 9. The same buffer served as a negative control. In each trial, 128 neonates of *S. frugiperda* were used, 16 neonates per dose, individually placed in each well. Trays were maintained in a climatic chamber at the same conditions as for colony rearing. All bioassays were scored at 10 days for mortality and functional mortality (dead larvae plus larvae arrested in L1). Bioassays were replicated three times. The insecticidal potency, regressions lines, and $LC_{50}$ were calculated with the Polo-PC Probit analysis program (LeOra-software, Berkeley, CA). $LC_{50}$ values were considered significantly different when fiducial limits did not overlap.

## 5.3. Results

### 5.3.1. Protein Expression and Proteolytic Band Pattern

The constructs carrying the mutations were able to expressed correctly the Vip3Af mutant proteins. Only mutants E483Q and the triple mutant T167S-E168D-P171G did not achieve the expression of enough protein to work with and were dismissed for further analysis. The remaining 10 mutants were successfully expressed and purified. Half of the mutants (E483D, M34L, K284Q, W552F and W552Y) rendered the expected main fragments of 62 kDa and 20 kDa after trypsin treatment (Fig. 5. 1). This proteolytic band pattern was described in Chapter IV as pattern “a”. The previously named pattern “e”, consisting on the main bands of 62 kDa, 53 kDa and 20 kDa, was also represented in mutants N682K-G689S, G689S and G689E. The proteolytic band patterns “b” (40 kDa and 20 kDa) and “f” (a single band of 27 kDa) were also represented in mutants W552H and E483H, respectively.

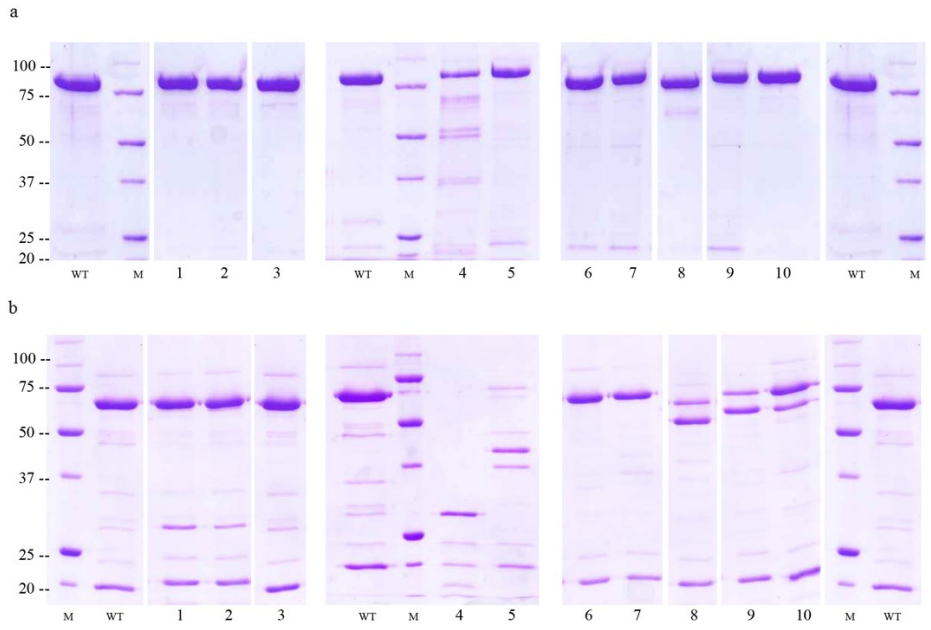


***Fig. 5. 1. Representative proteolytic band patterns of the site directed mutated proteins of Vip3Af1(WT) after SDS-PAGE.***

*Protein samples (5 μg) were incubated with 5:100 trypsin (trypsin:Vip, w:w) (B) or without trypsin as control treatment (A). Incubations were performed at 37 ºC for 1 h. Lanes 1: M34L, 2: K284Q, 3: E483D, 4: E483H, 5: W552H, 6: W552F, 7: W552Y, 8: N682K-G689S, 9: G689S, 10: G689E. "WT": Vip3Af1(WT). "M": molecular weight marker (kDa).*

### 5.3.2. Emission Spectra and Overall Protein Conformation

The emission curves of the the 10 expressing mutant protoxins were shown to be similar to that of the Vip3Af1(WT) (Fig. 5. 2). The emission peaks ranged from 335 nm to 340 nm, in all cases below the maximum of 348 nm expected for the emission of free Trp when excited at 280 nm in aqueous solutions (Bortolotti et al., 2016; Teale and Weber, 1957)), indicating that the 3 triptophan residues in the Vip3Af sequence face an hydrophobic environment in native conditions.

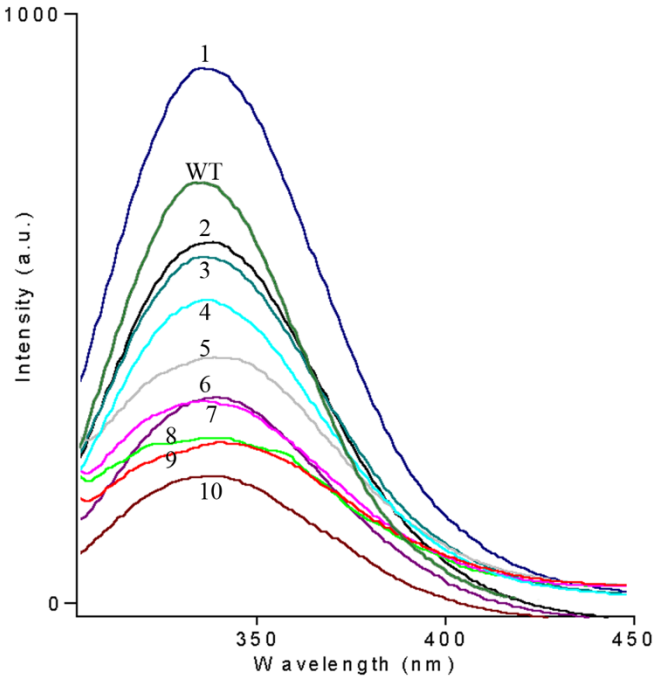


*Fig. 5. 2. Emission spectra of the intrinsic fluorescence of the protoxin form of the Vip3Af1(WT) and the site directed mutated Vip3Af proteins.*

*Proteins (3 -8 µg/mL) were excited at 280 nm and the emission was scanned from 300 to 450 nm. WT: Vip3Af1(WT), 1: M34L, 2: E483D, 3: K284Q, 4: G689E, 5: W552F, 6: E483H, 7: G689S, 8: W552Y, 9: W552H and 10: N682K-G689S. The maximum emission peak ranged from 335 to 340 nm.*

### 5.3.3. Insecticidal activity of the site-directed mutants

None of the site-directed mutants significantly altered the insecticidal activity against *S. frugiperda* compared to the reference Vip3Af1(WT) protein (Table 5. 3). Nevertheless, some differences between mutants might be pointed out. Mutants E483H and W552H markedly decrease their $LC_{50}$ up to 4-fold in comparison to the wild type and showed a significant difference with that of the slightly more active mutant M34L ($LC_{50}$ 32 ng/cm$^2$, F.L. $_{(99\%)}$: 13-79). Following mutant M34L, mutants E483D and K284Q were the most active ones with relative potencies of 4 and 2.8 respectively.

## 5.4. Discussion

Reverse genetics is one of the most used approach to deepen in the protein knowledge, especially when the protein structure is unknown (Bordo and Argos, 1991). As a logical step forward after the systematic study of the Vip3Af core toxin's sequence by alanine scanning, 12 mutations were build up based on theoretically favourable amino acid changes. Only 2 out of the 12 site-directed mutants, the triple

mutant T167S-E168D-P171G and the E483Q, prevented protein expression. Since the gene sequence and the plasmid were correct, the failure in expressing these mutants might account only for the nature in the mutation, perhaps by disrupting their structural integrity or by rendering such high unstable proteins that are quickly degraded after expression, as described in the previous chapter. The slight shifts in the emission peak obtained from the intrinsic fluorescence spectra (Fig. 5. 2) of the other 10 expressed mutants suggest that only minor conformational changes occur, which might be locally compensated. Accordingly, although some differences in the insecticidal potency among different variants were observed, none of them significantly differed from that on the Vip3Af1(WT) (Table 5. 3). However, unless these mutant proteins are tested against other insect species, we cannot discard that some of the mutations increase the insecticidal activity of Vip3Af.

***Table 5. 3. Quantitative parameters from concentration-mortality responses (at 10 days) of Vip3Af1(WT) and SDM-Vip3Af proteins purified by affinity chromatography on*** S. frugiperda.

| Treatment | $LC_{50}$ | 99% F. L.[†] | | Regression line | | Relative | 99% F. L.[†] | |
|---|---|---|---|---|---|---|---|---|
| | ($ng/cm^2$) | Lower | Upper | Slope±SE | a[◇]±SE | Potency | Lower | Upper |
| Vip3Af1(WT) | 116 ab | 48 | 300 | 0.9 ± 0.1 | 3.1 ± 0.3 | 1 | - | - |
| M34L | 32 a | 13 | 79 | 0.8 ± 0.1 | 3.8 ± 0.2 | 3.6 | 1 | 13.6 |
| K284Q | 51 ab | 19 | 140 | 0.9 ± 0.1 | 3.5 ± 0.2 | 2.3 | 0.6 | 8.7 |
| E483D | 29 ab | 8 | 109 | 1.1 ± 0.2 | 3.5 ± 0.4 | 4 | 0.8 | 20.3 |
| E483H | 445 b | 80 | 2919 | 0.8 ± 0.2 | 2.9 ± 0.4 | 0.3 | 0.1 | 1.8 |
| W552H | 520 b | 107 | 2850 | 0.4 ± 0.1 | 3.6 ± 0.3 | 0.2 | 0.1 | 1.4 |
| W552F | 41 ab | 9 | 180 | 0.9 ± 0.2 | 3.5 ± 0.5 | 2.8 | 0.5 | 16.9 |
| W552Y | 228 ab | 58 | 959 | 0.5 ± 0.1 | 3.8 ± 0.3 | 0.5 | 0.1 | 2.7 |
| N682K-G689S | 159 ab | 34 | 819 | 0.7 ± 0.2 | 3.3 ± 0.3 | 0.7 | 0.1 | 4.4 |
| G689S | 94 ab | 27 | 345 | 0.9 ± 0.2 | 3.3 ± 0.4 | 1.2 | 0.3 | 5.9 |
| G689E | 135 ab | 34 | 565 | 0.7 ± 0.2 | 3.5 ± 0.5 | 0.9 | 0.2 | 4.5 |

[†] *Fiducial limits.*
[◇]*a: intercept*

Mutantions M34L and K284Q were chosen from a protein sequence comparison among different Vip3A. The residue $Lys^{284}$ is highly conserved among Vip3A proteins; only in some Vip3Aa sequences, such as the Vip3Aa1, the lysine is substituted to a non-homologous $Gln^{284}$ (Fig. 5. 3). Both lysine and glutamine residues have amphipathic side chains and are frequently found forming part of binding or catalytic active sites. In agreement to that, the residue in site-284 is expected to be exposed to the protein environment (Fig. 5. 3), which in the lepidopteran larvae guts is of alkaline nature (pH> 8). Therefore, K284Q accounts for the removal of the positive net charge in the protein local surface in comparison to the wild type which does not have a critical effect on the integrity of the protein or its function, since no significant differences in the toxicity against *S. frugiperda* were found (Table 5. 3).

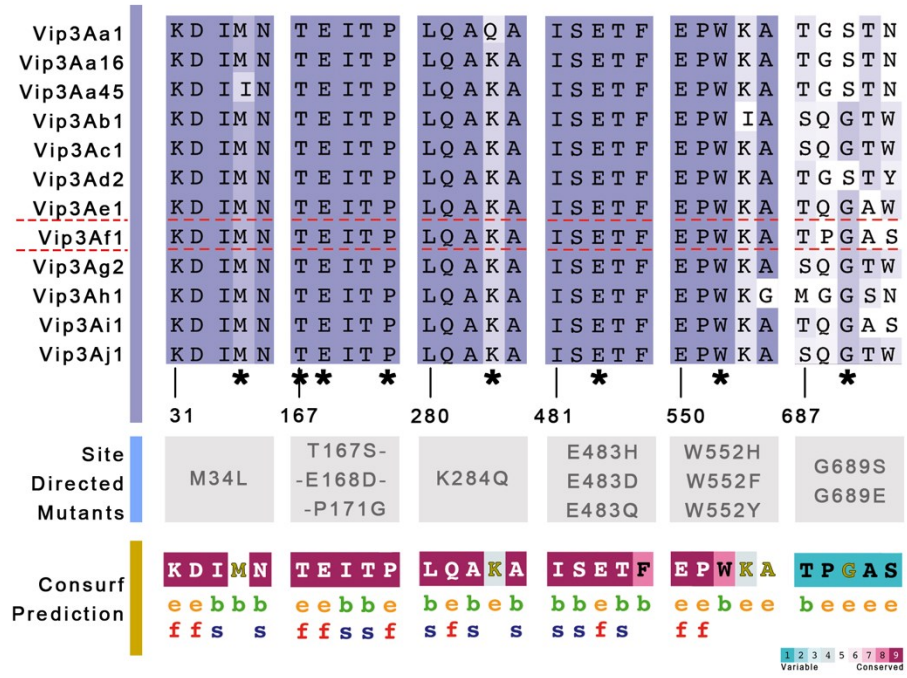


***Fig. 5. 3. Multiple sequence alignment and consurf prediction of residues buried and exposed for the regions concerning the site-directed mutations of the Vip3Af1(WT).***

*Conservation of these sites was evaluated by Clustal Omega msa* (Sievers et al., 2011) *of different Vip3A proteins from Bacillus thuringiensis: Vip3Aa1 (GenBank accession number AAC37036), Vip3Aa16 (GenBank accession number AAW65132), Vip3Aa45 (GenBank accession number JF710269), Vip3Ab1 (accession number AAR40284), Vip3Ac1 (named PS49C with Seq. ID 7 in U.S. patent application 20.040.128.716 (Narva and Merlo)), Vip3Ad2 (accession number CAI43276), Vip3Ae1 (accession number CAI43277), Vip3Af1 (accession number CAI43275), Vip3Ag2 (accession number ACL97352), Vip3Ah1 (accession number ABH10614), Vip3Ai1 (accession number KC156693) and Vip3Aj1 (accession number KF826717). The msa (purple panel) is coloured according to BLOSUM62 colour scheme. Amino acid conservation, quality (BLOSUM62 score based on observed substitutions) as visualised by Jalview* (Waterhouse et al., 2009). *Asterisks (*) highlight the positions that were mutated. The Consurf prediction* (Berezin et al., 2004) *(yellow panel) represents the predicted functional (f) or structural (s), roles of the residues and the predicted location exposed (e) or buried (b). Residues in yellow indicates low confidence in the prediction due to insufficient data. The conservation-code scale of the consurf prediction is presented at the bottom.*

The functional and structural role of the N-terminus (upstream the processing site 192-XXKVKX-199 (Rang et al., 2005)) of Vip3 proteins is not without controversy, though it is widely accepted that this fragment is cleaved, but not removed, after protease activation in the insect midguts (Bel et al., 2017; Chakroun et al., 2016a, 2012; Chakroun and Ferré, 2014; Estruch and Yu, 2001; Gayen et al., 2015, 2012; Hernández-Martínez et al., 2013; Lee et al., 2006, 2003; Li et al., 2007; Liu et al., 2011; Palma et al., 2014). While Li and colleagues (Li et al., 2007b) argued that the 20 kDa band from the N-terminus was crucial for the correct folding of the functional Vip3A protein, Gayen et al., (2015, 2012) succeed in cloning a highly active 62 kDa of a Vip3A (without the first 200 amino acids from the N-terminus). It was recently shown that

the insecticidal activity of the whole protein is not compromised by point mutations in the N-terminus of a Vip3A protein (Liu et al., 2017). We found position $Met^{34}$ the most attractive candidate to seek for a response driven from the N-terminus of the protein. On the one hand, this position falls at the end of the signal peptide (SP) according to some authors (Chen et al., 2003; Doss et al., 2002; Estruch et al., 1996; Rang et al., 2005), although other authors claim that the SP might be shorten up to the first 11 residues (Doss et al., 2002, chapter IV of this thesis). Deletion of the first 27, 33 or 39 residues has led to unpredictable results, from the total loss of insecticidal activity to no changes in the toxicity depending on the species tested (Bhalla et al., 2005; Chen et al., 2003; Selvapandiyan et al., 2001). Additionally, $Met^{34}$ also falls in a predicted conserved *Tar* multidomain (COG0840, a chemotaxis protein motif) with transmembrane properties (Chakroun et al., 2016a). On the other hand, $Met^{34}$ is a highly-conserved residue among most of the Vip3 proteins (Fig. 5. 3) and is expected to be buried in the protein hydrophobic environment, most likely in a $\alpha$-helix structure. This is the only different residue between the Vip3Aa1 and the Vip3Aa45 ($34^{Met \rightarrow Ile}$), being both proteins biologically active and phylogenetically close-related to the Vip3Af1 (Palma et al., 2013b, 2012). There has been a slight increase in the insecticidal activity of M34L against *S. frugiperda* (Table 5. 3). The leucine amino acid has a higher helical preference than either methionine or isoleucine and thus, it is likely that this change contributes to the stabilization of the $\alpha$-helix and eases the insertion into the cell membrane during protein secretion. A more drastic mutation attempt in the N-terminus was intended by creating a triple mutant (T167S-E168D-P171G) based on the three consecutive key residues reported in the previous chapter. These three positions are predicted to be functional and exposed residues (Fig. 5. 3) and even when the single substitutions were chosen to be "safe-mutations", three close and simultaneous mutations in a highly-conserved area appeared to be unbearable for the protein structure and stability.

The proteolytic activation of M34L and K284Q gave two main bands of 62 kDa and of 20 kDa, which is the expected proteolytic fragments reported in the Vip3Af1(WT). Therefore, it is assumed that these mutations do not affect the correct folding of the Vip3Af protein. This was also the case for the mutations E483D, W552F and W552Y. Positions $Glu^{483}$, $Trp^{552}$ and $Gly^{689}$ in the Vip3Af1(WT) were identified in chapter IV as key residues for the insecticidal activity against *S. frugiperda* and *Agrotis segetum* (Lepidoptera: Noctuidae). The substitution of the native residue to an alanine resulted in unique proteolytic patterns that was not observed in any other substitution: E483A gave a single band of 27 kDa (pattern "f"), W552A displayed pattern"b" consisting in two main bands of 40 kDa and the 20 kDa, and G689A gave pattern "e" (62 kDa, 53 kDa and 20 kDa). Interestingly, the trypsin treatment of mutants E483H, W552H and the three mutants in position 689 (G689S, G689E and N682K-G689S) displayed the same proteolytic patterns described when the native residue in these positions were substituted to an alanine (Fig. 5. 1). Since alanine does not share any specific physicochemical characteristics with either histidine, serine or glutamate, non-synonymous changes in these sites might locally alter the

conformation, making trypsin accessible to different cleavage sites other than the native ones.

The position $Glu^{483}$ is a predicted functional and exposed key residue (Fig. 5. 3). The substitution of glutamate to aspartate (E483D), glutamine (E483Q) or histidine (E483H) are thought to be either favorable or neutral. The fact that E483Q impairs protein expression suggests that the side chain of the glutamic acid, negatively charged due to its low p$K_a$, contributes to the protein conformation by establishing ionic interactions or salt bridges with other spatially-close residues, especially with those positively-charged. This is further supported by the non-deleterious effect of mutant E483D, in which the negative charge contribution is ensured by the side chain of the aspartic acid. Contrarily to the deleterious effect of the substitution to a Gln, the exchange to a histidine provides either a local positive or negative charge depending on the local pH, which might disrupt local contacts but yet is able to retain some insecticidal activity (Table 5. 3). The alike effect reported for the E483A might respond to different constraints. While histidine is highly versatile due to its p$K_a$ near to neutral pH, alanine might reduce the steric impairments between the residues in the vicinity, limiting the impact of the mutation. A similar result can also be found in the $Trp^{552}$ when is changed to an A or to a H. However, unlike $Glu^{483}$, $Trp^{552}$ is probably buried in a hydrophobic core in the protein (Fig. 5. 3), and was predicted to form a ligand site in the putative CBM of the Vip3Af1(WT) (Fig 5. 4), together with the $Pro^{551}$ and the $Lys^{553}$. Thus, the change to a histidine might modify the interactions with the surrounding residues, perhaps by removing the stacking interactions arising between tryptophan and proline, by increasing the local net charge, or by both, causing eventually a local misfolding that accounts for a non-functional activation of the protein by the insect gut proteases. The insecticidal performance still retained by both E483H and W552H is likely explained by the toxic fragment of 62 kDa before is completely processed to the main bands of 27 kDa and 40 kDa, as it was suggested for E483A and W552A.

With only one exception known so far (Vip3Ba1), Vip3 proteins share a highly conserved domain identified as a Carbohydrate Binding Motif (CBM type 4, 9) which spans from $Ser^{536}$ to $Gln^{652}$ in the Vip3Af1(WT) sequence (Chakroun et al., 2016a). The alanine-scanning in the whole region revealed only one critical residue for the toxicity, the $Trp^{552}$. Aromatic residues Phe, Tyr and Trp are known to be involved in the binding to carbohydrates in CBM by stacking interactions of the aromatic-shape side-chain with the pyranose ring of sugars and by hydrogen bonding (Asensio et al., 2013; Boraston et al., 2004). No significant differences in the $LC_{50}$ were found when tryptophan was exchanged with the other aromatic amino acid with a ring in their side chain (Table 5. 3), suggesting that the aromaticity may be an important trait in position W552 (strongly conserved among Vip3A sequences) playing a role in protein stability.

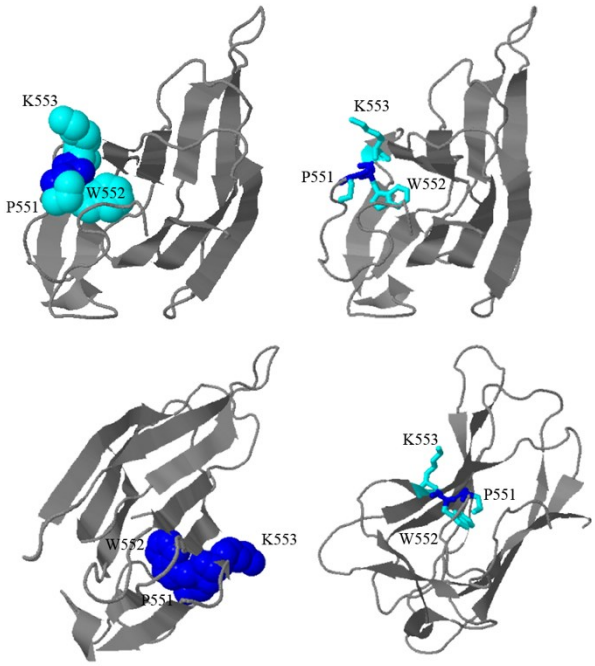


***Fig. 5. 4. Structural view of the ligand binding site prediction for the Vip3Af1(WT) using 3DLigandSite*** (Wass et al., 2010).
*Protein sequence used: (accession number CAI43275). Job Id: 5a14750999445eea: cluster IV. The Phyre2 confidence score was 96.1, and MAMMOTH Score for Cluster IV was 11.7. Different images show different orientations of the fragment predicted in the C-terminal region of the protein ($Asn^{537}$ – $Ile^{667}$).*

Finally, position $Gly^{689}$ was described as being potentially subjected to positive Darwinian selection, though the exchange of the glycine to an alanine was not favorable (Wu et al., 2007). This position is predicted to be functional (Fig. 5. 3) with the side chain facing the protein surface, in agreement to the model of the C-terminal end of Vip3 proteins in which this site was located in a loop of a structure predominantly formed by ß-sheets. The *in silico* model of the Vip3Af1 also supports this configuration. The C-terminal end of the Vip3 proteins is thought to determine the target specificity and thus, it exists a higher sequence divergence among Vip3 proteins (Chakroun et al., 2016a; Palma et al., 2014, 2012; Rang et al., 2005; Ruiz de Escudero et al., 2014; Wu et al., 2007). Glycine is the smallest of the amino acids with a short and polar side chain. The substitution of $Gly^{689}$ either to a serine or to a glutamic acid did not affect the insecticidal activity of the Vip3Af protein (Table 5. 3), contrary to what was observed when the glycine was substituted to an alanine. This is likely explained by the non-polar nature of the Ala, which might disrupt the functional reactivity of a putative functional site. The outcome of the site directed mutagenesis of $Gly^{689}$ further supports the prediction of site-689 being subjected to a high mutation freedom as predicted by Wu (Wu et al., 2007) and placed in a exposed loop. Otherwise, the substitution to an alanine would had been favorable by

compacting the hydrophobic pocket whereas the polar and charged residues, with larger side chains, would likely disrupt the hydrophobic moiety.

Site-directed mutagenesis is a useful tool to identify sites with critical implications to the function and structure of a protein with unknown spatial conformation. The substitutions performed in this study did not lead to statistical differences in the insecticidal activity of the Vip3Af against *S. frugiperda*. Nevertheless, the slight differences found help to shed light on the structural implications of Vip3 proteins. It is proposed that site-483, site-552 and site-689 play a key role for the folding of the protein, while site-689 may also constitute a functional residue placed in a loop. Despite the lack of an unequivocally relationship of the N-terminus with the insecticidal response, the presence of the N-terminal fragment might indirectly contribute to the Vip3A function, yet contributing to the final outcome.

With the increasing demand of a more sustainable agriculture and the high time and economical costs of development of new active substances, synthetic diversification of the genetic bank of Vip3 proteins might be a shortcut strategy in agricultural biotechnology (Palma and Berry, 2016). Protein engineering is one of such strategies for target diversification; Unfortunately, the few changes introduced in the sequence of Vip3Af in this study did not allow to improve the insecticidal potency against *S. frugiperda* larvae for its application in biotech solutions. However, it is still to be proven whether the mutations studied here contribute to broaden the target specificity or the insecticidal potency against other insects and, therefore, further study is necessary.

# GENERAL DISCUSSION

Worldwide agriculture is a living scenario continuously adapting. With the increase of the global population, arable land surface has increased only 14%, whereas the overall yield reached almost 80% increase since the earlies 60's (Alexandratos and Bruinsma, 2012). As a consequence of the agriculture intensification and the lack of extensive knowledge on agricultural chemistry, an unsustainable overuse of chemicals became a common practice, which have caused serious contamination problems to aquifers and soil and have threatened wild life and food and feed safety. In response to this situation, there is a global commitment of reducing the chemicals inputs to agriculture, either by optimising the pesticides application methods and the cropping systems management, or by the development of more sustainable plant protection products. Biostimulants, biotechnology-based solutions and biological and microbial control are promising tools that help to reduce the delivery of conventional pesticides to the environment. In this context, *Bacillus thuringiensis* (Bt) is by far the most widely used and well-known microbial control agent. Vip3A proteins are insecticidal resources present in bioformulations and in transgenic crops, although the mode of action is not completely understood and the crystallographic structure is still unknown. Different to chemical pesticides, natural compounds such as insecticidal proteins are huge and their biocidal response is complex, often multi-factorial. Thus, in order to ensure the success on the use of Vip3A proteins for crop protection, characterise the mode of action, the protein structure and the insecticidal spectrum in detail becomes essential.

Vip3A proteins are known to be active against lepidopteran, such as the Cry-tolerant *Agrotis ipsilon* (Lepidoptera: Noctuidae) or of many other species from the *Spodoptera* genus (Estruch and Yu, 2001; Gayen et al., 2012; Warren, 1997). Unfortunately, most of the literature available focuses on the insecticidal range of Vip3Aa subclass. In order to increase the pull of information available of the species targeted by different Vip3A proteins, in the first chapter of this thesis the toxicity of 5 different Vip3A proteins (Vip3Aa, Vip3Ab, Vip3Ad, Vip3Ae and Vip3Af) were screened against 8 different caterpillar pest species (*A. ipsilon*, *Helicoverpa armigera*, *Mamestra brassicae*, *S. exigua*, *S. frugiperda*, *S. littoralis*, *Ostrinia nubilalis* and *Lobesia botrana*). Seven out of these 8 species were susceptible to Vip3Aa, Vip3Ae and Vip3Af. Vip3Ad was not toxic to any of the species tested. Likewise, the European corn borer *O. nubilalis* was tolerant to all Vip3 proteins tested, although it showed marginally susceptibility to Vip3Af. Some specificity in the pest-protein combination was observed: *A. ipsilon*, *S. frugiperda* and *S. littoralis* were susceptible to Vip3Aa, Vip3Ab, Vip3Ae and Vip3Af; *S. exigua* was susceptible to Vip3Aa and Vip3Ae, and moderately susceptible to Vip3Ab; *M. brassicae* and *L. botrana* were susceptible to Vip3Aa, Vip3Ae and Vip3Af; *H. armigera* was moderately susceptible to Vip3Aa, Vip3Ae and Vip3Af. No major differences were found when comparing protoxins *vs*. trypsin-activated toxins.

Proteolytic processing is a key starting point on the insecticidal performance. Thus, the second and third chapter focused on the activation step of Vip3Aa16 and Vip3Af1

by commercial trypsin and midgut juice from the two susceptible insects *A. ipsilon* and *S. frugiperda*. The 89 kDa protoxin was firstly proposed to be cleaved into two fragments of 20 kDa (corresponding to the first 200 amino acids) and 65 kDa (considered as the "core" toxin, corresponding to the last ca. 600 amino acids). Secondary cleavage sites were also proposed to split the 65 kDa toxin into two overlapping fragments of 33 kDa and 42 kDa. The activation step and the complete degradation of the proteins by proteases have been often related to different insecticidal response (Abdelkefi-Mesrati et al., 2011b; Caccia et al., 2014; Chakroun et al., 2016c, 2012; Estruch and Yu, 2001; Hernández-Martínez et al., 2013; Li et al., 2007). However, the apparent degradation of the 62-66 kDa active toxin after proteolytic activation observed by SDS-PAGE might not be related to instability of Vip3A proteins to insect midgut peptidases. In chapter II and III is shown that the misleading degradation of the "core" toxin obtained by SDS-PAGE analysis is an *in vitro* effect caused by the denaturing interaction of the SDS present in the loading buffer. This effect is based on a partial denaturation resistance of the trypsin and other peptidases present in the insect midgut juice, while Vip3Aa proteins are progressively unfolded by the SDS and the high temperature gradually achieved during the sample heating step. Thus, the peptidases still retaining enzymatic activity cut upon inaccessible cleavage sites under Vip3Aa-native conditions. The empirical evidences to that were based on i) the kinetics of the activation of the Vip3Aa and the Vip3Af to high concentrations of trypsin, in which after an apparent degradation of the "core" toxin at the first-time points, a conspicuous band of 62-66 kDa fragment appeared after 72 h treatment, directly related to the vanishing of the band corresponding to trypsin; ii) the gel filtration chromatography of a sample with a completely-degraded SDS-PAGE profile of both Vip3Aa (treated with either trypsin or *A. ipsilon* midgut juice) and Vip3Af (treated with *S. frugiperda* midgut juice). These samples were biologically active against *A. ipsilon* and *S. frugiperda.* Furthermore, when the eluted fraction containing the Vip3A proteins free of peptidases were subjected to gel electrophoresis, the 62-66 kDa fragment was no longer degraded; iii) the inhibition of the trypsin reaction by the specific irreversible inhibitors AEBSF and E64 or by urea prior to the addition of the loading buffer containing SDS; and iv) the trypsin treatment of the Vip3Aa in presence of SDS or β-mercaptoethanol during the incubation.

Despite the influence of the SDS, the C-terminal end of the Vip3A proteins does not seem to be over-processed by peptidases, rendering a band of ca. 33 kDa in the Vip3Af and of 29 kDa corresponding to the sequence fragment from S-509 onwards in the Vip3Aa16. This suggests a more stable conformation of the C-terminal end of the Vip3A proteins predominantly formed by β-sheets as predicted *in silico*.

Moreover, further addition of trypsin to the Vip3Af toxin activated during 72 h did not caused an apparent degradation of the 62 kDa-core, suggesting some differences in the activated-toxin conformation. Thus, it is likely that once the protoxin is first treated with trypsin, the excision of the 200 amino acids from the N-terminus triggers a compaction of the "core" into a globular form, in agreement to Kunthic et al*.,* (2016). Furthermore, Lee et al*.,* (2003) showed that the activation step was crucial

for the formation of pores in brush border vesicles membranes (BBMV) of susceptible insects, perhaps facilitated by the compacting of the C-terminus.
Although the misleading degradation effect was observed in both Vip3Aa and Vip3Af, two minor differences were noticeable. Although in both proteins the 65 kDa fragment apparently accumulated over time as the trypsin self-digests, a complete digestion of the 65 kDa fragment at the first time-points of the kinetics was not observed in the Vip3Af, not even at the highest concentration of trypsin. With regards to the N-terminus, the fragment of 20 kDa almost completely disappeared in the Vip3Aa16, whereas in the Vip3Af1 this band was yet enough intense after 72 h incubation. Therefore, the differences found between Vip3Af1 and the Vip3Aa16 reflect a different interaction of both proteins to SDS molecules, which might account to some differences in their native structure.

Since the X-ray structure of Vip3 proteins is not yet disclosed, in order to further explore the molecular structure of Vip3A proteins an alanine scanning of a major part of the Vip3Af1 protein sequence was analysed in the 4$^{th}$ chapter. Alanine scanning is a successful technique for mapping crucial positions or epitopes in a protein and helps to infer on protein structure-function relationships. Only 10% of the residues analysed play a crucial role in either protein stability, protein folding, proteolytic processing or insecticidal activity of the Vip3Af1. Therefore, most of the substitutions to alanine, constituted neutral mutations even in the most conserved regions among the Vip3A subfamily, which stresses the high level of resilience and adaptability of Vip3A proteins to preserve protein function and homeostasis. In all, 54 positions were selected after a first screening of the alanine collection and the correct substitution was checked by DNA sequencing. From the initial 54, 19 positions were related to protein expression or protein lability. The remaining 35 substitutions caused a decrease in the insecticidal activity against *S. frugiperda* to different degrees. After a more accurate analysis, 19 substitutions were confirmed to cause a reduction in the insecticidal activity against *S. frugiperda.* The position of these 19 residues clustered mainly in two regions of the protein sequence (at the N-terminus between amino acids 167 and 272 and at the C-terminus between amino acids 689 and 741). For *S. frugiperda*, the top 11 positions driving the strongest activity inhibition (defined as mortality lower than 41% and functional mortality lower than 69%) were T167A, E168A, F229A, M238A, Y272A, E483A, W552A, G689A, I699A, Y719A, and G727A. Most of the substitutions that impaired the activity to *S. frugiperda* were also critical for the insecticidal activity against *Agrotis segetum*, with few differences. Substitutions T167A and E483A apparently were not as critical for *A. segetum* as for *S. frugiperda*, whereas mutations G689A, I699A, Y719A, and G727A in the C-terminus were more critical for the insecticidal activity against *A. segetum* than for *S. frugiperda*, supporting the role on target specificity of the C-terminus as proposed by Wu et al., 2007.
The proteolytic activation of the 35 selected mutants revealed differences that could also be clustered in defined regions of the Vip3Af sequence. These differences were characterised in 6 different proteolytic band profiles as evaluated by SDS-PAGE:

patterns “a” (corresponding to the wild type) and “d” contained the 62 kDa band and were found in those mutants clustering in the first half of the protein, whereas patterns “c” and “e” (both being very similar except for the faint presence of the 62 kDa band in “e”) were found in mutants clustering near the C-terminus, supporting the protein stabilisation role of the C-terminus. In this work is proposed that the stabilisation might be achieved by intra-chain interactions (e.g. hydrogen bonding, salt bridges) between the β-sheets of the C-terminus and the α-helices of the N-terminus. The disruption of these interactions by the mutation to a residue with different physicochemical properties might lead to the exposure of a secondary cleavage site downstream of the main first processing (192-XXKVKX-199 (Rang et al., 2005)), perhaps in sequence 259-KENVK-263 for the mutant in pattern “e” and 212-KEK-216 for pattern “c”. Additionally, there is evidence that after proteolytic digestion, the 62 kDa and the 20 kDa fragments remain bounded after cleavage (Chakroun and Ferré, 2014). Thus, there must be a relatively stable contact zone between those regions in the full-protein sequence. It is hypothesised that the contact regions between this pair could be from residues 53-65 and from residues 743-773, since these residual peptides always appeared in the mass fingerprinting of the main bands of the different proteolytic fragments, which in turns are closely placed to the two “*hot spots*” in the Vip3Af sequence described for the insecticidal activity.

Patterns “b” and “f”, which did not contain the 62 kDa band either, were found only in W552A and E483A, respectively, placed at the central region of the “core” sequence. It was shown that these band patterns, were not an artefactual effect due to the interaction with the SDS. The 20 kDa band was not present in patterns “d” and “f”, which showed a major band of 27 kDa. The single 27 kDa band of the mutant E483A was identified to start at position I-528, closely related to the SDS-resistant 29 kDa fragment in the Vip3Aa16.

The characterisation of these pattern bands was consistent either with commercial trypsin treatment or with midgut juice from both *S. frugiperda* and *A. segetum*. Thus the lack of toxicity of the mutants not maintaining the 62 kDa fragments is related to the instability to proteases *in vivo.* Although some of the mutants not containing the 62 kDa fragment were yet capable to exert some insecticidal activity to one or the other insect species, it is likely that the marginal toxicity is achieved by the 62 kDa fragment prior to further cleavage.

Only slight shifts on the fluorescence emission peak were detected between the protoxin and the activated form of the wild type Vip3Af, indicating that only minor changes in the overall conformation takes place after activation, in agreement to the recently published study on the conformation of the Vip3Ag4 (Palma et al., 2017). Likewise, only minor changes on the fluorescence emission spectra among the protoxin of the wild type and the selected mutants were observed, indicating that the mutations do not disrupt the overall conformation of the protein and that the minor changes are locally compensated. An *in silico* modelled 3D structure of a single molecule of Vip3Af1 is proposed for the first time which helps to visualize the “hot spots” of the Vip3Af. In the Vip3A sequences known so far, there are only 3 cysteines

which are highly conserved. No disulphide bonds were predicted in the Vip3Af sequence, although $Cys^{401}$ was predicted to be oxidized. In agreement to that, none of the cysteine substitutions in C292A, C401A or C507A affected the toxicity against *S. frugiperda*, suggesting the absence of disulphide bonds stabilizing the chain structure. Nevertheless, the substitution of a half-cystine could be locally compensated by either the surrogate residue or its vicinity with other type of interactions, yet resulting in a functional protein. The half-cystine predicted in position 401 could be involved in a dilusphide bridge between subunits pairs of the tetramer described by Palma et al., (2017).
Oligomerization and disulphide bonding engineering are mechanisms for which proteins can improve their stability and functional diversity without increasing the genetic burden and complexity; this could be the functional role behind the insertion of a short sequence containing 8 cysteines along with the deletion of the $Cys^{507}$ in the Vip3B sequences (Rang et al., 2005; Chakroun et al., 2016a). However, further experimental data is required to elucidate the role of the cysteines in Vip3 structure and evolution.

In the 5th and final chapter, 12 different mutants were generated by site-directed mutagenesis all along the Vip3Af1 protein sequence. Reverse genetics is one of the most used approach to deepen in the protein knowledge, especially when the protein structure is unknown. Ten of these mutants were successfully expressed without major folding changes and were functionally active. It was not possible to significantly improve the insecticidal potency against *S. frugiperda* in any of the Vip3Af mutants.
Mutations in position 689 (G689S, G689E and N682K-G689S), as well as mutations E483H and W552H gave proteolytic patterns different to the native profile of the wild type but equivalent to those obtained in the same positions mutated in chapter IV.
Mutation M34L in the N-terminal was significantly more active against *S. frugiperda* than E483H and W552H, but no differences were found with the wild type Vip3Af.
The position $Glu^{483}$ is a predicted functional and exposed key residue whose negatively-charge side chain might be crucial for the structure, being that its substitution to a non-charged amino-acid or to a positively charged residue either limits the insecticidal function or impairs protein expression.
Position $Trp^{552}$ was found to be strongly conserved among Vip3A sequences and falls into the predicted Carbohydrate Binding Motif (CBM). No significant differences in the $LC_{50}$ were found when $Trp^{552}$ was exchanged with other aromatic amino acids with a ring in their side chain, suggesting that the aromaticity may be an important trait in position W552 playing a structural role rather than in the binding to carbohydrates.
Finally, position $Gly^{689}$ was predicted to be functional and placed in a loop. Although the exchange of the glycine to an alanine in chapter IV was not favorable, the substitution to a Ser or a Glu did not cause a significant effect on the insecticidal function of the Vip3Af, supporting the prediction that this position was subjected to positive Darwinian selection (Wu et al., 2007).

When the empirical evidence of the spatial conformation of a protein is unknown, a holistic approach is needed for the structure- function relationship inference. If taken together all the available literature and the results presented herein, we might venture to make a general role proposal of the main regions in the Vip3A proteins. Assuming that the cloning of the 62-66 kDa "core" renders a functional and properly folded toxin (Gayen et al., 2015, 2012) and that the removal of the first 200 residues from the N-terminus (20 kDa fragment) is necessary for the formation of pores (Lee et al., 2003), it is likely that the N-terminus do not play an essential role in the toxicity (Chakroun et al., 2016a; Rang et al., 2005; Wu et al., 2007). Nevertheless, such a big and extremely conserved sequence might be retained among homologues due to a positive fitness outcome (Fay and Wu, 2003). Jiang et al. (2016) suggested that the insecticidal activity of Vip3A proteins might be achieved by multiple mechanisms, which could have a cumulative effect on the insecticidal outcome. The protoxin form of Vip3Aa is able to exert cytotoxic activity on Sf9 and Sf21 cells (Estruch and Yu, 2001; Jiang et al., 2016; Singh et al., 2010). Thus, it is likely that the N-terminus, which is predominantly formed by α-helices, is involved in an alternative but not exclusive mechanism, perhaps the apoptosis pathway. This mechanism would account for a delayed response compared to the formation of pores, and could be the underlying mechanism for the big difference found with the Vip3Aa16 protoxin and activated toxin against *S. exigua* described in Chakroun et al. (2012).
The high divergence of the C-terminus amongst Vip3A sequences is related to functional diversification and target specificity (Fang et al., 2007; Selvapandiyan et al., 2001; Wu et al., 2007). The higher divergence is found from position 450 onwards, in which a second processing site (450-LNKKKVES-459) has been proposed and after which a short sequence of 20 residues (mostly Cys) is inserted in Vip3B (Estruch and Yu, 2001; Rang et al., 2005). Active and not-active toxins are able to bind to specific receptors in the BBMV of tolerant and resistant species (Chakroun et al., 2016c; Chakroun and Ferré, 2014; Lee et al., 2003), thus is likely that the binding to specific receptor occur in a highly conserved region. Therefore the central region of the protein, might be responsible to the specific binding. This regiod could span from residue 200 to residue 455, which corresponds to the 33 kDa band initially proposed as the minimum active fragment (Estruch and Yu, 2001). Finally, the end of the protein composed mostly by β-sheets, is predicted in two domain structures in the Vip3Af1, one of them consists in the CBM. Thus, the C-terminal end of the sequence could account for two different features: i) protein stability, by bonding interactions with the α-helices of the N-terminus, and ii) target specificity. Proteolytic activation might trigger a compaction of the β-sheets structure, facilitating the insertion into the cell membrane by disrupting the permeability or by forming pores (Lee et al., 2003; Liu et al., 2011).

Understanding the pest and protein interactions and their relation to the protein structure is necessary to design tailored measures for pest control. The results obtained in this Thesis give a better understanding of the protein structure and function of Vip3A proteins, which will be helpful for the decision making when and

how using *B. thuringiensis* or its insecticidal Vip3A proteins as a phytosanitary resource in pest management programs and resistance management strategies.

# CONCLUSIONS

## CONCLUSIONS (CAT)

1. Caracterització l'espectre insecticida de diferents proteïnes Vip3A.
   1.1. Es va realitzar un cribratge de l'activitat insecticida de 5 proteïnes Vip3A contra 8 plagues d'erugues. Les proteïnes Vip3A difereixen entre elles en l'especificitat i en diferent nivells de dosi -resposta. Cap de les proteïnes investigades fou tòxica contra *Ostrinia nubilalis,* que només va mostrar una mortalitat marginal front la Vip3Af. La Vip3Ad no és activa contra cap de les 8 espècies estudiades. No es van trobar diferències significatives entre les protoxines i les toxines activades amb tripsina.
   1.2. La combinació considerada òptima per desenvolupar l'estudi de la relació estructure-funció va ser Vip3Af front *Spodoptera frugiperda.*

2. Anàlisi de l'estabilitat front l'acció de les proteases digestives en presència de detergent (SDS). Inferir en aspectes estructurals de la Vip3Aa i de la Vip3Af.
   2.1. La interacció de la SDS amb les proteïnes Vip3A abans de l'electroforesi i en presència de serín-proteases, produeix un fals perfil de degradació de la toxina. A altes concentracions de serín-proteases, els enzims són encara actius durant el pas d'escalfament, mentre que les proteïnes Vip3A es despleguen per l'acció del SDS i de la temperatura, exposant llocs de talls no accessibles en estat natiu. Les diferències en les cinètiques d'activació observades entre la Vip3Aa i la Vip3Af revelen possibles diferències en la seva estructura.
   2.2. L'efecte aparent de degradació desapareix després de l'addició d'inhibidors de proteases irreversibles o d'agents caotròpics forts- com ara urea, i també per la separació de les proteases i les proteïnes Vip3 per cromatografia d'exclusió molecular.
   2.3. El fragment de 62-66 kDa de les proteïnes Vip3A és altament estable i representa el principal fragment responsable de l'acció insecticida. El fragment de 19-22 kDa es correspon amb la part N-terminal de la proteïna. Els llocs d'escissió secundaris foren identificats en una regió d'estructures-ß predites a l'extrem C-terminal.
   2.4. La major estabilitat front les proteases de la toxina activada podria indicar una lleu compactació de les estructures-ß de la regió central-final de la proteïna, fent-la més resistent a l'acció desnaturant del SDS i prevenint per tant l'exposició de llocs de talls no natius.

3. Escaneig d'alanina de la Vip3Af
   3.1. Una proteïna Vip3A va ser analitzada sistemàticament per mitjà de l'escaneig d'alanina per primera vegada. Només un 10% dels residus de la Vip3Af analitzats resultaren ser crítics bé afectant l'estabilitat, el plegament, el processament proteolític o l'activitat insecticida, la qual cosa fa patent

l'alta resiliència i adaptabilitat de les proteïnes Vip3A a compensar els canvis mantenint l'homeostasi i la funcionalitat. De les 558 substitucions estudiades, 19 afectaren l'expressió de la proteïna. Les 11 mutacions que més negativament afectaren l'activitat contra *S. frugiperda* van ser T167A, E168A, F229A, M238A, Y272A, E483A, W552A, G689A, I699A, Y719A, i G727A. Estos resultats es varen confirmar en *Agrotis segetum*. Les mutacions situades a la C-terminal tingueren major repercussió en l'activitat insecticida contra *A. segetum* que contra *S. frugiperda*, fet que recolza el paper de l'extrem C-terminal en l'especificitat.

3.2. Els mutants seleccionats van donar 6 perfils proteolítics diferents. El perfils proteolítics de les protoxines tractades amb tripsina o amb extracte de suc intestinals tant de S. *frugiperda* com de *A. segetum* no revelaren diferències. La pro-toxina Vip3Af es talla en la posició $Asp^{199}$ després de l'activació, generant dos fragments principals de 62 kDa i de 20 kDa.

3.3. S'ha identificat dues regions crítiques a la seqüència de la Vip3Af, on es concentren les mutacions considerades crítiques per l'acció insecticida: la regió N-terminal entre els residus 167 i 272, i l'extrem C-terminal entre els residus 689 i 741. Els patrons d'activació a les mutacions de la regió N-terminal mantingueren el fragment de 62 kDa, mentre a la regió C-terminal no, recolzant el paper estabilitzador de la C-terminal.

3.4. La reducció de l'activitat insecticida de les mutacions no es conseqüència de canvis importants en l'estructura terciària, en base a les dades de fluorescència intrínseca.

3.5. La predicció *ab initio* de la conformació de la Vip3Af va revelar una estructura α - ß en 5 dominis, formada per regions desordenades, α-hèlixs a la N-terminal i fulles-ß a la regió C-terminal.

## 4. Mutagènesi dirigida de la Vip3Af:

4.1. Es varen generar 12 diferents mutants amb èxit. La triple mutació a la regió N-terminal i la mutació E483Q comprometeren la correcta expressió de la proteïna o la seva estabilitat. Les mutacions generades no comportaren diferències significatives en l'activitat insecticida contra *S. frugiperda* tot i que algunes de les mutacions revelaren diferències en l'estabilitat proteolítica.

## CONCLUSIONS (EN)

1. Characterization of the insecticidal spectra of different Vip3A proteins.
   1.1. A screening of the insecticidal activity of 5 Vip3A proteins against 8 caterpillar pests was performed. Vip3A proteins revealed different target specificity and dose –response behavior. *Ostrinia nubilalis* was found to be tolerant to all Vip3A tested and only marginal mortality was caused by the Vip3Af. Vip3Ad protein was no toxic to any of the tested species. No major differences were found when comparing protoxins vs. trypsin-activated toxins.
   1.2. Vip3Af was selected for further structure and function relationship due to the overall high toxicity. *S. frugiperda* was shown to be susceptible to a broad range of Vip3A proteins.

2. Analysis of the stability against digestive proteases in the presence of SDS and inference of structural aspects of the Vip3Aa and Vip3Af proteins.
   2.1. The interaction of the SDS with the Vip3A proteins during the heating step prior to SDS-PAGE in the presence of serine proteases leads to a misleading degradation profile of the toxin. High concentrations of serine proteases of the insect midgut juice are able to display enzymatic activity during the heating step whereas the Vip3A proteins become unfolded by the action of the SDS and the temperature, exposing non-native cleavage sites. Some differences are noticed between the Vip3Aa and the Vip3Af activation kinetics, suggesting differences in their structure.
   2.2. The misleading degradation disappears after the addition of irreversible protease inhibitors or strong chaotropic agents such as urea or by the separation of the proteases and the Vip3 molecules by size exclusion chromatography.
   2.3. The 62-66 kDa band of the Vip3A proteins is highly stable and represents the main active fragment for the insecticidal activity. The 19-22 kDa fragment correspond to the N-terminus of the protein. Secondary cleavage sites were identified in a region of predicted ß-structures at the C-terminus.
   2.4. During the time course of the activation process, a compaction of the ß-structures from the mid-end of the sequence might take place, making the protein more resistant to unfolding denaturation by the SDS.

3. Alanine-scanning of the Vip3Af.
   3.1. A Vip3A protein was systematically analysed by alanine-scanning for the first time. Only 10% of the residues analysed play a crucial role in either protein stability, protein folding, proteolytic processing or insecticidal activity of the Vip3Af1(WT), which stresses the high level of resilience and adaptability of Vip3A proteins to preserve protein function and

homeostasis. From the 558 residue substitutions analysed by alanine-scanning, 19 impaired protein expression. The 11 positions driving the strongest activity inhibition against *S. frugiperda* were T167A, E168A, F229A, M238A, Y272A, E483A, W552A, G689A, I699A, Y719A, and G727A. These results were confirmed on *Agrotis segetum*. Critical positions in the C-terminal had a more markedly negative effect on the insecticidal function against *A. segetum* than against *S. frugiperda*, supporting the role of the C-terminal end in target specificity.

3.2. The selected mutants gave 6 different proteolytic profiles. These profiles were consistent regardless the use of commercial trypsin or midgut juice from *S. frugiperda* or *A. segetum*. The protoxin is splitted at position $Asp^{199}$ after proteolysis digestion in two main fragments of 62 kDa and 20 kDa.

3.3. Two "hot spots" are identified in the primary sequence of the Vip3Af protein: one in the N-terminal region, clustering residues 167 to 272, and the other in the C-terminal end, between residues 689 and 741. The proteolytic profile of these mutants is also consistent with the above proposal: mutations in the N-terminal part gave a proteolytic pattern containing the core active fragment of 62 kDa whereas mutations in the C-terminal region gave proteolytic fragment of smaller size, supporting the stability role of the C-terminal end.

3.4. Only minor changes in the tertiary structure occurred in the ala-mutants selected as revealed by intrinsic fluorescence emission spectra.

3.5. The *ab initio* prediction of the Vip3Af structure revealed a 5 domains α - ß protein dominated by α-helix structures at the N-terminal and ß-sheet structures in the C-terminal region with a considerable amount of disordered regions.

4. Site-directed mutagenesis of the Vip3Af.

4.1. 12 different site-directed mutants were successfully generated. The triple mutant in the N-terminal region and E483Q impaired the protein expression or the stability. The mutations did not significantly alter the insecticidal activity but some of the mutations revealed differences in the proteolytic stability against *S. frugiperda.*

# REFERENCES

Abdelkefi-Mesrati, L., Boukedi, H., Chakroun, M., Kamoun, F., Azzouz, H., Tounsi, S., Rouis, S., Jaoua, S., 2011a. Investigation of the steps involved in the difference of susceptibility of *Ephestia kuehniella* and *Spodoptera littoralis* to the *Bacillus thuringiensis* Vip3Aa16 toxin. J. Invertebr. Pathol. 107, 198–201. doi:10.1016/j.jip.2011.05.014

Abdelkefi-Mesrati, L., Boukedi, H., Dammak-Karray, M., Sellami-Boudawara, T., Jaoua, S., Tounsi, S., 2011b. Study of the *Bacillus thuringiensis* Vip3Aa16 histopathological effects and determination of its putative binding proteins in the midgut of *Spodoptera littoralis*. J. Invertebr. Pathol. 106, 250–254. doi:10.1016/j.jip.2010.10.002

Abdelkefi-Mesrati, L., Rouis, S., Sellami, S., Jaoua, S., 2009. *Prays oleae* midgut putative receptor of *Bacillus thuringiensis* vegetative insecticidal protein Vip3LB differs from that of Cry1Ac toxin. Mol. Biotechnol. 43, 15–19. doi:10.1007/s12033-009-9178-4

Abulreesh, H.H., Osman, G.E.H., Assaeedi, A.S.A., 2012. Characterization of insecticidal genes of *Bacillus thuringiensis* strains isolated from arid environments. Indian J. Microbiol. 52, 500–503. doi:10.1007/s12088-012-0257-z

Adamczyk, J.J.J., Mahaffey, J.S., 2008. Efficacy of Vip3A and Cry1Ab transgenic traits in cotton against various lepidopteran pests. Florida Entomol. doi:10.1653/0015-4040-91.4.570

Adang, M.J., Crickmore, N., Jurat-Fuentes, J.L., 2014. Diversity of *Bacillus thuringiensis* crystal toxins and mechanism of action., in: Dhadialla, T.S., Gill, S.S. (Eds.), Advances in Insect Physiology , Vol 47. Eds. Oxford: Academic Press, pp. 39–87.

Alexandratos, N., Bruinsma, J., 2012. World agriculture towards 2030/2050: the 2012 revision. Land Use Policy. 20, 375.

Ali, M.I., Luttrell, R.G., 2011. Susceptibility of *Helicoverpa zea* and *Heliothis virescens* (Lepidoptera: Noctuidae) to Vip3A insecticidal protein expressed in VipCot (TM) cotton. J. Invertebr. Pathol. 108, 76–84. doi:DOI 10.1016/j.jip.2011.06.013

An, J., Gao, Y., Wu, K., Gould, F., Gao, J., Shen, Z., Lei, C., 2010. Vip3Aa tolerance response of *Helicoverpa armigera* populations from a Cry1Ac cotton planting region. J. Econ. Entomol. 103, 2169–2173. doi:10.1603/ec10105

Anilkumar, K.J., Rodrigo-Simón, A., Ferré, J., Pusztai-Carey, M., Sivasupramaniam, S., Moar, W.J., 2008. Production and characterization of *Bacillus thuringiensis* Cry1Ac-resistant cotton bollworm *Helicoverpa zea* (Boddie). Appl. Environ. Microbiol. 74, 462–9. doi:10.1128/AEM.01612-07

Arora, N., Selvapandiyan, A., Agrawal, N., Bhatnagar, R.K., 2003. Relocating expression of vegetative insecticidal protein into mother cell of *Bacillus thuringiensis*. Biochem. Biophys. Res. Commun. 310, 158–162. doi:10.1016/j.bbrc.2003.08.137

Asensio, J.L., Ardá, A., Cañada, F.J., Jiménez-Barbero, J., 2013. Carbohydrate–Aromatic Interactions. Acc. Chem. Res. 46, 946–954. doi:10.1021/ar300024d

Asokan, R., Swamy, H.M.M., Arora, D.K., 2012. Screening, Diversity and Partial Sequence Comparison of Vegetative Insecticidal Protein (vip3A) Genes in the Local Isolates of *Bacillus thuringiensis* Berliner. Curr. Microbiol. 64, 365–370. doi:DOI 10.1007/s00284-011-0078-z

Baranek, J., Kaznowski, A., Konecka, E., Naimov, S., 2015. Activity of vegetative insecticidal proteins Vip3Aa58 and Vip3Aa59 of *Bacillus thuringiensis* against lepidopteran pests. J Invertebr Pathol 130, 72–81. doi:10.1016/j.jip.2015.06.006

Barkhade, U.P., Thakare, A.S., 2010. Protease Mediated Resistance Mechanism to Cry1C and Vip3A in *Spodoptera litura*. Egypt. Acad. J. Biol. Sci. 3 (2).

Barth, H., Aktories, K., Popoff, M.R., Stiles, B.G., 2004. Binary bacterial toxins: biochemistry, biology, and applications of common *Clostridium* and *Bacillus* proteins. Microbiol. Mol. Biol. Rev. 68, 373–402. doi:10.1128/MMBR.68.3.373-402.2004

Barth, H., Hofmann, F., Olenik, C., Just, I., Aktories, K., 1998. The N-terminal part of the enzyme component (C2I) of the binary *Clostridium botulinum* C2 toxin interacts with the binding component C2II and functions as a carrier system for a Rho ADP-ribosylating C3-like fusion toxin. Infect. Immun. 66, 1364–9.

Beard, C.E., Court, L., Boets, A., Mourant, R., Van Rie, J., Akhurst, R.J., 2008. Unusually high frequency of genes encoding vegetative insecticidal proteins in an Australian *Bacillus thuringiensis* collection. Curr. Microbiol. 57, 195–199. doi:10.1007/s00284-008-9173-1

Bel, Y., Banyuls, N., Chakroun, M., Escriche, B., Ferré, J., 2017. Insights into the Structure of the Vip3Aa Insecticidal Protein by Protease Digestion Analysis. Toxins (Basel). 9, 131. doi:10.3390/toxins9040131

Bel, Y., Jakubowska, A.K., Costa, J., Herrero, S., Escriche, B., 2013. Comprehensive analysis of gene expression profiles of the beet armyworm *Spodoptera exigua* larvae challenged with *Bacillus thuringiensis* Vip3Aa toxin. PLoS One 8, e81927. doi:10.1371/journal.pone.0081927

Ben Hamadou-Charfi, D., Boukedi, H., Abdelkefi-Mesrati, L., Tounsi, S., Jaoua, S., 2013. *Agrotis segetum* midgut putative receptor of *Bacillus thuringiensis* vegetative insecticidal protein Vip3Aa16 differs from that of Cry1Ac toxin. J Invertebr Pathol 114, 139–143. doi:10.1016/j.jip.2013.07.003

Berezin, C., Glaser, F., Rosenberg, J., Paz, I., Pupko, T., Fariselli, P., Casadio, R., Ben-Tal, N., 2004a. ConSeq: the identification of functionally and structurally important residues in protein sequences. Bioinformatics 20, 1322–1324. doi:10.1093/bioinformatics/bth070

Bergamasco, V.B., Mendes, D.R., Fernandes, O.A., Desidério, J.A., Lemos, M. V, 2013. *Bacillus thuringiensis* Cry1Ia10 and Vip3Aa protein interactions and their toxicity in *Spodoptera* spp. (Lepidoptera). J. Invertebr. Pathol. 112, 152–158. doi:10.1016/j.jip.2012.11.011

Bernardi, O., Amado, D., Sousa, R.S., Segatti, F., Fatoretto, J., Burd, A.D., Omoto, C., 2014. Baseline Susceptibility and Monitoring of Brazilian Populations of *Spodoptera*

*frugiperda* (Lepidoptera: Noctuidae) and *Diatraea saccharalis* (Lepidoptera: Crambidae) to Vip3Aa20 Insecticidal Protein. J. Econ. Entomol. 107, 781–790. doi:10.1603/EC13374

Bernardi, O., Bernardi, D., Ribeiro, R.S., Okuma, D.M., Salmeron, E., Fatoretto, J., Medeiros, F.C.L., Burd, T., Omoto, C., 2015. Frequency of resistance to Vip3Aa20 toxin from *Bacillus thuringiensis* in *Spodoptera frugiperda* (Lepidoptera: Noctuidae) populations in Brazil. Crop Prot. 76, 7–14. doi:10.1016/j.cropro.2015.06.006

Betts, M.J., Russell, R.B., 2003. Amino Acid Properties and Consequences of Substitutions, in: Bioinformatics for Geneticists. John Wiley & Sons, Ltd, Chichester, UK, pp. 289–316. doi:10.1002/0470867302.ch14

Bhalla, R., Dalal, M., Panguluri, S.K., Jagadish, B., Mandaokar, A.D., Singh, A.K., Kumar, P.A., 2005. Isolation, characterization and expression of a novel vegetative insecticidal protein gene of *Bacillus thuringiensis*. FEMS Microbiol. Lett. 243, 467–472. doi:S0378-1097(05)00013-3 [pii]

Bi, Y., Zhang, Y., Shu, C., Crickmore, N., Wang, Q., Du, L., Song, F., Zhang, J., 2015. Genomic sequencing identifies novel *Bacillus thuringiensis* Vip1/Vip2 binary and Cry8 toxins that have high toxicity to *Scarabaeoidea* larvae. Appl. Microbiol. Biotechnol. 99, 753–760. doi:10.1007/s00253-014-5966-2

Blaustein, R.O., Koehler, T.M., Collier, R.J., Finkelstein, A., 1989. Anthrax toxin: channel-forming activity of protective antigen in planar phospholipid bilayers. Proc. Natl. Acad. Sci. U. S. A. 86, 2209–13.

Boets, A., Arnaut, G., Van Rie, J., Damme, N., 2011. Toxins. US patent 7,919,609 B2.

Boraston, A.B., Bolam, D.N., Gilbert, H.J., Davies, G.J., 2004. Carbohydrate-binding modules: fine-tuning polysaccharide recognition. Biochem. J. 382, 769–781. doi:10.1042/BJ20040892

Bordo, D., Argos, P., 1991. Suggestions for 'safe' residue substitutions in site-directed mutagenesis. J. Mol. Biol. 217, 721–729. doi:10.1016/0022-2836(91)90528-E

Bortolotti, A., Wong, Y.H., Korsholm, S.S., Bahring, N.H.B., Bobone, S., Tayyab, S., van de Weert, M., Stella, L., 2016. On the purported 'backbone fluorescence' in protein three-dimensional fluorescence spectra. RSC Adv. 6, 112870–112876. doi:10.1039/C6RA23426G

Boukedi, H., Ben Khedher, S., Triki, N., Kamoun, F., Saadaoui, I., Chakroun, M., Tounsi, S., Abdelkefi-Mesrati, L., 2015. Overproduction of the *Bacillus thuringiensis* Vip3Aa16 toxin and study of its insecticidal activity against the carob moth *Ectomyelois ceratoniae*. J. Invertebr. Pathol. 127, 127–129. doi:10.1016/j.jip.2015.03.013

Bradford, M.M., 1976. A rapid and sensitive method for the quantitation of microgram quantities of protein utilizing the principle of protein-dye binding. Anal. Biochem. doi:10.1016/0003-2697(76)90527-3

Burkness, E.C., Dively, G., Patton, T., Morey, A.C., Hutchison, W.D., 2010. Novel Vip3A *Bacillus thuringiensis* (Bt) maize approaches high-dose efficacy against *Helicoverpa*

*zea* (Lepidoptera: Noctuidae) under field conditions: Implications for resistance management. GM Crops 1, 337–343. doi:10.4161/gmcr.1.5.14765

Caccia, S., Chakroun, M., Vinokurov, K., Ferré, J., 2014. Proteolytic processing of *Bacillus thuringiensis* Vip3A proteins by two *Spodoptera* species. J. Insect. Physiol. 67, 76–84. doi:10.1016/j.jinsphys.2014.06.008

Caccia, S., Di Lelio, I., La Storia, A., Marinelli, A., Varricchio, P., Franzetti, E., Banyuls, N., Tettamanti, G., Casartelli, M., Giordana, B., Ferré, J., Gigliotti, S., Ercolini, D., Pennacchio, F., 2016. Midgut microbiota and host immunocompetence underlie *Bacillus thuringiensis* killing mechanism. Proc. Natl. Acad. Sci. 113, 201521741. doi:10.1073/pnas.1521741113

Calvete, J.J., Marcinkiewicz, C., Monleon, D., Esteve, V., Celda, B., Juarez, P., Sanz, L., 2005. Snake venom disintegrins: evolution of structure and function. Toxicon 45, 1063–1074. doi:S0041-0101(05)00071-1

Calvete, J.J., Moreno-Murciano, M.P., Theakston, R.D., Kisiel, D.G., Marcinkiewicz, C., 2003. Snake venom disintegrins: novel dimeric disintegrins and structural diversification by disulphide bond engineering. Biochem. J. 372, 725–734. doi:10.1042/BJ20021739

Carrière, Y., Crickmore, N., Tabashnik, B.E., 2015. Optimizing pyramided transgenic Bt crops for sustainable pest management. Nat. Biotechnol. 33, 161–168. doi:10.1038/nbt.3099

Carroll, J., Convents, D., Van Damme, J., Boets, A., Van Rie, J., Ellar, D.J., 1997. Intramolecular proteolytic cleavage of Bacillus thuringiensis Cry3A δ-endotoxin may facilitate its coleopteran toxicity. J. Invertebr. Pathol. 70, 41–49. doi:10.1006/jipa.1997.4656

Carvalho, F.P., 2006. Agriculture, pesticides, food security and food safety. Environ. Sci. Policy 9, 685–692. doi:10.1016/j.envsci.2006.08.002

Ceroni, A., Passerini, A., Vullo, A., Frasconi, P., 2006. DISULFIND: a disulfide bonding state and cysteine connectivity prediction server. Nucleic Acids Res. 34, W177–W181. doi:10.1093/nar/gkl266

Chakroun, M., Banyuls, N., Bel, Y., Escriche, B., Ferré, J., 2016a. Bacterial Vegetative Insecticidal Proteins (Vip) from Entomopathogenic Bacteria. Microbiol. Mol. Biol. Rev. 80, 329–350. doi:10.1128/MMBR.00060-15

Chakroun, M., Banyuls, N., Bel, Y., Escriche, B., Ferré, J., 2016b. Correction for Chakroun et al., Bacterial Vegetative Insecticidal Proteins (Vip) from Entomopathogenic Bacteria. Microbiol. Mol. Biol. Rev. 80, iii. doi:10.1128/MMBR.00039-16

Chakroun, M., Banyuls, N., Walsh, T., Downes, S., James, B., Ferré, J., 2016c. Characterization of the resistance to Vip3Aa in *Helicoverpa armigera* from Australia and the role of midgut processing and receptor binding. Sci. Rep. 6, 24311. doi:10.1038/srep24311

Chakroun, M., Bel, Y., Caccia, S., Abdelkefi-Mesrati, L., Escriche, B., Ferré, J., 2012. Susceptibility of *Spodoptera frugiperda* and *S. exigua* to *Bacillus thuringiensis* Vip3Aa insecticidal protein. J. Invertebr. Pathol. 110, 334–339. doi:10.1016/j.jip.2012.03.021

Chakroun, M., Ferré, J., 2014. *In vivo* and *in vitro* binding of Vip3Aa to *Spodoptera frugiperda* midgut and characterization of binding sites by (125)I radiolabeling. Appl Env. Microbiol 80, 6258–6265. doi:10.1128/AEM.01521-14

Chen, J., Yu, J., Tang, L., Tang, M., Shi, Y., Pang, Y., 2003. Comparison of the expression of *Bacillus thuringiensis* full-length and N-terminally truncated vip3A gene in *Escherichia coli*. J. Appl. Microbiol. 95, 310–316.

Christensen, S., Valnickova, Z., Tøgersen, I.B., Olsen, E.H.N., Enchild, J.J., 1997. Assignment of a single disulphide bridge in human α2-antiplasmin: implications for the structural and functional properties. Biochem. J. 323, 847–852. doi:10.1042/bj3230847

Crickmore, N., Baum, J., Bravo, A., Lereclus, D., Narva, K., Sampson, K., Schnepf, E., Sun, M., Zeigler, D.R., 2014. *Bacillus thuringiensis* toxin nomenclature. http://www.btnomenclature.info/

Cunningham, B.C., Wells, J.A., 1989. High-resolution epitope mapping of hGH-receptor interactions by alanine-scanning mutagenesis. Science (80). 244, 1081–1085. doi:10.1126/science.2471267

De, A., Bose, R., Kumar, A., Mozumdar, S., 2014. Targeted Delivery of Pesticides Using Biodegradable Polymeric Nanoparticles. Fundam. Appl. Control. Release Drug Deliv. 629–639. doi:10.1007/978-81-322-1689-6

de Maagd, R.A., Bravo, A., Berry, C., Crickmore, N., Schnepf, H.E., 2003. Structure, diversity, and evolution of protein toxins from spore-forming entomopathogenic bacteria. Annu. Rev. Genet. 37, 409–433. doi:10.1146/annurev.genet.37.110801.143042

de Maagd, R.A., Bravo, A., Crickmore, N., 2001. How *Bacillus thuringiensis* has evolved specific toxins to colonize the insect world. Trends Genet. 17, 193–199. doi:10.1016/S0168-9525(01)02237-5

Dong, F., Shi, R., Zhang, S., Zhan, T., Wu, G., Shen, J., Liu, Z., 2012a. Fusing the vegetative insecticidal protein Vip3Aa7 and the N terminus of Cry9Ca improves toxicity against *Plutella xylostella* larvae. Appl. Microbiol. Biotechnol. 96, 921–929. doi:10.1007/s00253-012-4213-y

Dong, F., Zhang, S., Shi, R., Yi, S., Xu, F., Liu, Z., 2012b. Ser-substituted mutations of Cys residues in *Bacillus thuringiensis* Vip3Aa7 exert a negative effect on its insecticidal activity. Curr. Microbiol. 65, 583–588. doi:10.1007/s00284-012-0201-9

Donovan, W.P., Donovan, J.C., Engleman, J.T., 2001. Gene knockout demonstrates that vip3A contributes to the pathogenesis of Bacillus thuringiensis toward *Agrotis ipsilon* and *Spodoptera exigua*. J.Invertebr.Pathol. 78, 45–51.

Donovan, W.P., Engleman, J.T., Donovan, J.C., Baum, J.A., Bunkers, G.J., Chi, D.J., Clinton, W.P., English, L., Heck, G.R., Ilagan, O.M., Krasomil-Osterfeld, K.C., Pitkin,

J.W., Roberts, J.K., Walters, M.R., 2006. Discovery and characterization of Sip1A: a novel secreted protein from *Bacillus thuringiensis* with activity against coleopteran larvae. Appl. Microbiol. Biotechnol. 72, 713–719. doi:10.1007/s00253-006-0332-7

Doss, V., K., A.K., Jayakumar, R., Sekar, V., 2002. Cloning and expression of the vegetative insecticidal protein (vip3V) gene of *Bacillus thuringiensis* in *Escherichia coli*. Protein Expr. Purif. 26, 82. doi:10.1016/S1046-5928(02)00515-6

Dubois, T., Faegri, K., Perchat, S., Lemy, C., Buisson, C., Nielsen-LeRoux, C., Gohar, M., Jacques, P., Ramarao, N., Kolstø, A.-B., Lereclus, D., 2012. Necrotrophism Is a Quorum-Sensing-Regulated Lifestyle in *Bacillus thuringiensis*. PLoS Pathog. 8, e1002629. doi:10.1371/journal.ppat.1002629

EFSA, 2012. Scientific Opinion on application ( EFSA-GMO-DE-2010-82 ) for the placing on the market of insect-resistant genetically modified maize MIR162 for food and feed uses , import and processing under Regulation (EC) No 1829/2003 from Syngenta, EFSA Journal. doi:10.2903/j.efsa.2012.2756.

EPA, 2017. Pesticides Industry Sales and Usage 2008 - 2012 Market estimates.

Espinasse, S., Chaufaux, J., Buisson, C., Perchat, S., Gohar, M., Bourguet, D., Sanchis, V., 2003. Occurrence and linkage between secreted insecticidal toxins in natural isolates of *Bacillus thuringiensis*. Curr. Microbiol. 47, 501–7.

Estruch, J.J., Carozzi, N.B., Desai, N., Duck, N.B., Warren, G.W., Koziel, M.G., 1997. Transgenic plants: An emerging approach to pest control. Nat. Biotechnol. 15, 137–141. doi:10.1038/nbt0297-137

Estruch, J.J., Warren, G.W., Mullins, M. a, Nye, G.J., Craig, J. a, Koziel, M.G., 1996. Vip3A, a novel *Bacillus thuringiensis* vegetative insecticidal protein with a wide spectrum of activities against lepidopteran insects. Proc. Natl. Acad. Sci. 93, 5389–5394.

Estruch, J.J., Yu, C.G., 2001. Plant pest control.

EU Pesticides database - European Commission http://ec.europa.eu/food/plant/pesticides/eu-pesticides-database/ (accessed 3.18.17).

EUROSTATS. Agri-environmental indicator - consumption of pesticides - Statistics Explained. http://ec.europa.eu/eurostat/statistics-explained/index.php/Agri-environmental_indicator_-_consumption_of_pesticides (accessed 3.19.17).

Fang, J., Xu, X., Wang, P., Zhao, J.Z., Shelton, A.M., Cheng, J., Feng, M.G., Shen, Z., 2007. Characterization of chimeric *Bacillus thuringiensis* Vip3 toxins. Appl. Env. Microbiol. 73, 956–961. doi:10.1128/AEM.02079-06

Fay, J.C., Wu, C.I., 2003. Sequence divergence, functional constraint, and selection in protein evolution. Annu. Rev. Genomics Hum. Genet. 4, 213–235. doi:10.1146/annurev.genom.4.020303.162528

Federici, B.A., 1998. Transgenic Bt crops and resistance: Broadscale use of pest-killing plants to be true test. Calif. Agric. 52, 14–20. doi:10.3733/ca.v052n06p14

Feitelson, J.S., Schnepf, H.E., Narva, K.E., Stockhoff, B.A., Schmeits, J., Loewer, D., Dullum, C.J., Muller-Cohn, J., Stamp, L., Morrill, G., Finstad-Lee, S., 2003. Pesticidal toxins and nucleotide sequences which encode these toxins. US patent 6,656,908 B2.

Ferrè, F., Clote, P., 2006. DiANNA 1.1: an extension of the DiANNA web server for ternary cysteine classification. Nucleic Acids Res. 34, W182–W185. doi:10.1093/nar/gkl189

Franco-Rivera, A., Benintende, G., Cozzi, J., Baizabal-Aguirre, V.M., Valdez-Alarcón, J.J., López-Meza, J.E., 2004. Molecular characterization of *Bacillus thuringiensis* strains from Argentina. Antonie Van Leeuwenhoek 86, 87–92. doi:10.1023/B:ANTO.0000024913.94410.05

Gasteiger, E., Hoogland, C., Gattiker, A., Duvaud, S., Wilkins, M.R., Appel, R.D., Bairoch, A., 2005. Protein Identification and Analysis Tools on the ExPASy Server, in: Walker, J.M. (Ed.), The Proteomics Protocols Handbook. Humana Press, pp. 571–607. doi:10.1385/1-59259-890-0:571

Gayen, S., Hossain, M.A., Sen, S.K., 2012. Identification of the bioactive core component of the insecticidal Vip3A toxin peptide of *Bacillus thuringiensis.* J. Plant Biochem. Biotechnol. 21, 128–135. doi:10.1007/s13562-012-0148-8

Gayen, S., Samanta, M.K., Hossain, M.A., Mandal, C.C., Sen, S.K., 2015. A deletion mutant ndv200 of the *Bacillus thuringiensis* vip3BR insecticidal toxin gene is a prospective candidate for the next generation of genetically modified crop plants resistant to lepidopteran insect damage. Planta. 242, 269–281. doi:10.1007/s00425-015-2309-1

Gomis-Cebolla, J., Ruiz de Escudero, I., Vera-Velasco, N.M., Hernández-Martínez, P., Hernández-Rodríguez, C.S., Ceballos, T., Palma, L., Escriche, B., Caballero, P., Ferré, J., 2017. Insecticidal spectrum and mode of action of the *Bacillus thuringiensis* Vip3Ca insecticidal protein. J. Invertebr. Pathol. 142, 60–67. doi:10.1016/j.jip.2016.10.001

Gouffon, C., Van Vliet, A., Van Rie, J., Jansens, S., Jurat-Fuentes, J., 2011. Binding Sites for *Bacillus thuringiensis* Cry2Ae Toxin on Heliothine Brush Border Membrane Vesicles Are Not Shared with Cry1A, Cry1F, or Vip3A Toxin. Appl. Environ. Microbiol. 77, 3182–3188. doi:10.1128/AEM.02791-10

Graser, G., Walters, F.S., Burns, A., Sauve, A., Raybould, A., 2017. A General Approach to Test for Interaction Among Mixtures of Insecticidal Proteins Which Target Different Orders of Insect Pests. J. Insect Sci. 17, 532–536. doi:10.1093/jisesa/iex003

Greene, G.L., Leppla, N.C., Dickerson, W.A., 1976. Velvetbean Caterpillar: A Rearing Procedure and Artificial Medium. J. Econ. Entomol. 69, 487–488. doi:10.1093/jee/69.4.487

Gulzar, A., Pickett, B., Sayyed, A.H., Wright, D.J., 2012. Effect of temperature on the fitness of a Vip3A resistant population of *Heliothis virescens* (Lepidoptera: Noctuidae). J. Econ. Entomol. 105, 964–970. doi:Doi 10.1603/Ec11110

Han, S., Arvai, A.S., Clancy, S.B., Tainer, J.A., 2001. Crystal structure and novel recognition motif of Rho ADP-ribosylating C3 exoenzyme from *Clostridium botulinum*: structural insights for recognition specificity and catalysis. J. Mol. Biol. 305, 95–107. doi:10.1006/jmbi.2000.4292

Han, S., Craig, J.A., Putnam, C.D., Carozzi, N.B., Tainer, J.A., 1999. Evolution and mechanism from structures of an ADP-ribosylating toxin and NAD complex. Nat. Struct. Biol. 6, 932–936. doi:10.1038/13300

Hernández-Martínez, P., Hernández-Rodríguez, C., Rie, J. V, Escriche, B., Ferré, J., 2013. Insecticidal activity of Vip3Aa, Vip3Ad, Vip3Ae, and Vip3Af from *Bacillus thuringiensis* against lepidopteran corn pests. J Invertebr Pathol 113, 78–81. doi:10.1016/j.jip.2013.02.001

Hernández-Rodríguez, C.S., Boets, A., Van Rie, J., Ferré, J., 2009. Screening and identification of vip genes in *Bacillus thuringiensis* strains. J. Appl. Microbiol. 107, 219–225. doi:10.1111/j.1365-2672.2009.04199.x

Hernández-Rodríguez, C.S., Ruiz de Escudero, I., Asensio, A.C., Ferré, J., Caballero, P., 2013. Encapsulation of the *Bacillus thuringiensis* secretable toxins Vip3Aa and Cry1Ia in *Pseudomonas fluorescens*. Biol. Control 66, 159–165. doi:10.1016/j.biocontrol.2013.05.002

Huang, F., Qureshi, J.A., Meagher, R.L., Reisig, D.D., Head, G.P., Andow, D.A., Ni, X., Kerns, D., Buntin, G.D., Niu, Y., Yang, F., Dangal, V., 2014. Cry1f resistance in fall armyworm *Spodoptera frugiperda*: single gene versus pyramided Bt maize. PLoS One 9, e112958. doi:10.1371/journal.pone.0112958

ISAA. ISAA GM Approval Database. http://www.isaaa.org/gmapprovaldatabase/ (accessed 4.24.17).

Jackson, R.E., Marcus, M.A., Gould, F., Bradley J., J.R., Van Duyn, J.W., 2007. Cross-resistance responses of Cry1Ac-selected *Heliothis virescens* (Lepidoptera: Noctuidae) to the *Bacillus thuringiensis* protein vip3A. J Econ.Entomol 100, 180–186.

Jagtap, D.D., Narahari, A., Swamy, M.J., Mahale, S.D., 2007. Disulphide bond reduction and S-carboxamidomethylation of PSP94 affects its conformation but not the ability to bind immunoglobulin. Biochim. Biophys. Acta - Proteins Proteomics 1774, 723–731. doi:10.1016/j.bbapap.2007.03.017

James, C., 2015. Global Status of Commercialized Biotech/GM Crops: 2015. ISAAA Brief No. 51. ISAAA. Executive summary.

James, C., 2014. Global Status of Commercialized Biotech/GM Crops: 2014- ISAAA Brief No. 51. ISAA, Ithaca, NY.

Jamoussi, K., Sellami, S., Bdelkefi-Mesrati, L., Givaudan, A., Jaoua, S., 2009. Heterologous expression of *Bacillus thuringiensis* vegetative insecticidal protein-encoding gene *vip3LB* in *Photorhabdus temperata* strain K122 and oral toxicity against the lepidoptera *Ephestia kuehniella* and *Spodoptera littoralis*. Mol. Biotechnol. 43, 97–103.

Jiang, K., Mei, S.Q., Wang, T.T., Pan, J.H., Chen, Y.H., Cai, J., 2016. Vip3Aa induces apoptosis in cultured *Spodoptera frugiperda* (Sf9) cells. Toxicon 120, 49–56. doi:10.1016/j.toxicon.2016.07.019

Jouzani, G.S., Valijanian, E., Sharafi, R., 2017. *Bacillus thuringiensis*: a successful insecticide with new environmental features and tidings. Appl. Microbiol. Biotechnol. doi:10.1007/s00253-017-8175-y

Juárez, P., Comas, I., González-Candelas, F., Calvete, J.J., 2008. Evolution of snake venom disintegrins by positive Darwinian selection. Mol. Biol. Evol. 25, 2391–2407. doi:10.1093/molbev/msn179

Jucovic, M., Walters, F.S., Warren, G.W., Palekar, N. V., Chen, J.S., 2008. From enzyme to zymogen: engineering Vip2, an ADP-ribosyltransferase from *Bacillus cereus*, for conditional toxicity. Protein Eng. Des. Sel. 21, 631–638. doi:10.1093/protein/gzn038

Kearse, M., Moir, R., Wilson, A., Stones-Havas, S., Cheung, M., Sturrock, S., Buxton, S., Cooper, A., Markowitz, S., Duran, C., Thierer, T., Ashton, B., Meintjes, P., Drummond, A., 2012. Geneious Basic: An integrated and extendable desktop software platform for the organization and analysis of sequence data. Bioinformatics 28, 1647–1649. doi:10.1093/bioinformatics/bts199

Knapp, O., Benz, R., Gibert, M., Marvaud, J.C., Popoff, M.R., 2002. Interaction of *Clostridium perfringens* iota-toxin with lipid bilayer membranes: Demonstration of channel formation by the activated binding component Ib and channel block by the enzyme component Ia. J. Biol. Chem. 277, 6143–6152. doi:10.1074/jbc.M103939200

Kunthic, T., Surya, W., Promdonkoy, B., Torres, J., Boonserm, P., 2016. Conditions for homogeneous preparation of stable monomeric and oligomeric forms of activated Vip3A toxin from *Bacillus thuringiensis*. Eur. Biophys. J. doi:10.1007/s00249-016-1162-x

Kupferschmidt, K., 2013. A lethal dose of RNA. Science 341, 732–3. doi:10.1126/science.341.6147.732

Kurtz, R.W., 2010. A review of Vip3A mode of action and effects on Bt Cry protein-resistant Colonies of lepidopteran larvae. Southwest. Entomol. 35, 391–394. doi:10.3958/059.035.0321

Kurtz, R.W., McCaffery, A., O'Reilly, D., 2007. Insect resistance management for Syngenta's VipCot transgenic cotton. J Invertebr Pathol 95, 227–230. doi:10.1016/j.jip.2007.03.014

Lacey, L.A., Frutos, R., Kaya, H.K., Vail, P., 2001. Insect Pathogens as Biological Control Agents: Do They Have a Future? Biol. Control 21, 230–248. doi:10.1006/bcon.2001.0938

Lacey, L.A., Grzywacz, D., Shapiro-Ilan, D.I., Frutos, R., Brownbridge, M., Goettel, M.S., 2015. Insect pathogens as biological control agents: Back to the future. J. Invertebr. Pathol. 132, 1–41. doi:10.1016/j.jip.2015.07.009

Larkin, M.A., Blackshields, G., Brown, N.P., Chenna, R., McGettigan, P.A., McWilliam, H., Valentin, F., Wallace, I.M., Wilm, A., Lopez, R., Thompson, J.D., Gibson, T.J.,

Higgins, D.G., 2007. Clustal W and Clustal X version 2.0. Bioinformatics 23, 2947–2948. doi:10.1093/bioinformatics/btm404

Lee, M.K., Curtiss, A., Alcantara, E., Dean, D.H., 1996. Synergistic effect of the Bacillus thuringiensis toxins CryIAa and CryIAc on the gypsy moth, *Lymantria dispar*. Appl. Environ. Microbiol. 62, 583–6.

Lee, M.K., Miles, P., Chen, J.S., 2006. Brush border membrane binding properties of *Bacillus thuringiensis* Vip3A toxin to *Heliothis virescens* and *Helicoverpa zea* midguts. Biochem Biophys.Res.Commun. 339, 1043–1047. doi:10.1016/j.bbrc.2005.11.112

Lee, M.K., Walters, F.S., Hart, H., Palekar, N., Chen, J.S., 2003. The mode of action of the *Bacillus thuringiensis* vegetative insecticidal protein Vip3A differs from that of Cry1Ab d-endotoxin. Appl. Environ. Microbiol. 69, 4648–4657. doi:10.1128/AEM.69.8.4648-4657.2003

Lemes, A.R.N., Davolos, C.C., Legori, P.C.B.C., Fernandes, O.A., Ferré, J., Lemos, M.V.F., Desiderio, J.A., 2014. Synergism and antagonism between *Bacillus thuringiensis* Vip3A and Cry1 proteins in *Heliothis virescens*, *Diatraea saccharalis* and *Spodoptera frugiperda*. PLoS One 9, e107196. doi:10.1371/journal.pone.0107196

LeOra-software, 1987. Polo-PC a user's guide to probit or logit analysis.

Leuber, M., Orlik, F., Schiffler, B., Sickmann, A., Benz, R., 2006. Vegetative Insecticidal Protein (Vip1Ac) of *Bacillus thuringiensis* HD201: Evidence for Oligomer and Channel Formation. Biochemistry 45, 283–288. doi:10.1021/BI051351Z

Li, C., Xu, N., Huang, X., Wang, W., Cheng, J., Wu, K., Shen, Z., 2007. *Bacillus thuringiensis* Vip3 mutant proteins: Insecticidal activity and trypsin sensitivity. Biocontrol Sci. Technol. 17, 699–708. doi:10.1080/09583150701527177

Li, T., Liu, B., Spalding, M.H., Weeks, D.P., Yang, B., 2012. High-efficiency TALEN-based gene editing produces disease-resistant rice. Nat. Biotechnol. 30, 390–392. doi:10.1038/nbt.2199

Lisansky, S.G., Quinlan, R., Tassoni, G., 1993. The *Bacillus thuringiensis* production handbook: laboratory methods, manufacturing, quality control, registration. CPL Scientific Ltd, Newbury, UK.

Liu, J., Song, F., Zhang, J., Liu, R., He, K., Tan, J., Huang, D., 2007. Identification of *vip3A*-type genes from *Bacillus thuringiensis* strains and characterization of a novel *vip3A*-type gene. Lett.Appl.Microbiol 45, 432–438.

Liu, J.G., Yang, A.Z., Shen, X.H., Hua, B.G., Shi, G.L., 2011. Specific binding of activated Vip3Aa10 to *Helicoverpa armigera* brush border membrane vesicles results in pore formation. J. Invertebr. Pathol. 108, 92–97. doi:10.1016/j.jip.2011.07.007

Liu, M., Liu, R., Luo, G., Li, H., Gao, J., 2017. Effects of Site-Mutations Within the 22 kDa No-Core Fragment of the Vip3Aa11 Insecticidal Toxin of *Bacillus thuringiensis*. Curr. Microbiol. 1–5. doi:10.1007/s00284-017-1233-y

Liu, Y.-J., Liu, J., Ying, S.-H., Liu, S.-S., Feng, M.-G., 2013. A fungal insecticide engineered for fast per os killing of caterpillars has high field efficacy and safety in

full-season control of cabbage insect pests. Appl. Environ. Microbiol. 79, 6452–8. doi:10.1128/AEM.01594-13

Llewellyn, D.J., Mares, C.L., Fitt, G.P., 2007. Field performance and seasonal changes in the efficacy against *Helicoverpa armigera* (Hübner) of transgenic cotton expressing the insecticidal protein Vip3A. Agric. For. Entomol. 9, 93–101. doi:10.1111/j.1461-9563.2007.00332.x

Loguercio, L.L., Barreto, M.L., Rocha, T.L., Santos, C.G., Teixeira, F.F., Paiva, E., 2002. Combined analysis of supernatant-based feeding bioassays and PCR as a first-tier screening strategy for *Vip* -derived activities in *Bacillus thuringiensis* strains effective against tropical fall armyworm. J. Appl. Microbiol. 93, 269–277. doi:10.1046/j.1365-2672.2002.01694.x

Mahadeva Swamy, H.M., Asokan, R., 2013. *Bacillus thuringiensis* as 'Nanoparticles'- a Perspective for Crop Protection. Nanosci. Nanotechnology-Asia. doi:10.2174/22106812112029990006

Mahon, R.J., Downes, S.J., James, B., Gregg, P., Knight, K., 2012. Vip3A resistance alleles exist at high levels in Australian targets before release of cotton expressing this toxin. PLoS One 7, e39192. doi:10.1371/journal.pone.0039192

Marchler-Bauer, A., Lu, S., Anderson, J.B., Chitsaz, F., Derbyshire, M.K., DeWeese-Scott, C., Fong, J.H., Geer, L.Y., Geer, R.C., Gonzales, N.R., Gwadz, M., Hurwitz, D.I., Jackson, J.D., Ke, Z., Lanczycki, C.J., Lu, F., Marchler, G.H., Mullokandov, M., Omelchenko, M. V., Robertson, C.L., Song, J.S., Thanki, N., Yamashita, R.A., Zhang, D., Zhang, N., Zheng, C., Bryant, S.H., 2011. CDD: a Conserved Domain Database for the functional annotation of proteins. Nucleic Acids Res. 39, D225–D229. doi:10.1093/nar/gkq1189

Martin, P.A.W., 1994. An Iconoclastic View of *Bacillus thuringiensis* Ecology. Am. Entomol. 40, 85–91. doi:10.1093/ae/40.2.85

Marucci, S.C., Figueiredo, C.S., Tezza, R.I.D., Alves, E.C. da C., Lemos, M.V.F., Desidério, J.A., 2015. Relação entre toxicidade de proteínas Vip3Aa e sua capacidade de ligação a receptores intestinais de lepidópteros-praga. Pesqui. Agropecuária Bras. 50, 637–648. doi:10.1590/s0100-204x2015000800002

Melo, A.L. de A., Soccol, V.T., Soccol, C.R., 2016. *Bacillus thuringiensis* : mechanism of action, resistance, and new applications: a review. Crit. Rev. Biotechnol. 36, 317–326. doi:10.3109/07388551.2014.960793

Mesrati, L.A., Tounsi, S., Kamoun, F., Jaoua, S., 2005. Identification of a promoter for the vegetative insecticidal protein-encoding gene vip3LB from *Bacillus thuringiensis*. FEMS Microbiol. Lett. 247, 101–104.

Mesrati, L., Tounsi, S., Jaoua, S., 2005. Characterization of a novel vip3-type gene from Bacillus thuringiensis and evidence of its presence on a large plasmid. FEMS Microbiol. Lett. 244, 353–358. doi:10.1016/j.femsle.2005.02.007

Milne, R., Liu, Y., Gauthier, D., Van, F.K., 2008. Purification of Vip3Aa from *Bacillus thuringiensis* HD-1 and its contribution to toxicity of HD-1 to spruce budworm

(*Choristoneura fumiferana*) and gypsy moth (*Lymantria dispar*) (Lepidoptera). J Invertebr.Pathol. 99, 166–172.

Moar, W.J., Berry, C., Narva, K.E., 2017. The structure/function of new insecticidal proteins and regulatory challenges for commercialization. J. Invertebr. Pathol. 142, 1–4. doi:10.1016/j.jip.2017.02.001

Morrison, K.L., Weiss, G.A., 2001. Combinatorial alanine-scanning. Curr. Opin. Chem. Biol. 5, 302–307. doi:S1367-5931(00)00206-4

Murawska, E., Fiedoruk, K., Bideshi, D.K., Swiecicka, I., 2013. Complete genome sequence of *Bacillus thuringiensis* subsp. *thuringiensis* strain IS5056, an isolate highly toxic to *Trichoplusia ni*. Genome Announc. 1, e0010813. doi:10.1128/genomeA.00108-13

NCBI NCBI C Toolkit Cross Reference - BLOSUM 80. URL https://www.ncbi.nlm.nih.gov/IEB/ToolBox/C_DOC/lxr/source/data/BLOSUM80 (accessed 4.16.17).

Ni, M., Ma, W., Wang, X., Gao, M., Dai, Y., Wei, X., Zhang, L., Peng, Y., Chen, S., Ding, L., Tian, Y., Li, J., Wang, H., Wang, X., Xu, G., Guo, W., Yang, Y., Wu, Y., Heuberger, S., Tabashnik, B.E., Zhang, T., Zhu, Z., 2017. Next generation transgenic cotton: pyramiding RNAi and Bt counters insect resistance. Plant Biotechnol. J. doi:10.1111/pbi.12709

Nicholas, Nicholas, H., Deerfield, D., 1997. GeneDoc: analysis and visualization of genetic variation. EMBNEW. NEWS 4.

Nielsen, M.M., Andersen, K.K., Westh, P., Otzen, D.E., Mascher, E., Lundahl, P., Almgren, M., Pastore, A., 2007. Unfolding of beta-sheet proteins in SDS. Biophys. J. 92, 3674–85. doi:10.1529/biophysj.106.101238

Palma, L., Berry, C., 2016. Understanding the structure and function of *Bacillus thuringiensis* toxins. Toxicon. 109, 1–3. doi:10.1016/j.toxicon.2015.10.020

Palma, L., de Escudero, I.R., Maeztu, M., Caballero, P., Muñoz, D., 2013a. Screening of vip genes from a Spanish *Bacillus thuringiensis* collection and characterization of two Vip3 proteins highly toxic to five lepidopteran crop pests. Biol. Control 66, 141–149. doi:10.1016/j.biocontrol.2013.05.003

Palma, L., de Escudero, I.R., Maeztu, M., Caballero, P., Muñoz, D., 2013b. Screening of vip genes from a Spanish *Bacillus thuringiensis* collection and characterization of two Vip3 proteins highly toxic to five lepidopteran crop pests. Biol. Control 66, 141–149. doi:10.1016/j.biocontrol.2013.05.003

Palma, L., Hernández-Rodrí-guez, C.S., Maeztu, M., Hernández-Martí-nez, P., Ruiz, de E., Escriche, B., Munoz, D., Van Rie, J., Ferré, J., Caballero, P., 2012. Vip3C, a novel class of vegetative insecticidal proteins from *Bacillus thuringiensis*. Appl. Environ. Microbiol. 78, 7163–7165. doi:10.1128/AEM.01360-12

Palma, L., Muñoz, D., Berry, C., Murillo, J., Caballero, P., 2014. *Bacillus thuringiensis* toxins: an overview of their biocidal activity. Toxins (Basel) 6, 3296–3325. doi:10.3390/toxins6123296

Palma, L., Scott, D., Harris, G., Din, S.-U., Williams, T., Roberts, O., Young, M., Caballero, P., Berry, C., 2017. The Vip3Ag4 Insecticidal protoxin from *Bacillus thuringiensis* adopts a tetrameric configuration that is maintained on proteolysis. Toxins (Basel). 9, 165. doi:10.3390/toxins9050165

Panetta, J.D., 1993. Engineered microbes: the Cell Cap system., in: Kim, L. (Ed ). (Ed.), Advanced Engineered Pesticides. Marcel Decker, pp. 379–382.

Parker, W., Song, P.S., 1992. Protein structures in SDS micelle-protein complexes. Biophys. J. 61, 1435–1439. doi:10.1016/S0006-3495(92)81949-5

Pickett, B.R., 2009. Studies on resistance to vegetative (Vip3a) and crystal (Cry1a) insecticidal toxins of *Bacillus thuringiensis* in *Heliothis virescens* (Fabricius). Imperial College London.

Qin, Y., Ying, S.-H., Chen, Y., Shen, Z.-C., Feng, M.-G., 2010. Integration of insecticidal protein Vip3Aa1 into *Beauveria bassiana* enhances fungal virulence to *Spodoptera litura* larvae by cuticle and per Os infection. Appl. Environ. Microbiol. 76, 4611–8. doi:10.1128/AEM.00302-10

Rang, C., Gil, P., Neisner, N., Van Rie, J., Frutos, R., 2005. Novel Vip3-related protein from *Bacillus thuringiensis*. Appl. Environ. Microbiol. 71, 6276–6281. doi:10.1128/AEM.71.10.6276-6281.2005

Raybould, A., Quemada, H., 2010. Bt crops and food security in developing countries: realised benefits, sustainable use and lowering barriers to adoption. Food Secur. 2, 247–259. doi:10.1007/s12571-010-0066-3

Rice, W.C., 1999. Specific primers for the detection of vip3A insecticidal gene within a *Bacillus thuringiensis* collection. Lett. Appl. Microbiol. 28, 378–382. doi:10.1046/j.1365-2672.1999.00536.x

Ruiu, L., 2013. *Brevibacillus laterosporus*, a pathogen of invertebrates and a broad-spectrum antimicrobial species. Insects 4, 476–92. doi:10.3390/insects4030476

Ruiz de Escudero, I., Banyuls, N., Bel, Y., Maeztu, M., Escriche, B., Muñoz, D., Caballero, P., Ferré, J., 2014. A screening of five *Bacillus thuringiensis* Vip3A proteins for their activity against lepidopteran pests. J. Invertebr. Pathol. 117, 51–55. doi:10.1016/j.jip.2014.01.006

Ruiz de Escudero, I., Estela, A., Escriche, B., Caballero, P., 2007. Potential of the *Bacillus thuringiensis* toxin reservoir for the control of *Lobesia botrana* (Lepidoptera: Tortricidae), a major pest of grape plants. Appl. Environ. Microbiol. 73, 337–40. doi:10.1128/AEM.01511-06

Russell, R.B., Betts, M.J., Barnes, M.R., n.d. Amino acid properties. URL http://www.russelllab.org/aas/ (accessed 4.15.17).

Sanahuja, G., Banakar, R., Twyman, R.M., Capell, T., Christou, P., 2011. *Bacillus thuringiensis*: a century of research, development and commercial applications. Plant Biotechnol. J. 9, 283–300. doi:10.1111/j.1467-7652.2011.00595.x

Sanchis, V., 2011. From microbial sprays to insect-resistant transgenic plants: history of the biospesticide *Bacillus thuringiensis*. A review. Agron. Sustain. Dev. 31, 217–231. doi:10.1051/agro/2010027

Saraswathy, N., Nain, V., Sushmita, K., Kumar, P.A., 2008. A fusion gene encoding two different insecticidal proteins of *Bacillus thuringiensis*. Indian J. Biotechnol. 7, 204–209.

Sattar, S., Biswas, P.K., Hossain, M.A., Maiti, M.K., Sen, S.K., Basu, A., 2008. Search for Vegetative Insecticidal Proteins (VIPs) from local isolates of *Bacillus thuringiensis* effective against lepidopteranand homopteran insect pests. J. Biopestic. 1, 216–222.

Sattar, S., Maiti, M.K., 2011. Molecular characterization of a novel vegetative insecticidal protein from *Bacillus thuringiensis* effective against sap-sucking insect pest. J. Microbiol. Biotechnol. 21, 937–46.

Schmid, A., Benz, R., Just, I., Aktories, K., 1994. Interaction of Clostridium botulinum C2 toxin with lipid bilayer membranes formation of cation-selective channels and inhibition of channel function by chloroquine. JJournal Biol. Chem. 269, 16706–16711.

Schnepf, H.E., Narva, K.E., Stockhoff, B.A., Lee, S.F., Waltz, M., Sturgis, B., 2003. Pesticidal toxins and genes from Bacillus laterosporus strains. US patent 6,605,701 B2.

Schrödinger, L.L.C., 2015. The PyMOL Molecular Graphics System, Version~1.8.

Sellami, S., Cherif, M., Abdelkefi-Mesrati, L., Tounsi, S., Jamoussi, K., 2015. Toxicity, activation process, and histopathological effect of *Bacillus thuringiensis* vegetative insecticidal protein Vip3Aa16 on *Tuta absoluta*. Appl. Biochem. Biotechnol. 175, 1992–1999. doi:10.1007/s12010-014-1393-1

Sellami, S., Jamoussi, K., Dabbeche, E., Jaoua, S., 2011. Increase of the *Bacillus thuringiensis* secreted toxicity against lepidopteran larvae by homologous expression of the *vip3LB* gene during sporulation stage. Curr. Microbiol. 63, 289–294. doi:10.1007/s00284-011-9976-3

Selvapandiyan, A., Arora, N., Rajagopal, R., Jalali, S.K., Venkatesan, T., Singh, S.P., Bhatnagar, R.K., 2001. Toxicity analysis of N- and C-terminus-deleted vegetative insecticidal protein from *Bacillus thuringiensis*. Appl. Environ. Microbiol. 67, 5855–5858. doi:10.1128/AEM.67.12.5855-5858.2001

Sena, J.A., Hernandez-Rodriguez, C., Ferre, J., 2009. Interaction of *Bacillus thuringiensis* Cry1 and Vip3A proteins to *Spodoptera frugiperda* midgut binding sites. Appl. Environ. Microbiol.

Shan, Q., Wang, Y., Li, J., Zhang, Y., Chen, K., Liang, Z., Zhang, K., Liu, J., Xi, J.J., Qiu, J.-L., Gao, C., 2013. Targeted genome modification of crop plants using a CRISPR-Cas system. Nat. Biotechnol. 31, 686–688. doi:10.1038/nbt.2650

Shelton, A.M., 2012. Genetically engineered vegetables expressing proteins from *Bacillus thuringiensis* for insect resistance. GM Crops Food 3, 175–183. doi:10.4161/gmcr.19762

Shi, Y., Ma, W., Yuan, M., Sun, F., Pang, Y., 2007. Cloning of *vip1/vip2* genes and expression of Vip1Ca/Vip2Ac proteins in *Bacillus thuringiensis*. World J. Microbiol. Biotechnol. 23, 501–507. doi:10.1007/s11274-006-9252-z

Shi, Y., Mowery, R.A., Ashley, J., Hentz, M., Ramirez, A.J., Bilgicer, B., Slunt-Brown, H., Borchelt, D.R., Shaw, B.F., 2012. Abnormal SDS-PAGE migration of cytosolic proteins can identify domains and mechanisms that control surfactant binding. Protein Sci. 21, 1197–1209. doi:10.1002/pro.2107

Shi, Y., Xu, W., Yuan, M., Tang, M., Chen, J., Pang, Y., 2004. Expression of *vip1/vip2* genes in *Escherichia coli* and *Bacillus thuringiensis* and the analysis of their signal peptides. J. Appl. Microbiol. 97, 757–765. doi:10.1111/j.1365-2672.2004.02365.x

Shingote, P.R., Moharil, M.P., Dhumale, D.R., Deshmukh, A.G., Jadhav, P.V., Dudhare, M.S., Satpute, N.S., 2013. Distribution of *vip* Genes, Protein Profiling and Determination of Entomopathogenic Potential of Local Isolates of *Bacillus thuringiensis*. Bt Res. 4, 14–20. doi:10.5376/bt.2013.04.0003

Shingote, P.R., Moharil, M.P., Dhumale, D.R., Jadhav, P. V, Satpute, N.S., Dudhare, M.S., 2013. Screening of *vip1/vip2* binary toxin gene and its isolation and cloning from local *Bacillus thuringiensis* isolates. ScienceAsia 39, 620–624. doi:10.2306/scienceasia1513-1874.2013.39.620

Sievers, F., Wilm, A., Dineen, D., Gibson, T.J., Karplus, K., Li, W., Lopez, R., McWilliam, H., Remmert, M., Soding, J., Thompson, J.D., Higgins, D.G., 2011. Fast, scalable generation of high-quality protein multiple sequence alignments using Clustal Omega. Mol. Syst. Biol. 7, 539. doi:10.1038/msb.2011.75

Singh, G., Sachdev, B., Sharma, N., Seth, R., Bhatnagar, R.K., 2010. Interaction of *Bacillus thuringiensis* vegetative insecticidal protein with ribosomal S2 protein triggers larvicidal activity in *Spodoptera frugiperda*. Appl. Environ. Microbiol. 76, 7202–7209. doi:10.1128/AEM.01552-10

Song, F., Chen, C., Wu, S., Shao, E., Li, M., Guan, X., Huang, Z., 2016a. Transcriptional profiling analysis of *Spodoptera litura* larvae challenged with Vip3Aa toxin and possible involvement of trypsin in the toxin activation. Sci. Rep. 6, 23861. doi:10.1038/srep23861

Song, F., Lin, Y., Chen, C., Shao, E., Guan, X., Huang, Z., 2016b. Insecticidal Activity and Histopathological Effects of Vip3Aa Protein from *Bacillus thuringiensis* on *Spodoptera litura*. J. Microbiol. Biotechnol. 26, 1774–1780. doi:10.4014/jmb.1604.04090

Song, R., Peng, D., Yu, Z., Sun, M., 2008. Carboxy-terminal half of Cry1C can help vegetative insecticidal protein to form inclusion bodies in the mother cell of *Bacillus thuringiensis*. Appl. Microbiol. Biotechnol. 80, 647–654. doi:10.1007/s00253-008-1613-0

Srinivasan, A., Giri, A.P., Gupta, V.S., 2006. Structural and functional diversities in lepidopteran serine proteases. Cell. Mollecular Biol. Lett. 11, 132–154. doi:10.2478/s11658-006-0012-8

Strohalm, M., Hassman, M., Košata, B., Kodíček, M., 2008. mMass data miner: an open source alternative for mass spectrometric data analysis. Rapid Commun. Mass Spectrom. 22, 905–908. doi:10.1002/rcm.3444

Sullivan, L.H., 1896. The tall office building artistically considered. Lippincott's Mag. March, 403–409.

Tamura, K., Peterson, D., Peterson, N., Stecher, G., Nei, M., Kumar, S., 2011. MEGA5: Molecular evolutionary genetics analysis using maximum likelihood, evolutionary distance, and maximum parsimony methods. Mol. Biol. Evol. 28, 2731–2739. doi:10.1093/molbev/msr121

Teale, F.W.J., Weber, G., 1957. Ultraviolet fluorescence of the aromatic amino acids. Biochem. J. 65, 476–482.

Thamthiankul Chankhamhaengdecha, S., Tantichodok, A., Panbangred, W., 2008. Spore stage expression of a vegetative insecticidal gene increase toxicity of *Bacillus thuringiensis* subsp. *aizawai* SP41 against *Spodoptera exigua*. J. Biotechnol. 136, 122–128. doi:10.1016/j.jbiotec.2008.05.013

Thangudu, R.R., Manoharan, M., Srinivasan, N., Cadet, F., Sowdhamini, R., Offmann, B., 2008. Analysis on conservation of disulphide bonds and their structural features in homologous protein domain families. BMC Struct. Biol. 8, 55. doi:10.1186/1472-6807-8-55

Thompson, J., Gibson, T.J., Plewniak, F., Jeanmougin, F., Higgins, D.G., 1997. The CLUSTAL_X Windows interface: flexible strategies for multiple sequence alignment aided by quality analysis tools. Nucleic Acids Res. 25, 4876–4882. doi:10.1093/nar/25.24.4876

Tilman, D., Fargione, J., Wolff, B., D'Antonio, C., Dobson, A., Howarth, R., Schindler, D., Schlesinger, W.H., Simberloff, D., Swackhamer, D., 2001. Forecasting Agriculturally Driven Global Environmental Change. Science (80-. ). 292, 281–284. doi:10.1126/science.1057544

van Frankenhuyzen, K., 2009. Insecticidal activity of Bacillus thuringiensis crystal proteins. J. Invertebr. Pathol. 101, 1–16. doi:10.1016/j.jip.2009.02.009

Van Frankenhuyzen, K., Nystrom, C., 2009. The Bacillus thuringiensis toxin specificity database. URL http://www.glfc.forestry.ca/bacillus/BtSearch%0A.cfm. (accessed 2.4.16).

Vélez, A.M., Spencer, T.A., Alves, A.P., Moellenbeck, D., Meagher, R.L., Chirakkal, H., Siegfried, B.D., 2013. Inheritance of Cry1F resistance, cross-resistance and frequency of resistant alleles in *Spodoptera frugiperda* (Lepidoptera: Noctuidae). Bull. Entomol. Res. 103, 700–713. doi:10.1017/S0007485313000448

Walsh, T.K., Downes, S.J., Gascoyne, J., James, W., Parker, T., Armstrong, J., Mahon, R.J., 2014. Dual Cry2Ab and Vip3A Resistant Strains of *Helicoverpa armigera* and *Helicoverpa punctigera* (Lepidoptera: Noctuidae); testing linkage between loci and monitoring of allele frequencies. J. Econ. Entomol. 107, 1610–1617. doi:10.1603/ec13558

Wang, Y., Cheng, X., Shan, Q., Zhang, Y., Liu, J., Gao, C., Qiu, J.-L., 2014. Simultaneous editing of three homoeoalleles in hexaploid bread wheat confers heritable resistance to powdery mildew. Nat. Biotechnol. 32, 947–951. doi:10.1038/nbt.2969

Warren, G., Koziel, M., Mullin, M., Nye, G., Carr, B., Desai, N., Kostichka, K., Duck, N., Estruch, J., 1998. Auxiliary proteins for enhancing the insecticidal activity of pesticidal proteins. US patent 5,770,696.

Warren, G.W., 1997. Vegetative insecticidal proteins: novel proteins for control of corn pests, in: Carozzi NB, K.M. (Ed.), Advances in Insect Control, the Role of Transgenic Plants. Taylor & Francis Ltd, London, United Kingdom., pp. 109–121.

Wass, M.N., Kelley, L.A., Sternberg, M.J.E., 2010. 3DLigandSite: predicting ligand-binding sites using similar structures. Nucleic Acids Res. 38, W469–W473. doi:10.1093/nar/gkq406

Waterhouse, A.M., Procter, J.B., Martin, D.M., Clamp, M., Barton, G.J., 2009. Jalview Version 2--a multiple sequence alignment editor and analysis workbench. Bioinformatics 25, 1189–1191. doi:10.1093/bioinformatics/btp033

Welch, K.L., Unnithan, G.C., Degain, B.A., Wei, J., Zhang, J., Li, X., Tabashnik, B.E., Carrière, Y., 2015. Cross-resistance to toxins used in pyramided Bt crops and resistance to Bt sprays in *Helicoverpa zea*. J. Invertebr. Pathol. 132, 149–156. doi:10.1016/j.jip.2015.10.003

Wu, J., Zhao, F., Bai, J., Deng, G., Qin, S., Bao, Q., 2007. Evidence for positive darwinian selection of Vip gene in *Bacillus thuringiensis*. J.Genet.Genomics 34, 649–660. doi:10.1016/S1673-8527(07)60074-5

Wu, J.H., Luo, X.L., Zhang, X.R., Shi, Y.J., Tian, Y.C., 2011. Development of insect-resistant transgenic cotton with chimeric TVip3A*accumulating in chloroplasts. Transgenic Res. 20, 963–973. doi:DOI 10.1007/s11248-011-9483-0

Wu, Z.L., Guo, W.Y., Qiu, J.Z., Huang, T.P., Li, X.B., Guan, X., 2004. Cloning and localization of vip3A gene of *Bacillus thuringiensis*. Biotechnol.Lett. 26, 1425–1428.

Yamagiwa, M., Esaki, M., Otake, K., Inagaki, M., Komano, T., Amachi, T., Sakai, H., 1999. Activation process of dipteran-specific insecticidal protein produced by *Bacillus thuringiensis* subsp. *israelensis*. Appl. Environ. Microbiol. 65, 3464–9.

Yamaguchi, T., Sahara, K., Bando, H., Asano, S., 2010. Intramolecular proteolytic nicking and binding of *Bacillus thuringiensis* Cry8Da toxin in BBMVs of Japanese beetle. J. Invertebr. Pathol. 105, 243–247. doi:10.1016/j.jip.2010.07.002

Yeates, T.O., 2007. Protein Structure: Evolutionary Bridges to New Folds. Curr. Biol. 17, 48–50. doi:10.1016/j.cub.2006.12.003

Yu, C.G., Mullins, M.A., Warren, G.W., Koziel, M.G., Estruch, J.J., 1997. The *Bacillus thuringiensis* vegetative insecticidal protein Vip3A lyses midgut epithelium cells of susceptible insects. Appl. Environ. Microbiol. 63, 532–536.

Yu, X., Liu, T., Liang, X., Tang, C., Zhu, J., Wang, S., Li, S., Deng, Q., Wang, L., Zheng, A., Li, P., 2011a. Rapid detection of *vip1*-type genes from *Bacillus cereus* and

characterization of a novel vip binary toxin gene. FEMS Microbiol. Lett. 325, 30–36. doi:10.1111/j.1574-6968.2011.02409.x

Yu, X., Zheng, A., Zhu, J., Wang, S., Wang, L., Deng, Q., Li, S., Liu, H., Li, P., 2011b. Characterization of Vegetative Insecticidal Protein vip Genes of *Bacillus thuringiensis* from Sichuan Basin in China. Curr. Microbiol. 62, 752–757. doi:10.1007/s00284-010-9782-3

Yu, X.M., Liu, T., Sun, Z.G., Guan, P., Zhu, J., Wang, S.Q., Li, S.C., Deng, Q.M., Wang, L.X., Zheng, A.P., Li, P., 2012. Co-expression and Synergism Analysis of Vip3Aa29 and Cyt2Aa3 Insecticidal Proteins from *Bacillus thuringiensis*. Curr. Microbiol. 64, 326–331. doi:DOI 10.1007/s00284-011-0070-7

Zheng, L., Baumann, U., Reymond, J.-L., 2004. An efficient one-step site-directed and site-saturation mutagenesis protocol. Nucleic Acids Res. 32, e115. doi:10.1093/nar/gnh110

Zhu, C., Ruan, L., Peng, D., Yu, Z., Sun, M., 2006. Vegetative insecticidal protein enhancing the toxicity of *Bacillus thuringiensis* subsp *kurstaki* against *Spodoptera exigua*. Lett. Appl. Microbiol. 42, 109–114. doi:10.1111/j.1472-765X.2005.01817.x

# ANNEX

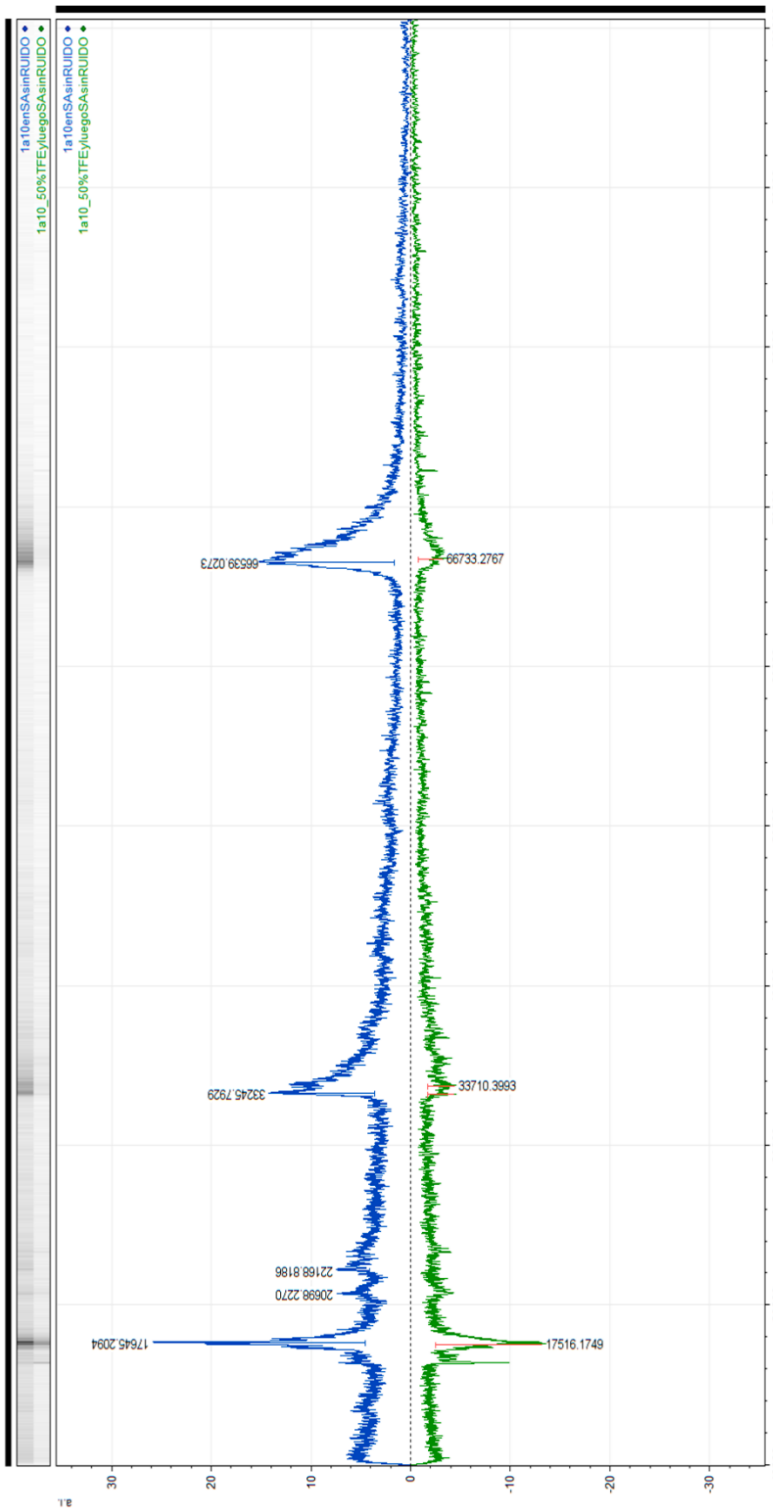


*Fig. S-2.1. Molecular mass determination by MALDI TOF/TOF of the 66 kDa polypeptide formed after treatment of the Vip3Aa protoxin with trypsin (24:100 trypsin:Vip3A, w:w) for 3 days.*

*Table S-4.1. Primers used for testing out the correct change in the Ala-mutated proteins and the results of the sequencing.*

| Primer | Sequence | Position† in the reference gene | Product size‡ (bp) | Vip3Af mutated protein | Codon (aa) (mutation/ wt) |
|---|---|---|---|---|---|
| *wt1.fw* | 5' CGATGCGATAAATACGATGCTTCATA 3' | 321 - 1078 | 757 | T167A | GCT (A)/ ACT (T) |
| *wt1.rev* | 5' ACCCAACCAATGCATGTCCT 3' | | | E168A | GCA (A)/ GAA (E) |
| | | | | P171A | GCT (A)/ CCT (P) |
| | | | | F229A | GCT (A)/ TTT (F) |
| | | | | M238A | GCG (A)/ ATG (M) |
| | | | | N242A | GCT (A)/ AAT (N) |
| | | | | F244A | GCC (A)/ TTC (F) |
| | | | | R246A | GCT (A)/ CGT (R) |
| | | | | Y272A | GCT (A)/ TAT (Y) |
| | | | | C292A | GCC (A)/ TGC (C) |
| | | | | I301A | GCT (A)/ ATT (I) |
| *wt2.fw* | 5' CGGAGGTTATTTATGGTGATACGG 3' | 1166 - 1793 | 627 | C401A | GCT (A)/ TGT (C) |
| *wt2.rev* | 5' TGGATTACATACTCAGTTTTCGGT 3' | | | E483A | GCA (A)/ GAA (E) |
| | | | | C507A | GCT (A)/ TGT (C) |
| | | | | D519A | GCC (A)/ GAC (A) |
| | | | | W552A | GCG (A)/ TGG (W) |
| *wt3.fw* | 5' AAGGACGGAGGATTTTCACAA 3' | 1729 - 2281 | 552 | G689A | GCG (A)/ GGG (G) |
| *wt3.rev* | 5' TCTACATATAATCCGGTATTATTGG 3' | | | I699A | GCT (A)/ ATT (I) |
| | | | | L711A | GCT (A)/ CTT (L) |
| | | | | Y719A | GCT (A)/ TAT (Y) |
| | | | | G727A | GCT (A)/ GGA (G) |
| | | | | F741A | GCT (A)/ TTT (F) |

*Table S-5.1. Characteristics of primer design for the site directed mutagenesis and comparison between $T_m$.*

| Primer | *Tm* (ºC) | Self-annealing *Tm* (ºC) | % GC | length/ mutations (bases) | Complementarity of primer pair (bases) |
|---|---|---|---|---|---|
| *M34L-Fwd* | 78 | 70 | 34 | 38/ 2 | 27 |
| *M34L-Rev* | 76 | 68 | 29 | 38/ 2 | 27 |
| *T167S-E168D-P171G-Fwd* | 83 | 80 | 37 | 49/ 4 | 40 |
| *T167S-E168D-P171G-Rev* | 82 | 79 | 35 | 48/ 4 | 40 |
| *K284Q-Fwd* | 78 | 67 | 36 | 36/ 2 | 23 |
| *K284Q-Rev* | 79 | 66 | 33 | 42/ 2 | 23 |
| *E483D-Fwd* | 76 | 64 | 35 | 34/ 2 | 21 |
| *E483D-Rev* | 74 | 65 | 37 | 30/ 1 | 21 |
| *E483Q-Fwd* | 76 | 64 | 35 | 34/ 1 | 21 |
| *E483Q-Rev* | 74 | 65 | 37 | 30/ 1 | 21 |
| *E483H-Fwd* | 77 | 65 | 38 | 34/ 2 | 21 |
| *E483H-Rev* | 75 | 66 | 40 | 30/ 2 | 21 |
| *W552H-Fwd* | 81 | 69 | 41 | 39/ 1 | 23 |
| *W552H-Rev* | 81 | 71 | 47 | 34/ 2 | 23 |
| *W552F-Fwd* | 80 | 68 | 38 | 39/ 2 | 23 |
| *W552F-Rev* | 80 | 70 | 44 | 34/ 2 | 23 |
| *W552Y-Fwd* | 80 | 68 | 38 | 39/ 2 | 23 |
| *W552Y-Rev* | 80 | 70 | 44 | 34/ 2 | 23 |
| *G689S-Fwd* | 79 | 71 | 45 | 33/ 2 | 23 |
| *G689S-Rev* | 79 | 72 | 48 | 31/ 2 | 23 |
| *G689E-Fwd* | 79 | 71 | 45 | 33/ 2 | 23 |
| *G689E-Rev* | 79 | 72 | 48 | 31/ 2 | 23 |
| *N682K-G689S-Fwd* | 86 | 82 | 51 | 41/ 3 | 33 |
| *N682K-G689S-Rev* | 84 | 78 | 42 | 45/ 3 | 33 |